Synthesis of heterocyclic scaffolds using reagentless techniques

Sergi Ortoll

Thesis submitted for the degree of Doctor of Philosophy

Completed with supervision by

Professor Mark Bagley and Professor John Spencer

Declaration

I hereby declare that this thesis is my own work and effort and that it has not been submitted anywhere for any award of another degree. I also undertake that any quotation or paraphrase from the published work of other people has been acknowledged. This work was supervised by Prof Mark C. Bagley.

Sergi Ortoll Diaz

Acknowledgements

I have been very fortunate to receive a great deal of support throughout my PhD. First and foremost, I would like to thank my supervisor Prof. Mark C. Bagley for giving me the opportunity of conducting my PhD under his supervision, directing, encouraging, and inspiring me from start to finish.

I would like to thank my co-supervisors Prof. John Spencer and Dr Eddy Visseux for their expertise and guidance in formulating this thesis.

This project would not have been possible without the funding from the European Regional Development Fund (ERDF) via the Interreg France (Channel) England program, and I would like to acknowledge them at this occasion.

I would like to thank Dr Alaa Abdul-Sada and Dr. Ramon Gonzalez at the University of Sussex and Dr. Iain Goodall at the University of Greenwich for carrying out all the mass spectrometry, service and Dr Iain Day and Dr Manvendra Sharma at the University of Sussex for NMR studies and support.

Special thanks to my friends Mary, Andy, Arathy, Raysa, Hugo and all the people I have met during this journey for making my PhD life all the brighter, as well as Gonzalo and Angel for starting this adventure with me and Julia for her support during all this journey. And finally, I would like to thank my partner Gemma, my sister Judit, my parents and the rest of my family and friends for believing in me and cheering me on, all the way.

Abstract

This thesis focuses on the utilization of reagentless techniques, especially flow chemistry, for the synthesis of useful quantities of carbazole scaffolds and some of its derivatives. It also explores the potential biological activity of the scaffolds synthesised, as well as the scope of this type of new techniques in the synthesis of carbazole containing natural products, and the adaptation of this methodology to the synthesis of carbolines.

Chapter 2 describes the development of a novel synthetic pathway for the synthesis of *N*-ethylated carbazoles using reagentless scaffolds, starting with readily commercially available haloanilines and boronic acids. Although each step of the synthesis is investigated, optimized and discussed separately, alhough the integrated methodology is all described together as a linear synthesis and total isolated yields are reported, as well as the possibility of scaling up the whole process for the continous production of carbazoles in gram scale. The data for the compound characterization is discussed and rationalized.

Chapter 3 investigates the reactivation of the p53 gene when it suffers the Y220C mutation. Synthetic alternatives to PK083 analogues are explored, and 5 new candidates are sent to be tested in biological assays. The biological results of these new candidates are reported and the data is discussed. Also, computational docking is carried out using the Schrödinger interface *Maestro* to predict the acitivty of some of the scaffolds.

Chapter 4 explores the adaptation of the methodology developed in Chapter 2 to synthesise a series of carbazole-based natural products, comparing the data to the previously published in the literature. Moreover, the adaptation of the method to the synthesis of carbolines is evaluated.

Chapter 5 concludes the thesis and proposes possible future directions.

Abbreviations

Å	angstrom
ACP	acyl carrier protein
APIs	active Pharmaceutical Ingredients
Asp	aspartic acid
ATP	adenosine triphosphate
Boc	*tert*-butyloxycarbonyl
cat.	catalyst
CDK	cyclin-dependent kinase
CNS	central nervous system
cod	1,5-cyclooctadiene
COX	cyclooxygenase
CTD	carboxy-terminal domain
Cys	cysteine
d	doublet
Da	dalton
DavePhos	2-dicyclohexylphosphino-2'-(*N,N*-dimethylamino)biphenyl
DCE	1,2-dichloroethane
DCM	dichloromethane
DDQ	2,3-dichloro-5,6-dicyanobenzoquinone
DIBAL-H	diisobutylaluminium hydride
DMAD	dimethylacetylene dicarboxylate
DMF	*N,N*-dimethylformamide
DMSO	dimethyl sulfoxide
DMU/(+)-TA	dimethylurea/(+)-tartaric acid
DNA	deoxyribonucleic acid
DPF	*N,N*-diphenylformamide
dppf	1,1'-bis(diphenylphosphino)ferrocene
DSF	differential scanning fluorimetry
DYRK	dual-specificity tyrosine phosphorylation-regulated kinases
EDC	1-ethyl-3-(3-dimethylaminopropyl)carbodiimide
EDG	electron donating group
ESI	electrospray ionization
Et	ethyl

EWG	electron withdrawing group
FA	fluoroacetate
g	gram
GHz	gigahertz
Gln	glutamine
Glu	glutamic acid
Gly	glycine
HDM2	human double minute
His	histidine
HIV	human immunodeficiency virus
HOBt	1-hydroxy benzotriazole
HRMS	high resolution mass spectra
Hz	hertz
IPA	isopropyl alcoholIR infrared
IR	infrared
IC_{50}	half maximal inhibitory concentration
ITC	isothermal calorimetry
IUPAC	International Union of Pure and Applied Chemistry
KAS	*β*-ketoacyl-ACP synthase
K_D	dissociation constant
kDa	kilodalton
LED	light-emitting diodes
LCMS	liquid chromatography–mass spectrometry
Leu	leucine
Lys	lysine
M	molar
m	multiplet
MAO	monoamine oxidase
Me	methyl
MDM2	mouse doble minute 2
MFOs	Metal Organic Frameworks
MHz	megahertz
mg	milligram
mL	millilitre
MM	mixer mill

mmol	milli-mole
MW	microwave
NBS	*N*-bromosuccinimide
NGFR	nerve growth factor receptor
nM	nanomolar
NMM	*N*-methylmorpholine
NMP	*N*-methyl-2-pyrrolidone
NMR	nuclear magnetic resonance
NOESY	nuclear overhauser effect spectroscopy
Nzc	neocarazostatin
OAc	acetate
p	pentet
Pd	palladium
PLK	polo-like kinases
PFA	perfluoroalkoxy
Ph	phenyl
PivOH	pivalic acid
PPh_3	triphenylphosphine
ppm	parts per million
ppy	2-phenylpyridine
Pro	proline
PTFE	polytetrafluoroethylene
Py	pyridine
q	quartet
QSAR	quantitative structure activity relationship
R&D	research and development
RAM	Rink amide
RNA	ribonucleic acid
rt	room temperature
s	singlet
SAR	structure activity relationship
SDS-PAGE	sodium dodecyl-sulfate polyacrylamide gel electrophoresis
SM	starting material
SMB	simulated moving bed chromatography
S_n	singlet level

S_N2	second order nucleophilic substitution
SS	subsite
STAB	sodium triacetoxyborohydride
Sw	water solubility
t	triplet
TAD	topologically associating domains
ThDP	thiamine diphosphate
THF	tetrahydrofuran
TFA	trifluoroacetic acid
Thr	threonine
TLC	thin layer chromatography
T_m	melting temperature
TMS	trimethylsilyl
T_n	triplet level
TR	trypanothione reductase
*t*R	retention times
TRI	trypanothione reductase inhibitors
Trp	Transient receptor potential
Tyr	tyrosine
UV	ultraviolet
Val	valine
V_n	vibrational states
W	watt
WT	wild type
µM	micromolar
°C	celsius degree

Schemes, Figures and Tables

Table of contents

CHAPTER 1: Introduction

Emerging in the nineteenth century, organic synthesis is defined as the capability to synthesise and determine the structure of carbon-containing molecules. The continuous evolution of structural chemistry and organic synthetic methods over the last two centuries has been rather dramatic, in terms of both molecular complexity and diversity, and so has the impact of this evolution on science and society.[1]

The synthesis of urea (**1.1**) by Friedrich Wöhler in 1828 is widely recognised as the first reported synthesis of an organic compound from an inorganic precursor and the starting point of modern organic chemistry (**Scheme 1**).[2] Since that date organic chemistry has been constantly evolving. In the 19th century, in 1865, Friedrich August Kekulé von Stradonitz discovered the benzene (**1.2**) ring structure,[3] which led to further discoveries about how this and other organic compounds react. The year 1874 also saw important advances in organic chemistry when Jacobus van 't Hoff and Joseph-Achille Le Bel discovered that carbon is tetrahedral in geometry and developed a 3D stereochemical representation system to describe how atoms were arranged in space about a tetrahedral centre.[3]

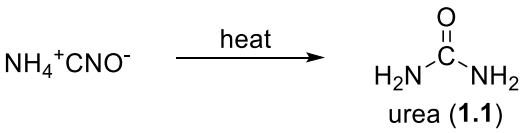

Scheme 1. *Synthesis of Urea (Wöhler, 1828),[2] considered as the starting point of modern organic chemistry.*

More dramatic developments took place in the 20th century. In 1906, Mikhail Tsvet described a chromatographic method for the separation of organic compounds in two papers in the German botanical journal *Berichte der Deutschen Botanischen Gesellschaft.*[4,5] In 1938, Isidor Rabi developed the extremely powerful technique of nuclear magnetic resonance spectroscopy,[6] and only two years later, in 1940, Carbon-14 was first discovered by Martin Kamen and Samuel Ruben at the University of California.[7] The number of discoveries continued to increase: from the 1950s countless theories and key reactions have been discovered and reported, focusing on understanding reactivity and the bond making and breaking processes involved in reaction mechanism.

Later in that century, Robert Woodward and his research group developed new synthetic methods that focused on the synthesis of natural products, with remarkable target syntheses including those of cholesterol (**1.3**),[8] cortisone (**1.4**),[9] chlorophyll (**1.5**)[10] and Vitamin B_{12} (**1.6**).[11] The synthesis of these compounds, among others, are the precursors of modern natural product synthesis, which nowadays pursues the synthesis of compounds with incredible complexity, not only for the size of the molecules, but also for their rich density of functionality and stereochemistry.[12] Notable examples include the first total synthesis of taxol (**1.7**) by R. Holton *et al.* in 1994,[13,14] the synthesis of the antibiotic (-)-madumycin II (**1.8**), reported by F. Tavares *et al.* in 1996[15] and the more recent enantioselective total synthesis of the cytotoxic natural product (+)-psiguadial B (**1.9**) achieved by Sarah Reisman's group in 2016 (**Figure 1**).[16]

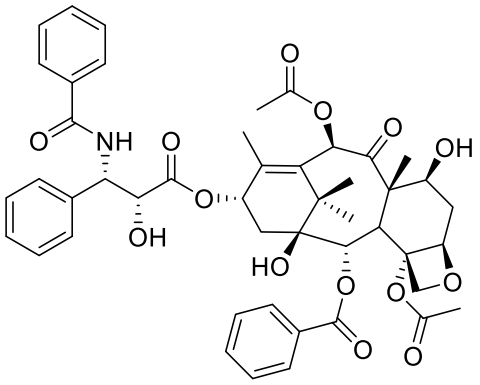

taxol (**1.7**)

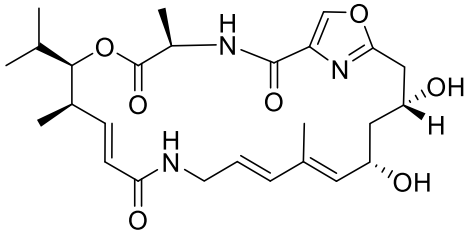

(-)-madumycin II (**1.8**)

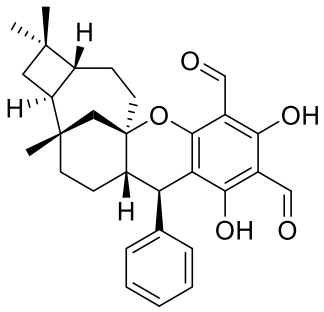

(+)-psiguadial B (**1.9**)

Figure 1. *Structures of taxol (**1.7**), (-)-madumycin II (**1.8**) and (+)-psiguadial B (**1.9**).*

Although the synthesis of these complex natural products is one of the most important fields of modern organic and medicinal chemistry, the discovery and optimization of drug synthesis has been directed to the generation of simpler compound collections for screening. The paradigm of "drug-like-ness" altered the behaviour of medicinal chemistry in terms of designing and synthesising target compounds, whose structures are currently more focused on meeting key drug-like properties.[17]

To meet that need, click chemistry appeared as a modular approach that used only practical and reliable chemical transformations for the assembly of specifically designed building blocks at the beginning of the century. The first definition of click chemistry was given by K. B. Sharpless in 2001,[18] who stated that click reactions must be of wide scope, giving consistently high yields with a variety of readily available starting materials, generate only inoffensive by products and be stereospecific. A click chemistry process should involve only simple reaction conditions, the use of no solvent or a solvent that is easily removed, and simple product isolation. Two years later, in 2003, H. C. Kolb and Sharpless himself published a review reaffirming an increasing number of applications of click chemistry in the drug discovery sector. This new approach does not substitute, but enhances, existing methods and techniques, combining with structure-based design techniques through the choice of appropriate building blocks. It enables rapid structure-activity relationships (SAR) profiling through the generation of analogue libraries.[19] The most common examples of click chemistry include cycloadditions of unsaturated species, especially 1,3-dipolar cycloaddition reactions of an azide and alkyne to form a 1,2,3-triazole,[20,21] but nucleophilic ring-opening reactions and carbonyl chemistry of the non-aldol type are also reliable.

Chemical synthesis also recognises its own limitations, especially in a drive towards more sustainable chemical practices to protect our natural resources. The needs of improved productivity and efficiency lead the modern chemist to explore alternative approaches to compound synthesis. The current cost, scale-up issues, and lack of reproducibility among others make change inevitable. Hence, synthetic chemistry is reaching an impressive level of sophistication. Nowadays, modern synthetic methods provide access to a wide range of compounds, from healing drugs to plastics and polymers, that display structural or beneficial properties and function. Newly emerging technologies include biochemical methods, parallel synthesis tools, fast serial processing using focussed microwave methods or microfluidic devices and advances in the nanoscience field.[22] Automation and computational advances also have the potential for widespread impact.

This work was funded under the LabFact programme. LabFact is a cooperation project that involves 6 institutes within the France (Channel)-England (FCE) region, (Universities of Sussex, Southampton, Rouen, Caen, ENSICAEN and CNRS) and an industrial partner (Pareon Chemicals) to bring together world experts in reagentless chemistry. Its vision is to produce scaffolds with little to no waste using flow and reagentless technologies in combination, such as heat, light, high-pressure or microwaves, under flow, microwave or mechanochemical conditions. Using reagentless techniques adds a significant competitive advantage by reducing costs, enhancing sustainability, and reducing waste streams. Thus, it is ideally placed to forge business-research partnerships and trigger investment in the region. LabFact will help small and medium-sized enterprises to innovate production, add products to their portfolio and meet sustainability needs in accord with FCE Common Challenges.

LabFact's deliverables include:

a) Promoting open innovation mechanisms.

b) Promoting smart technology innovation through research industry partnerships.

c) Promoting multidisciplinary business R&D knowledge.

d) Innovating R&D skills in SMEs through learning, teaching, and training.

e) Building new partnerships for business-research cooperation and innovation.

Figure 2. *The University of Sussex is a partner in the LabFact Project, which involves multiple academic institutes in the France (Channel)-England region, bringing together world experts in reagentless techniques.*

1.1 Emerging technologies

The International Union of Pure and Applied Chemistry (IUPAC) described an emerging technology as "one that is between a new scientific discovery and a fully commercialized technology".[23] They recently highlighted a number of emerging technologies in the chemical sciences that stand out as innovative technologies promising to make significant improvements in laboratories and industry in the future. Nanopesticides, enantioselective organocatalysis, Metal Organic Frameworks (MFOs) and flow chemistry were some of their top ranked emerging technologies in 2019, with the potential to make chemistry more sustainable in the future.[24]

As a matter of fact, one of the significant challenges for modern chemists since the beginning of the century has been the development of more sustainable methods to establish new and "greener" chemistry. In 1999, Prof. James H. Clark published the first article in a newly released journal called Green Chemistry,[25] reviewing the challenges for the chemical industry, as well as providing examples of significant advances in several synthetic methods and highlighting the importance of education and academia's role.

Green Chemistry is a concept driven by efficiency coupled to environmental responsibility. Synthetic objectives must be achieved with additional consideration given to the unnecessary

environmental burden created during manufacturing operations.[26] The twelve principles of green chemistry have played a major role in defining its aims, since they were first proposed by Paul Anastas and John Warner (**Figure 3**).[27] Thereby, when developing a new method or investigating a synthetic pathway, the aim must not be only to meet the target goal, but also to satisfy as many of these principles as possible. Indeed, application of the twelve principles could reduce environmental impact whilst providing higher efficiency in chemical synthesis. These principles are 'design rules', as design is probably the main aspect of Green Chemistry. The twelve principles guide chemists in the pursuit of experimental outcomes whilst reducing undesired environmental impact.

1. Prevention of Waste
2. Atom Economy
3. Less Hazardous Chemical Syntheses
4. Designing Safer Chemicals
5. Safer Solvents and Auxiliaries
6. Design for Energy Efficiency
7. Use of Renewable Feedstock
8. Reduce Derivatives
9. Catalysis
10. Design for Degradation
11. Real-time analysis for Pollution Prevention
12. Inherently Safer Chemistry for Accident Prevention

Figure 3. *12 Principles of Green Chemistry.*[28]

The pharmaceutical industry, and medicinal chemistry, probably represents one of the major challenges for green chemistry. The deliverables are usually well defined, and it may be of short-term interest to simply reach delivery than the potential improvement of synthetic efficiency. In fact, intellectual property concerns can frequently preclude innovation. However, the principles of Green Chemistry encourage scientists to develop their own novel processes to improve efficiency according to their need. The investigation of more efficient synthetic routes, reducing the costs of starting materials and waste treatments, or decreasing the energy demands, can also lead to higher economic benefits. In conclusion, improved economic and environmental performance, accompanied by technological development, increases scientific excellence.[26]

In any case, the whole chemical Industry has a key role to play in maintaining and improving our quality of life, the competitiveness of the chemical industry and the natural environment. The drive towards cleaner technologies with a reduction of waste requires a level of innovation that the chemical industry has not seen in many years. Some chemical processes developed in the first half of the 20th century may no longer be acceptable.[27] The challenge, therefore, is to develop new products and processes that achieve the societal, economic and environmental benefits that are now required. The development of new synthetic pathways using alternative or more selective chemistry, improvement of selectivity, energy minimisation and employing safer chemicals are good examples of "greener"

practices. To sum up, the ideal will be a balanced combination of a number of environmental, health and safety, and economic factors.[25,26]

As future challenges demand more efficient scientific technologies are adopted for chemical processes, reagentless techniques will emerge as novel processes that can reduce or even avoid the use of reagents and solvents, increasing the reaction efficiency in terms of time and yield and minimizing waste. The LabFact team at the University of Sussex is particularly focused on a selection of these techniques, using microwave, mechanochemistry and flow processes, the last one of which is the key feature of this thesis.

1.1.1 Microwave-assisted chemistry

Microwave-assisted chemistry is an "old emerging technology" that has been in laboratory use since the 1980s. In 1986, Richard Gedye and Frank Smith used a domestic microwave oven to investigate four typical organic reactions: the acid-catalysed hydrolysis of benzamide, the oxidation of toluene with $KMnO_4$, the esterification of benzoic acid with alcohols and the S_N2 reaction of sodium 4-cyanophenoxide and benzyl chloride.[29] All the reactions were carried out in sealed Teflon vessels under reflux conditions, and the authors compared the results to a classic reflux method in batch, observing significant enhancements in reaction times. In the same year, J. Giguere *et al.* published a study on the use of a microwave oven on eight more reaction examples, mainly pericyclic reactions including the Diels-Alder and Claisen processes.[30]

Microwaves are electromagnetic radiation of wavelengths between 1 nm and 0.1 m (300 to 3 GHz) and consist of an oscillating, orthogonal electric and magnetic field. For most practical purposes related to microwave synthesis, it is the electric component of the electromagnetic field that is of importance for wave–material interactions.[31] This technique provides a number of advantages in organic synthesis, as it can reduce significantly reaction times and increase yields with the direct heating of the reaction medium (**Figure 4**), but it can also reduce side reactions and increase reproducibility.

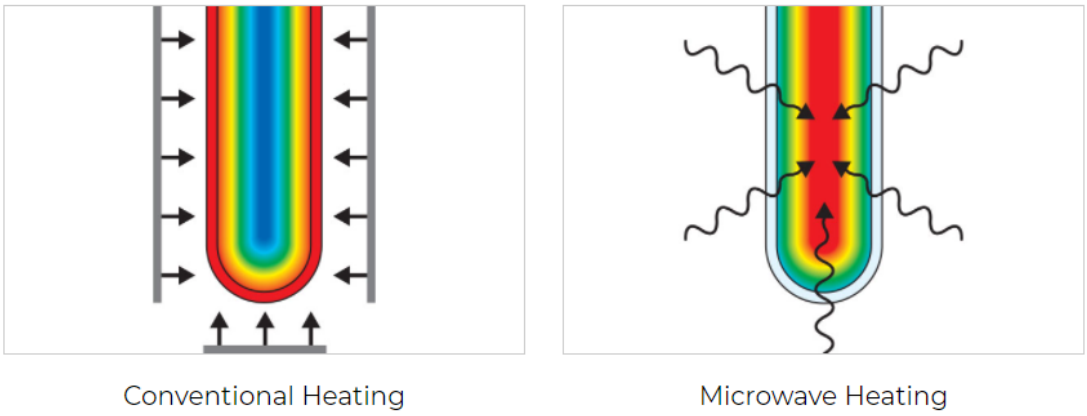

Figure 4. *The temperature profile after 60 s as affected by microwave irradiation compared to conventional heating in an oil-bath. Microwave irradiation raises the temperature of the whole reaction volume simultaneously, whereas in the oil heated tube, the reaction mixture in contact with the vessel wall is heated first.*[32]

The electric component causes heating by two mechanisms: dipolar polarization, and ionic conduction. The dipolar polarization is produced by the displacement of charges or rotation of dipoles of the matrix with an applied oscillating electric field. A substance needs to possess a dipole moment to generate heat when irradiated. The dipoles align with the applied electric field when the sample is under microwave irradiation, and when the field oscillates, they will attempt to realign themselves. During this process energy is lost in form of heat through molecular friction and dielectric loss. The ability of the matrix to reorientate in an applied electric field (known as the Maxwell displacement) is directly related to the amount of heat generated.[33,34] If the dipole does not have enough time to realign (high-frequency irradiation), or reorients too quickly (low-frequency irradiation) with the applied field, no heating occurs. Non-polar solvents, which have no permanent dipole moment, are ineffective as solvents for microwave reactions. The second heating mechanism is ionic conduction, which is observed when a matrix contains ions that can oscillate under the microwave irradiation. From this oscillation, collisions will occur between molecules generating heat. Such ionic conduction effects are particularly important for ionic liquids.[34,35]

Currently, microwave reactors with efficient temperature control systems for safe microwave synthesis at laboratory scale are available on the market. For this project, microwave-assisted reactions were carried out using a CEM Discover SP Explorer™ (**Figure 5**). The magnitude of microwave power available is up to 300 W, and heating can occur up to 300 °C with highly accurate infrared (IR) temperature control. This instrument operates with a single-mode microwave cavity, with automated samplers, and can accept 10 mL or 35 mL sealed vessels.

Figure 5. *CEM Discover SP Explorer*[32]

Medicinal chemistry has benefited from microwave technology which has had a significant impact on the development of methods and technologies to accelerate the design, synthesis, purification, and analysis of compound libraries. Its capability to dramatically reduce reaction times allows many reaction parameters to be evaluated in a few hours to optimize the desired chemistry and prepare compound libraries rapidly. Besides, microwave synthesis allows for the discovery of novel reaction pathways, often providing higher yields, with a more efficient use of expensive and limited resources. For the pharmaceutical industry and for medicinal chemistry, time equals money. Hence, microwave chemistry has emerged as extremely beneficious.[35]

1.1.2 Mechanochemistry

A mechanochemical reaction is a chemical reaction induced by the direct absorption of mechanical energy, complementing the conventional methods of activation: heat, irradiation and electrochemistry.[36] Evidence on the use of mechanical activation has been dated to the Holocene and Pleistocene Epochs some 1.6 million years ago as a means of grinding husks off grain by our ancestors.[37] With further refinement, the technology took the form of what we recognise today as a pestle and mortar, the use of which is thought to have been confined to mixing, grinding and mincing. More recently, the first documented chemical transformation utilising mechanical activation is considered to be the extraction of mercury from its ore, cinnabar (mercury sulphide).[38]

In addition to the usual variables for conventional reactions, such as stoichiometry, reaction time and temperature, in mechanochemical reactions three new variables appear. The first one is the kinetic energy of the ball(s) before collision, which will be the maximum amount of energy transferred during the collision. The second one is how that energy is transferred in a collision. Different types of energy absorption can lead to different outcomes.[39] The last one is how frequently collisions happens.

Nonetheless, these three variables are directly related to conventional parameters, as the energy produced by collisions will increase the vessel temperature.

In comparison to conventional methods, mechanochemistry offers a number of important advantages. The most obvious one, especially regarding green chemistry, is that reactions can be performed under solvent-free conditions. Mechanochemistry can promote reactions between solids quickly and quantitatively.[40] Reducing solvent usage during a reaction, and also during any purification, is a significant safety and environmental improvement.

Figure 6. *Retsch Mixer mill MM 400 (left) and set of jars and balls (right).*[41]

There are different types of ball-mill reactors: oscillating (shaker/mixer), planetary, magnetic, gravity, and roller mills. Among the designs, oscillating and planetary mills are the ones currently commercially available for small scale batch chemical transformations. For this project, a Retsch mixer mill MM 400 (**Figure 6**) was used. The mixer mill MM 400 is a compact versatile bench-top unit, with a powerful grinding action by impact and friction, that can oscillate up to 30 Hz for reaction times between 1 and 90 min and can accept grinding jar volumes from 1.5 mL to 50 mL.

1.1.3 Ultrasound

The first mathematical model describing the processes involved in sonochemistry was published by Lord Rayleigh in 1917.[42] However, it was not used in chemical reactions until 1927, when Loomis first reported the chemical and biological effects of ultrasound.[43,44] Sonochemistry is the use of ultrasound to promote chemical reactions. Ultrasound has been widely used as a method of chemical activation for the synthesis of *N*-heterocycles during the last few decades. The first example of this method was reported by Ando *et al.* in 1984,[45] when he irradiated of a mixture of benzyl bromide, potassium cyanide, and alumina in an aromatic solvent and obtained benzyl cyanide, whereas mechanical agitation gave the Friedel-Crafts type product. They realized sonication could change the main reaction pathway from electrophilic aromatic substitution to aliphatic nucleophilic substitution.

Sonochemistry is considered as a green chemistry method, as it can use smaller quantities of chemicals, reduce energy consumption, and increase product selectivity. The chemical effects of ultrasound do not come from a direct interaction with molecular species. The produced effect, known as cavitation, consists in the formation, growth, and implosive collapse of stable and transient microbubbles in a liquid.[46] These microbubbles absorb energy from the ultrasound waves and reach an energy saturation stage. Then, the cavity can no longer sustain itself and implodes. The collapse of the cavity produces intense local heating, high pressures, and very short lifetimes, an unusual environment for chemical reactions.[47] A more detailed explanation about the theory and the kinetic analysis of sonochemistry, including bubble dynamics and factors affecting cavitation, was published in a review by L. H. Thompson and L. K. Doraiswamy in 1999.[48]

The simple ultrasonic cleaning bath is the most available and cheapest source of ultrasonic irradiation for the chemical laboratory. The normal usage therefore involves the immersion of standard glass reaction vessels into the bath which enables the distribution of energy into the reaction medium. The ultrasonic bath used for this project was a Fisherbrand FB150051 model (**Figure 7**).[49]

Figure 7. *Ultrasonic bath Fisherbrand FB150051.*[49]

An ultrasonic bath system uses indirect sonication, and the ultrasonic power which reaches the reaction vessel is relatively low as compared to other ultrasonic systems. Nowadays other types of systems are available, such as probes that are capable of delivering large amounts of power directly to the reaction mixture or planar transducers, which can be connected to a vessel which contains either the reaction mixture (direct sonication) or a coupling fluid into which the reaction vessel is immersed (indirect sonication).[50]

1.2 Flow chemistry

A flow reaction is a chemical reaction in which the reactants and solvents are pumped through a tubular coil, that can be placed in a heated reactor, or through prepacked supported reagent columns (**Scheme 2** shows a general scheme). The solutions can be pumped from a bottle or injected through an injecting loop placed after the pumps. The output can be directly analysed, collected and/or recycled if necessary.[22] One of the first continuous flow purification operations was Simulated Moving Bed Chromatography (SMB), an automated continuous liquid chromatography system, which has been used to produce a wide range of pharmaceutical intermediates and, eventually, Active Pharmaceutical Ingredients (APIs). As with many emerging technologies, it was originally considered to be too expensive for practical use, but continuous processing continued and continues to evolve and find increased acceptance and applications in the manufacture of molecules.

Flow reactors offer advantages to the synthetic chemists including controlled heat transfer, increased photon-flux in photochemical reactions, increased solution-solid and solution-gas phase interactions, controlled use of highly reactive and/or toxic materials, and increased capacity to run reactions in series. Furthermore, flow chemistry offers new capabilities such as the integration of reactor components, and on-line monitoring and purification.[51] Currently, a worthwhile goal is the design of flow processes that permit efficient assembly of small molecules in useful quantities for biological evaluation, allowing the facile scale-up of resulting hit compounds to significant quantities for full biological or other functional evaluation.

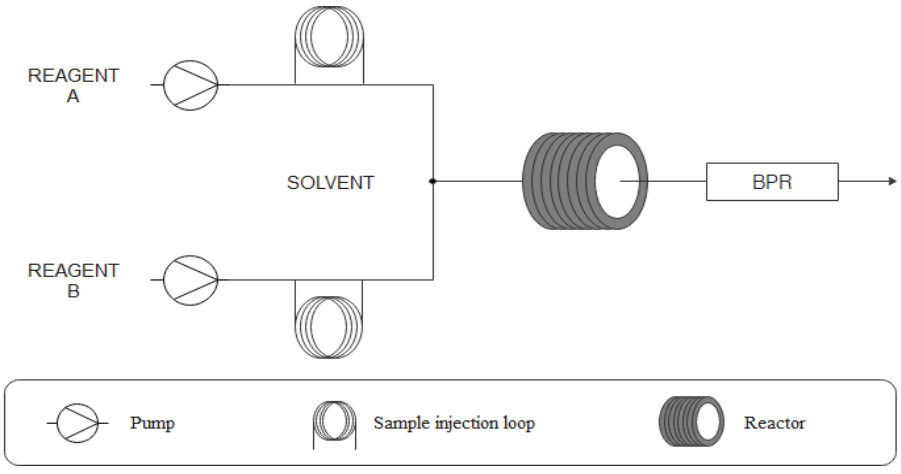

Scheme 2. *General scheme for a flow reaction.*

Flow procedures are defined by high standards of safety, efficiency and reproducibility. The higher control of variables, efficient mixing and superior heat exchange can lead to shorter and well-defined reaction times. However, the major advantage of flow chemistry is the small reaction volume, enabling the optimization of the reaction conditions for a reaction on trial scale. Hence, these optimized

conditions can be directly translated to the production of larger quantities, simply by increasing the quantities of reagent, running the process for longer and/or changing the reactor volume. Safety is also an important improvement when scaling up exothermic or hazardous reactions, or the in-situ generation of highly reactive species. Hazardous chemistry requires extensive safety assessments in order to scale up batch reactions, especially when the reaction is performed on large scale.[52] Examples include, but are not limited to, the generation and use of ozone, azides, diazonium species as well as cryogenic or high temperature reactions.[53] To understand the advantages of performing such reactions in a flow reactor the kinetics of the reaction and the potential energy released are key considerations. As the reaction takes place in a tube, the reaction volume at each point of the tube is small, and the heat produced is therefore less significant and easily dissipated.[54]

Reactions under flow conditions are carried out under a controlled backpressure. A backpressure regulator allows solvents to be used in the process at higher temperatures than their boiling points, enabling reactions to be conducted at high temperature whilst maintaining the homogeneity of the solution.[55] On the other hand, it also offers advantages when using reactive gases. Under high pressure conditions, there is a better dilution of the gas into the solvent, providing a homogeneous solution of the solvent and the gas. The solution can be saturated with the gas before the reaction or during the process, by feeding the gas into the reactor under a controlled temperature. Thus, not only is the solubility of the gas no longer a problem, but also the gas can be fed into the reaction as it is consumed. These gases are easily removed from the reaction mixture as they evaporate when the solution is returned to atmospheric pressure. There are also safety factors involved when using pressured gas bottles in the laboratory, and especially in large scale industrial gas-liquid reactors. These safety issues are significantly improved when using gas-liquid flow reactors.[56]

Mediating transformations in continuous flow systems offers another advantage compared to reactions in a round bottom flask, with the possibility of running multistep synthesis. Usually, useful organic compounds require several steps, involving different reactions or methods. In multistep flow synthesis, the general approach starts as a single step reaction, mixing the components in a suitable flow reactor. The outcome of the first reaction is then either mixed with a new reagent or directly flushed to a new reactor with different applications (UV reactor, copper reactor, gas-liquid reactor, etc.), or both.[57]

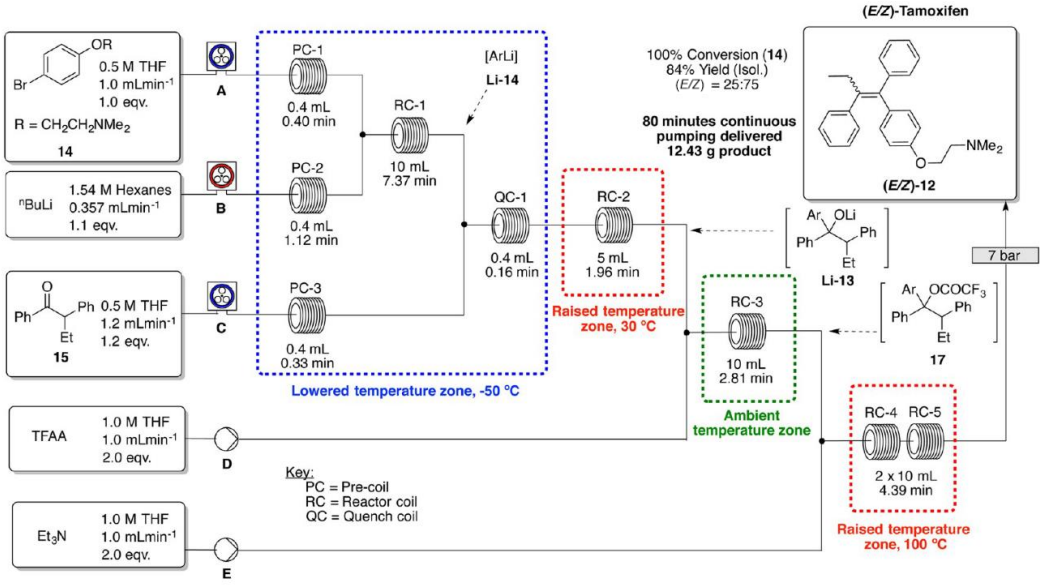

Scheme 3. *Continuous-flow telescoped synthesis of (E/Z)-tamoxifen.*[58]

A multistep synthesis may require inline separation of the components of the reaction. This can be achieved by connecting columns loaded with resins which are able to trap the non-desired product. These columns can also be connected at the end of the synthesis to purify the final compound online. Those multistep syntheses where the intermediate separation is not required are termed as 'one pot' synthesis, or 'telescopic' synthesis when carried out in a continuous mode.[57] Several examples of the multistep synthesis of active pharmaceutical ingredients in flow have been recently published, like the continuous flow synthesis of olanzapine,[59] amitriptyline[60] or tamoxifen, showed in **Scheme 3**.[58] This last example shows a peristaltic pump capable of pumping at smooth flow rates and elevated pressure, equipped with fluoropolymer flow tubing compatible with organometallic air-sensitive reagents such as *n*-butyllithium, Grignard reagents, and DIBAL-H on multigram scale which allowed the optimisation for a 80 min of continuous collection of the breast cancer drug tamoxifen with an 84% yield (*E*/*Z* =25:75).

Some laboratories construct their own equipment from readily available parts; however, most organic solvents are not compatible or recommended to be used with certain tubing materials. Perfluoroalkoxy (PFA) tubing is a suitable starting point when considering the material of choice for flow reaction chemistries.[55] Commercially available benchtop flow chemistry platforms, though, have made flow chemistry widely accessible, not only for industrial processes but also for research laboratories.

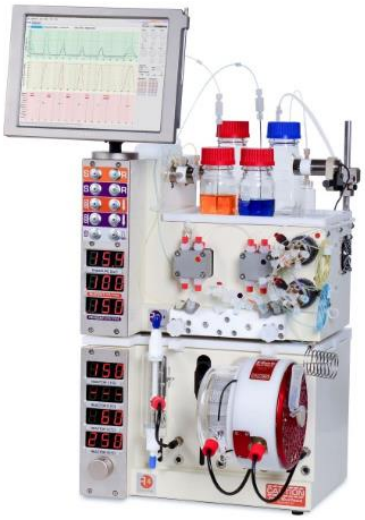

Figure 8. *Vapourtec R2C+/R4 system. Displayed with permission from Vapourtec Ltd.*[61]

A Vapourtec R2C+/R4 flow reactor was used for this project (**Figure 8**). The R2C+ is the pumping unit containing two adapted acid resistant pumps. The tubing is made from PFA or polytetrafluoroethylene (PTFE or Teflon) plastics, and the pump heads are ceramic. The R4 is the heater unit with four heating positions and two cooling positions. Each 10 mL reactor unit contains tubing wrapped into a coil (13 m of tubing), with temperature sensor located on the wall of the tubing. The reactor tubing can be made of PFA (standard heated reactor), stainless-steel (high temperature reactor) or a fluoropolymer (photochemical reactor).

Flow chemistry started to be introduced into the core business of the pharmaceutical industry at the beginning of the century, in different stages of the discovery and development process. Nowadays, this technology is used in many different aspects, and even has been integrated into standard drug discovery and development activities.[62] Benefits and opportunities have already been recognised in natural product synthesis.

Flow chemistry is a disruptive technology in the research environment that constitutes a large change in the philosophy of synthesis. If one reflects on how the laboratory of the future might be, flow chemistry techniques have real potential in extending current capabilities. Moreover, the tools of molecular engineering will change to reflect the demand of a more environmentally conscious society, and the continuous implementation of modern tools such as computer software and remote monitoring.[63]

1.2.1 Photochemistry and the photochemical flow reactor

Organic photochemistry is a re-emerging feature in sustainable chemistry. Photochemical reactions are induced via an electronically excited state possessing a different electronic configuration than the corresponding ground states, altering the reactivity of the species involved. It offers numerous advantages such as simplified multi-step synthesis and, often, the absence of chemical catalysts.[64]

A general representation of a photochemical reaction mechanism divided into 3 stages is shown in **Figure 12**. The first step is always the absorption of a photon (***hν***) by a molecule (**R**) in its ground state. This generates the excited state of the molecule (**R***). The second stage is called the primary photochemical process and it is a step or series of steps that occur from the excited state of the molecule. This process can lead to 3 different species: a ground state intermediate (**I**), an excited intermediate (**I***) or product (**P***) or a species called a funnel (**F**) which is a structure that it is neither a stable intermediate nor a product but involves crossing from the excited state to the ground state.[65]

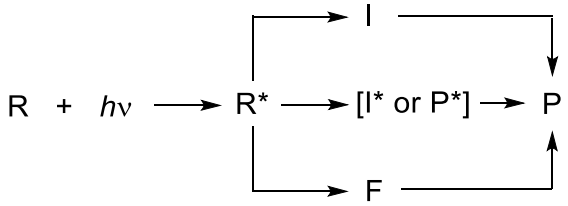

Scheme 4. *General representation for photochemical reaction mechanisms.*

To explain the absorption and emission of energy during a photochemical process it is common to employ a Jablonski diagram (**Figure 9**). Firstly, there are pathways by which an electron can access different excited state. Starting from the antiparallel spin of the electrons in the ground state, the electron can be promoted to the higher energy level without changing its spin, which results in maintaining a spin multiplicity of 1; or it can change its spin, which results in a spin multiplicity of 3. In either case, the electron can occupy different excited states. If the electron retains its spin and multiplicity of 1, the energy levels are known as singlets and are represented as S_n, and if the electron changes its spin and multiplicity to 3 those levels are known as triplets, represented as T_n. Within each energy level, there are different vibrational states (v_n).[65,66]

The first step is the absorption of a photon, which will promote an electron from the ground state to an excited electronic state and excited vibrational state, so the electron is excited vibrationally and electronically. In **Figure 9** example the electron has been promoted to the first excited singlet state, but it can go to other excited states. Once the molecule is in the excited state, in the second step there is a vibrational relaxation, where the molecule gives up vibrational energy as heat and the electron relaxes to the lowest vibrational level of the excited state. In the third step, different processes can happen. One

such process is fluorescence, and this phenomenon consists of the electron relaxing and returning to the singlet ground state releasing a photon. Another process that can happen is vibrational relaxation and internal conversion, where the electron goes back to the singlet ground state by giving up its energy as heat. It is called vibrational relaxation because it is releasing energy as heat, and it is called internal conversion because it is changing electronic states. The last process than can happen is intersystem crossing, a transition from a singlet state to a triplet state. In this case, after the vibrational relaxation, the spin of the electron changes and goes to the triplet state without changing energy. Once in the triplet state, the electron is again in an excited vibrational state, so it undergoes vibrational relaxation again to the ground state of the triplet and finally phosphorescence takes place when the electron goes back down to the original ground state, emitting a photon.[67]

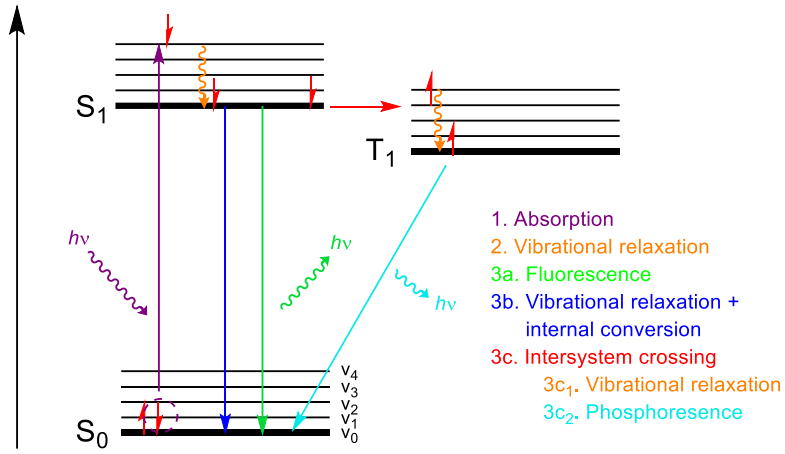

Figure 9. *Jablonski diagram.*

Some important things to keep in mind are that the emitted light is lower energy than the absorbed light because of the loss of energy in the vibrational relaxation, and for this reason phosphorescence is lower energy than fluorescence. Also, phosphorescence is slower than fluorescence as the electron has to change its spin before relaxing.[65]

Photochemical transformations have been performed on laboratory and industrial scales within the commodity chemical industry for decades. [68] Photopolymerizations and radical chain synthesis have been conducted under milder conditions with greater functional-group compatibility due to the high selectivity of individual light reactions, independent of temperature. However, over the past decades the field of synthetic photochemistry has experienced a significant resurgence.

The optimal conditions for a photochemical reaction are given by a high photon-flux. The photon penetration depth into the reaction mixture is dependent on its optical properties, as described by the Beer–Lambert–Bouguer law. Thus, without a sufficiently large surface area, the photon penetration depth can be insufficient, and part of the solution may remain unirradiated. The last decade has

witnessed a remarkable development towards improved and new photochemical transformations in response to greener and more sustainable chemical synthesis needs. The introduction of modern continuous flow reactors has enabled a remarkable improvement, as they help to overcome limitations inherent to photochemistry. Light-permeable tubing placed inside the reactor coil (**Figure 10**), ensures that light can easily penetrate a solution of substrate with very efficient and uniform irradiation of the reaction mixture, minimizing the limitations arising from the Beer–Lambert law. The availability of suitable light sources, ranging from light-emitting diodes (LED) to continuous fluorescent lamps and powerful UV lamps, have also contributed significantly to recent developments.[69]

Moreover, continuous flow processing provides a simple scale-up of a photochemical reaction without any alteration of the reaction conditions, and over-irradiation and consequent decomposition is avoided as the solution will remain in the reactor only for the specified reaction time.

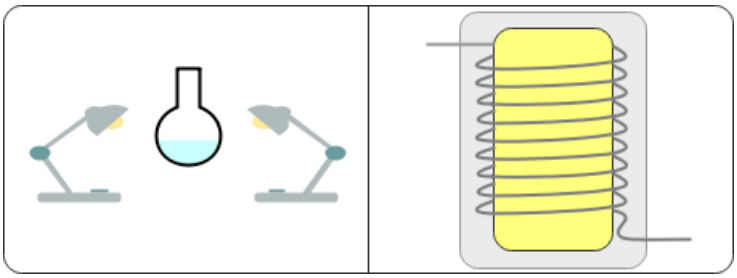

Figure 10. *Schematic comparison between a) batch and b) flow set up.*

Vapourtec has developed the UV-150, a pioneering photochemical reactor that provides more efficient, precise, consistent, safe and scalable photochemical synthesis (**Figure 11**). The “plug and play” reactor is designed to complement Vapourtec’s existing systems with an easy and quick set up. Tubing is assembled into cartridges which can be easily removed and replaced within seconds and standard reactor cartridges are available in 2, 5 or 10 mL volumes. The UV-150 allows for safe access to photochemical processes with the design of a compact, high intensity 150 Watt medium pressure mercury lamp and wavelength filters which allow the selection of desired wavelengths, whilst eliminating unwanted wavelengths that might cause side reactions or the decomposition of products. Filters also have a key role in reducing the heating effect of the lamp. Wavelength filters are positioned between the lamp and the reactor and can be quickly and easily changed by hand. The reactor operates between -5 and 80 °C.[70]

Figure 11. *Vapourtec UV-150 photochemical reactor (left). 10 mL tubing cartridge (top right). Wavelength filters (bottom right).*[297]

Despite most applications of photochemical reactions currently being based on photo-cycloadditions and photo-rearrangement reactions,[71] photochemistry is also starting to find application in the synthesis of natural products, to afford more sustainable and easily scalable processes. Furthermore, the fine chemical industries are becoming interested in synthetic photoredox chemistries for its potential to offer new bond disconnection options.[72]

New reactor designs are constantly being investigated and developed to offer better alternatives for photochemical reactions. Likewise, more energy-efficient LEDs, and even solar light are being studied to achieve greener chemical synthesis.[73]

1.3 Medicinal chemistry

From the oldest records on the use of therapeutic plants and minerals utilized by ancient civilizations to the basic studies of chemistry and physics from the Greco-Roman and Arabian alchemists between the thirteenth and sixteenth centuries, chemical compounds derived from plants and other natural sources have been used by humans to alleviate pain and other maladies. Until the nineteenth century, these “remedies” were primarily crude preparations of plant material of unknown constitution. The revolution in synthetic organic chemistry during the nineteenth century produced a concerted effort towards the identification of the structures of active constituents of these naturally derived medicinal, and the synthesis of what could be anticipated to be more efficacious, agents. By determining the molecular structures of the active components of these complex mixtures through refined and extended techniques of chemical analysis, it was thought that a better understanding of how these components worked could be elucidated.[74] The first effective synthetic drug against bacterial infections was reported

by Domagk in 1932 when he discovered Prontosil, a sulfonamide that cured gram-positive bacterial infections in man and animals. Together with the discovery of penicillin by Fleming in 1929, a significant change was introduced into medical practice which set the stage for organic chemistry and pharmacognosy, the science that deals with medicinal products of plant, animal, or mineral origin in their crude state, and its refinement to physiological chemistry.[75] The emergence of the pharmaceutical industry took place in conjunction with advances in organic/medicinal/pharmaceutical chemistry, pharmacology, bacteriology, biochemistry, and medicine as distinct fields of science. Current research efforts are now focused not only on discovering new, biologically active compounds using ever increasingly sophisticated technology but also on gaining a better understanding of how and where drugs exert their effects at the molecular level.[76]

The medicinal chemist attempts to design and synthesise a pharmaceutical agent that has a desired biological effect on the human body or some other living system, a compound called a 'drug'. Thus, medicinal chemistry is the discipline concerned with determining the influence of chemical structure on biological activity. As such, it is necessary to understand not only the mechanism by which a drug exerts its effect but also the physicochemical properties of the molecule, and the relative contribution that each functional group makes to these properties. All these properties influence the absorption, distribution, metabolism, excretion, and toxicity of the molecule. Structure–activity relationships (SARs) studies define what structural features of the molecule contributes to, or takes away from, the desired biological activity of the molecule of interest.[67,76]

1.3.1 Drug design

As stated before, the efforts to isolate and purify the active principles of natural medicines to identify their structures and how they worked were not made until the mid-nineteenth century. Ever since, many naturally-occurring drugs have been identified, synthesised and their structures determined, and these natural products have initiated efforts to synthesise analogues attempting to improve on what nature provides. This work started on a trial-and-error basis, but the results obtained over the years have disclosed general principles and relationships between molecular structure and biological activity for use in drug design. Subsequently, drug research has focused on a lead compound – an active principle isolated from a natural source or synthesised in a laboratory. Nonetheless, in recent years medicinal chemistry has changed, and drug design has become a multi-step, multidisciplinary and multi-year process which is a science unto itself. A better understanding of how the human body functions on a cellular and molecular level leads to the capability to identify a target in the body (drug receptors) and its properties, and consequently the design of a drug that can interact with that target. Therefore, drug design is divided in two parts: identifying the biomacromolecules that are involved in a disease (targets

or receptors) to understand its properties and knowing what properties turn a molecule into a drug, identifying the sub-unit parts that enable the drug to interact with the receptor and to be absorbed, distributed, metabolized and excreted by the body.[74]

The first part of the process of drug design is, as mentioned, the identification of the biomacromolecules that are involved in a disease and knowing the structures, properties, and functions of those macromolecules. Receptor macromolecules are frequently proteins or glycoproteins (enzymes and receptors) and DNA or RNA. These are macromolecules that have molecular weights of thousands of atomic mass units. Ideally, the receptor must be directly connected with the disease but not too many other processes. The interaction of the receptor with the designed drug is called binding, and it usually happens in a specific area of the macromolecule called the binding side (**Figure 12**).[75] The bond strength between the receptor and the drug must be enough to allow the drug to cause the desired pharmacological effect but also weak enough to release it when the job is done. The study of how drugs interact with their targets through binding interactions and produce a pharmacological effect is known as pharmacodynamics.

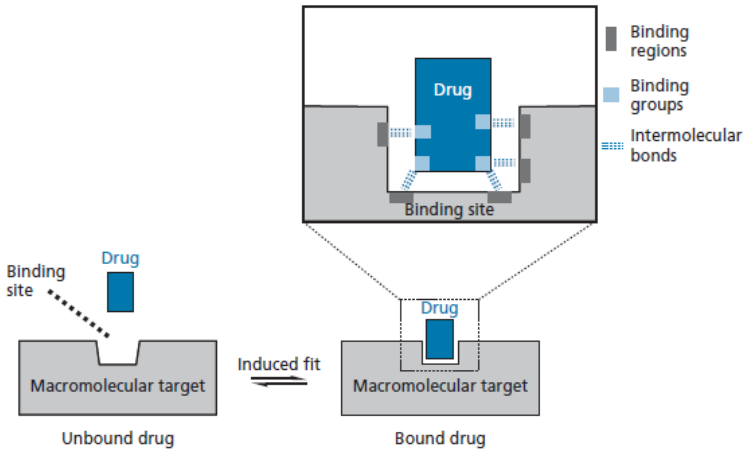

Figure 12. *Schematic representation of a drug binding to a target.*[74]

Once the target is recognized and studied, the second part of the process is the design of a molecule that will act as a drug to bind with the target and produce the biological effect. The first step is to find a lead compound which shows the desired pharmacological activity and that provides a start for the optimization process. This lead compound might be obtained from a natural source or from a library of synthesised compounds by pharmaceutical companies and they are usually small organic molecules (molecular weight below 800 g/mol, often below 500).[76] Molecules with similar structures have similar properties and interact similarly with the target. Subsequently, the drug must be optimized in terms of selectivity and activity while reducing the side effect or the toxicity. To achieve this purpose, some fragments or functional groups of the molecule may be replaced or interchanged, modifying the drug structure and therefore its properties. The number of interactions as well as the strength of these bindings

is a critical factor. The fragments or functional groups that bind with the target binding site are called binding groups, and they are one of the key factors of the activity of the molecule, although the carbon skeleton will also be important to interact with the target through Van der Waals interactions. The study of all of these factors and the impact on the pharmacological effects are called structure–activity relationships (SARs).[75] The goal of these studies is to discover what functional groups within a specific structure are important for its pharmacologic activity and how can these groups be modified to produce more potent, selective, and safer compounds that are easy to synthesise and chemically stable.

1.3.2 Flow chemistry in medicinal chemistry

Flow chemistry has become widespread in medicinal chemistry, especially in the pharmaceutical industry. Major pharmaceutical companies and organizations alike have made an unremitting investment in flow chemistry for the last few years, in many cases having entire manufacturing plants dedicated to this technology. This technology offers valuable advantages such as the capability of continous processing, process intensification, improved safety of hazardous reactions and ease of scale up opportunities.[22]

The implementation of flow chemistry in the drug discovery process is increasing. The benefits of using flow chemistry can be found at high temperatures (being able to attenuate the pressure of a flow reactor using a back-pressure regulator) or cryogenic temperatures; reaction exotherms, which can be problematic in batch reactors, can be easily handled in flow because of the high surface area to volume ratios providing excellent heat transfer and greater temperature control. Also, nonstandard reaction conditions, such as electrochemistry or photochemistry, have advantages in flow (see **section 1.2.1**) and can lead to more economic and safer synthetic routes. Consequently, flow chemistry facilities may enable the synthesis of libraries of new compounds, high-throughput reaction screening, building block scale-up and, in some cases, integrated analysis or bioassay.

As stated previously, several examples of multistep synthesis of API in flow have been recently published, like the continuous flow synthesis of olanzapine (**1.10**),[59] amitriptyline (**1.11**)[60] or tamoxifen (**1.12**),[58] shown in **Figure 13**. The implementation of these methods in the pharmaceutical industry could mean a turning point in terms of production costs and time.

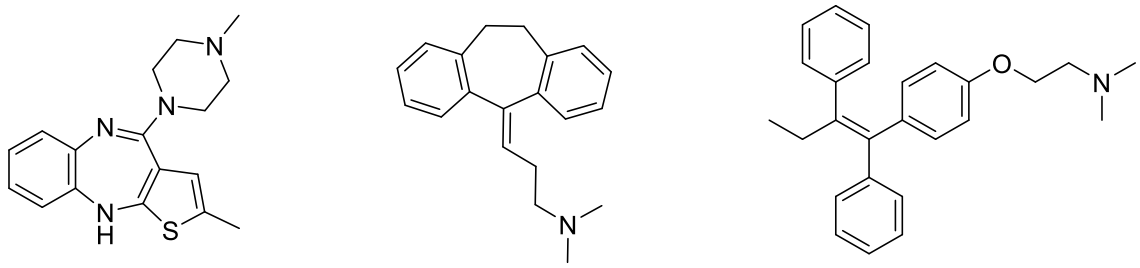

olanzapine (**1.10**) amitriptyline (**1.11**) tamoxifen (**1.12**)

Figure 13. *Structures of olanzapine (**1.10**), amitriptyline (**1.11**) and tamoxifen (**1.12**).*

1.3.3. Fluorine in medicinal chemistry

The use of organofluorine molecules in medicinal chemistry is relatively recent. This class of compounds are almost absent in natural products, and it was not until the 1970s that fluorinated compounds were regularly used in medicines. The main characteristics of fluorine are its very small size (1.47 Å diameter) and its highly electron withdrawing property, being the most electronegative element. This makes fluorine an exceptional atom that, with the substitution of an organic compound with a single fluorine atom or trifluoromethyl group located in a key position of a biologically active molecule, can result in a profound pharmacological change.[77]

Since the synthesis and evaluation of the antimetabolite drug, 5-fluorouracil (**1.13**) in 1957 (**Figure 14**),[78] drug candidates with one or more fluorines have become commonplace. Fluorine changes both the pharmacodynamics and pharmacokinetics of the molecule, providing a variety of properties to medicines such as intrinsic potency by enhancing binding interactions, metabolic stability and membrane permeability, bioavailability, influence on conformation and selective reactivities.[79] The trifluoromethyl group (-CF_3) has an intermediate electronegativity between the electronegativities of fluorine and chlorine.[80] Therefore, trifluoromethyl-substituted compounds are often strong acids, such as trifluoroacetic acid. The introduction of the difluoromethyl and trifluoromethyl groups into ligands has become increasingly popular and serves as a promising strategy in lead optimization to enhance protein-ligand interactions for biological applications, resulting in the development of new inhibitors in drug discovery projects.[81]

The fluorination of compounds is commonly done by direct reaction with fluorinating reagents or by adding fluorinated functional groups on aromatic rings or in aliphatic chains.[82] These fluorination processes provide a range of synthetic fluorinated building blocks amenable to functional group manipulation.

There are numerous examples of drugs containing fluorine. Many of the drugs that act by blocking dopamine receptors in the central nervous system (CNS) contain either a CF_3 group or a fluorophenyl group, which contribute to the overall pharmacological activity of the compounds by enhancing CNS penetration and retarding metabolic degradation. Several clinically useful agents contain fluorine, such as fluorouracil (**1.13**) or the phenothiazine trifluoropromazine (**1.14**) (**Figure 17**).[83]

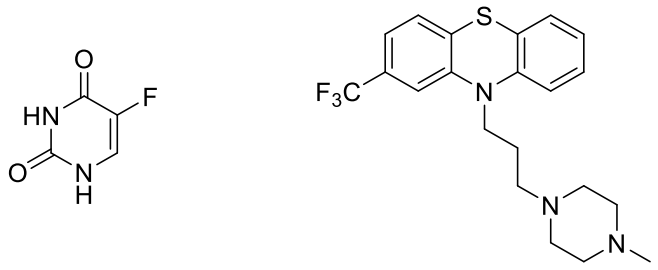

5-fluorouracil (**1.13**) trifluoropromazine (**1.14**)

Figure 14. *Structures of fluorinated drugs.*

1.4 Carbazoles

Carbazoles are aromatic heterocyclic compounds that belong to the alkaloid family and are defined as a cyclic organic compound containing nitrogen.[84] The structure is an aromatic system that is related to indole (**1.15**), but with a second benzene ring fused at the 2,3-positions (**Figure 15**).

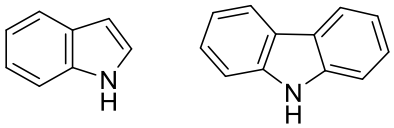

indole (**1.15**) carbazole (**1.16**)

Figure 15. *Carbazole and indole structures.*

The first compound of this class (**1.16**), whose structure is shown in **Figure 15**, was discovered in coal tar by Graebe and Glazer in 1872,[85] isolated for the first time in 1924 by Clemo and Perkin from the degradation of strychnine (**1.17**) (**Figure 16**).[86] Subsequently, *N*-vinyl carbazole (**1.18**) was synthesised and the chemistry of carbazoles emerged because of their use in the dye stuff and polymer industries up until the 1960s. In 1965, the discovery of the first carbazole alkaloid isolated from nature, murrayanine (**1.19**), by D. P. Chakraborty, B. K. Barman and P. K. Bose,[87] and the publication of their antibiotic properties,[88] reawakened the interest in and investigation of the biological and medicinal applications of carbazoles.

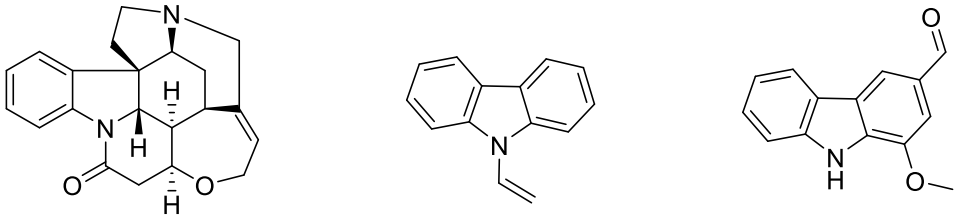

strychnine (**1.17**) *N*-vinylcarbazole (**1.18**) murrayanine (**1.19**)

Figure 16. *First discovered carbazoles structures.*

During the last few decades, several carbazole scaffolds have been reported to have prominent biological and physical properties that has made these compounds a distinguished target for synthetic chemists. Among their application in photophysical materials, carbazole-based polymers are widely used in the synthesis of highly efficient blue light-emitting materials, charge-transporting materials and host materials.[89] Their planar biphenyl structure with wide band gap, high luminescent efficiency and flexibility for skeletal modification highlights carbazoles as outstanding chromophores in organic electroluminescent (or organic light-emitting) materials.[90] Moreover, photorefractive properties of carbazole-based materials enable the creation of a new class of discotic, banana-shaped liquid crystalline materials;[91] carbazole-based polymers provide higher energy conversion efficiency and are being investigated as high efficiency organic solar cells.[92] Despite their commencement and the recent re-emergence of interest in the materials and polymer industries and associated chemistry, carbazoles have always been of topical interest due to their presence in natural products and numerous drugs. The biological and therapeutical properties of these compounds and their derivatives have been intensively studied making them play an important role in medicinal chemistry.

1.4.1. Biological and therapeutic properties of carbazoles

Carbazoles are privileged nitrogen heterocycles that are present in a wide range of natural products and pharmaceuticals. There are numerous natural or synthetic drugs containing this structure or a derivative thereof. These drugs possess anti-cancer, antibacterial, antifungal, anti-inflammatory, hepatoprotective, anti-HIV, anti-protozoan and sedative properties, or topoisomerase II inhibitory activity.[93] As an example, caprofen (**1.20**) (**Figure 17**) is probably the best-known carbazole derivative commercial drug, as a nonsteroidal anti-inflammatory agent that reduces inflammatory processes involving cyclooxygenase-2 (COX-2), which may have detrimental effects especially on brain regeneration.[94,95] More recently, in 2012, a novel series of 3-(substituted)-aryl-5-(9-methyl-3-carbazole)-1*H*-2-pyrazolines were synthesised and found to be anti-inflammatory and antioxidant agents.[96] Although caprofen was used in humans between 1988 and 1998, nowadays it is only used as a treatment for post-operative pain and inflammation in animals.

Clausenine (**1.21**) and clausenol (**1.22**)(**Figure 17**), plus other derivatives extracted from *Clausena anisata*, were found to be active against gram-positive and gram-negative bacteria and fungi,[97] and, as well as some new examples of *N*-substituted derivatives studied more recently (2010), showed promising antibacterial and antifungal activities.[98]

Some analogues of murrayanine (**1.19**), from the *Murraya koenigii* family (previously mentioned), such as koenidine (**1.23**) have been identified as a metabolically stable antidiabetic compounds.[99]

P7C3 (**1.24**) and related analogues have been reported to have neuroprotective properties with potent anti-oxidative activity, appearing as an alternative approach for treating Alzheimer's disease.[100–102] Carvedilol (**1.25**) is another important potential novel agent for the treatment of Alzheimer's disease as it also has a neuroprotective effect, in addition to therapeutic efficacy for treating cardiovascular diseases.[103–105]

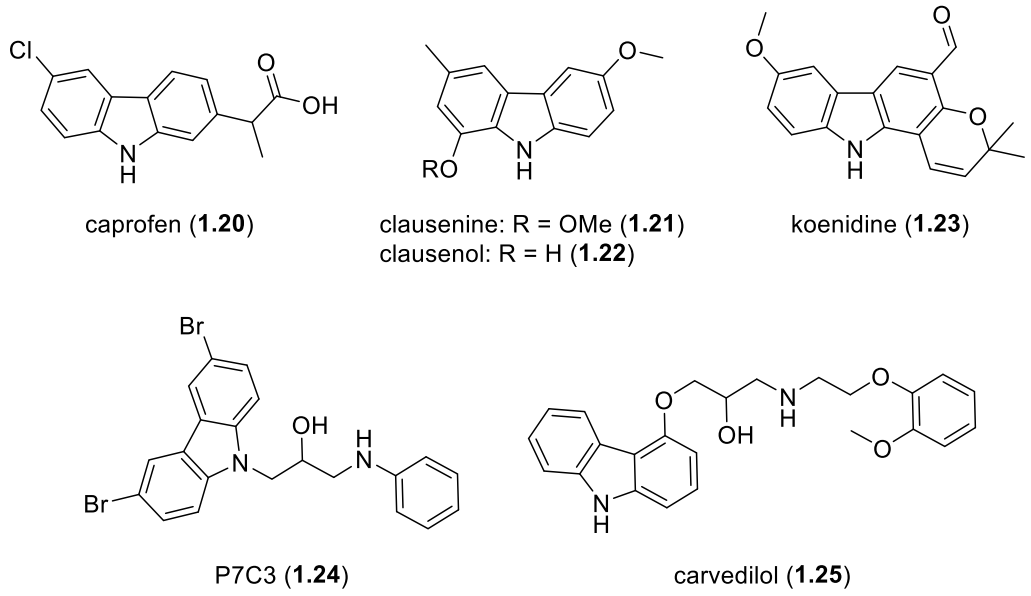

Figure 17. *Biologically active carbazole derived structures.*

1.4.1. Antitumour and tumour-promoting activities

Cancer is characterized by an uncontrolled growth of cells, which can spread throughout the body with severe health consequences. It is a major public health problem and is the second leading cause of death worldwide.[106] Among the existing anti-cancer drugs, carbazole scaffolds have been investigated for more than 50 years, being a key structural motif of many biologically active compounds, including natural and synthetic agents. Ellipticine (**1.26**) (**Figure 18**), discovered in 1959, is a natural

occurring carbazole derivative extracted from *Ochrosia elliptica* (Apocynacae) and considered the first lead compound in this carbazole analogue family.[107]

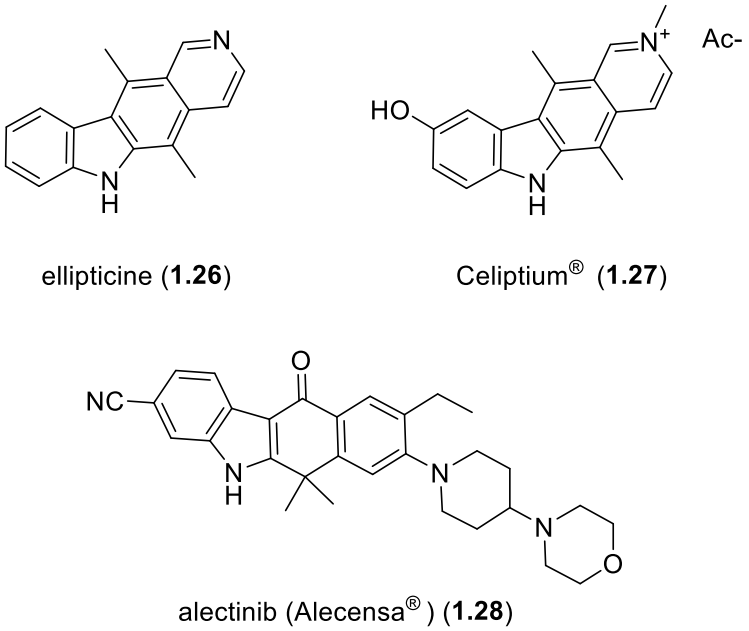

ellipticine (**1.26**) Celiptium® (**1.27**)

alectinib (Alecensa®) (**1.28**)

Figure 18. *Structures of carbazole-based commercial anticancer drugs.*

This compound led to the synthesis of new analogues, with Celiptium® (**1.27**) standing out as an anticancer agent used in the treatment of breast cancer since 1982 (**Figure 18**). Almost 30 years later, in 2015, alectinib (**1.28**) was the second analogue to be approved, as an orally available drug for the treatment of lung cancer.[108]

Over the years, medicinal chemists have investigated the biological activities of numerous carbazoles, including tricyclic, tetracyclic (with 5-, 6- and 7-membered rings), pentacyclic, hexacyclic and heptacyclic fused carbazoles. This interest is reflected in the large number of carbazole compounds in databases and publications, as well as the number of patents in the area. A large majority of carbazoles, including the lead compound ellipticine, exert their activity via an interaction with DNA because their structure features a flat polycyclic and aromatic chromophore. Although the optimal size for an intercalating chromophore is built by a tricyclic or tetracyclic ring system, the presence of additional rings and/or substituents provide a large diversity of biological properties. Besides, this DNA intercalation is only the first step in a series of processes that can confer antitumour activity to a drug.[109] **Figure 19** shows a simplified SAR of the tricyclic carbazole and the main functional groups that provide higher cytotoxic and biological activity.

Figure 19. *SAR of tricyclic carbazoles.*[110]

1.4.2. Synthesis of carbazoles

The first synthesis of carbazoles was achieved by C. Graebe und F. Ullmann in 1896[111] and it consists of the treatment of *o*-aminodiphenylamine (**1.29**) with nitrous acid to give 1-phenyl-1,2,3-benzotriazole (**1.30**), which when heated loses nitrogen to yield the carbazole (**1.16**) (**Scheme 5**). Ullmann synthesised a number of carbazoles by this method in 1904,[112] but other workers found that the presence of unsaturated groups gave negative results. Preston, Tucker, and Cameron were the first to show nitrocarbazoles, acetylcarbazoles and cyanocarbazoles were obtained with low yields.[113]

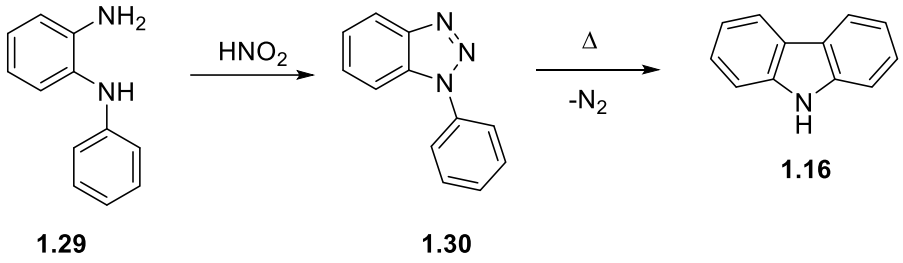

Scheme 5. *The Graebe-Ullmann Synthesis of carbazoles.*

Another classical method that has been often utilized for the synthesis of aromatic carbazoles is the dehydrogenation of 1,2,3,4-tetrahydrocarbazole (**1.31**) prepared by Borsche–Drechsel cyclization (**Scheme 6**), as described by Edmund Drechsel in 1888[114] and by Walter Borsche in 1907[115] with subsequent oxidation using lead oxide being an adaptation of the Fischer indole synthesis published in 1883.[116]

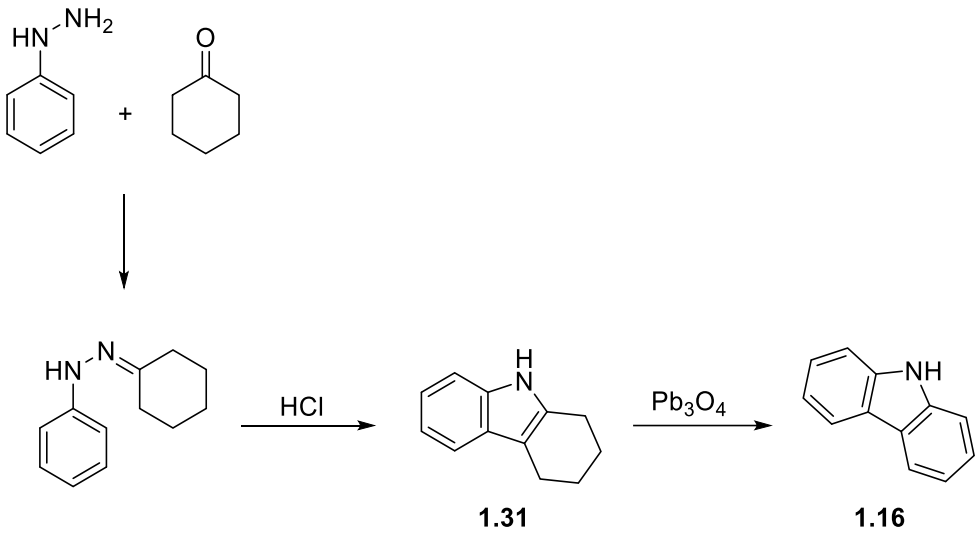

Scheme 6. *Borsche–Drechsel carbazole formation reaction.*

The triethyl phosphite catalysed intramolecular cyclization of 2-nitrobiaryls **1.32** described by Cadogan *et al.* in 1965[117] is another traditional method for the synthesis of carbazoles **1.16** (**Scheme 7**). Recently the same cyclisation has been reported using triphenylphosphine[118], in some cases in the presence of transition metal catalysts.[119]

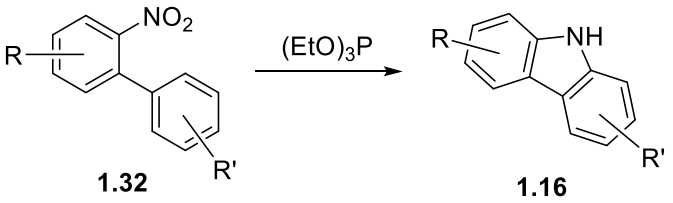

Scheme 7. *Cadogan cyclisation.*

1.4.2.1. Biosynthesis

Biosynthesis is a multi-step, enzyme-catalysed process where substrates are converted into more complex products in living organisms. Experimental knowledge on carbazole biosynthesis is limited and the number of enzymes in nature capable of catalysing the cyclisation for the formation of carbazoles is very small. Among them, StaP is responsible for the synthesis of indolocarbazoles **1.33**, and Xial for the synthesis of the antiviral xiamycin (**1.34**) (**Scheme 8**).[120]

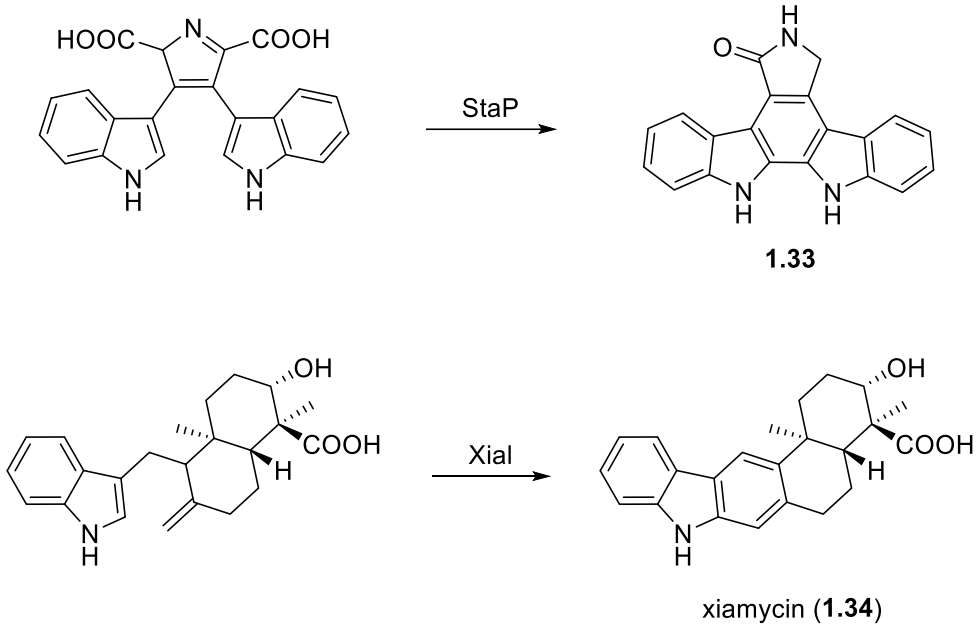

Scheme 8. *Biosynthesis of carbazole skeleton: StaP for indolocarbazole 1.33 biosynthesis and XiaI for xiamycin (**1.34**) biosynthesis.*[121]

One of the most relevant investigations was carried out by Huang and co-workers in 2015.[122] That study reports the discovery and characterization of the biosynthetic pathway of neocarazostatin A (**1.35**) through genome mining and gene inactivation. They describe the functions of five key enzymes, including the phytoene synthase-like prenyltransferase NzsG, the P450 hydroxylase NzsA , the thiamine diphosphate (ThDP)-dependent enzyme NzsH, a free-standing acyl carrier protein (ACP) NzsE, and the classical β-ketoacyl-ACP synthase (KAS) III NzsF. **Scheme 9** shows a simplified scheme for the biosynthesis of neocarazostatin A (**1.35**) and B (**1.36**) proposed by Huang's group.[123]

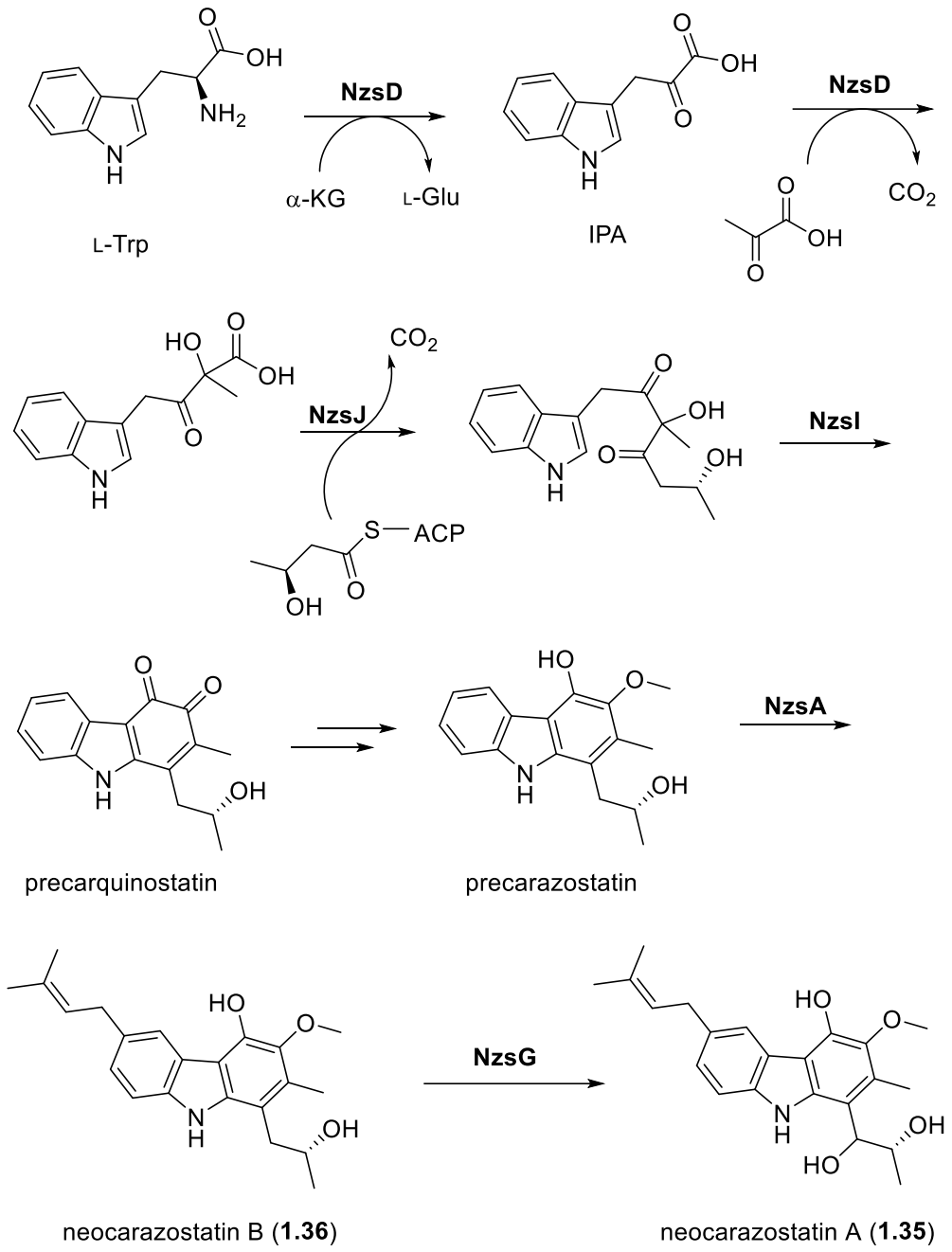

Scheme 9. *Biosynthetic pathways of neocarazostatin A (**1.35**) and B (**1.36**).*[123]

The same route performed by carbazole synthases leads to the same precarquinostatin intermediate **1.37** through the action of the enzymes CqsB1, 2, and 3, which are responsible for the cyclization of the acyl side chain moiety onto the unstable intermediate to form the ortho-quinone-containing ring of the carbazole intermediate. After the subsequent catalytic alkylation by the enzyme CqsB4, this route also yields the compound carquinostatin A (**1.38**) (**Scheme 10**).[124]

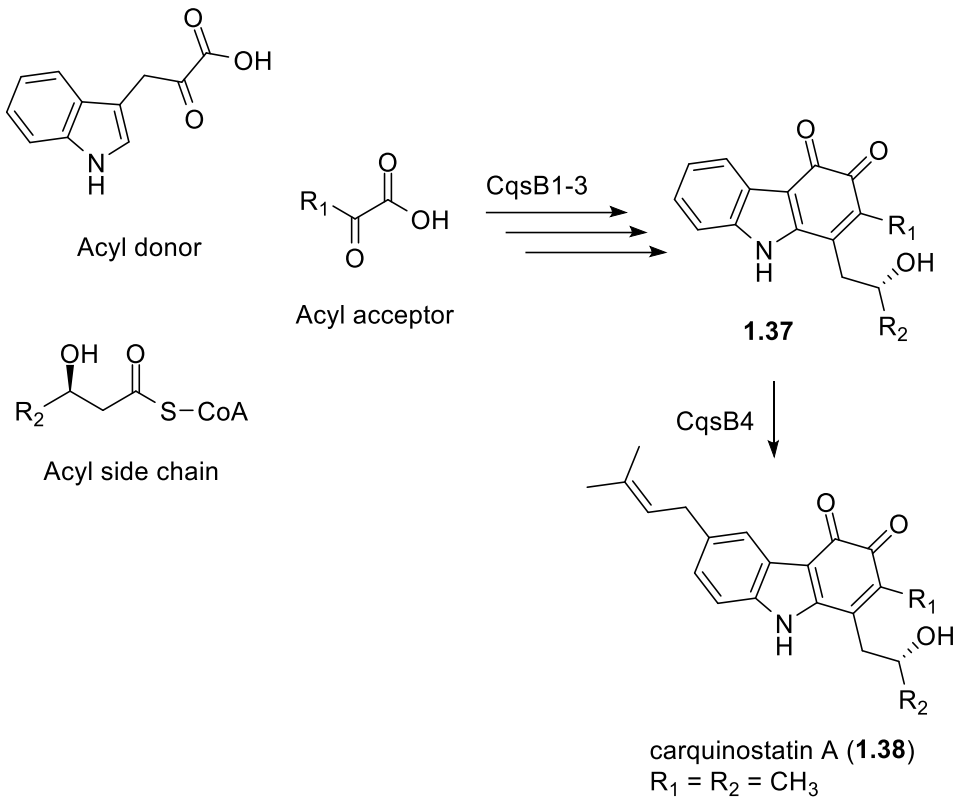

Scheme 10. *Biosynthetic route for the production of novel carbazole analogues.*[124]

1.4.2.2. Synthesis of carbazoles from indoles

For the past two decades, the conversion of indoles to carbazole derivatives has been widely examined because of the ready availability of indoles as starting substrates. Indoles are considered as an electron-rich heteroaromatic system that shows reactivity at C-2 and C-3 position for post functionalization.[125] The most widely-used synthetic methodologies for this process have been transition metal-catalysed reactions, cycloaddition chemistry, transition-metal-free cyclizations, Lewis-acid catalysed reactions and three component reactions.[125]

1.4.2.2.1. Transition metal-catalysed reactions

The transition metal mediated activation of C-H to form C-C or C-heteroatom bonds is one of the most used strategies adopted recently by chemists. Rh(III)-catalysed intermolecular annulation of *N*-pyrimidine indoles **1.39** has been exploited widely. Yi *et al.* designed a highly efficient one-pot route to carbazoles **1.40** using a Rh(III) catalytic system and terminal alkynes **1.41** (**Scheme 11**).[126] This route showed excellent functional group tolerance and regioselectivity, but the pyrimidyl group was necessary for the success of the reaction.

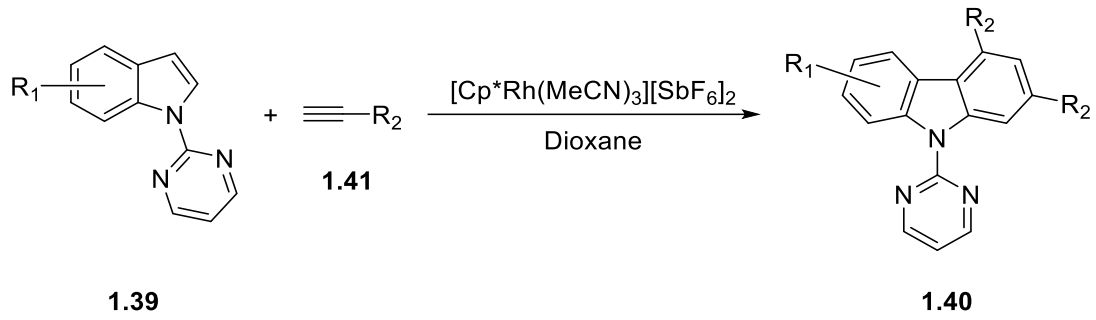

1.39 **1.40**

Scheme 11. *Rh-Catalysed synthesis of carbazoles using alkynes.*

Gold has also been used for a similar purpose. In 2012, Shengming Ma's group reported a $AuCl_3$-catalysed reaction of 1-(indol-2-yl)-3-alkyn-1-ols **1.42** that provides substituted carbazoles **1.16** in moderate yields under mild conditions, with the carbocyclic ring formation occurring at room temperature (**Scheme 12**). [127]

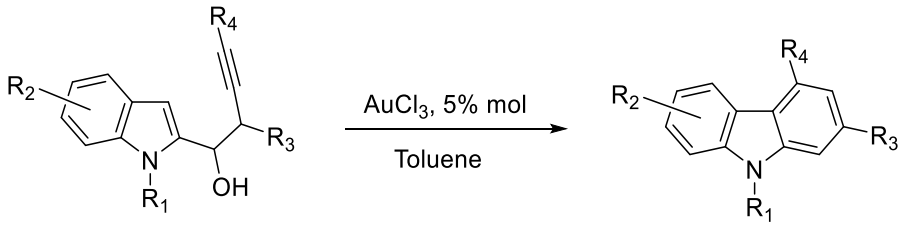

1.42 **1.16**

Scheme 12. *$AuCl_3$-catalysed synthesis of carbazoles **1.16** using 1-(indol-2-yl)-3-alkyn-1-ols **1.41**.*

The mechanism described for this reaction is shown in **Scheme 13**. It starts with the coordination of the Au^{3+} cation to activate the alkyne group in **1.42**, which is attacked at C3 of the indole to generate the C-C bond. After removal of a proton and protodemetallation, the elimination of H_2O affords the final carbazole structure **1.16**.[127]

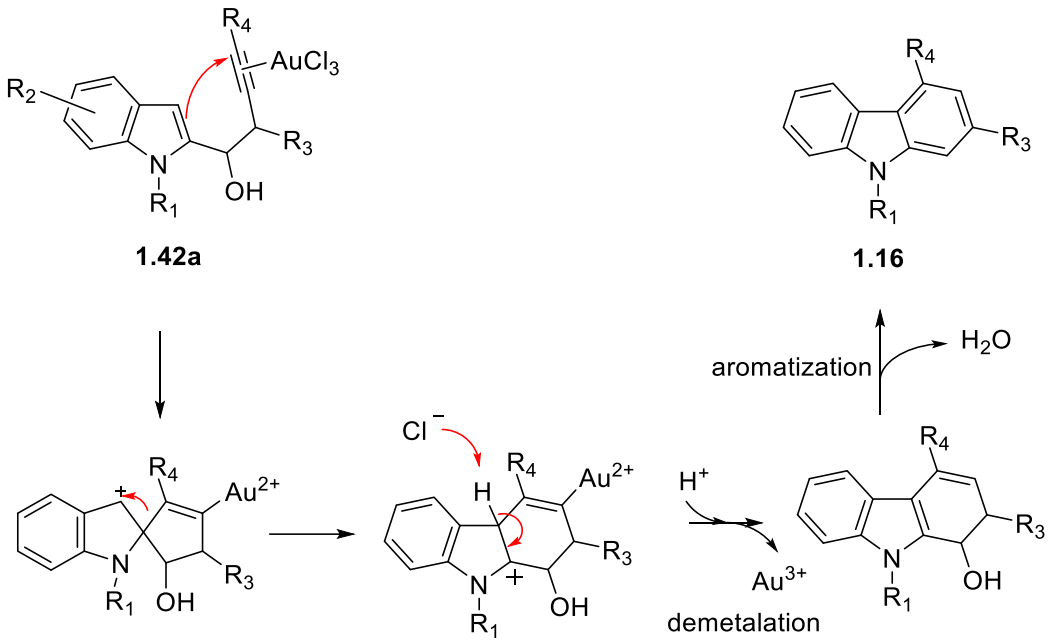

Scheme 13. *Mechanism for the gold catalysed cyclisation.* [127]

1.4.2.2.2 Cycloaddition

Many cycloaddition reactions under mild conditions have also been reported for the synthesis of carbazoles. Palladium-catalysed C-H activation is a broadly used strategy. Thus, Verma and co-workers published their work on the synthesis of carbazoles **1.16** from indoles **1.43** using a Pd(II)-Cu bimetallic system as catalyst for C-H activation followed by a triple successive oxidative Heck reaction, the subsequent cyclisation proceeding with high regioselectivity (**Scheme 14**).[128] The strategy was also successful in providing the tricyclic carbazole with an additional benzene ring.

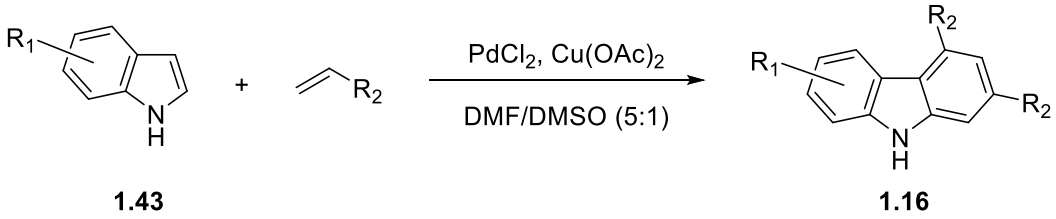

Scheme 14. *Pd(II)-Cu bimetallic catalytic system for the synthesis of carbazoles **1.16** from indoles **1.43** using alkenes.*

The mechanism for this reaction is shown in **Scheme 15a.** It starts with C3 C-H bond activation to generate a palladated species **1.44** which coordinates with the alkene **1.45**. Steric hindrance forces the *cis-trans* isomerization followed by β-hydride elimination which leads to a conjugation species **1.46** that will undergo a double Heck reaction. The double Heck reaction is shown in **Scheme 15b** and begins with palladium coordination to the double bond following deprotonation to form the palladium allyl system **1.47**. Due to steric hindrance, the olefin insertion must happen at the carbon adjacent to R_2, and this

creates Pd species coordinated by the imine **1.47**, followed by *β*-hydride elimination and *N*-protonation/C-H deprotonation. This intermediate **1.48** will then go through the same process to form the final carbazole compound **1.16**.[128]

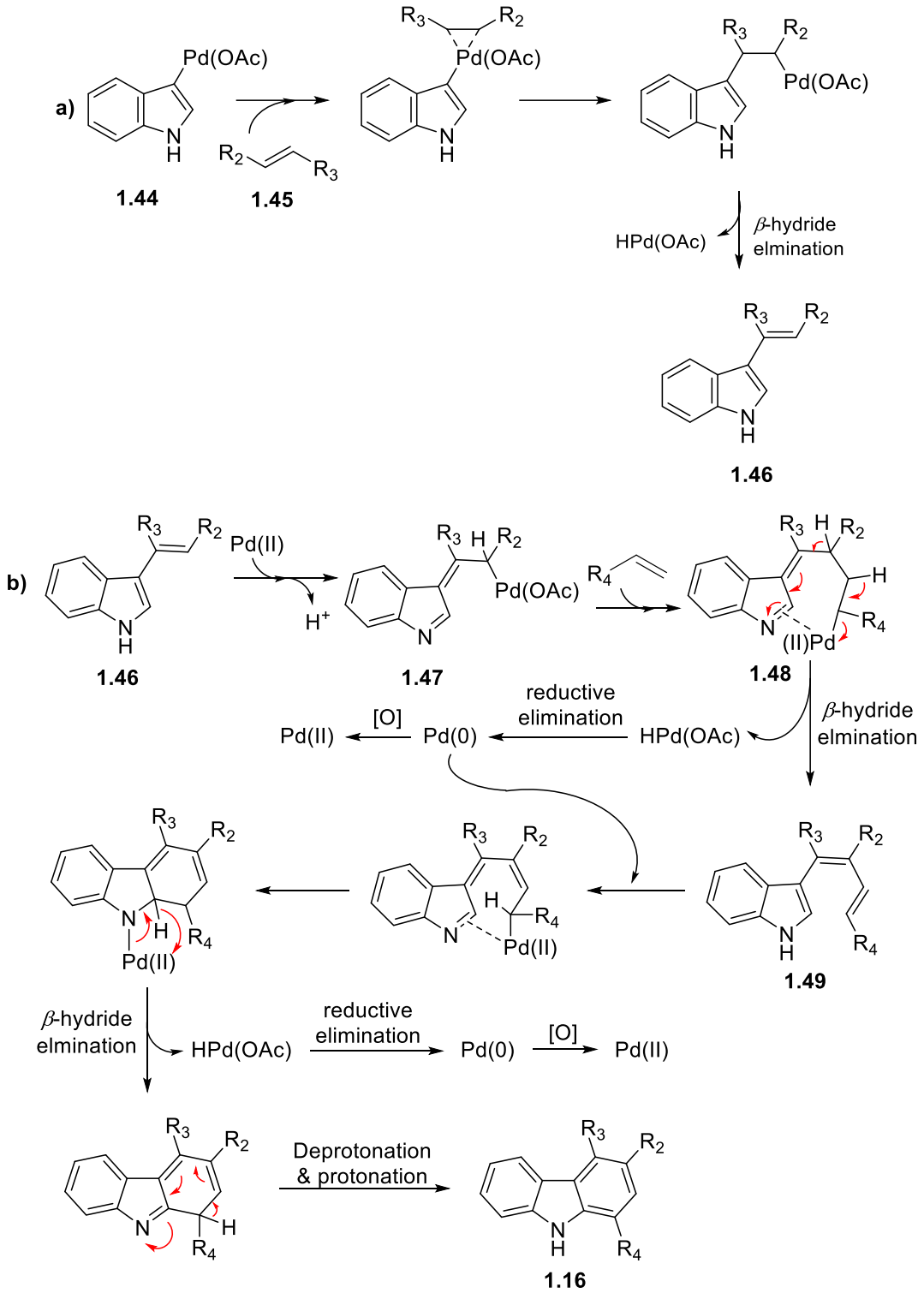

Scheme 15. *Mechanism for the palladium catalysed alkylation and double Heck reaction in series.*[128]

Environmentally benign processes have also received increasing attention in recent years. In 2017, Kotha *et al.* reported a metal-free benzannulation protocol to carbazoles from indoles, carbonyl compounds and dienophiles, by the Diels-Alder reaction of an in-situ generated diene **1.50**. Diene **1.50** is formed by the reaction of indole **1.51** and cyclohexanone (**1.52**) following dehydration, and and reacts with 1,4- naphthoquinone or dimethylacetylene dicarboxylate (DMAD) as a dienophile in *N,N*-dimethylurea/(+)-tartaric acid (DMU/(+)-TA) (**Scheme 16**). [129]

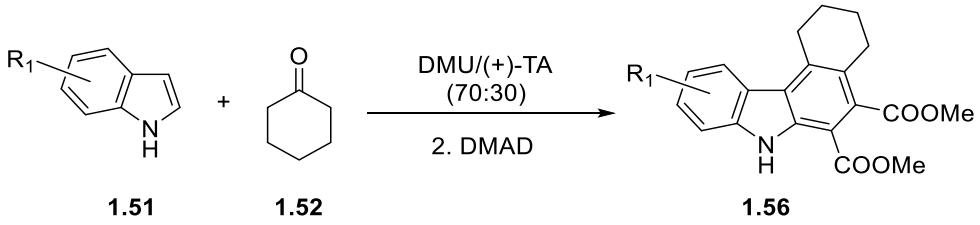

Scheme 16. *Metal-free benzannulation reaction to carbazoles **1.56** from indoles **1.51**, cyclohexanone (**1.52**) and dienophiles.*

The mechanism suggested for the reaction is explained in **Scheme 17** and starts with the attack of the indole at C3 by the carbonyl compound, which after elimination affords the diene. Then, a Diels–Alder reaction provides the intermediate derivative **1.55** which, after aromatization, yields the target carbazole scaffold **1.56**.[129]

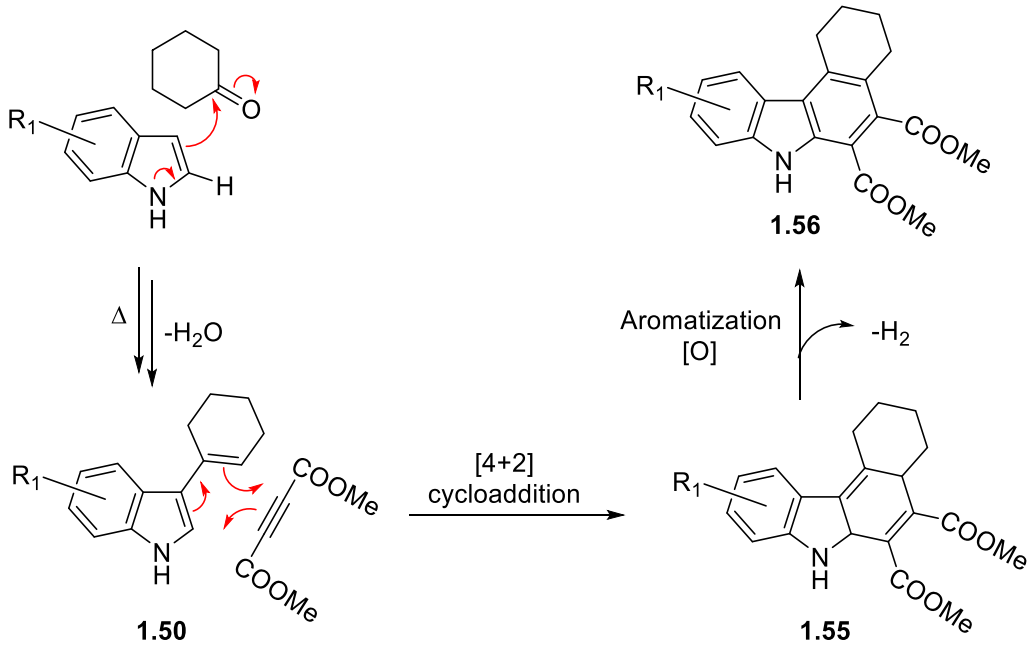

Scheme 17. *Mechanism for the metal free benzannulation.*[129]

1.4.2.2.3. Iodocyclization

Another strategy for the synthesis of carbazoles is a tandem iodocyclization to provide iodocarbazoles **1.57** (**Scheme 18**). This protocol, reported by Liang and co-workers,[130] suggests a

pathway involving a tandem iodocyclization with migration and aromatization. The cascade process is conducted at room temperature. The halide scaffolds **1.57** so produced can be further utilized in palladium-catalysed coupling reactions, turning these products into high value building blocks.

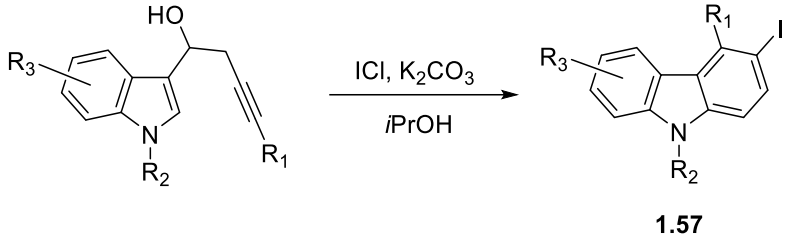

1.57

Scheme 18. *Tandem iodocyclization for the synthesis of iodocarbazoles **1.57**.*

The proposed reaction mechanism, shown in **Scheme 19**, starts with the activation of the alkyne using ICl forming a cyclic iodonium intermediate **1.58**, which is attacked by the indole ring at C3. Thereafter the 1,2-shift from C3 to C2 forms a benzylic cation **1.59**, which after deprotonation and aromatization by elimination of water provides the final iodocarbazole product **1.57**.[130]

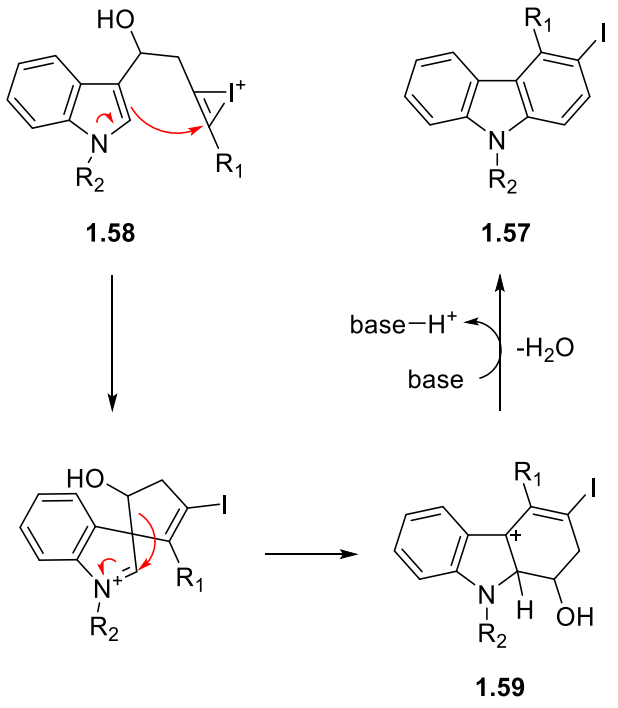

Scheme 19. *Mechanism for the iodocyclisation reaction.*[130]

1.4.2.2.4. Lewis acid-catalysed cyclization

Lewis acid-catalysed cyclization provides a complementary approach for carbazole synthesis, with ready availability of starting materials and mild reaction conditions. As an example, Wang's group

reported a trifluoroborane promoted cascade reaction between tryptophols **1.60** and propagylic alcohols **1.61** to furnish aryl substituted carbazoles **1.62** in good yields (**Scheme 20**).[131]

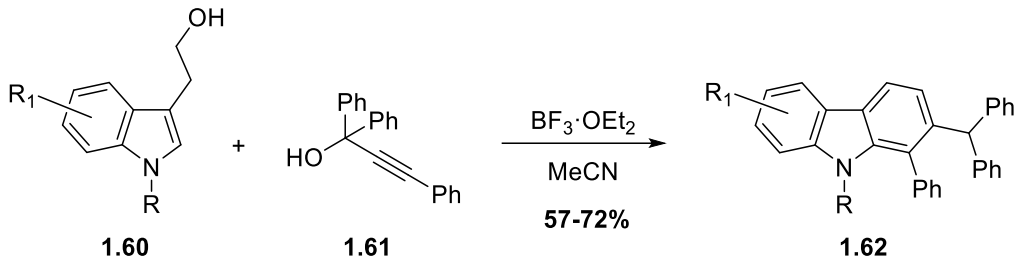

Scheme 20. *BF_3·OEt_2 catalysed reaction for the synthesis of carbazoles **1.62**.*

The first step of the mechanism is the activation of the propargylic alcohol **1.61** with BF_3 to become a more electron-deficient electrophile, which is subsequently attacked at the C3 of the indole **1.60a** providing the intermediate **1.63** (**Scheme 21**). A 1,2-migration of the allenyl group generates a carbocation that undergoes *β*-hydride elimination. Then, the propargylic alcohol is activated by BF_3 and undergoes a 6-*exo*-tet process to generate a tricyclic core carbocation skeleton, which upon deprotonation and H-shift leads to aromatization and formation of the final carbazole **1.62a**.[131]

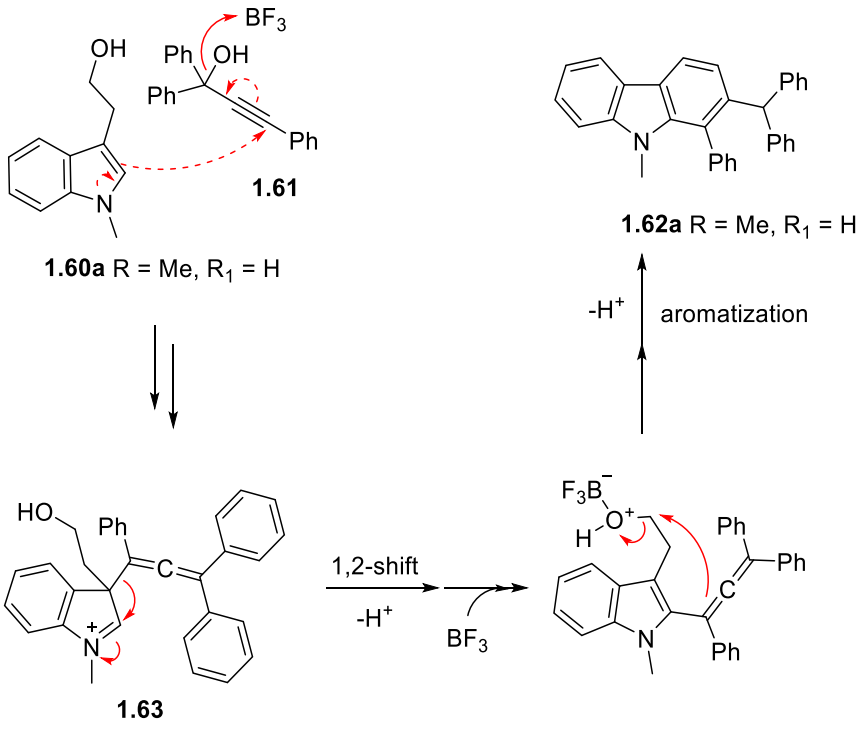

Scheme 21. *Mechanism for the BF_3 catalysed cyclization.*[131]

1.4.2.2.5. Three-component reaction

The main advantage of a 3-component reaction approach is the ready availability of simple indoles, ketones and alkenes. The Deng group developed a highly efficient method for carbazole formation using *N*-methylindoles, aromatic ketones, and nitroolefins under metal-free conditions (**Scheme 22**).[132] The indole-to-carbazole strategy was promoted by NH_4I with high regioselectivity through a formal [2 + 2 + 2] annulation, enabling the assembly of a large number of diverse carbazole products with good tolerance of a wide range of functional groups.

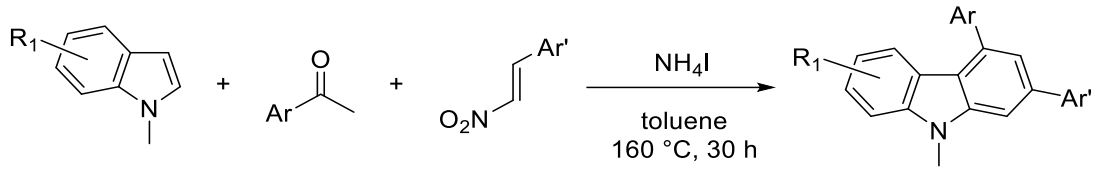

Scheme 22. *Three-component method for carbazole formation using indoles, ketones, and nitroolefins.*

A mechanism for this reaction has been proposed. As suggested in **Scheme 23**, it starts with nucleophilic attach by the indole **1.64** π-system at C3 to the carbonyl group of the aromatic ketone **1.65** followed by elimination of H_2O at 160 °C. Thereafter, Michael addition facilitated by attack of the diene on the nitroolefin **1.66**, with subsequent annulation, gave the carbazole carbon skeleton. Finally, the loss of nitrous acid and oxidative aromatization gave the final carbazole product **1.67**. Although this is the mechanism suggested, a Diels-Alder process is also plausible.[132]

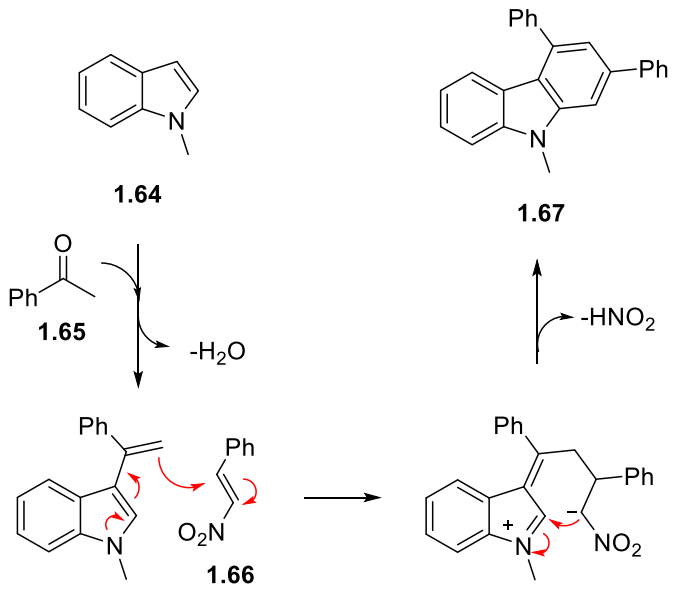

Scheme 23. *Mechanism for three component reaction with cyclisation.*[132]

1.4.2.2.6. Photochemistry

Photochemical activation has been also broadly studied recently as a route to carbazoles due to all of the advantages that this technique provides in synthetic organic chemistry. Thus, L.Q. Lu *et al.* developed a novel route to carbazole synthesis through a visible light-photocatalysed formal (4+2) cycloaddition of indole-derived bromides and alkynes (**Scheme 24**).[133] The optimized reaction conditions used ethyl 2-bromo-3-(1-methyl-1*H*-indol-3-yl)-3-oxopropanoate (**1.68**) with alkynes **1.69** and *fac*-$Ir(ppy)_3$ as a photocatalyst under blue LED irradiation (3 W) at room temperature. This novel protocol featured mild conditions, broad substrate scope and high reaction efficiency for the synthesis of carbazole carboxylates **1.70**.

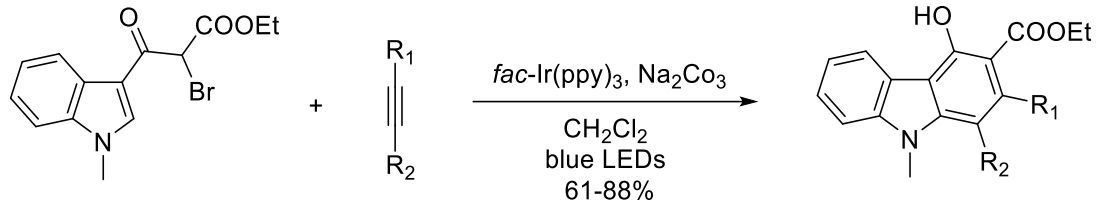

1.68 **1.69** **1.70**

Scheme 24. *Visible light-photocatalysed synthesis of carbazoles.*

The mechanism for this reaction involves the indispensable role of a photocatalyst (**Scheme 25**). A photocatalyst is a material which absorbs light to promote it to a higher energy level, from which it can provide energy to a reacting substance to facilitate chemical reaction, considering the photon as a reagent.[134] Thus, the reaction starts by elevating the photocatalyst [Ir(III)] to its excited state with blue light irradiation; this then activates the bromide providing radical intermediate **1.71**. Then, the nucleophilic attack of radical **1.71** onto the alkyne **1.69** generates a new radical intermediate **1.72** that undergoes cyclisation to the tricyclic skeleton **1.73**. This intermediate, in equilibrium with enol form **1.74**, is oxidised by the [Ir(IV)] previously formed on the first step of the bromide activation. Finally, a last deprotonation step leads to the target carbazole **1.70**.[133]

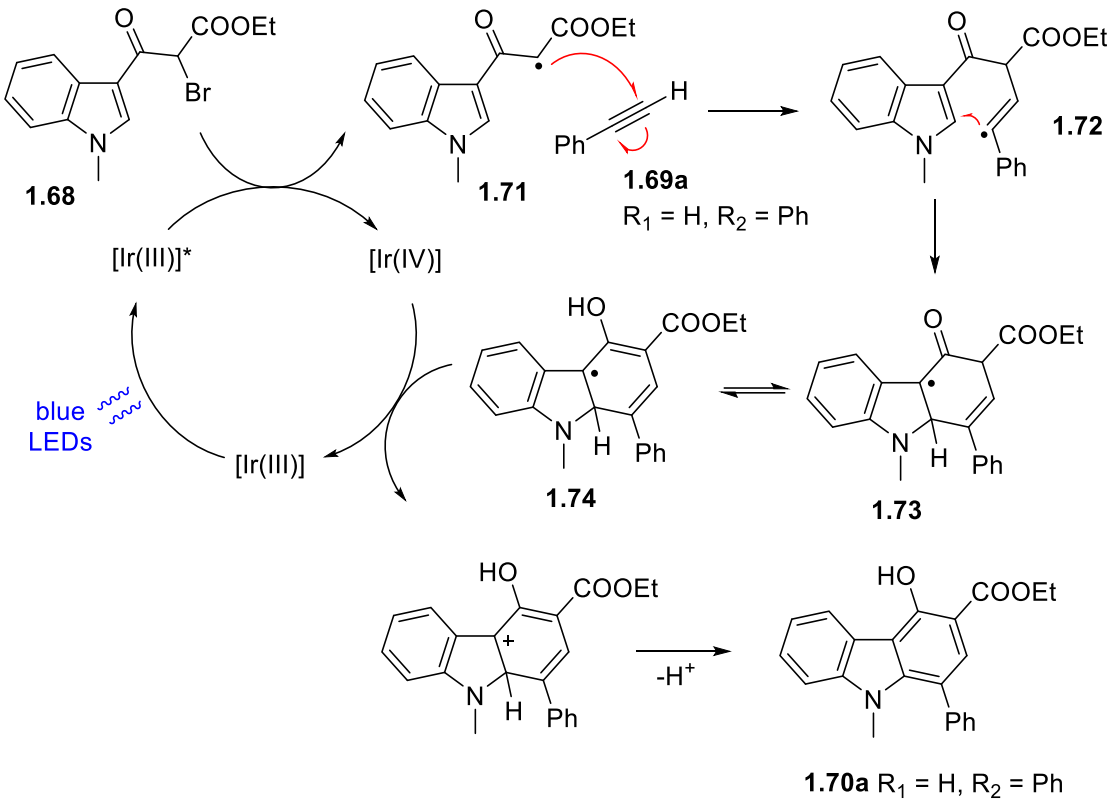

Scheme 25. *Modified mechanism for the photocatalysed cyclisation.*[133]

1.4.2.3. Synthesis of carbazoles from biaryl precursors

Although the formation of carbazoles from indole is the most widely adopted approach, there are also many examples of the synthesis of carbazoles from the corresponding biphenyl species by the activation of a nitrogen-containing group, such as amino, nitro or azido functionality. In 2008, Matthew J. Gaunt *et al.* published a Pd(II)-catalysed C-H bond amination reaction to form carbazoles.[135] The amination process operates under extremely mild conditions and produces *N*-alkylated carbazole products **1.75** in good to excellent yields (**Scheme 26**). Carbazoles possessing complex molecular architectures can also be formed using this reaction, highlighting its potential in natural product synthesis applications.

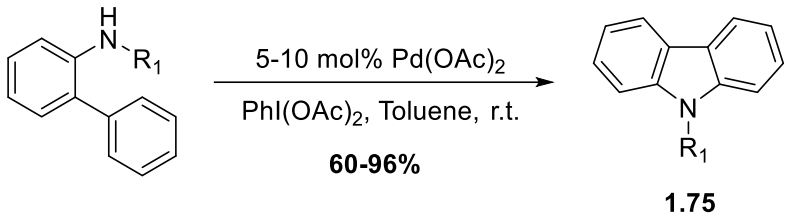

Scheme 26. *Pd(II)-catalysed C-H bond amination reaction to form carbazoles.*

In 2015, Miura's group also reported an iridium-catalysed dehydrogenative cyclization of 2-aminobiphenyls **1.76** in the presence of a copper co-catalyst under aerobic conditions, which led to carbazoles **1.16** through direct C-H amination (**Scheme 27**).[136]

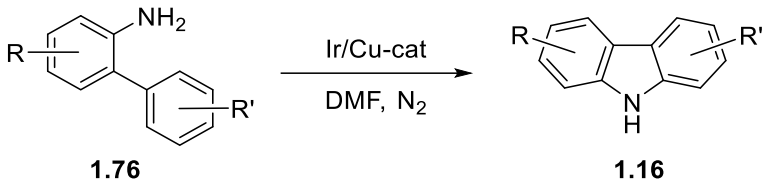

1.76 **1.16**

Scheme 27. *Iridium-catalysed dehydrogenative cyclization of 2-aminobiphenyls **1.76** to form carbazoles **1.16**.*

Similarly, intramolecular palladium(II)-catalysed oxidative carbon-carbon bond formation has also been described. In 2008, Keith Fagnou and co-workers reported this strategy using electron-rich diarylamines **1.77** and pivalic acid for the synthesis of carbazoles **1.16** in high yield with broad scope (**Scheme 28**), including the synthesis of the naturally occurring carbazole products such as clausenine (**1.21**, see section 1.4.1 and **Figure 17**).[137]

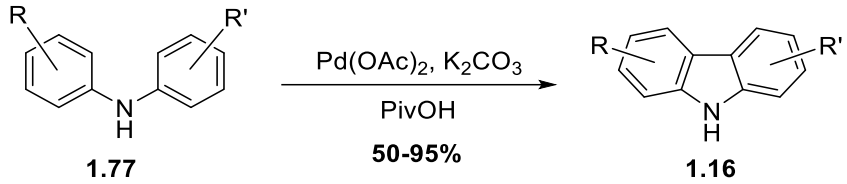

1.77 **1.16**

Scheme 28. *Intramolecular palladium(II)-catalysed carbon-carbon bond using diarylamines **1.77** and pivalic acid.*

Another efficient route to synthesise a variety of carbazoles starts from aniline and uses an intermolecular amination followed by intramolecular arylation. Zhijian Liu and Richard C. Larock reported in 2004 the reaction of *o*-iodoanilines **1.78** with silylaryl triflates **1.79** in the presence of caesium fluoride to afford the *N*-arylated products, which were subsequently cyclized using a palladium catalyst to carbazoles similar to previous (**Scheme 29a**).[138] A palladium-catalysed reaction sequence using substituted anilines **1.80** and 1,2-dihaloarenes **1.81** as electrophiles was published by Lutz Ackermann and co-workers in 2009 (**Scheme 29b**).[139] This chemistry tolerated a variety of functional groups and enabled highly regioselective synthesis of the same generic carbazole scaffold **1.16**.

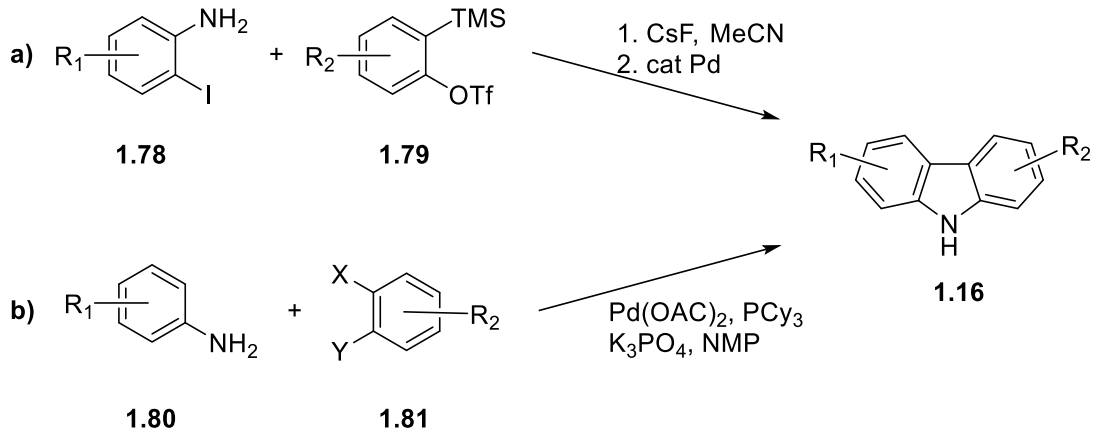

Scheme 29. *a) Reaction of o-iodoanilines **1.78** with silylaryl triflates **1.79** and subsequent cyclization to carbazoles **1.16** using a Pd catalyst. b) Palladium-catalysed reaction sequence for the synthesis of carbazoles **1.16** using substituted anilines **1.80** and 1,2-dihaloarenes **1.81**.*

Azides as amino group sources in C–H amination processes have unique advantages, such as ease of preparation and generation of N_2 gas as the only by-product. In combination with dirhodium(II) complexes they provide great prospects for the synthesis of pyrroles,[140] indoles,[141] and a range of *N*-heteroaromatic compounds.[142] Benjamin J. Stokes published an extended version of this method with biaryl azides **1.82** for the synthesis of carbazoles **1.16** (**Scheme 30**).[143]

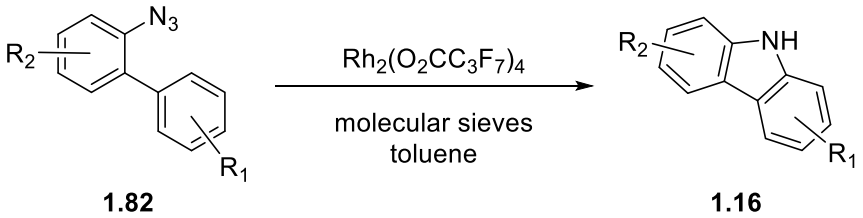

Scheme 30. *Dirhodium(II) catalysed synthesis of carbazoles **1.16** from biaryl azides **1.82**.*

More recently, direct nitrene insertions into C-H bonds have become an important tool for building C-N bonds in modern organic chemistry, and some chemists have focused on reporting milder conditions to avoid the use of transition metals, high temperatures, and ultraviolet or laser light. Hence, the synthesis of carbazoles and related building blocks through a visible light-induced intramolecular C-H amination reaction arose as a "greener" and efficient method for nitrene formation. In 2018, L. Yang's group published a new simple protocol for the synthesis of carbazoles **1.16** using azides upon irradiation with visible light with water as a co-solvent to enable the conversion of readily available 2-azidobiphenyls **1.82** under mild conditions (**Scheme 31**).[144]

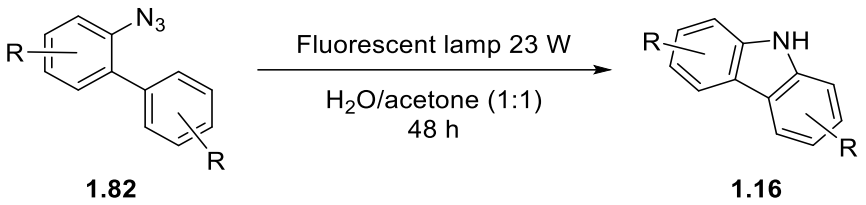

Scheme 31. *Synthesis of carbazoles **1.16** by the irradiation of azides **1.82** with visible light and water as a co-solvent.*

Under these conditions the azide **1.82** should be transformed into a nitrene intermediate **1.83** by release of N_2.The intermediate **1.83** should react rapidly by electrocyclic ring closure followed by a [1,5]-H shift, to give the final product (**1.16**) after tautomerization. This mechanism (**Scheme 32**) was proposed by L. Yang *et al.* in 2018.[144]

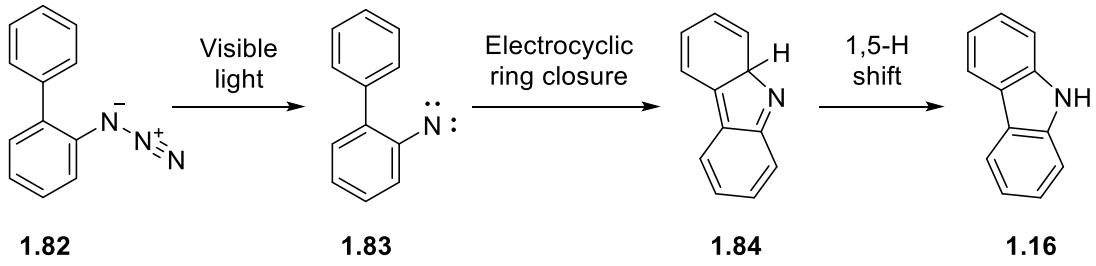

Scheme 32. *Proposed mechanism for the electrocyclisation.*[144]

More recently, in 2020, R. K. Saunthwal *et al.* published a new method using reactive aryl sulfilimines **1.85** instead of the corresponding azides **1.82**. The reaction scope was found to be broad with high yields for a range of substrates (**Scheme 33**). They also reported an efficient gram-scale synthesis of Clausine C.[145]

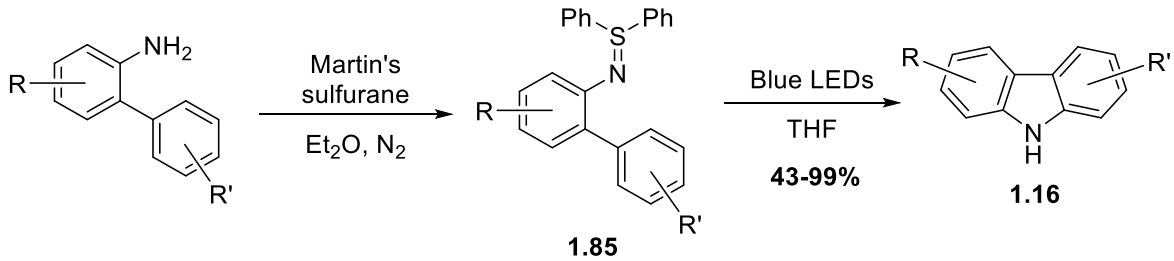

Scheme 33. *Synthesis of carbazoles irradiating sulfilimines with visible light.*

After analysing the methods previously reported in the literature and following our principles of green chemistry, the visible light promoted synthesis of carbazoles from the corresponding biphenyl azide intermediates offers considerable promise. This approach would provide the possibility of being

adapted to a flow process and could be developed to provide a more efficient and sustainable approach to the carbazole scaffold. A related example for the synthesis of carbolines through an (azidophenyl)pyridine intermediate has been adapted in a synthetic route towards dimebolin (**1.86**) reported by Huijun Dong *et al.* in 2011 using batch techniques.[146] This approach provided access to γ-carboline derivatives in the first steps (**Scheme 34**). Palladium-catalysed Suzuki-Miyaura cross-coupling of *o*-bromoanilines **1.86** provided biaryl species **1.87**. Azidation, alkylation of the pyridine nitrogen and further ruthenium-catalysed cyclisation generated the corresponding γ-carbolines **1.88** from *ortho*-substituted aryl azide precursors **1.89**. This route seemed a good starting point for the development of a new synthetic pathway to carbazole scaffolds, adapted to reagentless techniques, performing the Suzuki-Miyaura cross-coupling reaction under microwave irradiation and the cyclization of the corresponding azide derivative into carbazole or carboline products under photochemical conditions in a flow photochemical reactor.

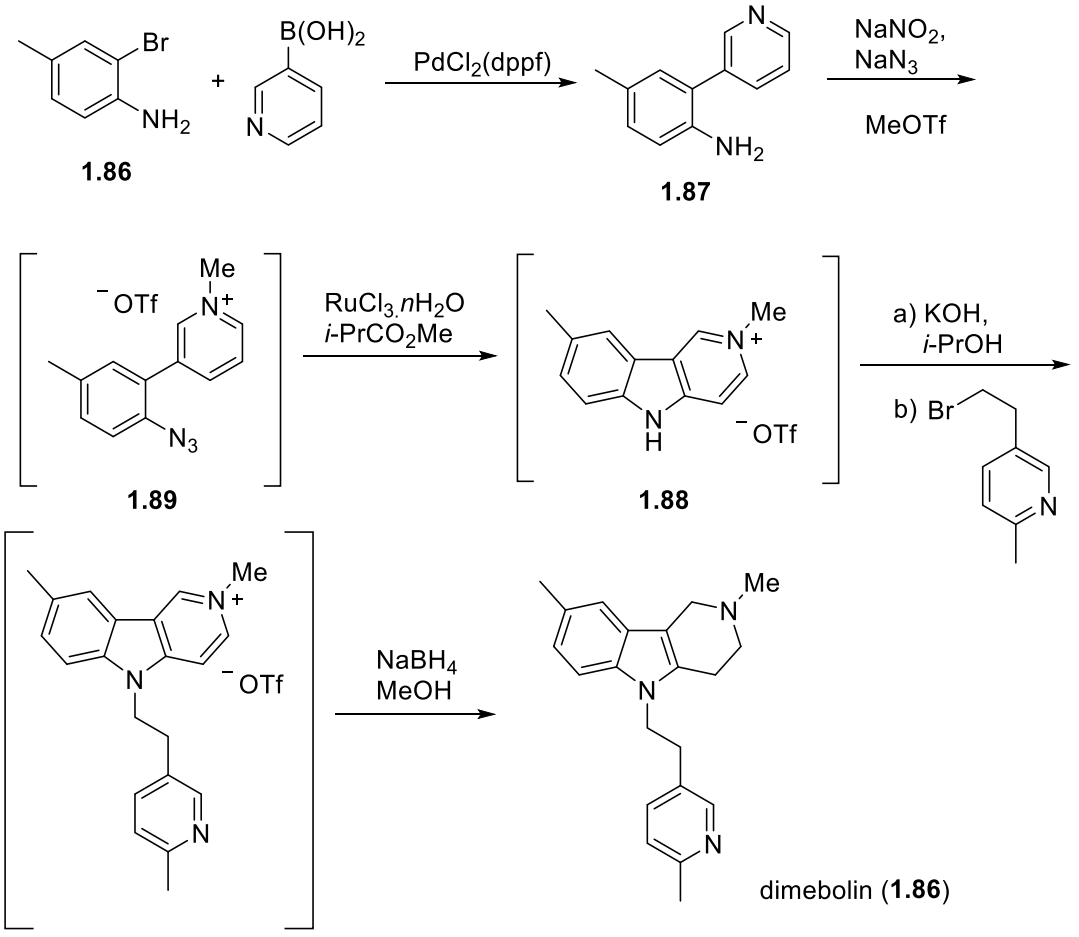

Scheme 34. *Synthesis of dimebolin (**1.86**).*

1.5 Objectives

Due to their widespread utility, the carbazole skeleton has been a key structural motif of many biologically active compounds, including natural and synthetic materials. There are many different methods for making carbazoles, including transition metal- or Lewis acid-catalysed reactions of indoles. However, there are notable difficulties in the synthesis, scope, and industrial production of this type of scaffold. Most of these synthetic strategies have poor atom efficiency, employ expensive reagents and give side products that need to be removed and disposed of safely. For these reasons, the investigation of biaryl substates as readily-accessible precursors for the synthesis of these compounds has increased significantly in recent years. The use of a photocyclization of biphenyl precursors as a greener, cleaner route to carbazoles has potential for incorporation into a flow process to increase efficiency and enable continuous production.

The general goals for this thesis are to investigate a new means of access to heterocyclic scaffolds by photocyclization of biaryl precursors to give, for example, carbazoles efficiently using, if possible, reagentless technologies. With the synthesis of suitable precursors, the incorporation of a photocyclization step into a continuous flow process could be studied, and this improved method then utilized for the production of diverse carbazoles of biological interest and adapted for the synthesis of other heterocyclic scaffolds with similar structural features.

Thus, the main objective of this thesis is the development of a new reagentless process that permits the assembly of carbazole scaffolds using reagentless techniques, in order to provide a route of access that was more efficient, sustainable and reproducible. The first step of the synthesis would involve a carbon–carbon cross-coupling reaction between a haloaniline, or equivalent, and a phenylboronic acid to provide the key biphenyl intermediate scaffold (**Scheme 35**). This type of coupling reaction can experience problems with solubility, especially at room temperature; therefore, flow chemistry was discarded in favour of a more expedient access using established technologies. Microwave assisted chemistry appeared as an attractive approach, although a solvent-free mechanochemical procedure could be a potential alternative.

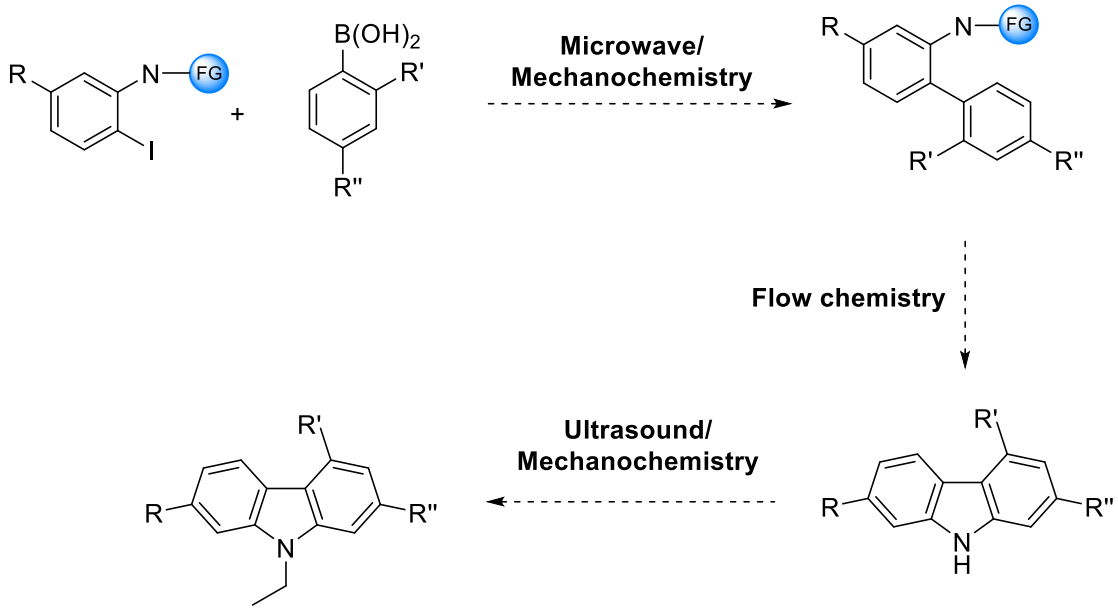

Scheme 35. *Carbazole synthetic proposal.*

With the coupled product to hand, a nitro, azido or amine containing biphenyl would be processed under flow conditions to promote cyclization to the corresponding carbazole derivative. For this step, the aim was to provide a more efficient alternative to the Cadogan reaction previously studied in the group, which not only proved to be low yielding and inconsistent, but also generated phosphine oxide as a wasteful by-product. The advantages of conducting photochemical reactions under flow conditions led to the consideration of azide formation and subsequent photocyclization as a favourable starting point. The subsequent *N*-alkylation reaction, as a transformation used for the derivatization of carbazole scaffolds, would be eligible to be adapted to many of the technologies described, although the use of ultrasound and mechanochemistry seemed to be the most promising options. If method development was successful, the next goal would be to process diverse compound libraries based upon this chemistry and prepare useful quantities for biological evaluation or test the synthetic approach by adapting it to a family of carbazole based natural products.

It was hoped at the design stage that any new method could be utilised for the synthesis of PhiKan083 carbazole analogues in useful quantities for biological testing. Hence, after assembling the carbazole scaffolds, a route towards substituted PK083 analogues could be investigated to yield reactivators of the p53 Y220C mutation. This will be discussed in greater detail in Chapter 4. As shown in **Scheme 36**, these reactivators must have an aminoalkyl chain. The addition of this group could be achieved by a formylation reaction to an *N*-ethylated carbazole, followed by reductive amination, and so would be accessible from the core carbazole scaffold, enabling the diversity of a photocyclization type approach to be utilized in providing new SAR on this important biological agent.

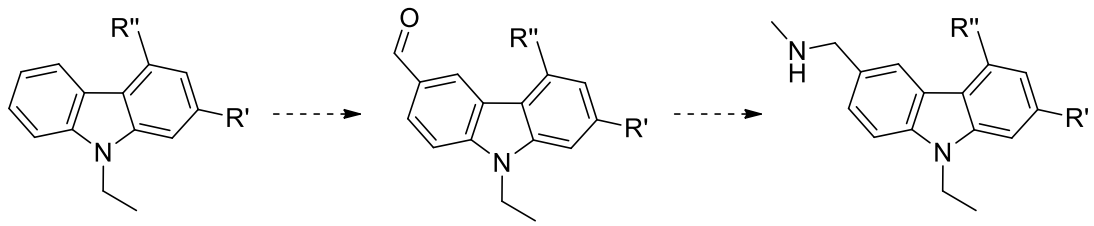

Scheme 36. *Synthetic proposal of PK083 analogues.*

The methods to be explored in this thesis could be adapted to the synthesis of other biologically interesting heterocycles, in order to develop a global methodology for the synthesis of small heterocycles using flow chemistry. Firstly, and due to their structural similarity, the method would first be tested towards *β*-carbolines. Although in this case the last alkylation step would not be required, the cross coupling and cyclization should happen under similar conditions to the synthesis of carbazole derivatives (**Scheme 37**), allowing the preparation of *β*-carbolines based on the structure of harmine.

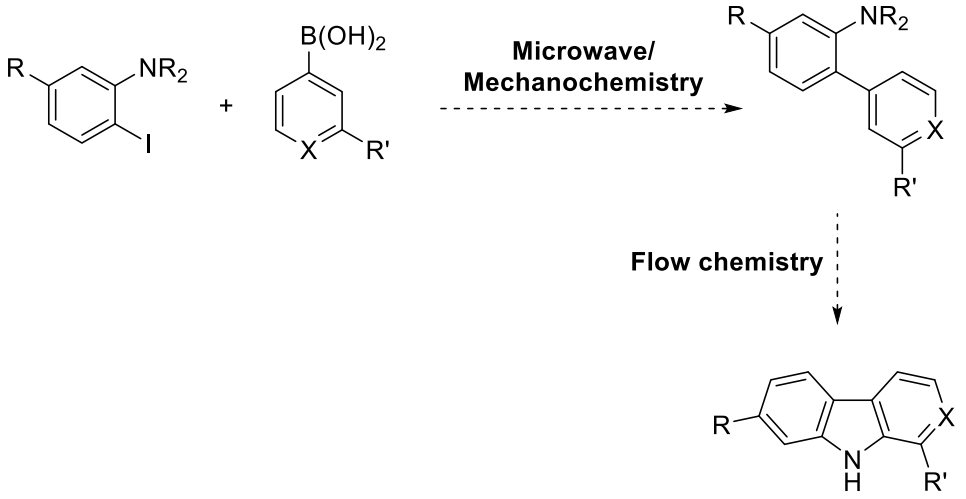

Scheme 37. *Synthetic approach towards carbazoles and β-carbolines.*

In conclusion, given the diversity of heterocyclic targets accessible by a photocyclization strategy and based upon good precedent, the discovery of a new method, that was both convergent and based upon qualifying green chemistry principles, was judged to be a worthwhile endeavour. Realizing this approach and adapting it to flow processing technologies is the subject of these studies, described in Chapter 2.

CHAPTER 2: New methods for the synthesis of carbazoles using a flow photochemical reactor

2.1 Retrosynthesis

A retrosynthetic pathway for the synthesis of carbazoles suitable to be adapted to reagentless techniques was designed (**Scheme 38**). The synthesis would start with a coupling reaction to give the biphenyl amines **2.1**. At first, haloanilines were chosen as, for the photochemical route, azide precursors would appear as a feasible option and these azides could be afforded in one step from the precursor amino group. This amine would be then converted into azide intermediate **2.2**, which would be irradiated with visible light to cyclize, by photochemical activation, on the contiguous phenyl group into the corresponding carbazole analogue **2.3**. Although the synthetic pathway is linear, each step has the potential to be studied and optimized individually. Thus, different substrates have been used in each step, and not all substrates have been tested in all reactions. The results for each step are further discussed below.

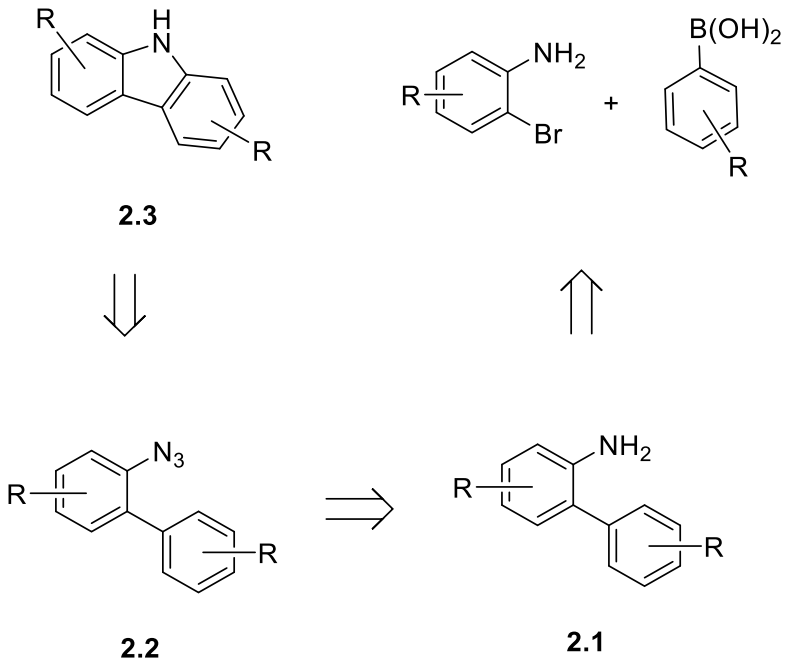

Scheme 38. *Proposed retrosynthetic scheme for the synthesis of carbazoles.*

2.2 Suzuki-Miyaura cross coupling reaction

The first step of the synthesis would then be the preparation of suitable biaryl precursors **2.1**, which often utilize a carbon–carbon cross-coupling reaction. A cross-coupling reaction is a reaction where two fragments are joined together with the aid of a transition metal catalyst (**Scheme 39**). In most cases, a main group (often an organometallic compound, R-M) reacts with an organic halide of the type R'-X with formation of a new carbon-carbon bond in the product R-R'. There are many examples of cross-coupling reactions using different substrates.

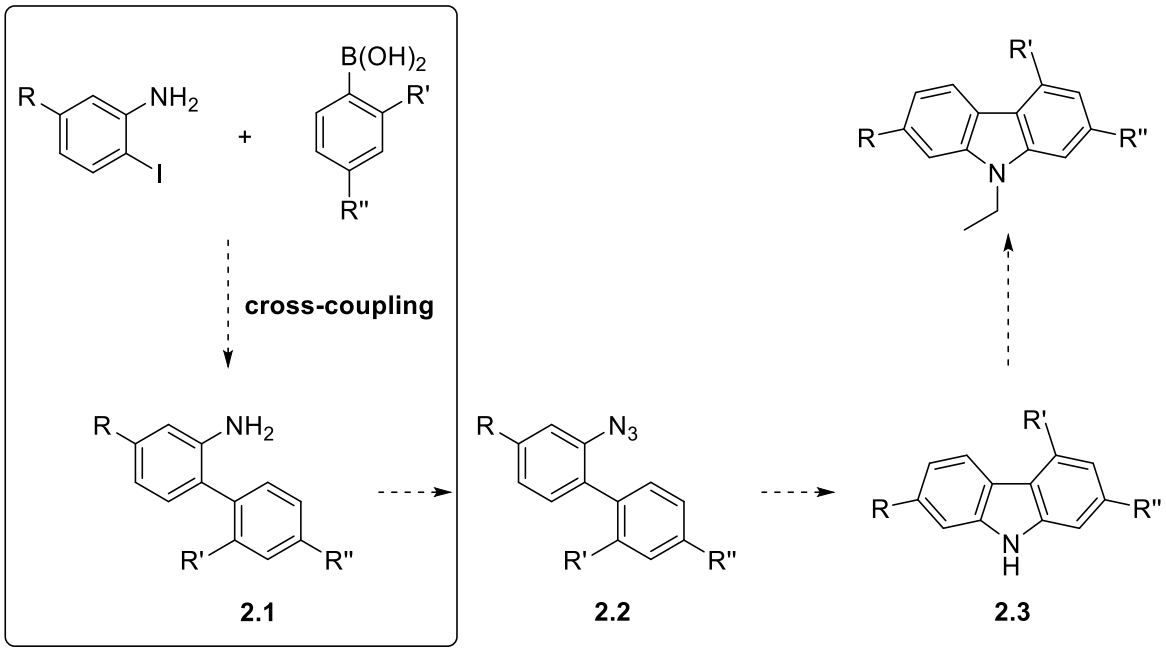

Scheme 39. *Cross-coupling reaction scheme.*

Among the reactions that accomplish the transformation needed to access a suitable biphenyl precursor, the Stille reaction is an example of a palladium-catalysed coupling reaction widely used for the coupling of two organic groups (**Scheme 40**),[147] one of which is an organostannane **2.4** (usually a vinyl, or aryl) and the other one is an organic halide of the type Ar-X (**2.5**), but triflates, sulfonates and phosphates can also be used. This type of reaction would be closer in scope to the proposed synthesis. The mechanism is shown below in **Scheme 44**.

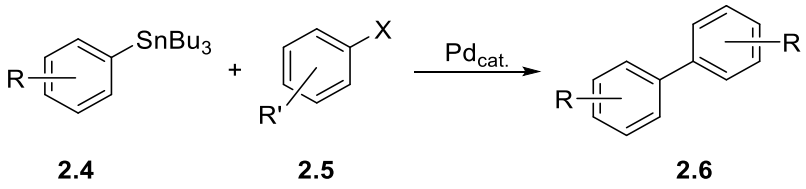

Scheme 40. *General Stille cross-coupling reaction.*

Nevertheless, there are two types of reactions that are more focused to the coupling of two benzene rings and are the most used examples for that purpose. The first one is the Negishi coupling. The process, first described by Ei-ichi Negishi in 1976,[148] involves the reaction of organic halides **2.5** or triflates with organozinc compounds **2.7** with a palladium or nickel catalyst. A general reaction scheme is shown in **Scheme 41**. The arylzinc reagents are usually synthesized from the corresponding aryl halides using iodine as a catalyst to activate the zinc towards nucleophilic addition. These organozinc species are often more reactive than both organostannanes and organoboronates which correlates to shorter reaction times.

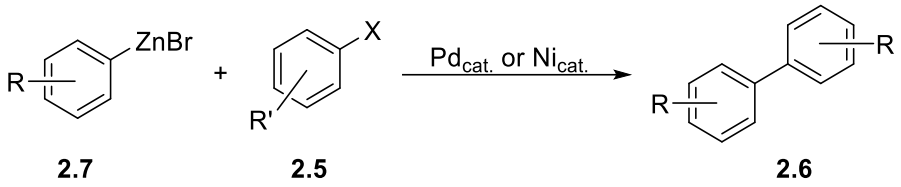

Scheme 41. *General Negishi coupling reaction scheme (X = halogen).*

The main drawback of this reaction is the necessity of synthesising the organozinc intermediate. These reactions are highly air sensitive and involve tedious procedures and workups. Accordingly, the approach that had been most used in the group, was the Suzuki-Miyaura cross coupling reaction. This reaction has been widely studied since its discovery by Akira Suzuki and Norio Miyaura[149] since it provides efficient tools for C-C bond formation, often in high yield and with broad functional group tolerance with uncomplicated protocols. It has been extensively used both in total synthesis and for the synthesis of compound libraries. In recent years, different approaches have been reported. In the late 1990s and early 2000s, the investigation of palladium clusters[150] and nanoparticles[151,152] gained importance to avoid the problems of separation and recovery of the catalyst. During the last couple of decades, greener strategies have emerged, from the use of alternative energy sources to solvent-free and benign solvent protocols. The first reports of microwave-mediated Suzuki reactions, published in 1996, were a turning point. After successfully carrying out the Heck reaction with different substrates,[12] Mats Larhed and Anders Hallberg published their work on Suzuki coupling using organoboronic acids **2.8** and 4-halobenzoic acid, linked to Rink amide (RAM) TentaGel **2.9** to provide a >99% conversion of the starting material within 3.8 min (**Scheme 42**).[13] The capability of conducting the reaction under microwave conditions provided high yields in just a few minutes, reducing dramatically the reaction times.

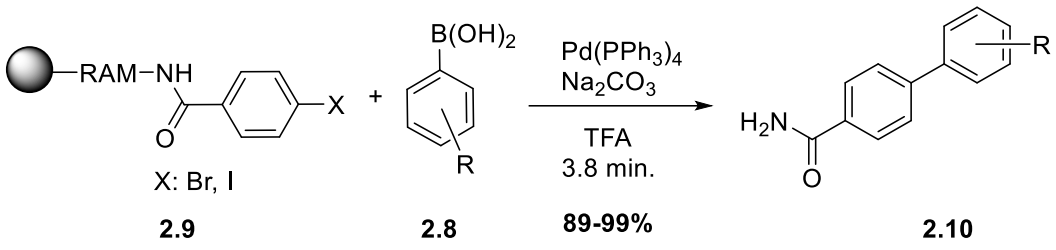

Scheme 42. *First Microwave-Assisted Suzuki Coupling on Solid-Phase.*[153]

The reaction could even be adapted to be conducted in water,[154] which is a more environmentally friendly solvent, and with its high dielectric constant is a very useful solvent for microwave-mediated synthesis. Besides, apart from the rate enhancement effects when water is heated well above its boiling point in sealed vessels, organic substrates can become more soluble. The appearance of microwave-assisted conditions allowed new methodologies to be explored to improve the efficiency and reduce the costs and environmental impact of cross-coupling reactions. Didier Villemin

and Fredéric Caillot used mono-mode microwave irradiation to perform different palladium-catalysed reactions using potassium fluoride on alumina as a base without solvent.[155] The emergence of mechanochemistry did not go unnoticed and in the year 2000, Axelsson and co-workers described the first Suzuki coupling reaction under mechanochemical conditions.[156] They reported the coupling of phenylboronic acids with a series of aryl bromides using $Pd(PPh_3)_4$ as the catalyst, and obtained excellent yields in a milling time of 30-60 min. The advantages of the mechanochemical treatment are among other things decreased reaction times, simplified work-up procedures, and especially the omission of solvents during the reaction course. Examples of these solid-state cross-coupling reactions are still few in number. Franziska Schneider's group published in 2009 their investigation into the parameters influencing the yield of reaction, such as revolutions per minute, milling time, and the size and number of milling balls,[157] but it was more recently, in 2019, when Tamae Seo *et al.* reported the first broadly applicable mechanochemical protocol for a solid-state cross-coupling reaction, using small amounts of olefins as additives in the presence of *in situ* generated palladium nanoparticles (**Scheme 43**).[158] However, the necessity of solvents for the work-up and purification processes is still a deficiency.

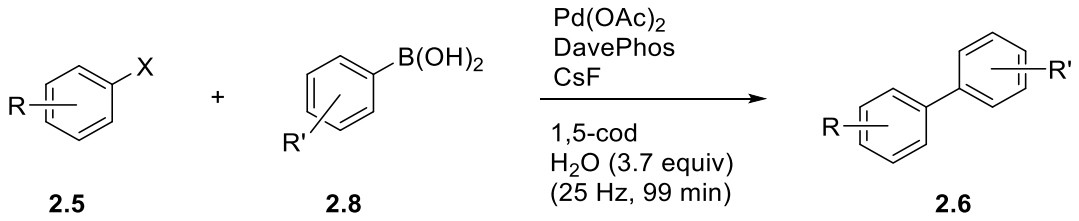

Scheme 43. *Tamae Seo's mechanochemical protocol for a solid-state Suzuki cross-coupling reaction.*[158]

Another approach that has been investigated under microwave irradiation is heterogeneous catalysis, using a catalyst immobilized on a solid support. In 2005, J. Freitag reported the application of porous glass carriers as an effective, reusable and sustainable catalytic system.[159] Not long after, Christine Schmöger and co-workers published their studies using palladium on porous glass as an active and easily recoverable ligandless catalyst in water under aerobic conditions.[160]

After analysing the key features of each reaction, the advantages of organoborane reagents, including their high stability, low toxicity, and simplicity of introduction into various substrates in comparison to the organostannane and organozinc species, render the Suzuki-Miyaura reaction the best candidate for the formation of the C-C bond needed for the purposes of this project. For this reason, the investigation of the cross-coupling step for the synthesis of the biphenyl intermediates started with haloanilines and phenylboronic acids.

2.2.1. Cross-coupling of haloanilines and boronic acids

The investigation started with the Suzuki cross coupling reaction to synthesise the biphenyl species. A range of phenylboronic acids were reacted with 2-bromoaniline, as haloanilines have been shown to be effective precursors for this kind of reaction.[138] The investigation started with two different electronic systems for the boronic acid: one electron-poor (4-nitrophenylboronic acid) and one electron-rich (4-methoxyphenylboronic acid). After that, two fluorinated boronic acids were explored as they would be of biological interest in future applications. The initial conditions employed, under microwave irradiation,[154] were at 125 °C for 35 min in a pressure-rated sealed tube, in basic media using sodium carbonate, with one of the most commonly used palladium catalysts, 1,1-bis(diphenylphosphino)ferrocenedichloropalladium(II), which had been reported to afford coupling products in high yields, after short periods of time.[161] This species is known to act as a precatalyst and is reduced to Pd(0) to initiate the catalytic cycle (**Table 1**).

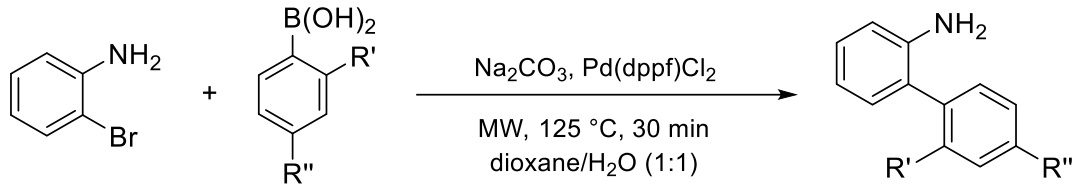

Table 1. *Initial study of the Suzuki coupling of 2-bromoaniline.*

Entry	R'	R''	Compound	Yield (%)[a]
1	H	NO_2	**2.11**	95
2	H	OCH_3	**2.12**	99
3	F	F	**2.13**	70
4	CF_3	CF_3	**2.14**	17

a) Isolated yield after purification by flash column chromatography.

As shown in **Table 1**, after a few experiments, it was observed that Pd(dppf)Cl_2 provided impressive results for the reaction of *para*-substituted boronic acids, with almost quantitative yields after flash column chromatographic purification for both electron-rich and electron-poor arylboronic acids (entries 1 and 2). Nevertheless, yields started to decline when a substituent was in the *ortho*-position of the boronic acid, with the largest reduction observed for the bulkier substituent (entries 3 and 4). This could be a consequence of, due to the size of its ligands, the catalyst experiencing steric hindrance in reaction with the boronic acid with an *ortho*-substituent or that protodeborylation in these cases is a competing side reaction.

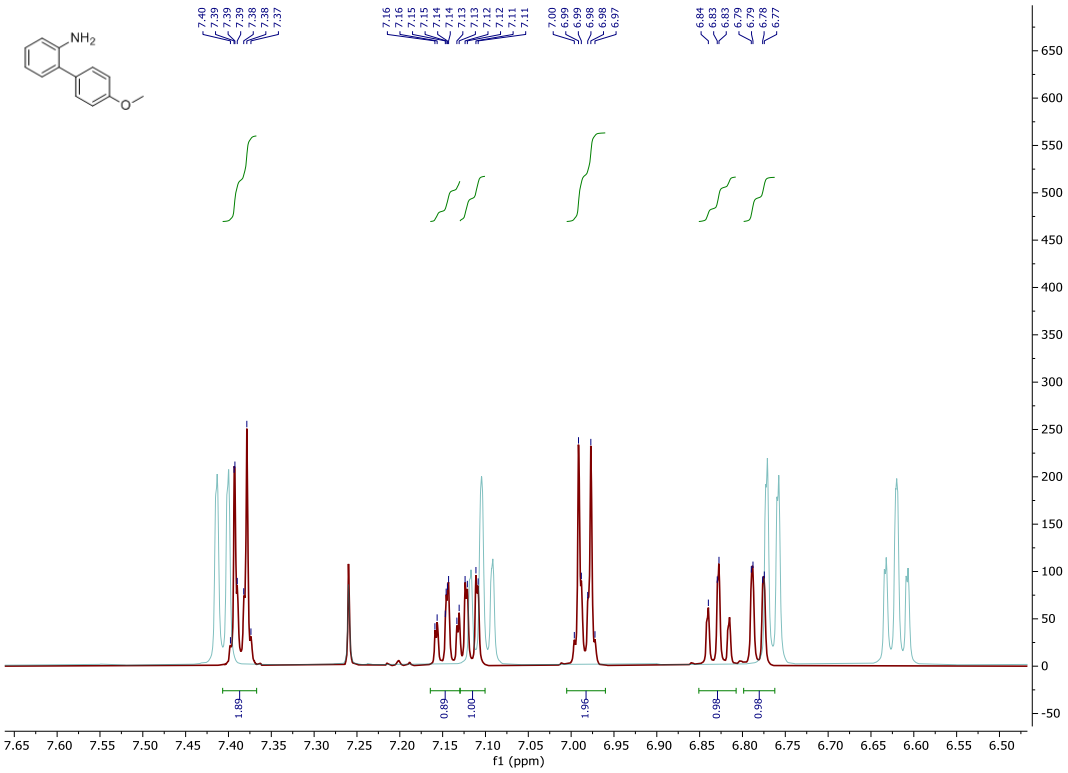

Figure 20. *[1]H-NMR spectrum of 2-(4'-methoxyphenyl)aniline (**2.12**). Red signals are attributed to the product, and blue signals are 2-bromoaniline used as a reference (the starting material).*

[1]H-NMR spectroscopic analysis showed good evidence for formation of the product, coupled biphenyl **2.12** (**Figure 20)**. When comparing the spectra of the product (red signals) with 2-bromoaniline (blue signals), two new signals integrating to 2H appeared at δ = 7.40 and 6.97 ppm, which are the 2 pairs of chemically equivalent protons in the ring adjacent to the aniline. The coupling responds to an AA'XX' system for *p*-disubstituted benzenes, where the protons are chemically equivalent but not magnetically equivalent. Besides, H3 (aniline proton on the *α* position of the phenyl group) shifted from δ = 7.42 ppm to 7.05 ppm due to the exchange of the bromine to an electron rich aromatic group. HRMS also showed the protonated molecular ion MH^+ at *m/z* 200.1073, matching with the theoretical mass of product **2.12**.

The mechanism for this reaction is shown in **Scheme 44**. The first step is the oxidative addition of *in situ* generated palladium(0) **2.15** to the haloaniline **2.16**, followed by substitution of the halogen atom on the resulting Pd(II) intermediate **2.17** by an hydroxyl group due to the presence of base. The boronate complex **2.18**, also formed by reaction of the boronic acid with the base, undergoes a transmetalation reaction forming a bis-arylated palladium(II) intermediate **2.19**. Eventually, reductive elimination releases the desired product **2.20**, restoring the original palladium(0) catalyst **2.15**. All of the methods previously mentioned have a very similar mechanism, including oxidative addition, transmetalation and reductive elimination as key steps.

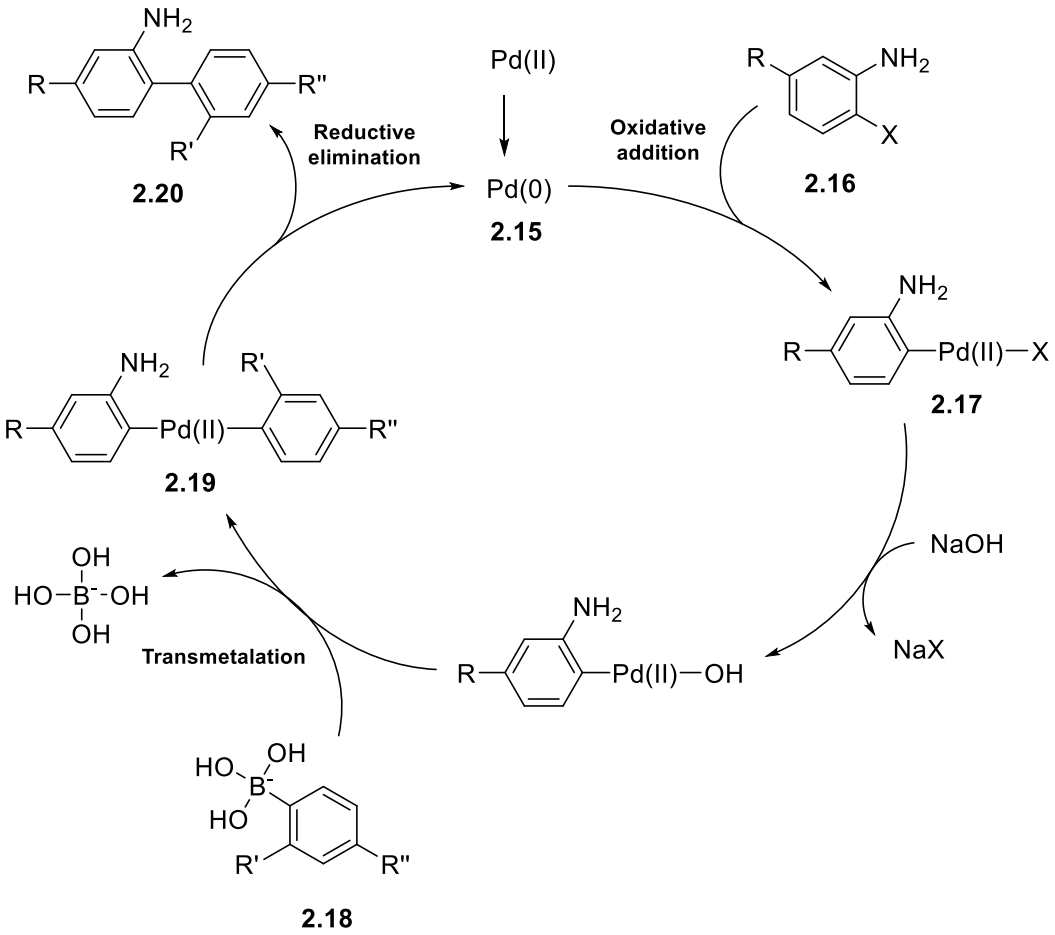

Scheme 44. *Suzuki-Miyaura cross-coupling reaction mechanism. Bidentate phosphine ligands omitted around palladium for clarity.*

Given the decrease in isolated yield observed in cases with an *ortho*-substituent, it was hypothesised that steric hindrance from the ligands attached to the Pd atom could be occurring when the boronic acid underwent transmetalation. The presence of the two (diphenylphosphino)ferrocene groups could affect the transmetalation step, where palladium bonds to the phenyl species previously attached to the boronic acid. To explore this possibility, tetrakis(triphenylphosphine)palladium(0) was tested with differently substituted boronic acids to compare the efficiency of this significantly reduced volume catalyst. A comparison between the structures of both catalysts is shown in **Figure 21.**

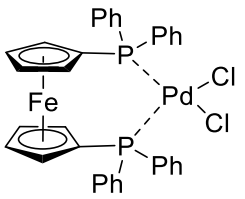

$Pd(dppf)Cl_2$

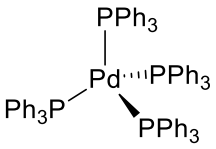

$Pd(PPh_3)_4$

Figure 21. *Structures of [1,1'-bis(diphenylphosphino)ferrocene]palladium(II) dichloride and tetrakis(triphenylphosphine)palladium(0)*

Additionally, 2-iodoaniline was selected to replace 2-bromoaniline in an attempt to optimize the yield, given that the oxidative addition of iodides should be more facile than for bromide compounds, and although bromide was providing good results iodine should maintain or improve them. A summary of the results for different compounds with each haloaniline and catalyst are shown in **Table 2**.

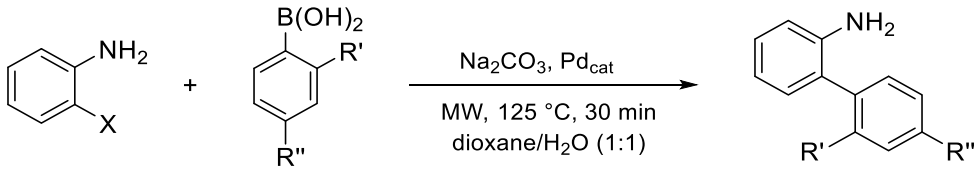

Table 2. *Comparison of the effects of the palladium catalyst on the reaction yield.*

Entry	X	R'	R''	Catalyst	Compound	Yield (%)[a]
1	Br	H	NO_2	$Pd(dppf)Cl_2$	**2.11**	**95**
2	I	H	NO_2	$Pd(PPh_3)_4$	**2.11**	61
3	I	H	NO_2	$Pd(dppf)Cl_2$	**2.11**	92
4	Br	H	OCH_3	$Pd(dppf)Cl_2$	**2.12**	**99**
5	I	H	OCH_3	$Pd(PPh_3)_4$	**2.12**	75
6	I	H	OCH_3	$Pd(dppf)Cl_2$	**2.12**	96
7	I	F	Br	$Pd(dppf)Cl_2$	**2.21**	56
8	I	F	Br	$Pd(PPh_3)_4$	**2.21**	36
9	Br	F	F	$Pd(dppf)Cl_2$	**2.13**	70
10	I	F	F	$Pd(PPh_3)_4$	**2.13**	**90**
11	I	CF_3	CF_3	$Pd(dppf)Cl_2$	**2.14**	17
12	I	CF_3	CF_3	$Pd(PPh_3)_4$	**2.14**	**68**

a) Isolated yield after purification by flash column chromatography.

The comparison between entries 1 and 3, and 4 and 6, suggested that the use of 2-iodoaniline over 2-bromoaniline does not detrimentally affect the yield in a negative way, so the iodide was used for subsequent studies as it may give better results than the bromo analogue for less efficient reactions. It can also be observed that the use of $Pd(PPh_3)_4$ led to improvements in yields for *ortho*-substituted phenylboronic acids (entries 10 and 12), although $Pd(dppf)Cl_2$ was still more efficient for *para*-substituted analogues (entries 3 and 6). This did not apply to compound **2.21** (entries 7 and 8), where a Br substituent was present on the boronic acid and competing reactions are possible. It was assumed that, although $Pd(dppf)Cl_2$ is very effective as a catalyst for the coupling of monosubstituted boronic acids, the presence of groups in the *ortho*-position decreased the efficiency of the catalysts, and therefore, for disubstituted boronic acids, $Pd(PPh_3)_4$ appeared to be more suitable due to its smaller ligand size. Subsequent reactions were carried out in accordance with this hypothesis.

Microwave-assisted reactions offer great advantages compared with batch reactions. The main advantage is the shortened reaction time: a Suzuki reaction in batch is typically carried out overnight, while a microwave assisted Suzuki reaction might usually take 35 minutes to reach completion. However, reaction scale is one of the limitations of this method, as the largest vials available for the CEM Discover™ microwave reactor have a capacity of 35 mL, and the maximum amount of solvent tends to be less than half the capacity of the vessel for sealed reaction operations (open vessel reactions can be performed in larger vessels, but are better performed with conductive heating). Although the concentration of reagents could be increased, there is not the possibility of carrying out the reaction on multigram scale as, at much higher concentrations, the yields would be expected to decrease. As large quantities of some of the biphenyl amines were required, a batch method for the cross-coupling reaction, previously studied in the group, was investigated to provide sufficient quantity of the desired products. This method, similar, to the microwave-assisted method, consisted of using the same reagents and stoichiometry, but in a THF-H_2O (1.1) solvent system, stirring at 80 °C overnight. The results for the synthesis of a range of biphenyl targets using both methods are shown in **Table 3.**

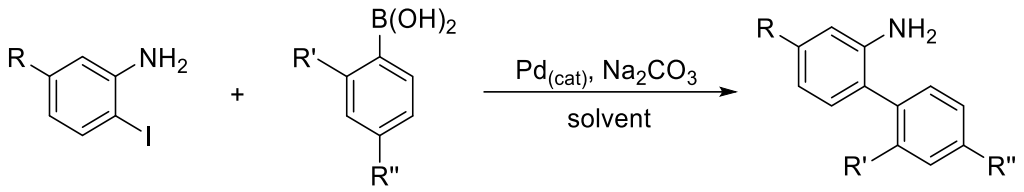

Table 3. *Microwave and batch methods comparation for the Suzuki-Miyaura cross-coupling reaction.*

Entry	R	R'	R''	Catalyst	Compound	Microwave yield (%)[a,b]	Batch Yield (%)[a,c]
1	H	H	OCH_3	$Pd(dppf)Cl_2$	**2.12**	99	91
2	H	F	F	$Pd(PPh_3)_4$	**2.13**	90	51
3	H	CF_3	CF_3	$Pd(PPh_3)_4$	**2.14**	68	74
4	H	F	CF_3	$Pd(PPh_3)_4$	**2.22**	85	84
5	H	F	CH_3	$Pd(PPh_3)_4$	**2.23**	80	99
6	H	OCH_3	F	$Pd(PPh_3)_4$	**2.24**	80	83
7	OCH_3	F	F	$Pd(PPh_3)_4$	**2.25**	60	29
8	OCH_3	H	OCH_3	$Pd(dppf)Cl_2$	**2.26**	87	89
9	OCH_3	F	CH_3	$Pd(PPh_3)_4$	**2.27**	77	35

a) Isolated yield after purification by flash column chromatography.
b) Reaction mixture was irradiated in a pressure-rated sealed tube at 125 °C (initial power 150 W) for 35 min in dioxane-water (1:1).
c) Reaction mixture was stirred at 80 °C overnight in THF-H_2O (1:1).

Both methods were roughly equally effective for monosubstituted boronic acids (entry 1), but with the addition of a substituent in the *ortho*-position of the boronic acid some differences appeared in certain cases. Entry 2 showed a significantly improved yield for compound **2.13** under microwave irradiation, which could indicate the use of electron-poor systems or the presence of a fluorine atom in the R' position would require harsher conditions and e.g. retard the transmetalation step due to the weaker nucleophilicity of the boronic acid. This hypothesis could justify the similar performance of both methods for compound **2.24** (entry 6)**,** as the presence of the methoxy group in the R' position should increase the electron density facilitating the transmetalation step. However, for compounds **2.14** and **2.22** both methods provided almost the same yield (entries 3 and 4), suggesting that electronic factors might not always be significant, as hypothesised. A better yield was obtained in batch for compound **2.23** (entry 5), which appeared an unusual result, which could suggest that in some cases the reaction time is more important than the temperature or the irradiation. Overall, no universal trends were observed for differences in the boronic acid substitution. The presence of a methoxy group in the aniline, as in entries 7 and 9 showed a clear improvement on the yield when the reaction was carried out under microwave

irradiation, and entry 8 showed the same effectiveness for both methods. Entries 7 and 9 also exhibited a reduction in efficiency, which could suggest that the presence of an electron-donating group on the aniline could disfavour the oxidative addition step. Although the batch method was proved to be efficient, the microwave assisted reaction provided similar or better yields in most cases and the reduced reaction time was a notable advantage. The microwave method was chosen for the synthesis of the biphenyl intermediates, and it was only substituted for the batch method when large amounts of product were required (over 2 g). Nineteen compounds were synthesised using a microwave assisted Suzuki-Miyaura cross-coupling reaction, following the considerations previously described, and are reported in **Table 4**.

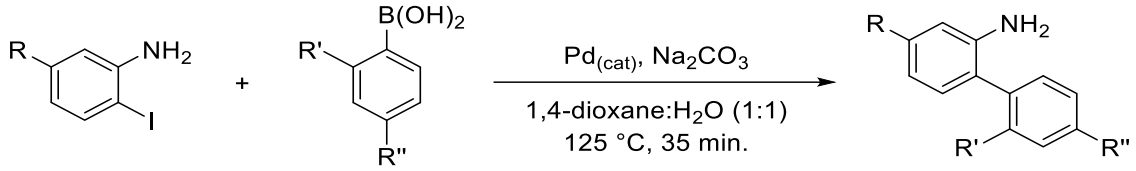

Table 4. *Optimum methods found for the synthesis of biphenyl amines.*

Entry	R	R'	R''	Catalyst	Compound	Yield (%)[a]
1	H	H	NO_2	$Pd(dppf)Cl_2$	**2.11**	95
2	H	H	OCH_3	$Pd(dppf)Cl_2$	**2.12**	99
3	H	H	CF_3	$Pd(dppf)Cl_2$	**2.28**	80
4	H	F	Br	$Pd(dppf)Cl_2$	**2.21**	56
5	H	F	F	$Pd(PPh_3)_4$	**2.13**	82
6	H	CF_3	CF_3	$Pd(PPh_3)_4$	**2.14**	68
7	H	F	CF_3	$Pd(PPh_3)_4$	**2.22**	85
8	H	F	CH_3	$Pd(PPh_3)_4$	**2.23**	80
9	H	OCH_3	F	$Pd(PPh_3)_4$	**2.24**	80
10	H	OCH_3	OCH_3	$Pd(PPh_3)_4$	**2.29**	85
11	H	OCH_3	CF_3	$Pd(PPh_3)_4$	**2.30**	85
12	OCH_3	H	OCH_3	$Pd(dppf)Cl_2$	**2.26**	83
13	OCH_3	F	F	$Pd(PPh_3)_4$	**2.25**	80
14	OCH_3	OCH_3	F	$Pd(PPh_3)_4$	**2.31**	85
15	OCH_3	F	CH_3	$Pd(PPh_3)_4$	**2.27**	77
16	F	H	OCH_3	$Pd(dppf)Cl_2$	**2.32**	88
17	F	F	F	$Pd(PPh_3)_4$	**2.33**	46
18	F	F	CH_3	$Pd(PPh_3)_4$	**2.34**	76
19	F	OCH_3	F	$Pd(PPh_3)_4$	**2.35**	77

a) Isolated yield after purification by flash column chromatography.

As stated before, the coupling with non-substituted haloanilines and *para*-substituted boronic acids provided excellent results for both electron-withdrawing and electron-donating groups (entries 1 and 2), although the yield decreased slightly when a CF_3 moiety was present (entry 3). The presence of a bromine gave the possibility of a side reaction for the boronic acid, thereupon entry 4 is considered an exception.

The addition of a functional group in position R' also moderately affected the yield of the reaction. The presence of a fluoro group (EWG) led to a lower yields (~80%), and this result was consistent for different electronic profiles (entries 5, 7 and 8). However, when a CF_3 group was present in that position, the yield decreased to less than 70% (entry 6). One possible reason could be the steric constraints of the group, which are more significant than the corresponding fluorine atom. This occurrence, however, was not observed for methoxy-containing analogues (entries 9-11), although the electronic effects of this EDG could counter any steric effects. The results suggest that electron-withdrawing groups on the boronic acid can decrease the effectiveness of the reaction, as well as bulky groups on the R' position. EDG on the boronic acid ring seem to favour the reaction and counter any steric effects from *ortho*-substitution.

The presence of a methoxy group on the bromoaniline did not have a positive effect on the outcome of the reactions. If entries 2 and 12 are compared, it can be deduced that for monosubstituted boronic acids the presence of this group decreased the efficiency of reaction. However, it did not have a significant impact on the reaction of disubstituted boronic acids, as the yields obtained were similar to those previously obtained for non-substituted haloanilines (entries 13-15). The reaction was also tested with a fluorine-containing haloaniline, which again gave reduced yields in reaction with monosubstituted boronic acids, but not in a discernible manner for disubstituted boronic acids (entries 16, 18 and 19). The synthesis of biaryl **2.33** proceeded in lower yield (entry 17), in comparison to the rest of compounds generated; this reaction was repeated to confirm the anomaly. The inductive effect of three fluorine atoms would have caused a significant decrease in the electron density of the system, negatively affecting its reactivity.

In summary, the microwave assisted Suzuki cross coupling reaction was proved to be an efficient method for the synthesis of differently substituted biphenyl amines, providing in most cases yields greater than 75% in 35 min reaction time. The method proved to be compatible with electron-donating and electron-withdrawing groups, although the presence of functional groups at positions R and R' could affect the yields. This technique was used to synthesise the biphenyl intermediates required in future steps for carbazole synthesis.

In order to make the process more sustainable, an alternative to microwave heating was also investigated, attempting to avoid the use of solvent in the reaction and, if possible, to develop a purification regime that avoided the use of flash column chromatography. Hence, the reaction was conducted under mechanochemical conditions (**Scheme 45**). Compound **2.12** was tested as the target of choice, as the reaction was known to be highly efficient in solution. Sodium carbonate was also used as it had been reported as an efficient base for the process,[160] with [1,1'-bis(diphenylphosphino)ferrocene]dichloropalladium(II) as catalyst. The reaction was carried out on 1 mmol scale, using a 50 mL vessel filled with 5 stainless steel balls shaking at 30 Hz for 90 min, the maximum frequency and time allowed by the instrument. The ^{1}H-NMR spectrum of the crude material showed poor conversion, and after purification by flash column chromatography the yield obtained was only 6%.

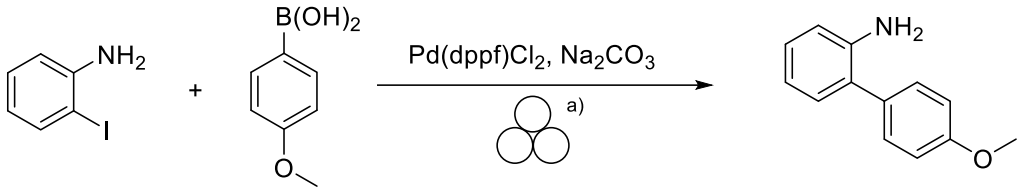

2.12

Scheme 45. *Mechanochemical Suzuki cross coupling approach. a) 90 min at 30 Hz in a 50 mL vessel with 5 balls.*

After this observation, it was found in the literature that in the absence of a supporting ligand[162] or an inorganic support material[163] this reaction provides the product in very low yield. Because of the addition of extra reagents, with extra waste products to remove, the necessity of further process optimization and the efficient results already obtained by a microwave-assisted method, further investigation of a mechanochemical route was discarded in favour of the established conditions.

2.3 Azide formation reaction

The second step of the synthesis would be the preparation of biaryl azide **2.2** (**Scheme 46**) as a suitable precursor for carbazole synthesis. The azide motif was chosen as it should undergo photochemical activation and provide the nitrene species that can react with an adjacent phenyl ring, cyclizing to the carbazole skeleton. The most general method for the preparation of aromatic azides is based on the reaction of diazonium salts with suitable azide sources.[164,165] This was previously studied in the group based on reported work by Galli *et al*. and applied to aminopyridines.[166]

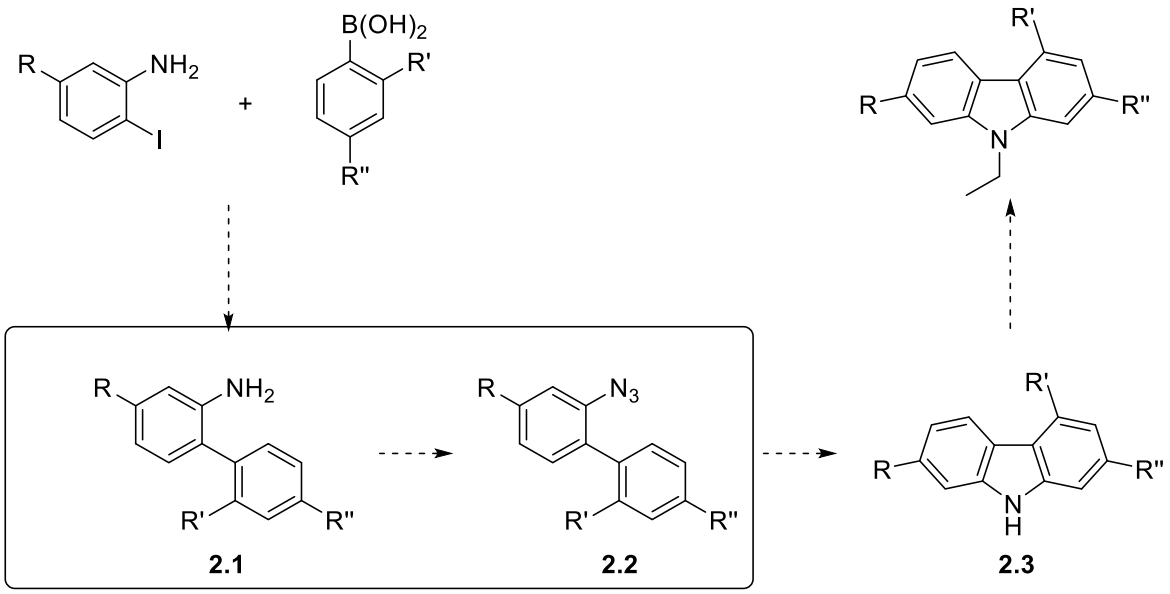

Scheme 46. *Azide formation reaction scheme.*

The chemistry of azides and nitrenes has attracted the attention of chemists since the discovery of phenyl azide by Griess over 100 years ago[167] and the first proposal of nitrenes as reaction intermediates by Tiemann in 1891.[168] However, interest in azides among organic chemists has been relatively modest due to the reported instability of these compounds. Low molecular weight azides are considered especially hazardous and were usually avoided, as they have poor thermal stability and explosive properties. Because of the hazards associated with their use, few azides were used commercially. This situation changed dramatically when Sharpless *et al.* reported the discovery of (3+2)-cycloadditions between nitriles **2.36** and organic azides **2.37** to yield the corresponding 5-membered heterocyclic compounds **2.38** (**Scheme 47**).[169]

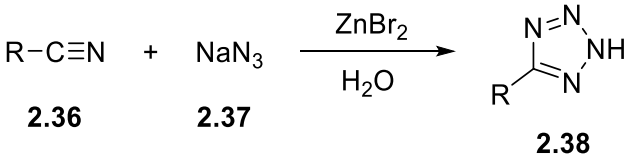

Scheme 47. *Reaction scheme for the preparation of 5-substituted 1H-tetrazoles.*

The generation and handling of organic azides normally involves a number of safety concerns, particularly on scale, which can limit the use of these important compounds. Thus, the utilization of flow processes to improve the safety of the reaction appears as a good approach to minimize the risk, carrying out the transformation in a tube reactor with precise control of the temperature and pressure. According to this, Catherine J. Smith's group published a flow process which provides the synthesis of these compounds either isolated as final products, purified in-line with the use of solid supported reagents, or carried on directly to further transformations without isolation within a contained flow system to deliver

high quality products in a safe and efficient manner.[170,171] **Scheme 48** shows the reaction scheme for the synthesis and in-line purification of azides in flow published by Smith. With the addition of more pumps and reactors after the columns, there is the possibility of conducting further reactions, such as aza-Wittig or the Staudinger reaction without the necessity of isolating the azide intermediate.

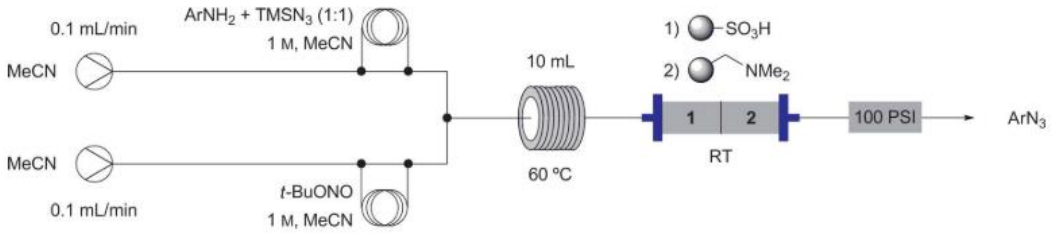

Scheme 48. *Reaction scheme for the synthesis and purification of aryl azides in flow.*[171]

2.3.1. Biaryl azide synthesis from biaryl amine precursors

In the early stages of the investigation, the synthesis of carbazoles was investigated in parallel with the synthesis of carbolines, due to the similarity in the structure. Therefore, the first steps of the study into the azide formation reaction started with both aminopyridines and biphenylamines, following work conducted previously in the group based upon Galli's publication.[166] First attempts were conducted with $NaNO_2$ and NaN_3 in acidic media (H_2SO_4 15%), and 3-aminopyridine was chosen as an electron poor substrate to explore, assuming that if it was successful for this substrate it should work even better for biphenyl and pyridoaniline precursors. The reaction provided poor yields, but it was discovered that the pH of the neutralized solution had a crucial effect on the solubility of the product in the organic phase when extracting with diethyl ether. Besides, the addition of urea after the diazonium salt formation to remove the excess of nitrosonium cation prevented its interaction with the azide anion instead of generating the target organic azide.[164,172] These two occurrences improved the yield significantly, and with the addition of urea before the addition of NaN_3 and eventual pH controlled neutralization 3-azidopyridine (**2.39**) and the pyridianiline analogue 3-azido-2-phenylpyridine (**2.40**) could be synthesised and isolated with a yield of 85% and 90% (**Scheme 49**).

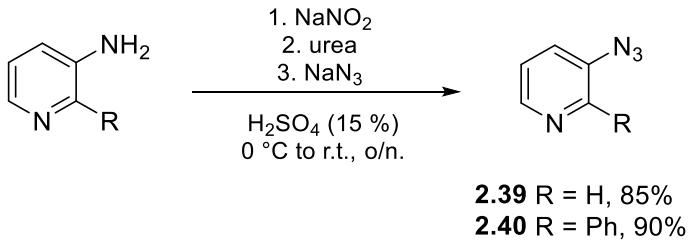

Scheme 49. *Synthesis of 3-azidopyridine (**2.39**) and 3-azido-2-phenylpyridine (**2.40**).*

After this success, different pyridoanilines and biphenyl amines were converted to the corresponding azides successfully under batch conditions (**Table 5**) in excellent yield in order to establish the viability of each process.

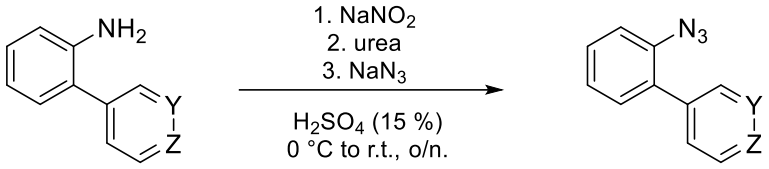

Table 5. *Azide formation under batch conditions.*

Entry	Y	Z	Compound	Yield (%)
1	CH	CH	**2.41**	97
2	N	CH	**2.42**	89
3	CH	N	**2.43**	91
4	CH	C-NO_2	**2.44**	95

a) Isolated yield after neutralization with sat. $NaHCO_3$ and extraction with diethyl ether.

The method seemed to work almost quantitatively for biphenylamines (entries 1 and 4) and in slightly reduced yield for pyridoaniline precursors (entries 2 and 3), but still was around 90% yield. The lower reactivity of the pyrido substrates was attributed as the reason for the reduction in isolated yield, although losses in the isolation process could not be ruled out. Although ^{1}H-NMR spectroscopic analysis provided good evidence of conversion, with a significant downfield shift of the proton adjacent to the amino group, for the first experiments infra-red spectroscopy was used to confirm the transformation had taken place. **Figure 22** shows the IR spectrum of 3-azido-2-phenylpyridine (**2.40**). The disappearance of the broad absorption for the N-H stretch and the appearance of a signal at 2106 cm^{-1} due to the N=N=N stretch indicated the success of reaction. LCMS was not useful to determine the mass due to the instability of these compounds, and due to the high toxicity and potential explosiveness of aryl azides they were reacted without further characterization.

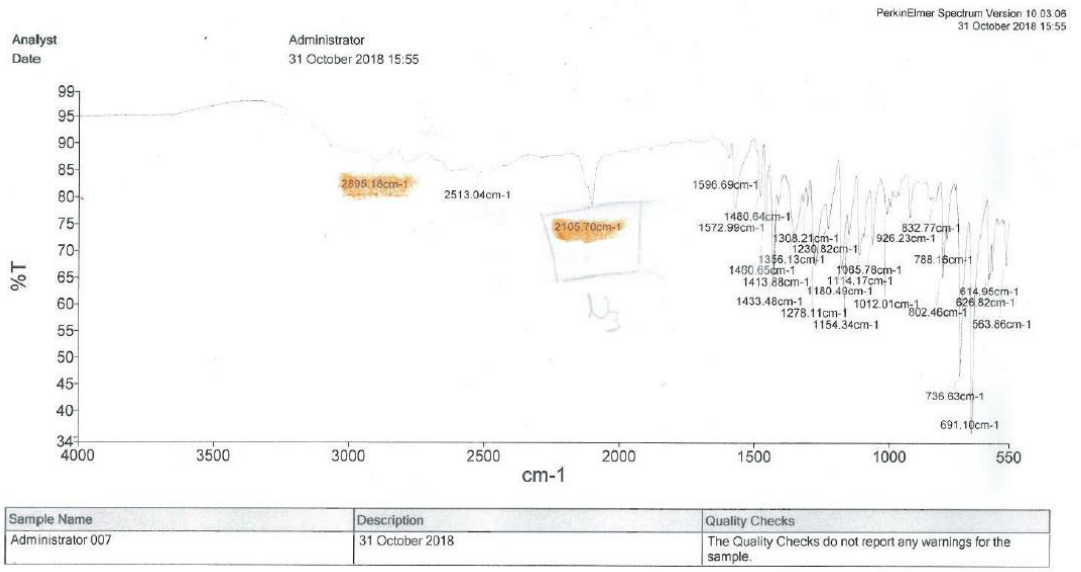

Figure 22. *IR spectrum of 3-azido-2-phenylpyridine (**2.40**).*

The transformation occurs in 2 main steps via a diazonium salt intermediate **2.45**, produced from the reaction between an amino group and the nitrosonium cation formed by protonation of the nitrite anion in acidic medium. (**Scheme 50**).

Step 1

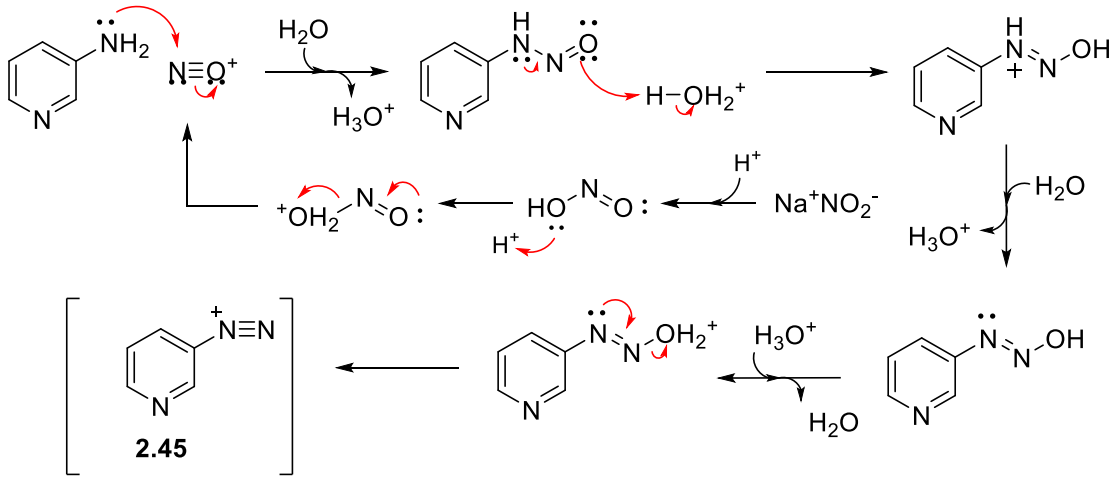

Scheme 50. *Diazonium salt intermediate **2.41** formation mechanism.*

In the second step, the mechanism of aryl azide formation from the diazonium intermediate **2.45**, generated *in situ*, and the azide ion has been extensively studied, and it is generally agreed that this reaction progresses via pentazene and pentazole intermediates **2.46** formed by attack of the azide species on the terminal nitrogen of the diazonium intermediate **2.45** (**Scheme 51**).[170]

Step 2

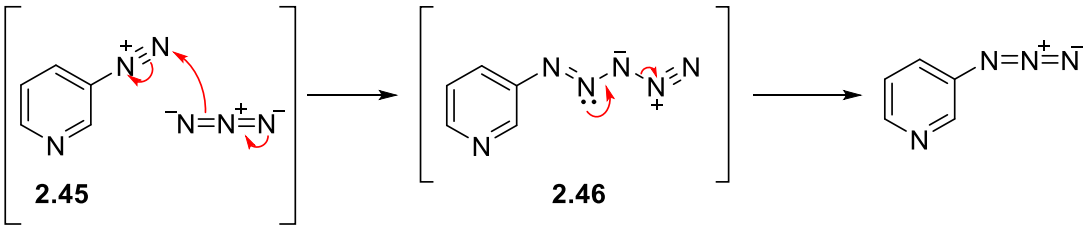

Scheme 51. *Pentazene intermediate* ***2.46*** *involved in the mechanism of azide formation.*[170]

Some substituted biphenyl amines, however, did not dissolve completely in the aqueous system, and in some cases the reaction did not proceed to completion. Given that solubility issues threatened an automated multistep flow process, and the non-acid resistant pumps of the flow reactor, a number of different acids and solvent systems were investigated for this reaction (**Table 6**).

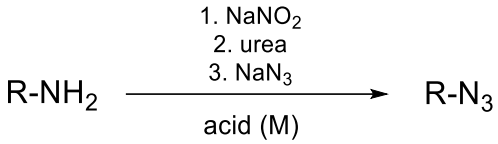

Table 6. *Results of acid and solvent screen in batch formation of the corresponding azide.*

Entry	R	Aqueous acid	Compound	Yield
1	3-Pyridinyl	H_2SO_4 (15%)	**2.39**	85
2	3-Pyridinyl	H_2SO_4 (0.017 M)	**2.39**	0
3	3-Pyridinyl	CH_3COOH (15%)	**2.39**	60
4	3-Pyridinyl	H_3PO_4 (15%)	**2.39**	65
5	2-Biphenyl	H_2SO_4 (15%)	**2.41**	97
6	2-Biphenyl	H_2SO_4 (15%), dioxane/water (3:2)	**2.41**	92

a) Isolated yield after neutralization with sat. $NaHCO_3$ and extraction with diethyl ether.

Sulphuric acid was efficient as an acid mediator for azide formation for both biphenylamine and pyridoaniline precursors (entries 1 and 5). However diluting or changing sulphuric acid to a weaker acid did not provide the same results (entries 2-4). The difference in the pH appeared to have a significant influence on the formation of the nitrosium cation. This led to the proposal to dilute the H_2SO_4 (15%) aqueous acid with an organic solvent to improve solubility without reducing the acidity of the mediator. A mixture of dioxane/water (3:2) provided excellent results (entry 6). Following these results the conditions described were used to synthesise four biphenyl azide analogues (**2.44-2.47**) for use in the

next photocyclization step. The four compounds, showed in **Table 7**, were synthesised in excellent yield under the described conditions to facilitate study of the subsequent photocyclization.

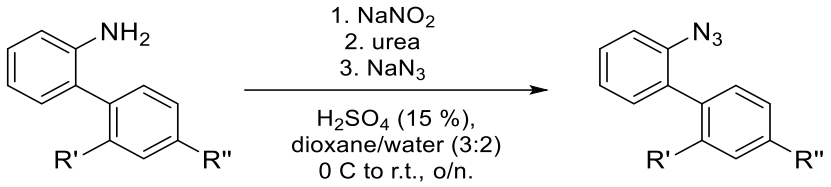

Table 7. *Azide formation under batch conditions.*

Entry	SM	R'	R''	Compound	Yield (%)[a]
1	**2.11**	H	NO_2	**2.44**	95
2	**2.12**	H	OCH_3	**2.45**	99
3	**2.13**	F	F	**2.46**	99
4	**2.21**	F	Br	**2.47**	90

a) Isolated yield after neutralization with sat. $NaHCO_3$ and extraction with diethyl ether.

After the success of the azide formation in batch, safety considerations over handling azides prompted the investigation an adaptation of this reaction to a flow process. Azide formation in flow was first studied with 3-aminopyridine and using two different methods. The first method was an adaptation of the method that provided promising results in batch, using $NaNO_2$, urea and NaN_3 in acidic medium. The second study followed previous work carried out by C.J. Smith *et al.* in 2011,[170] using $TMSN_3$ and ^tBuONO as a nitrosonium source. For both methods, different conditions were tested.

Flow process

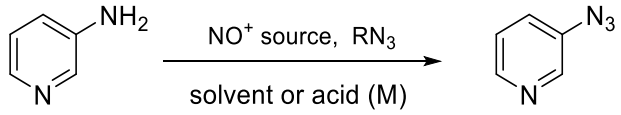

2.39

Table 8. *Azide formation with continuous flow processing.*

Entry	NO^+ source	Azide	Conditions (T, t)	Solvent	Conv. (%)
1	$NaNO_2$	NaN_3	60 °C, 50 min	CH_3COOH (0.1 M)	0
2	$NaNO_2$	NaN_3	60 °C, 50 min	CH_3COOH (1 M)	0
3	$NaNO_2$	NaN_3	60 °C, 120 min	H_3PO_4 (15%)	20
4	$NaNO_2$	NaN_3	145 °C, 120 min	H_3PO_4 (15%)	15
5	^{t}BuONO	$TMSN_3$	60 °C, 50 min	MeCN	20
6	^{t}BuONO	$TMSN_3$	80 °C, 50 min	MeCN	25
7	^{t}BuONO	$TMSN_3$	80 °C, 100 min	MeCN	10
8	^{t}BuONO	NaN_3	60 °C, 50 min	H_2O	0

a) Conversion calculated by integration of the ^{1}H-NMR signals of the crude material.

Table 8 shows the results for all of the reagents, conditions and solvents that were investigated. The first method investigated was an adaption of the method with sodium nitrite and sodium azide. Concerns about the resistance of the pumps to strong acids prompted the study of milder conditions. Although they did not provide promising results in batch, they could potentially be optimized under flow conditions. Acetic acid provided no transformation at all at different concentrations (entries 1 and 2). The acid was changed to phosphoric acid while increasing the time, and although a first result of 20% conversion seemed promising (entry 3), increasing the temperature to 145 °C made no difference to the outcome (entry 4). Hence, it was assumed that the reaction was not likely to proceed efficiently with a weaker acid under flow conditions. Similarly, Smith's method did not provide the yields expected when applied to a 3-aminopyridine precursor. Changing the solvent, the reaction time and the temperature from those given in the literature did not show any improvement in the conversion of starting material to the azide analogue (entries 5-8). When preparing the solution of $TMSN_3$ and the pyridoaniline, the evolution of a small quantity of gas was observed. It was assumed that the increased basicity of the aminopyridine must be impeding the progress of reaction or reacting in an alternative pathway with the azide reagent.

As the batch method could not be transferred to flow processing for pyrido substrates, perhaps due to a dependence on the pH of the reaction, and the alternative method using different azide and NO^+ sources could not be adapted from biphenyl substrates to pyridoanilines, it was assumed that the azide formation reaction for the synthesis of azidophenyl pyridines would have to be conducted in batch, using the previously described conditions. Hence, the investigation was then focused on the synthesis of carbazoles, changing the model substrate for azide formation from 3-aminopyridine to 2-biphenylamine. The results are displayed in **Table 9**.

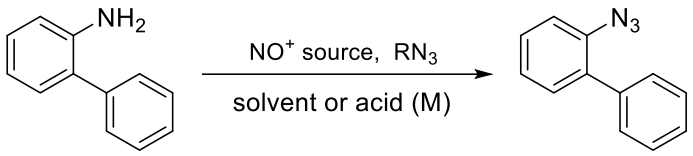

2.41

Table 9. *Azide formation under continuous flow.*

Entry	NO^+ source	Azide	Conditions (T, t)	Solvent	Conv. (%)
1	^{t}BuONO	$TMSN_3$	60 °C, 50 min	1, 4-dioxane	Quant.
2	$NaNO_2$	NaN_3	60 °C, 120 min	H_2SO_4 (15%) Dioxane/water (3:2)	80

a) Conversion calculated by integration of the ^{1}H -NMR signals of the crude material.

Despite different conditions being studied in this process, the adaptation of the simple method using $NaNO_2$, urea and NaN_3 in acidic medium H_2SO_4 (15%) in a mixture of 1,4-dioxane and water, as previously described, provided excellent results with 80% conversion to the biphenyl azide (entry 2). However, an adaptation of the method reported by C.J. Smith[170] with 1,4-dioxane (to avoid future issues with solubility) as solvent provided the best optimized method for the synthesis of arylazides with essentially a quantitative conversion (entry 1).

2.4 Photocyclisation reaction

The route required cyclisation of the biaryl azide intermediate **2.2** into the carbazole skeleton **2.3**. The first technology to be investigated for the synthesis of carbazoles was photochemistry. The reaction would occur through activation of the azide biphenyl to the nitrene form, which should cyclise into the carbazole target scaffold. It was hypothesised that the photocyclization of the azide biphenyl species into the corresponding carbazole could be easily adapted to a flow process (**Scheme 52**).

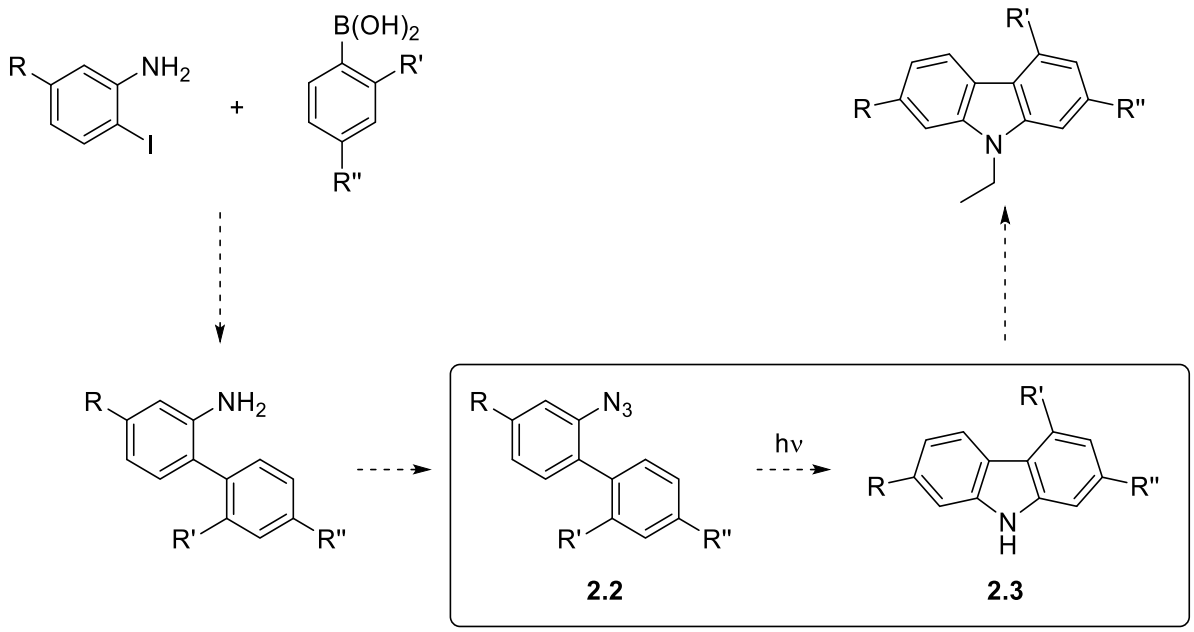

Scheme 52. *Flow process reaction scheme.*

A commercial photochemical reactor previously described was used in a flow processing study (Vapourtec UV-150). This photochemical reactor provides high intensity UV light from a high intensity medium pressure mercury lamp. **Figure 23** shows the wavelength range provided by the lamp inside the reactor. Under these conditions, the azide should be transformed into a nitrene intermediate.

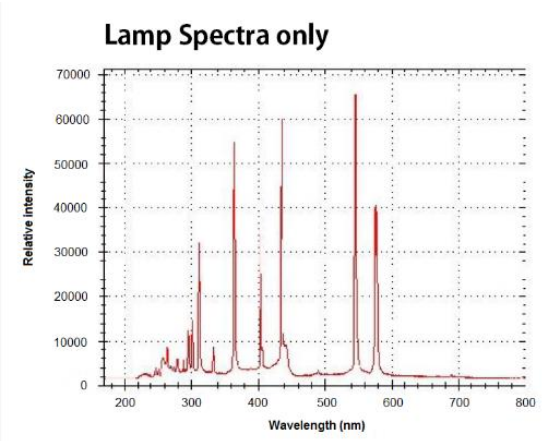

Figure 23*. Spectrum of the Hg lamp for the photochemical reactor*

As azides absorb at ~λ 350-380 nm,[173] a band-pass Type 2 filter (provided by Vapourtec) was used to ensure that the reactants were only exposed to light of the desired range of wavelengths. The filter selected, as shown in **Figure 24**, reduced the wavelength range to λ 300-400 nm.

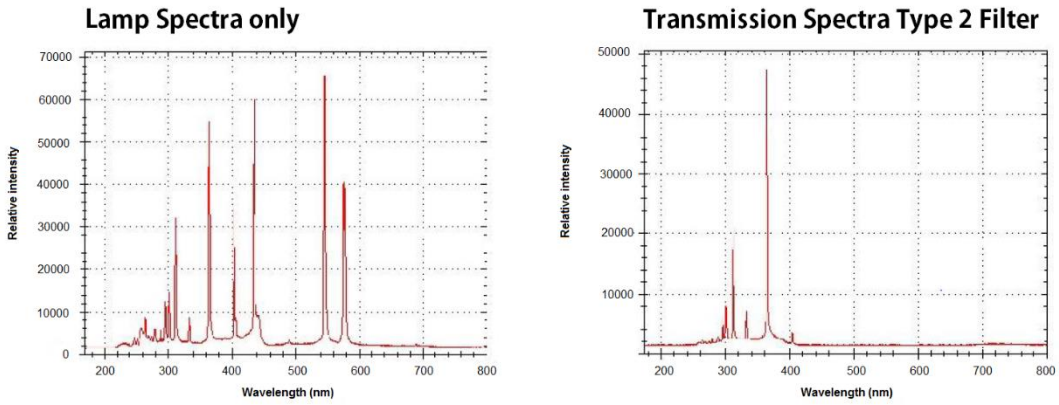

Figure 24. *Spectral profile with and without a Type 2 filter.*

2.4.1. Cyclization of photoactivated azides into carbazoles

Previous studies in Prof. John Spencer's group reported unoptimized conditions for the synthesis of the simple 9*H*-carbazole (**2.48**) using dichloromethane as solvent, with a 45% conversion obtained in 48 h under batch conditions using an UV lamp. The same reaction conducted in flow in our hands gave essentially full conversion by ^{1}H-NMR spectroscopic analysis in only 2 h with the photochemical reactor (**Scheme 53**). Although this reaction was successful for this simple precursor, the solubility of a diverse range of carbazole scaffolds under these conditions in CH_2Cl_2 was an issue of concern. For this reason, 1,4-dioxane was investigated as solvent for this reaction and provided the same conversion by ^{1}H-NMR spectroscopic analysis.

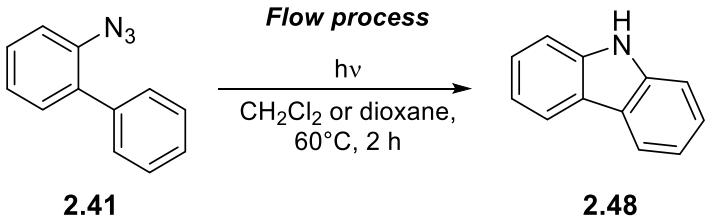

Scheme 53. *Flow photochemical cyclization reaction.*

Figure 25 shows the ^{1}H-NMR spectrum of the crude material after the flow processed photochemical reaction. It was observed that, after 2 hours, the cyclisation took place in almost full conversion. The ^{1}H-NMR was analysed in d_6-DMSO as solvent so the N-H proton could be observed, as a decisive indicator of the transformation. In this particular case, the symmetry of the product obtained after cyclisation also helped give a clear indicator of the formation of the product. As this compound is widely known and commercially available, the data could be compared to pure commercial material, confirming its identity.

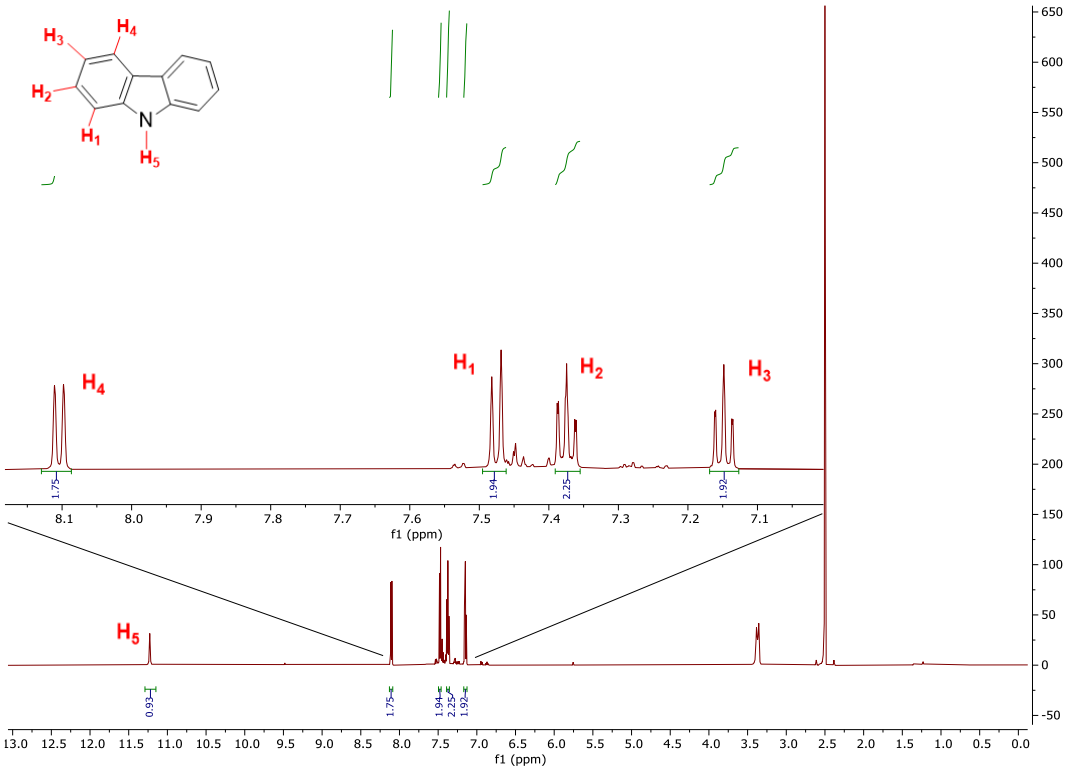

Figure 25. *^{1}H-NMR spectra of the carbazole **2.48** reaction crude after the flow process reaction.*

Given the success and efficiency improvement of transferring the 2-biphenylazide (**2.41**) photocyclization to a flow process, a number of the biphenyl azides obtained from the cross-coupling and azide formation reactions were processed in the photochemical reactor to give high conversion (by ^{1}H-NMR spectroscopic analysis, not isolated yield) in 1,4-dioxane as solvent (**Table 10**).

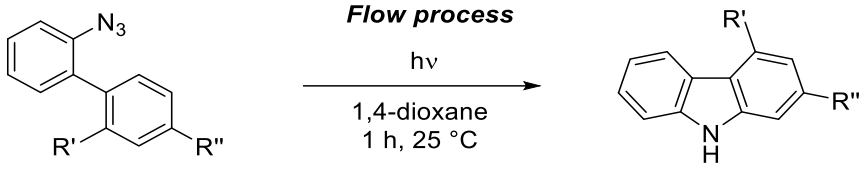

Table 10. *Results for the 2-step reaction under flow process.*

Entry	SM	R'	R''	Compound	Flow conv.(%)[a]	Yield (%)[b]
1	**2.41**	H	H	**2.49**	90	-
2	**2.44**	H	NO_2	**2.50**	-	-
3	**2.45**	H	OCH_3	**2.51**	87	28
4	**2.46**	F	F	**2.52**	88	22

a) Conversion calculated by integration of the ^{1}H -NMR signals of the crude material.

b) Isolated yield after flash column chromatography.

Entries 1, 3 and 4 proved the reproducibility of the method with EDG and EWG groups, but the nitro analogue (entry 2) did not provide the desired result. For this compound, a blockage in the reactor occurred and a mixture of different compounds was identified in the ^{1}H-NMR spectrum of the obtained crude material. Further studies of azides containing this functional group were discarded due to the suspected photoreduction of the nitro group to the corresponding hydroxylamine analogue.[174,175] Although compounds **2.51** and **2.52** provided high conversion, attempts at purification gave isolated yields that were much lower than expected. The two-step reaction showed conversions over 80% in all cases but, after purification, the amount of product obtained was unexpectedly small, despite different purification methods being investigated. It was suspected that crystallization during chromatographic purification, even in the presence of triethylamine, had dramatically affected the isolated yield and so flash column chromatography was ruled out. A range of solvents was employed to attempt to recrystallize the product, but none of them provided the corresponding carbazole in high purity or yield. Alternative methods were also tested such as extraction or trituration, employing different solvents and mixtures of solvents, unsuccessfully. The appearance of the crude material, which was more glue-like than an easily manipulated solid, frustrated further purification efforts. An inline purification using column immobilization after the two reactors was also suggested, but the increased pressure of the system caused by the presence of these columns was not compatible with the maximum pressure of the photochemical reactor (10 Bar), so was deemed to be unsuitable. Eventually, as the purification method had become a bottleneck and the conversions were high enough to proceed with the synthesis, it was decided to continue to the next step without purification.

2.5 Carbazole formation from biphenylamines in flow

As stated previously, the key step of this approach to carbazole formation is a photocyclization, proceeding via an azide intermediate. The investigation of flow processing first studied the reactions involved separately. At first, the azide formation was studied with no encouraging results. Then, attention focused on the photocyclization step which gave dramatically improved results when the photochemical reactor was employed in flow, compared to the batch conditions using a UV lamp. The method appeared to be more efficient when carrying out the azide formation step in batch, as illustrated in **Scheme 54**.

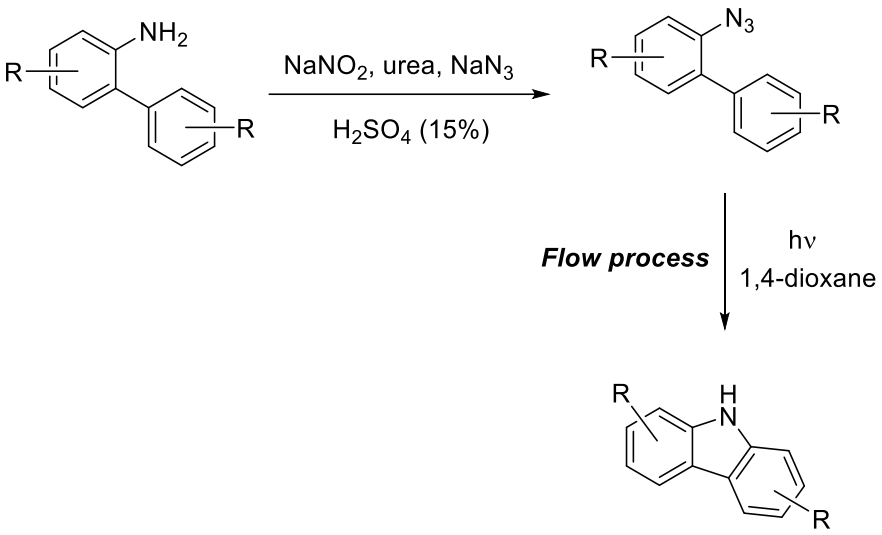

Scheme 54. *First method tested for the synthesis of carbazoles.*

However, the safety improvements from carrying out the azide reaction in flow, and the convenience of carrying out the two steps in series, in terms of time, solvent use and waste production, led us to study the azide formation in flow further to enable a two-step, one process, method. Given the success optimizing the two steps separately in flow, the immediate goal was to perform both reactions in cascade. Thus, the optimized flow process would consist of a two-step reaction conducted with two different reactors connected in series with a commercial Vapourtec R2C+/R4 system, using a standard PFA coil reactor and a UV-150 Photochemical Reactor. The azide formation reaction would take place in the PFA coil reactor when solution *A*, with the corresponding biphenyl amine and the trimethylsilyl azide, and solution *B*, containing *tert*-butyl nitrite, both in 1,4-dioxane, were mixed and heated for 50 min at 80 °C.[170] Although the three reagents could have been dissolved in the same solution, ^{t}BuONO was dissolved in a different reagent bottle to prevent the reaction from initiating outside of the reactor. Besides, as the two solutions were pumped from different pumps, and the efficiency of these pumps was often not constant during all of the process, the equivalents of the two reagents (especially ^{t}BuONO) were increased in order to minimise the effect of fluctuations in the flow rate. The product of this reaction, containing the biphenyl azide intermediate, was flushed directly to the photochemical reactor where it was irradiated for 50 min at λ 300 to 400 nm at a temperature of 80 °C. The reaction scheme is illustrated in **Scheme 55.**

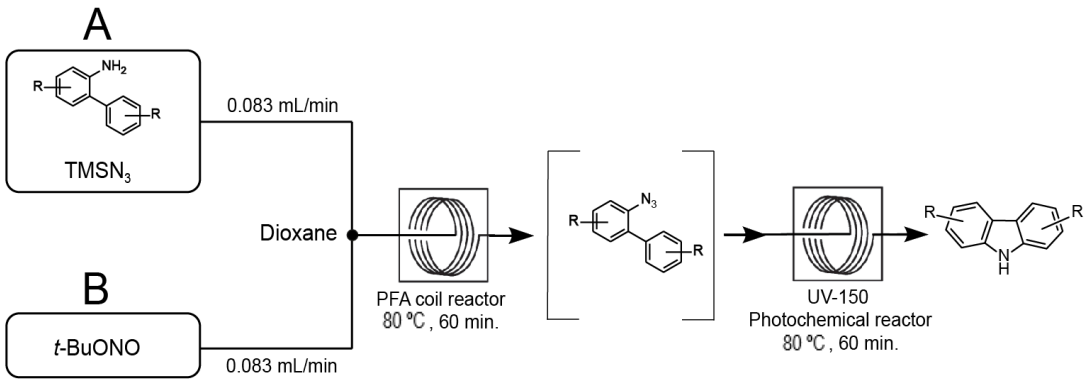

Scheme 55. *Flow reaction scheme.*

Using this method, 17 different carbazole scaffolds were synthesised from the biphenyl amine precursors with conversions over 75% (**Table 11**). Apart from compound **2.49**, the precursor for which was commercially available, all of the starting materials were obtained from the Suzuki cross-coupling step, previously described.

Flow process

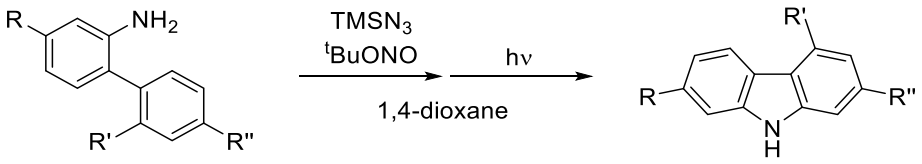

Table 11. *Results for the 2-step reaction under flow processing.*

Entry	SM	R	R'	R''	Compound	Flow conv.[a]
1	-	H	H	H	**2.49**	85
2	**2.23**	H	F	CH_3	**2.53**	91
3	**2.13**	H	F	F	**2.52**	79
4	**2.12**	H	H	OCH_3	**2.51**	87
5	**2.22**	H	F	CF_3	**2.54**	84
6	**2.24**	H	OCH_3	F	**2.55**	78
7	**2.28**	H	H	CF_3	**2.56**	80
8	**2.14**	H	CF_3	CF_3	**2.57**	76
9	**2.29**	H	OCH_3	OCH_3	**2.58**	87
10	**2.30**	H	OCH_3	CF_3	**2.59**	88
11	**2.27**	OCH_3	F	CH_3	**2.60**	77
12	**2.31**	OCH_3	OCH_3	F	**2.61**	91
13	**2.25**	OCH_3	F	F	**2.62**	82
14	**2.32**	F	H	OCH_3	**2.63**	83
15	**2.34**	F	F	CH_3	**2.64**	77
16	**2.33**	F	F	F	**2.65**	87
17	**2.35**	F	OCH_3	F	**2.66**	83

a) Conversion calculated by integration of the ^{1}H-NMR signals of the crude material.

Table 11 shows the conversion for all of the biphenyl species submitted to the flow process from the corresponding biphenylamine. In the initial experiments, only substitution on the 2-phenyl ring was studied (entries 1-10). The method showed good substrate compatibility, even with the most electron-rich (entries 4 and 9) and electron-poor (entries 3, 5 and 8) systems, with conversions from 76-91%. The presence of electron-withdrawing groups such as fluorine (entries 2, 3 and 5) or a relatively bulky group on position R' did not affect the efficiency of the reaction (a methoxy group in place, entries 6, 9 and 10), although the presence of a CF_3 group at that position, which combines rather big size with electronegativity, provided the most modest result of all of the compounds (entry 8). Overall, no difficulties were observed in the effectiveness of the method, in terms of electronics or with the presence

of a functional group in position R'. The addition of a fluorine as EWG (entries 15-17) or a methoxy as EDG (entries 11-14) on the position R of the aniline ring also did not have a noticeable impact on conversion, proving that the nature of the group at that position did not affect the reproducibility of the reaction. The flow process, therefore, allowed the formation of the carbazole skeleton for 17 differently substituted scaffolds from the corresponding biphenyl precursor in a reaction time of 2 hours, and all of the carbazoles were progressed to the next *N*-alkylation step without purification, although an additional attempt at purification and isolation was investigated for compound **2.53**. When purified, the observed problems in the purification process were again observed and an isolated yield of only 25% was obtained.

2.6 *N*-Alkylation of carbazole scaffolds

In order to isolate the carbazole products efficiently, all of the products from the photocyclization were investigated in an *N*-alkylation reaction, in this case with an ethyl group which will be necessary for biological activity (**Scheme 56**). The most common approach for this transformation is deprotonation with a base and subsequent attack to an R-X type electrophile. In most cases, the bases used are strong bases, using harsh conditions or with long reaction times. For the *N*-ethylation of carbazoles, although copper catalysis is a frequent method,[176–178] sodium hydride is one of the most efficient bases used, often acting in high efficiency with short reaction times.[179–182] Nevertheless, following the same principles of safety, atom economy, sustainability, cost and efficiency, an ultrasound-assisted synthesis of *N*-alkyl carbazoles (**2.67**) published by S. Zhao's group[183] appeared as a very suitable alternative to complete the last step of carbazole synthesis.

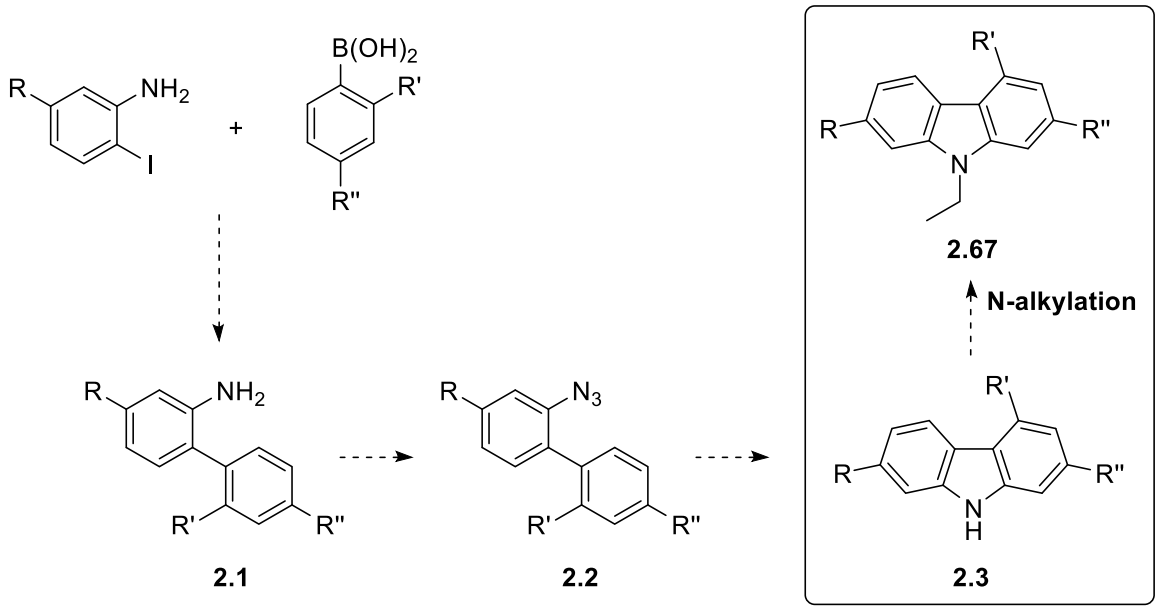

Scheme 56. *N-Ethylation step for the synthesis of carbazole derivatives* ***2.67****.*

Nitrogen-containing heterocycles such as *N*-arylpyrroles, *N*-arylindoles, *N*-arylimidazoles or *N*-arylcarbazoles are important natural products and biologically active pharmaceuticals. Since 1903, The copper-catalysed Ullmann-Goldberg coupling is a traditional method for the introduction of *N*-aryl functionality using aromatic halides.[184] As these molecules present similar reactivities, especially the pyrrole and indole derivatives, some methods are applicable for all of them. Among the copper catalysed methods, the work published by Heng-Chang Ma and Xuan-Zhen Jiang provides efficient arylation of pyrroles, indoles, and imidazole.[185] Although new approaches have been published, such as a palladium supported on zinc oxide nanoparticles for the ligand-free *O*-arylation and *N*-arylation of phenols and various N–H heterocycles with aryl halides,[186] we focused our attention on the S. Zaho *et al.* novel method using mild conditions and potassium hydroxide under ultrasonic irradiation[183] in accordance with our principles of green chemistry and the necessity of improving the sustainability of laboratory procedures (**Scheme 57**). In this publication they reported a method for the *N*-alkylation of indole, phenothiazine, and carbazole with a variety of alkylating agents under ultrasonic irradiation. The procedure is highly convenient, as a large number of *N*-alkylation reactions can be carried out in high yield, short reaction time, and milder conditions, avoiding the necessity of using hazardous reagents like sodium hydride.

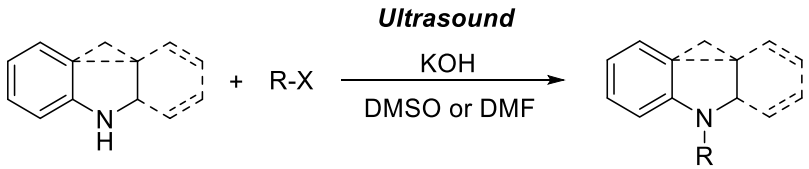

Scheme 57. *Ultrasound-assisted synthesis of N-alkyl derivatives of carbazole, indole, and phenothiazine.*[183]

Application of ball-milling techniques to accelerate substitution reactions, while avoiding the use of toxic organic solvents and reactants commonly required in these processes, has also gained interest in the last decade. Recently mechanochemical *N*-alkylations of secondary amines,[187,188] imines,[189] and imidazoles[190] among others have been reported, as well as the mechanochemical *N*-alkylation of imide derivatives by Anamarija Briš *et al.* described in **Scheme 58**,[191] which gave good yields and can be applied to various imides and alkyl halides. However, *N*-alkylations of carbazoles under mechanochemical condition have not been reported to date.

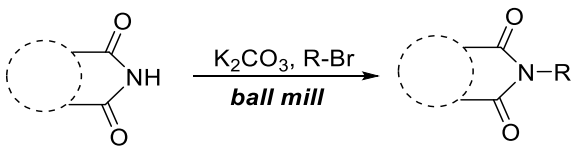

Scheme 58*. Reaction scheme for the mechanochemical N-alkylation of imide derivates.*

2.6.1. Carbazole *N*-ethylation using sonochemistry

For the reaction studied, the 9*H*-carbazole previously synthesised were transformed in accordance with the method of S. Zaho *et al.*[183] using solid KOH and iodoethane in DMSO in a commercial sonicator bath at 40 °C. This process required significantly shorter reaction times compared to other batch methods, affording full conversion in between 30 minutes and 2 hours (**Scheme 59**). The method avoided harsh conditions, hazardous bases such as sodium hydride, and was easily monitoring by TLC chromatography and ^{1}H-NMR spectroscopy to full conversion. At the end of the reaction, the mixture could be loaded directly onto a silica column due to the small quantities of DMSO required for the reaction.

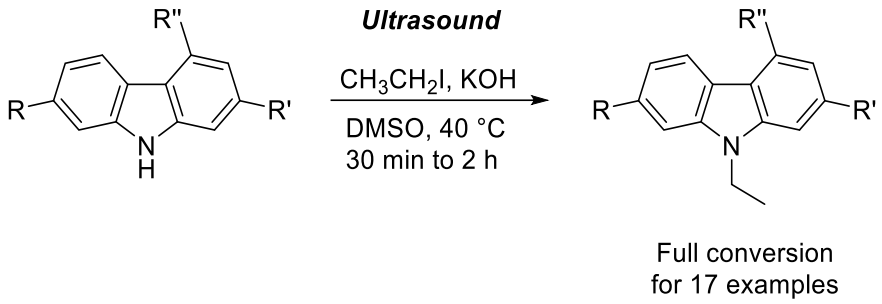

Scheme 59. *N-ethylation reaction scheme.*

Evidence for the success of the reaction was found in the ^{1}H-NMR spectrum by the disappearance of the N-H proton at δ 11-12 ppm, accompanied by the appearance of a quadruplet at ~4.5 ppm (integrating to 2H) and a triplet at ~1.5 ppm (integrating to 3H) due to the CH_2 and the CH_3 of the ethyl group, respectively (**Figure 26**). HRMS confirmed the theoretical mass of the product, the molecular ion exhibiting an additional 28 Daltons due to the introduction of the ethyl group.

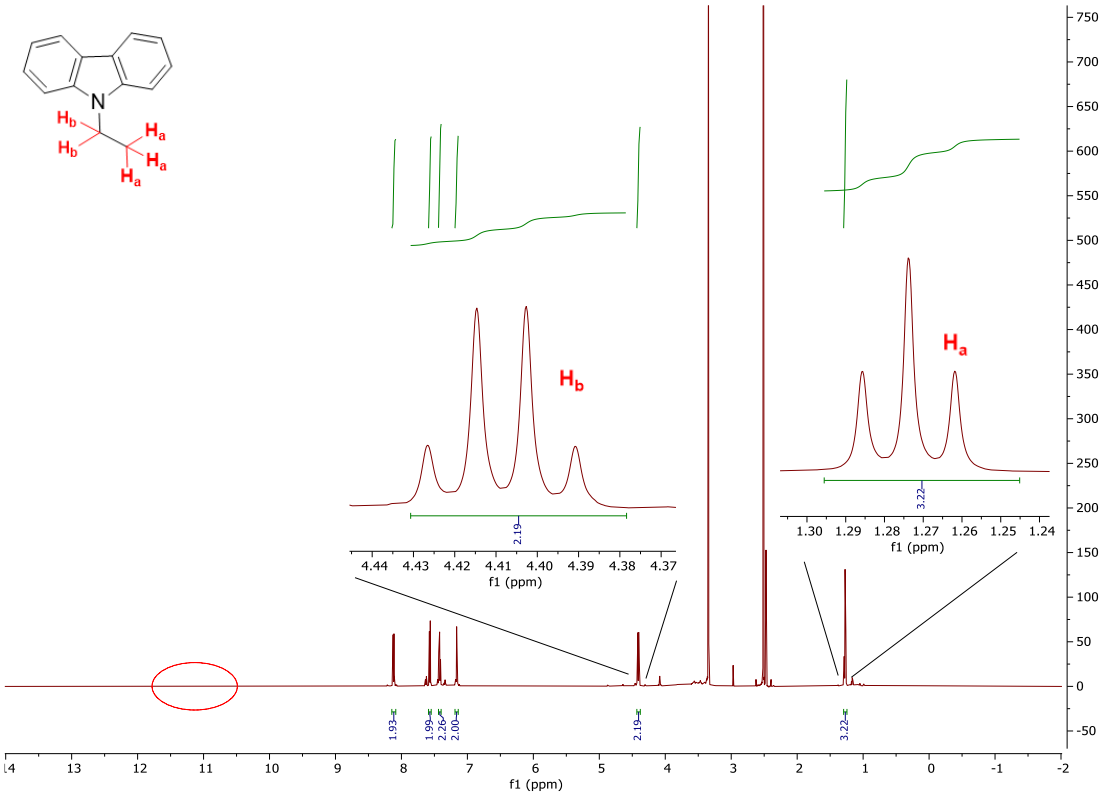

Figure 26. *^{1}H-NMR spectra of crude carbazole product* ***2.69***.

The reaction mechanism proceeds via S_N2: nucleophilic attack by the deprotonated nitrogen of the carbazole on the carbon atom of the iodoethane proceeds via a pentacoordinate transition state **[2.68]‡** (**Scheme 60**) and synchronous bond making and breaking, resulting in the final product **2.67**.

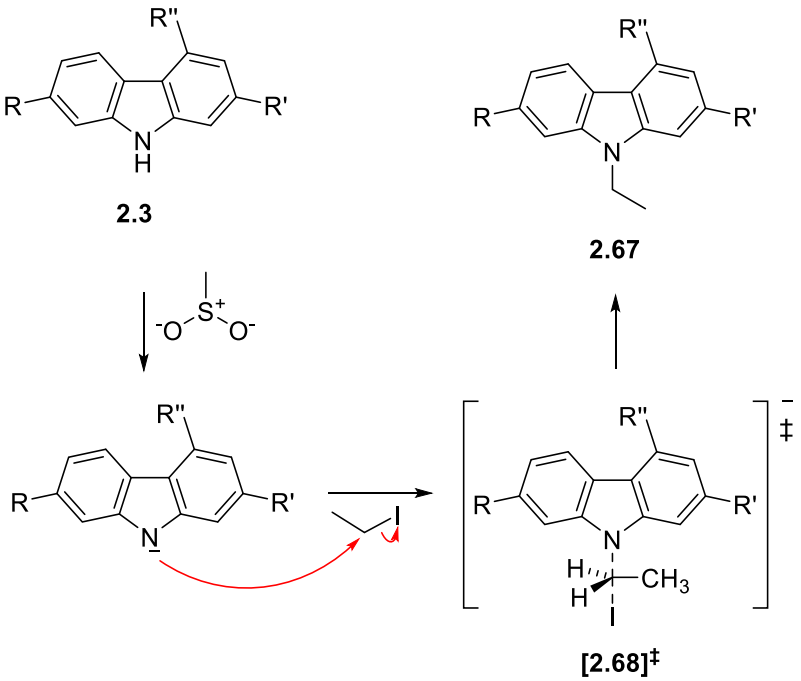

Scheme 60. *S_N2 mechanism for N-alkylation.*

The *N*-ethylation was the transformation studied on this project, as the ethyl group was required for future biological investigation, but S. Zaho's group demonstrated the compatibility of the method for several different alkyl groups, making it suitable for different synthetic demands.[183] Following these literature results, the *N*-functionalization was studied for two functionalized alkyl electrophiles, acetonitrile and *2,2,2*-trifluoroethyl trifluoromethane, but the reaction did not proceed, and only starting materials were observed after ^{1}H-NMR analysis.

The last step of the synthesis, the *N*-ethylation, provided full conversion of the non-purified carbazoles in a simple procedure, by reacting a solution of the crude carbazole product with iodoethane and potassium hydroxide in DMSO in an ultrasonic bath for reaction times that varied between 30 min and 2 h , monitoring reaction progress by TLC analysis. The aqueous workup for DMSO removal was found to be unnecessary on this scale as the employed quantities of solvent did not affect the separation under flash column chromatography. The final compounds obtained in this step could be isolated pure and characterised, completing the synthetic route and confirming the efficiency of the prior carbazole-forming step.

2.7 Synthetic route to *N*-ethylated carbazoles using reagentless techniques

After optimizing the four steps of the carbazole synthesis (cross-coupling, azide formation, photocyclization and *N*-ethylation) separately, a whole synthetic pathway from readily available haloanilines and boronic acids to the final *N*-ethylated carbazole scaffolds was developed. The method was used to synthesise 17 different compounds. The results of each step, the global yield of the synthesis and the purity of each compound are shown in **Table 12**. As the carbazoles were not isolated after the photocyclization step, the 3-step yield given refers to the azide formation reaction, photocyclization and *N*-ethylation reactions combined. For entry 1 commercially available 2-biphenylamine was used, skipping the cross-coupling reaction.

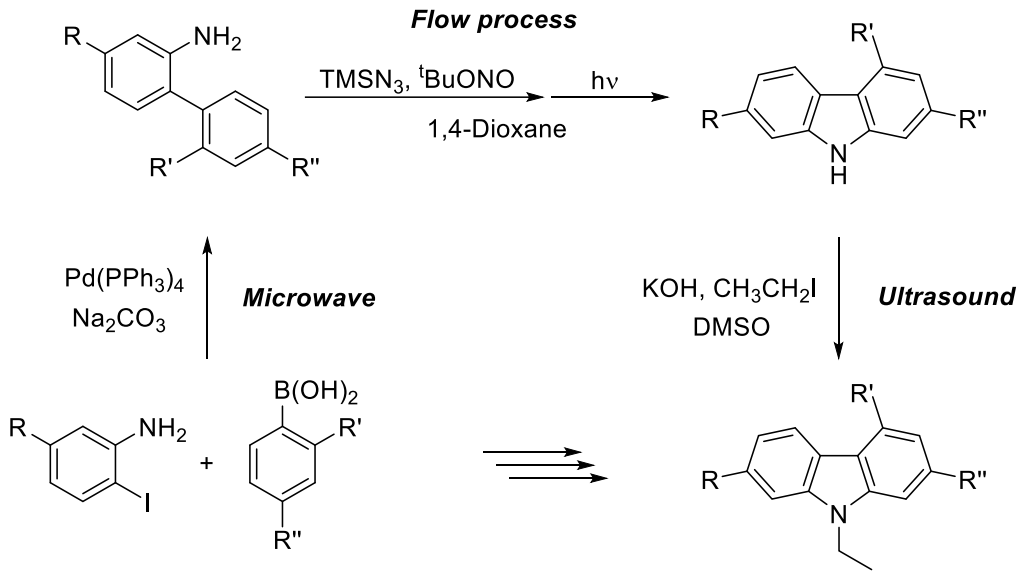

***Table 12**. Carbazole scaffolds synthetised using reagentless techniques.*

Entry	SM	R	R'	R''	Compound	Suzuki yield (%)[a]	3-step yield (%)[a,b]	Total Yield (%)[a]	Purity (%)[c]
1	-	H	H	H	**2.69**	-	56	-	*91*
2	**2.23**	H	F	CH_3	**2.70**	80	45	36	*96*
3	**2.13**	H	F	F	**2.71**	82	29	24	*97*
4	**2.12**	H	H	OCH_3	**2.72**	99	60	59	*93*
5	**2.28**	H	H	CF_3	**2.73**	80	43	34	*96*
6	**2.22**	H	F	CF_3	**2.74**	85	50	43	*95*
7	**2.24**	H	OCH_3	F	**2.75**	80	45	36	*95*
8	**2.14**	H	CF_3	CF_3	**2.76**	68	36	25	*91*
9	**2.29**	H	OCH_3	OCH_3	**2.77**	85	31	28	*94*
10	**2.30**	H	OCH_3	CF_3	**2.78**	85	55	47	*93*
11	**2.27**	OCH_3	F	CH_3	**2.79**	78	41	32	*96*
12	**2.31**	OCH_3	OCH_3	F	**2.80**	85	50	43	*97*
13	**2.25**	OCH_3	F	F	**2.81**	80	39	31	*95*
14	**2.32**	F	H	OCH_3	**2.82**	88	40	35	*98*
15	**2.34**	F	F	CH_3	**2.83**	77	57	44	*96*
16	**2.33**	F	F	F	**2.84**	46	49	23	*93*
17	**2.35**	F	OCH_3	F	**2.85**	77	55	42	*95*

a) Isolated yield after purification by flash chromatography.
b) Isolated yield after the flow process and following ultrasound N-ethylation.
c) Purity determined by LCMS analysis.

As stated before, no universal trends were observed on the efficiency of the method. The overall yields from the aniline and boronic acid to the corresponding carbazoles oscillated between 19% and 60% for a four-step synthesis, being in most of the cases between 31 and 47%. For the 3-step yield (flow process plus *N*-ethylation), the yields followed the trends for conversion showed in **Table 13**, except for **2.77** (entry 9), which provided one of the highest conversions (**Table 12**, entry 9) but after isolation the yield was lower than expected, and **2.83** (entry 15), which showed a rather low conversion in comparison to the isolated yield (**Table 12**, entry 15), which was one of the highest obtained. The low yield for compound **2.77** (entry 9) could be attributed to the purification by flash column chromatography. For the yields of the four-step synthesis, the low yield obtained for **2.84** is explained by the exceptionally low yield of the cross-coupling step (entry 16). In the case of compounds **2.71** and **2.77**, it was low yield of the flow process which compromised the global yield (entries 3 and 9), and for compounds **2.76** and **2.81** it was a combination of moderately low yields in both steps (entries 8 and 13). As mentioned before, **2.76** could be expected to be one of the most problematic due to the combination of electronic and steric effects (entry 8). On the other hand, the highest yield was obtained for **2.72,** which stands out with an overall yield of 60%, as a result of the high efficiency of the Suzuki cross coupling step and the highest yield for a flow process (entry 4). All the compounds displayed >90% purity after flash column chromatography, eluting on SiO_2 with a gradient of hexane/CH_2Cl_2 from 0 to 10% over 20 minutes. The compounds were submitted for LCMS analysis with no further purification, which makes the method convenient for providing high purity products without tedious workup or extra purification. The lowest purities were obtained for **2.69** (entry 1) and **2.76** (entry 8). For the first case, as the product was commercially available and was used as a reference, no further purification was attempted. For **2.76** (entry 8), an additional recrystallization from hexane was carried out, but the purity was not improved.

In conclusion, the method is effective for most of the examples and is tolerant of both electronic and steric effects in any of the positions. Hence, the method was confirmed to be an alternative and viable route to provide 17 highly pure *N*-alkylated carbazole scaffolds in good yields, fluctuating between 20 and 60% in a 4-step synthesis, starting from readily available and simple starting materials, haloanilines and phenylboronic acids, within a short period of time.

2.7.1. Scaling up

Following the future necessities of the project on the further functionalization of some of the compounds synthesised to study their biological properties and application, the scale of the reaction for the target compounds was increased from 200-300 mg (1-1.5 mmol) to 1-2 g scale (6-8 mmol). For the flow process, the reaction would proceed at the same concentration inside the reactor, so the only difference would be a longer time for the process. For the *N*-ethylation step, the larger quantity of DMSO

made it necessary to carry out an aqueous work up, extracting with dichloromethane, for loading on a solid cartridge with Celite for introduction to a SiO_2 column. The reaction time for this step was not altered and it provided the same quantitative conversion previously reported. After the three-step reaction the yields provided were equal to or greater than the yields reported for the synthesis of smaller quantities of material (**Table 13**).

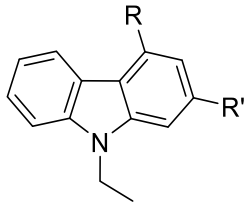

Table 13. *Carbazole scaffolds synthesized in larger quantities by this route (1-3 g).*

Entry	Compound	R'	R''	Yield (%)[a,b]	Previous yield (%)[a,b]
1	**2.70**	F	CF_3	43	45
2	**2.73**	H	CF_3	40	43
3	**2.76**	CF_3	CF_3	44	36
4	**2.75**	OCH_3	F	57	45
5	**2.78**	OCH_3	CF_3	65	55

a) Isolated yield after purification by flash chromatography.
b) Isolated yield after the flow process and following ultrasound N-ethylation.

For entries 1 and 2, the yield obtained was the same as that previously reported on a small scale, and for entries 3-5 it was significantly increased. Although there is not a clear explanation for this observation, the main hypothesis is that the small variation in the performance of the pumps, previously described, could have less impact when larger amounts of compound are used. In other words, inconsistencies in the flow rate over 2 minutes (showed by pressure chart on the flow reactor software) will have more of an impact if the whole process lasts 3-4 hours than if it lasts 8-9 hours. Considering this, the method proved to be appropriate for scaling up to produce grams of the desired carbazole in continuous flow with a potential increase of the yield.

2.8 Fluorine in ^{1}H and ^{13}C NMR spectroscopy

The major isotope of carbon, ^{12}C, is NMR-silent. However, ^{13}C, which has a natural abundance of 1.1%, has a nuclear spin of 1⁄2, so NMR spectra of this spin-active isotope can be obtained. The low natural abundance and relatively low resonance frequency of ^{13}C means that the signals are weaker than those of ^{1}H and more spectra need to be accumulated and summed to obtain spectra where the signals are strong. The low abundance means that it is very unlikely that two ^{13}C nuclei will be adjacent in a single molecule, so ^{13}C–^{13}C coupling is not observed in ^{13}C NMR spectra. Additionally, ^{13}C spectra are usually recorded with broadband ^{1}H decoupling, meaning that any coupling between ^{1}H and ^{13}C nuclei is eliminated by strongly irradiating all. Hence, this technique gives singlets for each unique carbon atom in the molecule. The ^{13}C NMR spectrum of compound **2.69**, shown in **Figure 27** as an example, displays only eight singlets. The six of them in the aromatic region are the equivalent carbons of the carbazole's carbocyclic rings, and the other two are the CH_2 and the CH_3 of the ethyl group. It can also be observed that the two quaternary carbons show a lower intensity in comparison to the other four carbons bonded to hydrogens, which eases their identification.

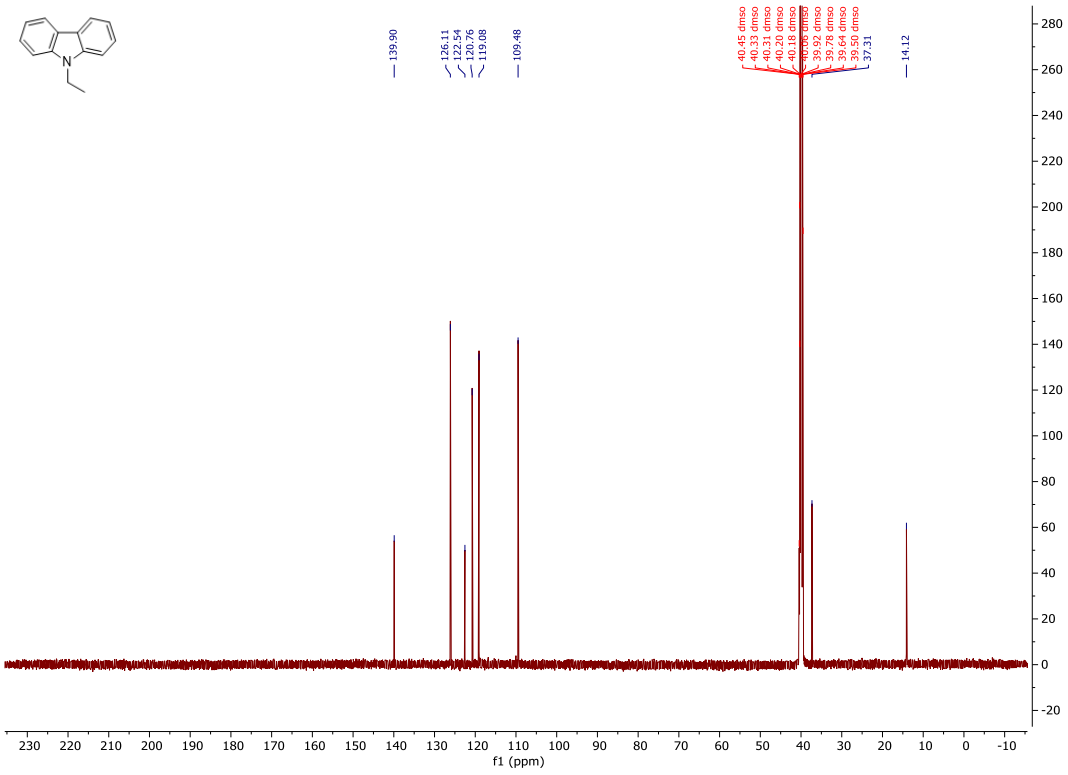

Figure 27. *^{13}C-NMR spectra of compound* ***2.69****.*

^{19}F (natural abundance 100%) has a spin quantum number *I* of ½, which makes it NMR-spin active. Thus, the presence of fluorine in a molecule is usually signalled by the appearance of splitting in ^{1}H and ^{13}C spectra due to ^{19}F–^{1}H and ^{19}F–^{13}C coupling, respectively. Due to the strong and long-range fluorine-carbon couplings, the signals of carbon atoms up to a distance of about four bonds are split by coupling to ^{19}F. One-bond ^{19}F–^{13}C coupling constants ($^{1}J_{CF}$) for fluorocarbons are in the range 160–280 Hz, with increasing fluorine substitution leading to larger coupling constants. In aromatic compounds, one-bond ^{19}F–^{13}C coupling constants are typically about 240 Hz.

On a practical basis, this means that ^{19}F alters the appearance of spectra by modifying the multiplicities of the existing signals. In ^{1}H-NMR spectra, it acts similar to an additional proton, but with an increased *J* value of approximately 10 Hz. The ^{1}H-NMR spectra of compound **2.71** is presented as an example in **Figure 28**, where it is shown how the presence of two ^{19}F nuclei converts two theoretical doublets with *J* ~ 2 Hz into a doublet of doublets (H-1: δ 7.45, dd, J_{HF} = 10.0, J_{HH} = 2.0 Hz) and a doublet of doublet of doublets (H-3: δ 7.01, ddd, J_{HF} = 10.5, J_{HF} = 10.5, J_{HH} = 2.0 Hz). The coupling of the protons with the ^{19}F of a CF_3 group at four bonds of distance is not observed by this technique.

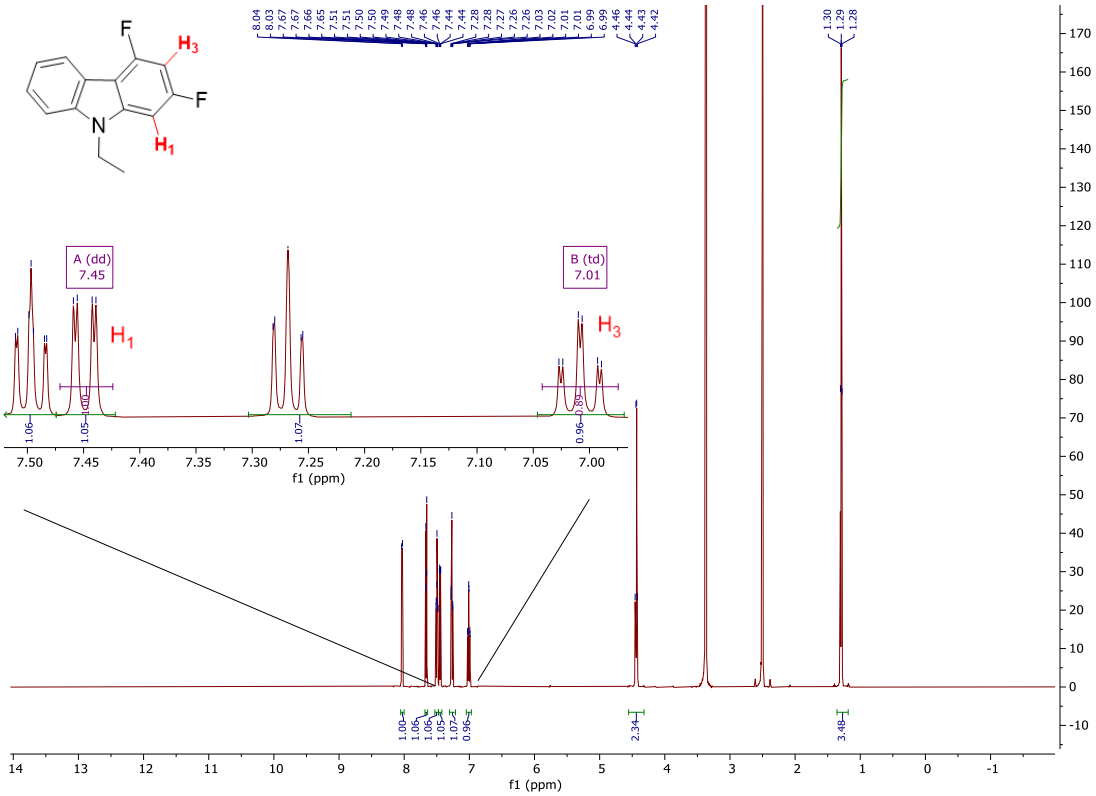

Figure 28. *^{1}H-NMR spectra of compound **2.71**.*

However, the spectra become more complicated in ^{13}C-NMR spectroscopy. As mentioned before, coupling with the ^{19}F nucleus generates splitting on distant ^{13}C nuclei. The ^{13}C-NMR spectra of the same compound **2.71** is presented as an example in **Figure 29**. Each fluorine couples with the

carbons at 1 to 4 bonds distance. The two C-F resonances can be observed at δ~160 ppm, which couple with their adjacent fluorine and the other CF, causing a doublet of doublets [δ 161.4 (dd, $^{1}J_{CF}$ = 241, $^{3}J_{CF}$ = 13 Hz), δ 157.6 (dd, $^{1}J_{CF}$ = 248, $^{3}J_{CF}$ = 16 Hz)]. Around δ 95 ppm, C-1 (δ 93.3, dd, $^{2}J_{CF}$ = 27, $^{4}J_{CF}$ = 4 Hz) and C-3 (δ 94.8 dd, $^{2}J_{CF}$ = 29, $^{2}J_{CF}$ = 24 Hz) can also be observed, and in this particular case they can be easily distinguished by the values of *J*.

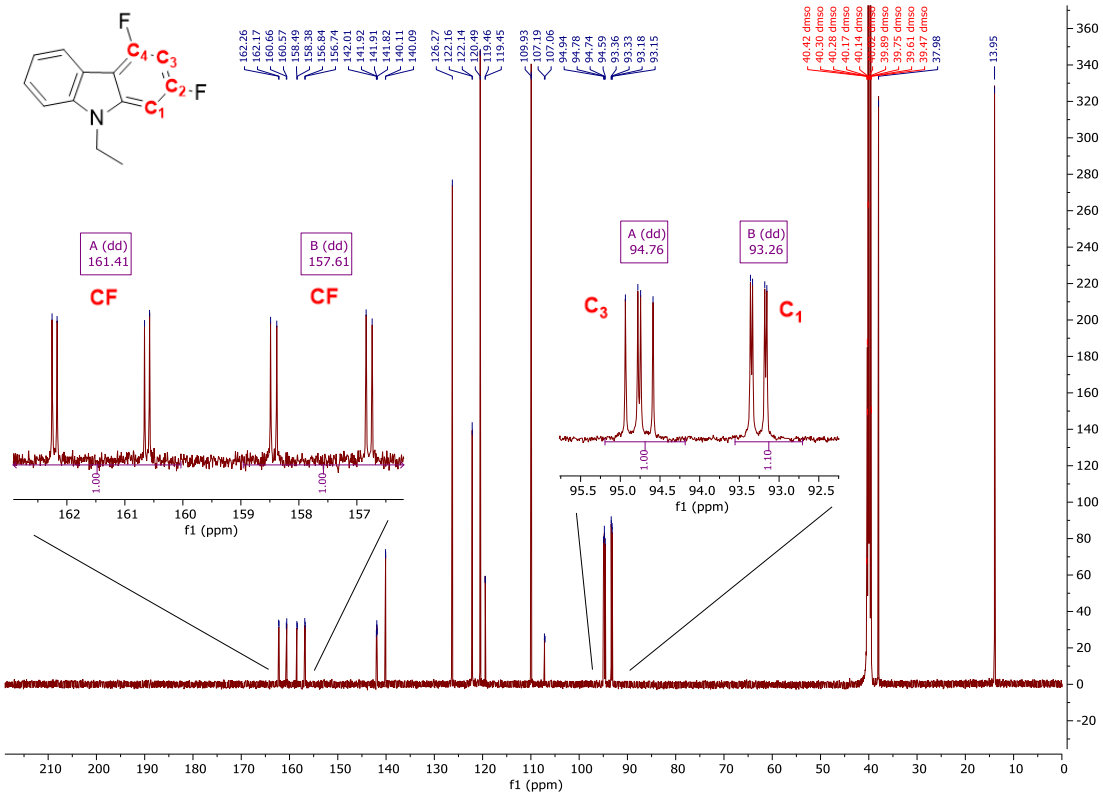

Figure 29. *^{13}C-NMR spectra of compound* ***2.71****.*

In this technique, the CF_3 group has a considerable effect on the observed spectrum. The trifluorinated carbon is often not easy to detect, as it appears around 100-150 ppm as a quartet with *J* ~ 270 Hz, which can be easily confused as 4 weak independent peaks. The ^{13}C-NMR spectrum of compound **2.73** shown in **Figure 30** is an excellent example to illustrate this statement. The four peaks of the quartet of the trifluorinated carbon (CF: δ 125.6 ppm, q, $^{1}J_{CF}$ = 272 Hz) are located in the middle of the spectrum, separated by ~ 2 ppm and overlapped by other signals. The carbon adjacent to the CF_3 is more obvious, as the signals are closer, and is displayed in an expansion in **Figure 31** (C-2: δ 126.3 ppm, q, $^{2}J_{CF}$ = 31 Hz). Although they are not expanded, C-1 and C-3 quartets can also be observed in the spectrum [δ 106.9 (q, $^{4}J_{CF}$ = 4 Hz), δ 115.4 (q, $^{4}J_{CF}$ = 4 Hz) ppm]. The addition of a second fluorine will result in more splitting, creating doublets of quartets and quartets of doublets for those carbons at less than 4 bonds of distance from both groups.

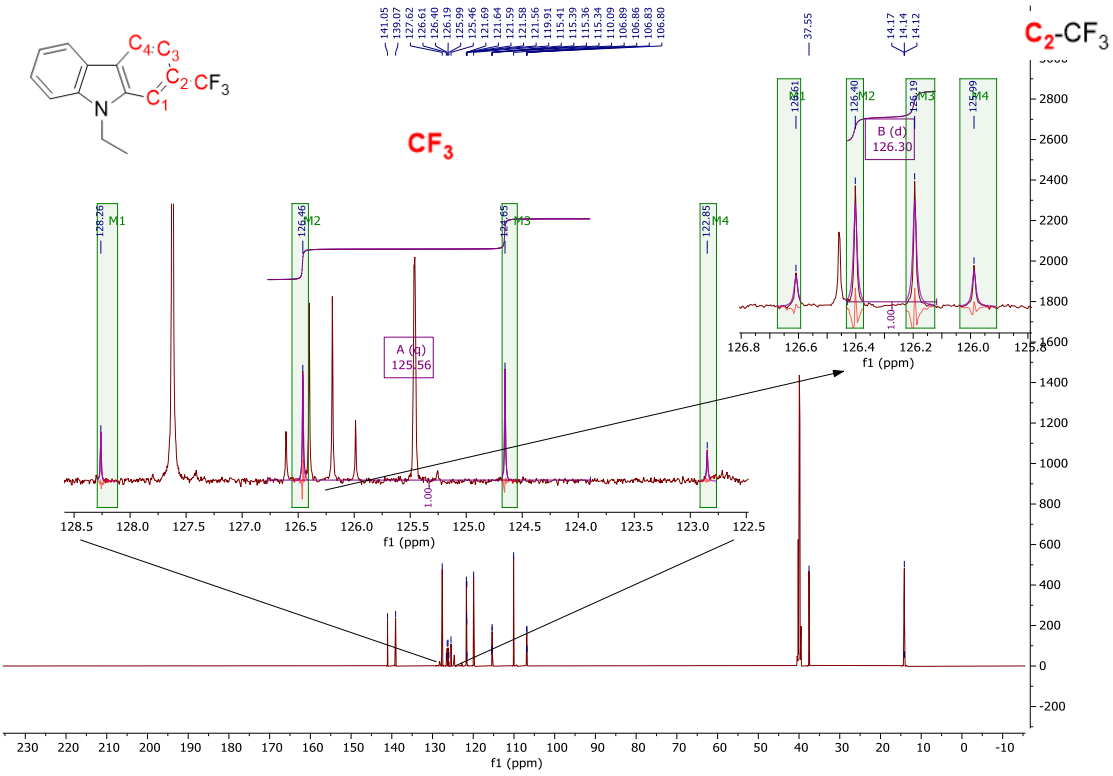

Figure 30. *^{13}C-NMR spectra of compound* ***2.73****.*

^{1}H and ^{13}C NMR spectroscopy are extremely useful techniques for identifying carbazole scaffolds. The variations in the multiplicities caused by the presence of fluorine atoms due to the spin quantum number of ½ for the ^{19}F isotope can be recognized and explained, being a further proof of the identity of the proposed structure. All of these data are supported by high-resolution mass spectrometry, which confirmed the mass of the compound precisely.

2.9 Conclusions

In conclusion, a new synthetic pathway adapted to reagentless techniques has been successfully developed and optimized for the synthesis of 17 *N*-ethylated carbazoles (16 of them novel) in good yields (25 to 59% for 4 steps), in high purities (>90%) and in a rapid, facile, and efficient manner. The method starts with a Suzuki-Miyaura cross-coupling reaction between commercially available, non-toxic and stable boronic acids with simple haloanilines. The reaction happens under microwave irradiation, providing excellent yields after a reaction time of 35 minutes. The obtained biphenyl species are then introduced into a mixing flow device with two reactors connected in series. Reactants are first pumped into a PFA temperature- controlled reactor at 80 °C where the azide analogue is formed, and the flow continues through a photochemical reactor where the solution is exposed to a photon flux to

promote the azide photoactivation and, following cyclization, provide the carbazole skeleton with high conversions in a total reaction time of 2 hours. The crude product is diluted in DMSO and *N*-ethylated with iodoethane using sonochemistry in the presence of potassium hydroxide, monitoring the reaction until completion after between 30 minutes and 2 hours, loading the solution mixture onto a silica column, where the final product can be obtained in high purity after flash column chromatography.

The method has been proved to be tolerant of electron-rich and electron-poor systems, and steric constraints in any of the investigated positions, to allow the continuous production of carbazoles in gram scale if necessary. Sufficient quantities of the desired scaffolds can be accessed, suitable for further functionalization and into potentially biological active compounds. All the compounds have been isolated, identified and fully characterised via ^{1}H and ^{13}C nuclear magnetic resonance spectroscopy, infrared spectroscopy and high-resolution mass spectrometry. The purity values have been obtained by liquid chromatography–mass spectrometry and the melting points have been reported. The characterisation data have been discussed, especially the ^{1}H and ^{13}C NMR spectra of fluorinated compounds, which present challenges but which can be understood based upon careful analysis of spectra.

After the success in developing a method for the synthesis of *N*-ethylated carbazole scaffolds in good quantities, it was decided that some of the examples should be functionalized in order to make them active as reactivators of the Y220C mutated p53 gene for testing in biological assays.

2.10 Experimental

General Methods

All procedures were carried out in the presence of air unless stated otherwise. Commercially available reagents were used without further purification. Analytical thin layer chromatography was carried out using aluminium-backed plates coated with Merck TLC Silicagel 60 F_{254} that were visualized under UV light (at λ 254 and/or 360 nm). NMR spectra were recorded using a Varian VNMRS instrument operating at 600, or 400 MHz for ^{1}H NMR and 151 MHz for ^{13}C NMR spectroscopy. *J* values were recorded in Hz to the nearest 0.5 Hz for ^{1}H NMR and to the nearest 1 Hz for ^{13}C NMR and multiplicities were expressed using the usual conventions. High resolution mass spectra were determined using a Bruker Daltronics Apex III instrument by electrospray ionization (ESI) and were captured by Dr. Alla K. Abdul-Sada of the University of Sussex Mass Spectrometry Centre. LCMS data were recorded on a on a Shimatzu Prominence Series coupled to a LCMS-2020 ESI and APcI mass spectrometer to meet the requirements of the project (>95%). Melting points were determined using a Stanford Research Systems Optimelt and are uncorrected. Flash chromatography was carried out using a Teledyne ISCO Combiflash Rf

instrument and Redisep Rf silica columns. Infra-red spectra were recorded in the range 4000–600 cm^{-1} on a Perkin–Elmer Spectrum One FTIR spectrometer using a Perkin–Elmer universal sampling accessory and are reported in cm^{-1}. Microwave-assisted reactions were carried out using a CEM Discover™ with a CEM Explorer at the given temperature using the instrument's in-built IR temperature measuring device, by modulating the initial power (given in parentheses). Flow reactions were conducted in a Vapourtec R2C+/R4 system, using a standard PFA coil reactor and a UV-150 Photochemical Reactor.

General Procedure A. Microwave-assisted synthesis of biphenylamines. A stirred solution of the the corresponding 2-haloaniline (1 equiv.), the corresponding boronic acid (1.3 equiv.), Na_2CO_3 (4 equiv.) and the palladium catalyst (5 mol%) in dioxane-water (1:1) was irradiated in a pressure-rated sealed tube at 125 °C (initial power 150 W) for 35 min using a CEM Discover microwave synthesizer. After cooling in a flow of compressed air, the reaction mixture was extractd with EtOAc. The organic layer was dried over anhydrous $MgSO_4$, filtered and concentrated under a reduced pressure. The crude product was purified by flash column chromatography on SiO_2, eluting with hexane-EtOAc, using a Teledyne ISCO Combiflash Rf instrument.

General Procedure B. Synthesis of biphenylamines. To a three-necked round bottomed flask was added the corresponding 2-haloaniline (1 equiv.), the corresponding boronic acid (1.3 equiv.) and potassium carbonate (2 equiv) in anhydrous THF/H_2O (1:1). The flask was evaculated and backfilled with argon 3 times and the corresponding palladium catalyst (5 mol%) was added to the reaction mixture. The resulting solution was stirred at 80 °C overnight. The reaction mixture product was extracted with EtOAc. The organic extracts were dried over anhydrous $MgSO_4$, filtered and concentrated under a reduced pressure to afford crude product that was purified by flash column chromatography on SiO_2, eluting with hexane-EtOAc, using a Teledyne ISCO Combiflash Rf instrument.

General Procedure C. Carbazole synthesis using biphenylamines in flow. A solution (A) of the corresponding biphenyl amine (0.1 M) and $TMSN_3$ (0.11 M) in dioxane and a solution (B) of *t*-BuONO (0.15 M) in dioxane were mixed, heated in a PFA coil reactor at 80 °C for 50 min and then irradiated with 300 to 400 nm at 80 °C for 50 min using a UV-150 Photochemical Flow Reactor connected in-series. The solvent was evaporated *in vacuo* and the crude product was used for the next step without further purification. Solid KOH (2 equiv.) was added to a suspension of the corresponding carbazole crude (1 equiv.) in DMSO. The reaction mixture was sonicated at 40 °C for 20 min. Then, iodoethane (2 equiv.) was added and the reaction mixture was further sonicated for 30 min at the same temperature. The reaction mixture loaded to a column and purified by flash column chromatography on SiO_2, eluting with hexane-CH_2Cl_2, using a Teledyne ISCO Combiflash Rf instrument.

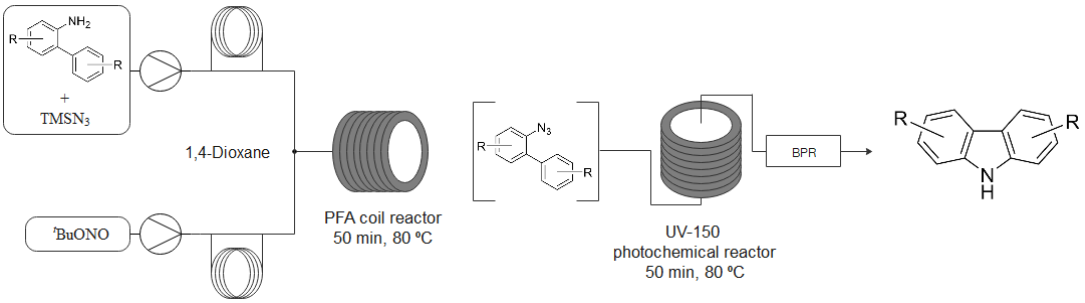

2.10.1 Synthesis of biphenyls

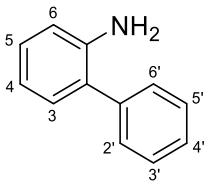

2-(4'-Nitrophenyl)aniline (2.11). Prepared according to General Procedure A using a solution of 2-bromoaniline (0.40 mL, 3.0 mmol, 1.0 equiv.), 4-nitrophenylboronic acid (650 mg, 3.9 mmol, 1.3 equiv.), Na_2CO_3 (1.27 g, 12.0 mmol, 4.0 equiv.) and $Pd(dppf)Cl_2$ (73 mg, 5 mol%) in dioxane-water (1:1) (14 mL) in a pressure-rated sealed tube (35 mL). Purification by flash column chromatography on on SiO_2 (24 g), eluting with hexane-EtOAc (9:1) gave the *title compound* (0.61 g, 95%) as an orange solid.

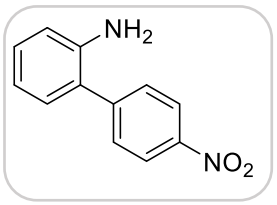

Mp: 156-159 °C (lit[192] 158-159 °C). **Purity (LCMS):** 94%. **Found [ESI]:** MH^+, 215.0826. $C_{12}H_{11}N_2O_2$ [MH] requires 215.0821 **IR** (neat) *v*/cm^{-1} 3470, 3385 (NH_2), 3070 (C-H), 1622 (ar C-C), 1500 (NO_2), 1105 (C-NO). **^{1}H NMR** (600 MHz, $CDCl_3$) δ 8.30 (2H, AA'XX', *J* 9.0, 2.5, 2.0, H-3'), 7.66 (2H, AA'XX', *J* 9.0, 2.5, 2.0, H-2'), 7.21 (1H, ddd, *J* 8.0, 7.5, 1.5, H-5), 7.12 (1H, dd, *J* 7.5, 1.5, H-3), 6.86 (1H, ddd, *J* 7.5, 7.5, 1.0, H-4), 6.79 (1H, dd, *J* 8.0, 1.0, H-6), 3.75 (2H, s, NH_2). **^{13}C NMR** (151 MHz, $CDCl_3$) δ 146.8 (C), 146.6 (C), 143.3 (C), 130.3 (CH), 129.9 (CH), 129.8 (CH), 125.1 (C), 124.1 (CH), 119.1 (CH), 116.2 (CH).

2-(4'-Methoxyphenyl)aniline (2.12). Prepared according to General Procedure A using a solution of 2-iodoaniline (329 mg, 1.5 mmol, 1.0 equiv.), 4-methoxyphenylboronic acid (269 mg, 2.0 mmol, 1.3 equiv.), Na_2CO_3 (636 mg, 6.0 mmol, 4.0 equiv.) and $Pd(dppf)Cl_2$ (173 mg, 10 mol%) in dioxane-water (1:1) (14 mL) in a pressure-rated sealed tube (35 mL). Purification by flash column chromatography on SiO_2 (12 g), eluting with hexane-EtOAc (9:1) gave the *title compound* (0.45 g, 75%) as a yellow oil.

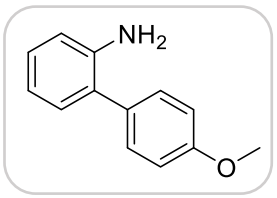

Purity (LCMS): 96%. **Found [ESI]:** MH^+, 200.1073. $C_{13}H_{14}NO$ [MH] requires 200.1070. **IR** (neat) *v*/cm^{-1} 3455, 3364 (NH_2 st), 3031 (ar C-H st), 1625 (ar C-C), 1239 (C-O). **^{1}H NMR** (600 MHz, $CDCl_3$) δ 7.39 (2H, AA'XX', *J* 8.5, 3.0, 2.0, H-2'), 7.14 (1H, ddd, *J* 8.0, 7.5, 1.5, H-5), 7.12 (1H, dd, *J* 7.5, 1.5, H-3), 6.98 (2H, AA'XX', *J* 8.5, 3.0, 2.0, H-3'), 6.83 (1H, ddd, *J* 7.5, 7.5, 1.0, H-4), 6.78 (1H, dd, *J* 8.0, 1.0, H-6), 3.85 (3H, s, OCH_3).N-H not observed. **^{13}C NMR** (151 MHz, $CDCl_3$) δ 158.8 (C), 143.0 (C), 131.6 (C), 130.5 (CH), 130.2 (CH), 128.2 (CH), 127.8 (C), 119.1 (CH), 115.9 (CH), 114.2 (CH), 55.3 (Me). (lit[143])

2-(2',4'-Difluorophenyl)aniline (2.13). Prepared according to General Procedure A using a solution of 2-iodoaniline (438 mg, 2.0 mmol, 1.0 equiv.), 2,4-difluorobenzeneboronic acid (481 mg, 2.6 mmol, 1.3 equiv.), Na_2CO_3 (848 g, 8.0 mmol, 4.0 equiv.) and $Pd(PPh_3)_4$ (115 mg, 5 mol%) in dioxane-water (1:1) (14 mL) in a pressure-rated sealed tube (35 mL). Purification by flash column chromatography on SiO_2 (12 g), eluting with hexane-EtOAc (9:1) gave the *title compound* (0.39 mg, 94%) as a colourless solid.

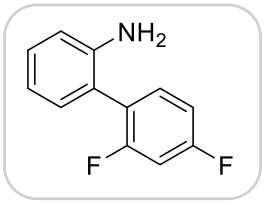

Mp: 80-82 °C (lit[193] 76-77 °C). **Purity (LCMS):** 96%. **Found [ESI]:** MH^+ 206.0783. $C_{12}H_{10}F_2N$ [MH] requires 206.0783. **IR** (neat) *v*/cm^{-1} 3478, 3389 (NH_2), 2970 (C-H), 1615 (C-C), 1102 (C-F), 762 (C-H). **^{1}H NMR** (600 MHz, $CDCl_3$) δ 7.35 (1H, ddd, J_{HF} 8.5, J_{HH} 8.2, J_{HF} 6.7, H-5'), 7.21 (1H, ddd, *J* 8.0, 7.5, 1.0, H-5), 7.09 (1H, dd, *J* 7.5, 1.0, H-3), 7.00 – 6.90 (2H, m, H-3', H-6'), 6.85 (1H, ddd, *J* 7.5, 7.5, 1.0, H-4), 6.81 (1H, dd, *J* 8.0, 1.0, H-6), 3.71 (2H, s, NH_2). **^{13}C NMR** (151 MHz, $CDCl_3$) δ 162.5 (dd, $^1J_{CF}$ 250, $^3J_{CF}$ 12, CF), 159.9 (dd, $^1J_{CF}$ 250, $^3J_{CF}$ 12, CF), 143.9 (C), 132.7 (dd, $^3J_{CF}$ 9, $^4J_{CF}$ 5, CH), 131.1 (CH), 129.4 (CH), 122.6 (dd, $^2J_{CF}$ 17, $^4J_{CF}$ 4, C), 120.7 (C), 118.7 (CH), 115.9 (CH), 111.8 (dd, $^2J_{CF}$ 21, $^4J_{CF}$ 4, CH), 104.4 (t, $^2J_{CF}$ 26, CH). **^{19}F NMR** (376 MHz, $CDCl_3$) δ -109.7 (q, J_{FF} 9), -110.5 (m).

2-(2',4'-Bis(trifluoromethylphenyl)aniline (2.14). Prepared according to General Procedure A using a solution of 2-iodoaniline (219 mg, 1.0 mmol, 1.0 equiv.), 2,4- bis(trifluoromethylphenylboronic acid (335 mg, 1.3 mmol, 1.3 equiv.), Na_2CO_3 (424 mg, 4.0 mmol, 4.0 equiv.) and $Pd(PPh_3)_4$ (115 mg, 10 mol%) in dioxane-water (1:1) (14 mL) in a pressure-rated sealed tube (35 mL). Purification by flash column chromatography on silica, eluting with hexane-EtOAc (9:1) gave the *title compound* (0.21 g, 68%) as a colourless oil.

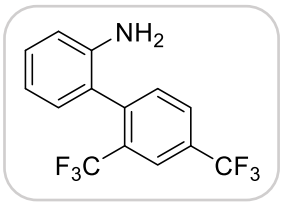

Purity (LCMS): 95%. **Found [ESI]:** MH^+, 306.0735. $C_{14}H_{10}F_6N$ [MH] requires 306.0717. **IR** (neat) *v*/cm^{-1} 3471, 3390 (NH_2), 3036 (C-H), 1624 (C-C), 1120 (C-F), 750 (C-H). **^{1}H NMR** (600 MHz, $CDCl_3$) δ 8.06 (1H, s, H-3'), 7.87 (1H, d, *J* 8.0, H-5'), 7.55 (1H, d, *J* 8.0, H-6'), 7.23 (1H, dd, *J* 8.0, 8.0, H-5), 6.99 (1H, d, *J* 7.5, H-3), 6.82 (1H, dd, *J* 8.0, 7.5, H-4), 6.78 (1H, d, *J* 8.0, H-6), 3.38 (2H, s, NH_2).

^{13}C NMR (151 MHz, $CDCl_3$) δ 143.5 (C), 142.1 (C), 133.5 (CH), 130.7 (q, $^2J_{CF}$ 31, C), 130.5 (q, $^2J_{CF}$ 34, C), 129.9 (CH), 129.7 (CH), 128.8 (q, $^3J_{CF}$ 4, CH), 123.9 (m, CH), 123.4 (q, $^1J_{CF}$ 272, CF_3), 123.2 (C), 123.1 (q, $^1J_{CF}$ 275, CF_3), 118.0 (CH), 115.6 (CH).

2-(4'-Bromo-2'-fluorophenyl)aniline (2.21). Prepared according to General Procedure A using a solution of 2-iodoaniline (438 mg, 2.0 mmol, 1.0 equiv.), 4-bromo-2-fluorophenylboronic acid (569 mg, 2.6 mmol, 1.3 equiv.), Na_2CO_3 (848 mg, 8.0 mmol, 4.0 equiv.) and $Pd(dppf)Cl_2$ (73 mg, 5 mol%) in dioxane-water (1:1) (14 mL) in a pressure-rated sealed tube (35 mL). Purification by flash column chromatography on SiO_2 (12 g), eluting with hexane-EtOAc (4:1) gave the *title compound* gave the *title compound* (0.29, 56%) as a brown oil.

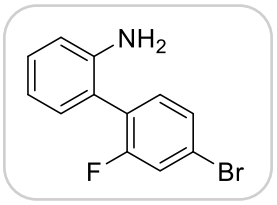

Purity (by LCMS): 96%. **Found [ESI]:** MH^+, 265.9977. $C_{12}H_{10}{}^{79}BrFN$ [MH] requires 265.9975. **IR** (neat) *v*/cm^{-1} 3470, 3376 (NH_2), 3027, 3065 (C-H), 1616 (C-C), 1205 (C-F). **^{1}H NMR** (600 MHz, $CDCl_3$) δ 7.39 – 7.33 (2H, m, H-4', H-6'), 7.27 (1 H, dd, J_{HF} 10.0, 8.5, 4.5, H-3'), 7.22 (1H, ddd, *J* 8.0, *J* 7.5, *J* 1.0, H-5), 7.09 (1H, dd, *J* 7.5, 1.0, H-3), 6.86 (1H, ddd, *J* 7.5, 1.0, H-4), 6.82 (1H, d, *J* 8.0, H-6), N-H not observed. **^{13}C NMR** (151 MHz, $CDCl_3$) δ 159.7 (d, $^1J_{CF}$ 251, CF), 143.4 (C), 133.0 (d, $^4J_{CF}$ 4, CH), 130.9 (d, $^4J_{CF}$ 1, CH), 129.5 (CH), 127.9 (d, $^4J_{CF}$ 4, (CH), 125.63 (d, $^2J_{CF}$ 17, C), 121.8 (d, $^3J_{CF}$ 9, CBr), 120.6 (C), 119.7 (d, $^2J_{CF}$ 26, CH), 119.0 (CH), 116.2 (CH).

2-(2'-Fluoro-4'-trifluoromethylphenyl)aniline (2.22). Prepared according to General Procedure A using a solution of 2-iodoaniline (438 mg, 2.0 mmol, 1.0 equiv.), 2-fluoro-4-trifluoromethylphenylboronic acid (541 mg, 2.6 mmol, 1.3 equiv.), Na_2CO_3 (848 mg, 8.0 mmol, 4.0 equiv.) and $Pd(PPh_3)_4$ (115 mg, 5 mol%) in dioxane-water (1:1) (14 mL) in a pressure-rated sealed tube (35 mL). Purification by flash column chromatography on SiO_2 (12 g), eluting with hexane-EtOAc (9:1) gave the *title compound* (0.43 g, 85%) as a yellow solid.

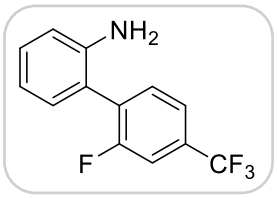

Mp: 50-51 °C. **Purity (LCMS):** 96%. **Found [ESI]:** MH^+, 256.0757. $C_{13}H_{10}F_4N$ [MH] requires 256.0749. **IR** (neat) *v*/cm^{-1} 3456, 3370 (NH_2), 3081 (C-H), 1620 (C-C), 1116 (CF_3) 1070 (C-F). **^{1}H NMR** (600 MHz, $CDCl_3$) δ 7.57 – 7.49 (2H, m, H-5', H-6'), 7.46 (1H, dd, $^3J_{HF}$ 10.0, J_{HH} 1.5, H-3'), 7.24 (1H, ddd, *J* 8.0, 7.5, 1.0, H-5), 7.11 (1H, dd, *J* 7.5, H-3), 6.86 (1H, ddd, *J* 7.5, 7.5, H-4), 6.82 (1H, d, *J* 8.0, H-6), 3.66 (2H, s, NH_2). **^{13}C NMR** (151 MHz, $CDCl_3$) δ 159.5 (d, $^1J_{CF}$ 249, CF), 143.9 (C), 132.8 (d, $^4J_{CF}$ 4, CH), 131.6 (qd, $^2J_{CF}$ 34, 34, 33, $^3J_{CF}$ 8, C-CF_3), 130.8 (CH), 130.6 (d, $^2J_{CF}$ 17, CF_3), 129.9 (CH), 123.3 (qd, $^1J_{CF}$ 272, $^4J_{CF}$ 3, CF_3), 121.4 (p, $^4J_{CF}$ 4, CH), 119.9 (C), 118.7 (CH), 116.0 (CH), 113.6 (dq, $^2J_{CF}$ 27, 4, CH).

2-(2'-Fluoro-4'-methylphenyl)aniline (2.23). Prepared according to General Procedure A using a solution of 2-iodoaniline (438 mg, 2.0 mmol, 1.0 equiv.), 2-fluoro-4-methylphenylboronic acid (397 mg, 2.6 mmol, 1.3 equiv.), Na_2CO_3 (848 mg, 8.0 mmol, 4.0 equiv.) and $Pd(PPh_3)_4$ (115 mg, 5 mol%) in dioxane-water (1:1) (14 mL) in a pressure-rated sealed tube (35 mL). Purification by flash column chromatography on SiO_2 (12 g), eluting with hexane-EtOAc (9:1) gave the *title compound* (0.32 g, 80%) as a colourless oil.

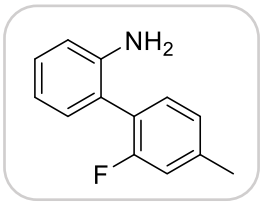

Purity (LCMS): 97%. **Found [ESI]:** MH^+, 202.1036. $C_{13}H_{13}FN$ [MH] requires 202.1032. **IR** (neat) *v*/cm^{-1} 3469, 3380 (NH_2 st), 2982 (C-H), 1615 (C-C), 1054 (C-F). **^{1}H NMR** (600 MHz, $CDCl_3$) δ 7.25 (1H, ddd, J_{HH} 8.0, J_{HF} 7.0, 1.5, H-6'), 7.20 (1H, m, H-5'), 7.12 (1H, dd, *J* 7.5, 1.5, H-3), 7.04 (1H, ddd, *J* 8.0, 1.0, 0.5, H-5), 7.00 (1H, dd, J_{HF} 11.0, J_{HH} 0.5, H-3'), 6.84 (1H, ddd, *J* 7.5, 7.0, 1.0, H-4), 6.81 (1H, dd, *J* 8.0, 1.0, H-6), 3.80 (2H, s, NH_2) 2.40 (3H, s, Me). **^{13}C NMR** (151 MHz, $CDCl_3$) δ 159.7 (d, $^1J_{CF}$ 246, C-F), 143.8 (C), 140.0 (d, $^3J_{CF}$ 8, C), 131.6 (d, $^3J_{CF}$ 5, CH), 131.1 (CH), 129.00 (CH), 125.3 (d, $^4J_{CF}$ 3, CH), 123.3 (d, $^2J_{CF}$ 17, C), 121.8 (C), 118.7 (CH), 116.5 (d, $^2J_{CF}$ 22, CH), 115.9 (CH), 21.1 (d, $^4J_{CF}$ 2, Me).

2-(4'-Fluoro-2'-methoxyphenyl)aniline (2.24). Prepared according to General Procedure A using a solution of 2-iodoaniline (438 mg, 2.0 mmol, 1.0 equiv.), 4-fluoro-2-methoxyphenylboronic acid (442 mg, 2.6 mmol, 1.3 equiv.), Na_2CO_3 (848 mg, 8.0 mmol, 4.0 equiv.) and $Pd(PPh_3)_4$ (115 mg, 5 mol%) in dioxane-water (1:1) (14 mL) in a pressure-rated sealed tube (35 mL). Purification by flash column chromatography on SiO_2 (12 g), eluting with hexane-EtOAc (9:1) gave the *title compound* (0.35 g, 80%) as a brown oil.

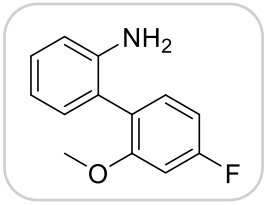

Purity (LCMS): 96%. **Found [ESI]:** MH^+, 218.0992. $C_{13}H_{13}FNO$ [MH] requires 218.0981. **IR** (neat) *v*/cm^{-1} 3459, 3372 (NH_2), 2981 (C-H), 1579 (C-C), 1276 (C-O), 1033 (C-F), 748 (C-H). **^{1}H NMR** (600 MHz, $CDCl_3$) δ 7.24 – 7.15 (2H, m, H-5, H-6'), 7.07 (1H, dd, *J* 7.5, 1.5, H-3), 6.84 (1H, ddd, *J* 7.5, 1.0, H-4), 6.81 – 6.70 (3H, m, H-6, H-3', H-5'), 3.80 (3H, s, OMe), 3.52 (2H, s, NH_2). **^{13}C NMR** (151 MHz, $CDCl_3$) δ 163.3 (d, $^1J_{CF}$ 246, CF), 157.8 (d, $^3J_{CF}$ 10, C), 144.1 (C), 132.4 (d, $^3J_{CF}$ 10, CH), 131.2 (CH), 128.7 (CH), 124.1, (C), 123.9 (d, $^4J_{CF}$ 3, C), 118.7 (CH), 115.8 (CH), 107.43 (d, $^2J_{CF}$ 21, CH), 99.4 (d, $^2J_{CF}$ 26, CH), 55.9 (OCH_3).

2-(2',4'-Difluorophenyl)-5-methoxyaniline (2.25). Prepared according to General Procedure A using a solution of 2-bromo-5-methoxyaniline (404 mg, 2.0 mmol, 1.0 equiv.), 2,4-difluorophenylboronic acid (411 mg, 2.6 mmol, 1.3 equiv.), Na_2CO_3 (848 mg, 8.0 mmol, 4.0 equiv.) and $Pd(PPh_3)_4$ (115 mg, 5 mol%) in dioxane-water (1:1) (14 mL) in a pressure-rated sealed tube (35 mL).

Purification by flash column chromatography on SiO_2 (12 g), eluting with hexane-EtOAc (9:1) gave the *title compound* (0.38 g, 80%) as a beige solid.

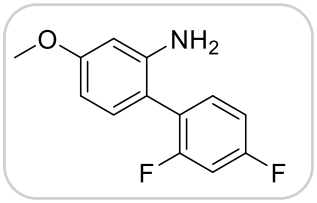

Mp: 93-95 °C. **Purity (LCMS):** 95%. **Found [ESI]:** MH^+, 236.0909. $C_{13}H_{12}F_2NO$ [MH] requires 236.0887. **IR** (neat) *v*/cm^{-1} 3707, 3665 (NH_2), 2981 (C-H), 1587 (C-C), 1292 (C-O), 1033 (C-F), 745, 715 (C-H). **^{1}H NMR** (600 MHz, $CDCl_3$) δ 7.32 (1H, ddd, J_{HF} 9, J_{HH} 8.5, J_{HF} 6.5, H-6'), 7.00 (1H, d, *J* 8.5, H-3), 6.98 – 6.88 (2H, m, H-3', H-5'), 6.43 (1H, dd, *J* 8.5, 2.5, H-4), 6.37 (1H, d, *J* 2.5, H-6), 3.80 (3 H, s, OMe). **^{13}C NMR** (151 MHz, $CDCl_3$) δ 162.3 (dd, $^1J_{CF}$ 249, $^3J_{CF}$ 12, CF), 160.7 (C), 160.1 (dd, $^1J_{CF}$ 249, $^3J_{CF}$ 12, CF), 144.9 (C), 132.9 (dd, $^3J_{CF}$ 10, $^3J_{CF}$ 5, CH), 132.0 (CH), 122.3 (dd, $^2J_{CF}$ 17, $^4J_{CF}$ 4, C), 113.6 (C), 111.7 (dd, $^2J_{CF}$ 21, $^4J_{CF}$ 4, CH), 104.7 (CH), 104.4 (dd, $^2J_{CF}$ 26, $^2J_{CF}$ 23, CH), 101.3 (CH), 55.2 (OCH_3).

2-(4'-Methoxyphenyl)-5-methoxyaniline (2.26. Prepared according to General Procedure A using a solution of 2-bromo-5-methoxyaniline (404 mg, 2.0 mmol, 1.0 equiv.), 4-methoxyphenylboronic acid (395 mg, 2.6 mmol, 1.3 equiv.), Na_2CO_3 (848 mg, 8.0 mmol, 4.0 equiv.) and $Pd(dppf)Cl_2$ (73 mg, 5 mol%) in dioxane-water (1:1) (14 mL) in a pressure-rated sealed tube (35 mL). Purification by flash column chromatography on SiO_2 (12 g), eluting with hexane-EtOAc (95:5) gave the *title compound* (0.38 g, 83%) as a beige solid.

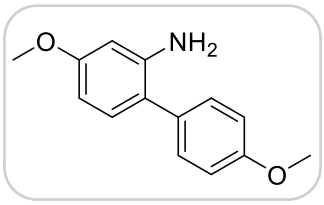

Mp: 114-116 °C (lit:[194] 110 °C). **Purity (LCMS):** 97%. **Found [ESI]:** MH^+, 230.1179. $C_{14}H_{16}NO_2$ [MH] requires 230.1181. **IR** (neat) *v*/cm^{-1} 3476, 3385 (NH_2), 2964 (C-H), 1605 (C-C), 1171 (C-O), 823, 786 (C-H). **^{1}H NMR** (600 MHz, $CDCl_3$) δ 7.34 (2H, AA'XX', *J* 8.5, 3.0, 2.0, H-2'), 7.02 (1H, d, *J* 8.5, H-3), 6.96 (2H, AA'XX', *J* 8.5, 3.0, 2.0, H-3'), 6.39 (1H, dd, *J* 8.5, 2.5, H-4), 6.33 (1H, d, *J* 2.5, H-6), 3.84 (3H, s, OMe), 3.79 (3H, s, OMe), NH_2 not observed. **^{13}C NMR** (151 MHz, $CDCl_3$) δ 155.1 (C), 153.8 (C), 139.7 (C), 126.7 (C), 126.6 (CH), 125.6 (CH), 115.9 (C), 109.4 (CH), 99.6 (OMe), 96.4 (OMe).

2-(2'-Fluoro-4'-methylphenyl)-5-methoxyaniline (2.27). Prepared according to General Procedure A using a solution of 2-bromo-5-methoxyaniline (404 mg, 2.0 mmol, 1.0 equiv.), 2-fluoro-4-methylphenylboronic acid (397 mg, 2.6 mmol, 1.3 equiv.), Na_2CO_3 (848 mg, 8.0 mmol, 4.0 equiv.) and $Pd(PPh_3)_4$ (115 mg, 5 mol%) in dioxane-water (1:1) (14 mL) in a pressure-rated sealed tube (35 mL). Purification by flash column chromatography on SiO_2 (12 g), eluting with hexane-EtOAc (95:5) gave the *title compound* (0.36 g, 77%) as a beige solid.

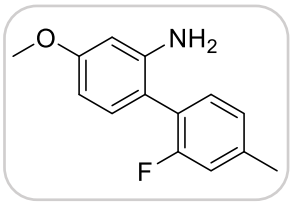

Mp: 112-114 °C. **Purity (LCMS):** 95%. **Found [ESI]:** MH^+, 232.1145. $C_{14}H_{15}FNO$ [MH] requires 232.1138. **IR** (neat) *v*/cm^{-1} 3472, 3373 (NH_2), 2972 (C-H), 1613 (C-C), 1207 (C-O), 1032 (C-F), 821, 800 (C-H). **^{1}H NMR** (600 MHz, $CDCl_3$) δ 7.22 (1H, dd, *J* 8.0, J_{HF} 8.0, H-6'), 7.02 (2H, m, H-3, H-5'), 6.98 (1H, d, $^3J_{HF}$ 11.0, H-3'), 6.42 (1H, dd, *J* 8.5, 2.5, H-4), 6.36 (1H, d, *J* 2.5, H-6), 3.80 (3H, s, OMe), 2.39 (3H, s, Me), NH_2 not observed. **^{13}C NMR** (151 MHz, $CDCl_3$) δ 160.4 (C), 159.8 (d, $^1J_{CF}$ 246, CF), 145.0 (C), 139.7 (d, $^3J_{CF}$ 8, CH), 132.0 (CH), 131.8 (d, $^4J_{CF}$ 4, CH), 125.2 (d, $^4J_{CF}$ 3, CH), 123.1 (d, $^2J_{CF}$ 16, C), 116.5 (d, $^2J_{CF}$ 22, CH), 114.7 (C), 104.5 (CH), 101.3 (CH), 55.2 (OMe), 21.1 (Me).

2-(4'-Trifluoromethylphenyl)aniline (2.28). Prepared according to General Procedure A using a solution of 2-iodoaniline (438 mg, 2 mmol, 1 equiv.), 4-trifluoromethylphenylboronic acid (494 mg, 2.6 mmol, 1.3 equiv.), Na_2CO_3 (848 mg, 8 mmol, 4 equiv.) and $Pd(dppf)Cl_2$ (74 mg, 5 mol%) in dioxane-water (1:1) (14 mL) in a pressure-rated sealed tube (35 mL). Purification by flash column chromatography on SiO_2 (12 g), eluting with hexane-EtOAc (9:1) gave the *title compound* (0.76 g, 80%) as a colourless solid.

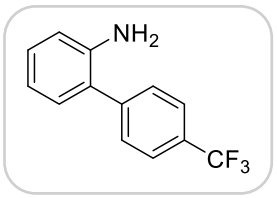

MP: 74-75 °C. **Purity (LCMS):** 95%. **Found [ESI]:** MH^+, 238.0828. $C_{13}H_{11}F_3N$ [MH] requires 238.0844. **IR** (neat) *v*/cm^{-1} 3463, 3368 (NH_2), 2933 (C-H), 1614 (C-C), 1068 (C-F), 754 (C-H). **^{1}H NMR** (600 MHz, $CDCl_3$) δ 7.70 (2H, d, *J* 8.0, H-3'), 7.59 (2H, d, *J* 8.0, H-2'), 7.19 (1H, ddd, *J* 8.0, 7.5, 1.5, H-5), 7.11 (1H, dd, *J* 7.5, 1.5, H-3), 6.84 (1H, ddd, *J* 7.5, 7.5, 1.0, H-4) 6.78 (1H, dd, *J* 8.0, 1.0, H-6), 3.73 (2H, s, NH_2). **^{13}C NMR** (151 MHz, $CDCl_3$) δ 143.3 (C), 143.2 (C), 130.3 (CH), 129.5 (CH), 129.3 (d, $^2J_{CF}$ 32, C), 129.3 (CH), 126.1 (C), 125.8 (q, $^3J_{CF}$ 4, CH), 124.2 (q, $^1J_{CF}$ 272, CF_3), 119.0 (CH), 115.9 (CH).

2-(2',4'-Dimethoxyphenyl)aniline (2.29). Prepared according to General Procedure A using a solution of 2-iodoaniline (438 mg, 2.0 mmol, 1.0 equiv.), 2,4-dimethoxyphenylboronic acid (473 mg, 2.6 mmol, 1.3 equiv.), Na_2CO_3 (848 mg, 8.0 mmol, 4.0 equiv.) and $Pd(PPh_3)_4$ (115 mg, 5 mol%) in dioxane-water (1:1) (14 mL) in a pressure-rated sealed tube (35 mL). Purification by flash column chromatography on SiO_2 (12 g), eluting with hexane-EtOAc (4:1) gave the *title compound* (0.31 g, 67%) as a beige solid.

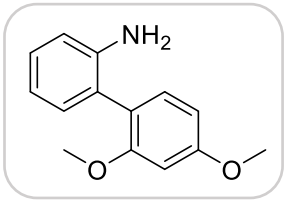

Mp: 59-61 °C (lit:[195] 69 °C). **Purity (LCMS):** 97%. **Found [ESI]:** MH^+, 230.1187. $C_{14}H_{16}NO_2$ [MH] requires 230.1181. **IR** (neat) *v*/cm^{-1} 3455, 3373 (NH_2), 2968 (C-H), 1607 (C-C), 1050 (C-O), 744 (C-H). **^{1}H NMR** (600 MHz, $CDCl_3$) δ 7.20 – 7.13 (2H, m, H-5, H-6'), 7.09 (1H, dd, *J* 7.5, 1.5, H-3), 6.83 (1 H, ddd, *J* 7.5, 7.5, 1.0, H-4), 6.78 (1H, dd, *J* 8.0, 1.0, H-6), 6.61 – 6.56 (2H, m, H-3', H-5'), 3.86 (3H, s, OMe), 3.79 (3H, s, OMe), 3.33 (2H, s, NH_2). **^{13}C NMR** (151 MHz, $CDCl_3$) δ 160.5 (C), 157.6 (C), 144.3

(C), 132.2 (CH), 131.3 (CH), 128.3 (CH), 124.9 (C), 120.7 (C), 118.6 (CH), 115.7 (CH), 104.7 (CH), 98.9 (CH), 55.7 (OMe), 55.4 (OMe).

2-(2'-Methoxy-4'-trifluoromethylphenyl)aniline (2.30). Prepared according to General Procedure A using a solution of 2-iodoaniline (438 mg, 2.0 mmol, 1.0 equiv.), 2-methoxy-4-trifluoromethylphenylboronic acid (559 mg, 2.6 mmol, 1.3 equiv.), Na_2CO_3 (848 mg, 8.0 mmol, 4.0 equiv.) and $Pd(PPh_3)_4$ (115 mg, 5 mol%) in dioxane-water (1:1) (14 mL) in a pressure-rated sealed tube (35 mL). Purification by flash column chromatography on SiO_2 (12 g), eluting with hexane-EtOAc (9:1) gave the *title compound* (0.45 g, 85%) as a colourless solid.

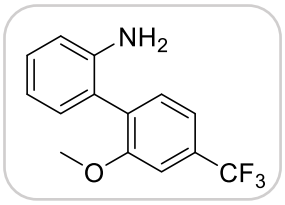

Mp: 88-89 °C. **Purity (LCMS):** 96%. **Found [ESI]:** MH^+, 268.0956. $C_{14}H_{13}F_3NO$ [MH] requires 268.0949. **IR** (neat) *v*/cm^{-1} 3707, 3581 (NH_2) , 2974 (C-H), 1623 (C-C), 1327 (C-O), 1116 (CF_3), 738 (C-H).**^{1}H NMR** (600 MHz, $CDCl_3$) δ 7.37 (1H, d, *J* 8.0, H-6'), 7.31 (1H, d, *J* 8.0, H-5'), 7.23 – 7.17 (2H, m, H-5, H-3'), 7.07 (1H, dd, *J* 7.5, 1.5, H-3), 6.84 (1H, ddd, *J* 7.5, 7.5, 1.0, H-4), 6.78 (1H, dd, *J* 8.0, 1.0, H-6), 3.86 (3H, s, OMe), 3.65 (2H, s, NH). **^{13}C NMR** (151 MHz, $CDCl_3$) δ 156.8 (C), 144.2 (C), 132.2 (CH), 132.1 (C), 131.0 (q, $^2J_{CF}$ 34, C), 130.9 (CH), 129.1 (CH), 124.0 (q, $^1J_{CF}$ 272, CF_3), 123.5 (C), 118.6 (CH), 117.9 (q, $^3J_{CF}$ 4, CH), 115.9 (CH), 107.9 (q, $^3J_{CF}$ 4, CH), 56.0 (OCH_3).

2-(4'-Fluoro-2'-methoxyphenyl)-5-methoxyaniline (2.31). Prepared according to General Procedure A using a solution of 2-bromo-5-methoxyaniline (404 mg, 2.0 mmol, 1.0 equiv.), 4-fluoro-2-methoxyphenylboronic acid (442 mg, 2.6 mmol, 1.3 equiv.), Na_2CO_3 (848 mg, 8.0 mmol, 4.0 equiv.) and $Pd(PPh_3)_4$ (115 mg, 5 mol%) in dioxane-water (1:1) (14 mL) in a pressure-rated sealed tube (35 mL). Purification by flash column chromatography on SiO_2 (12 g), eluting with hexane-EtOAc (9:1) gave the *title compound* (0.33 g, 67%) as a brown oil.

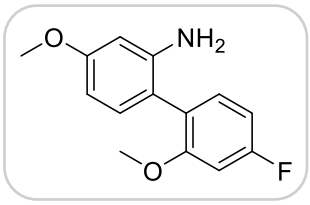

Purity (LCMS): 97%. **Found [ESI]:** MH^+, 248.1095. $C_{14}H_{15}FNO_2$ [MH] requires 248.1087. **IR** (neat) *v*/cm^{-1} 3708, 3681 (NH_2), 2981 (C-H), 1595 (C-C), 1205 (C-O), 1033 (C-F), 831 (C-H). **^{1}H NMR** (600 MHz, $CDCl_3$) δ 7.17 (1H, dd, J_{HH} 8.5, $^4J_{HF}$ 7.0, H-6'), 6.97 (1H, d, *J* 8.5, H-3), 6.76 – 6.68 (2H, m, H-5', H-3'), 6.40 (1H, dd, *J* 8.5, 2.5, H-4), 6.34 (1H, d, *J* 2.5, H-6), 3.79 (3H, s, OMe), 3.78 (3H, s, OMe). **^{13}C NMR** (151 MHz, $CDCl_3$) δ 163.2 (d, $^1J_{CF}$ 246, CF), 160.1 (C), 157.9 (d, $^3J_{CF}$ 10, C), 145.3 (C), 132.7 (d, $^3J_{CF}$ 10, CH), 132.0 (CH), 123.6 (d, $^4J_{CF}$ 3, C), 116.9 (C), 107.4 (d, $^2J_{CF}$ 21, CH), 104.2 (CH), 101.3 (CH), 99.4 (CH), (d, $^2J_{CF}$ 26), 55.9 (OCH_3), 55.1 (OCH_3).

2-(4'-Methoxyphenyl)-5-fluoroaniline (2.32). Prepared according to General Procedure A using a solution of 2-bromo-5-fluoroaniline (380 mg, 2.0 mmol, 1.0 equiv.), 4-methylphenylboronic acid (395 mg, 2.6 mmol, 1.3 equiv.), Na_2CO_3 (848 mg, 8.0 mmol, 4.0 equiv.) and $Pd(dppf)Cl_2$ (73 mg, 5 mol%)

in dioxane-water (1:1) (14 mL) in a pressure-rated sealed tube (35 mL). Purification by flash column chromatography on SiO_2 (12 g), eluting with hexane-EtOAc (4:1) gave the *title compound* (0.38 g, 88%) as a yellow solid.

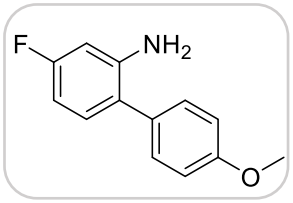

Mp: 97-99 °C. **Purity (LCMS):** 97%. **Found [ESI]:** MH^+, 218.0988. $C_{13}H_{12}FNO$ [MH] requires 218.0981. **IR** (neat) *v*/cm^{-1} 3457, 3371 (NH_2), 2959 (C-H), 1614 (C-C), 1236 (C-O), 1032 (C-F), 829, 798 (C-H). **^{1}H NMR** (600 MHz, $CDCl_3$) δ 7.32 (2H, AA'XX', *J* 8.5, 3.0, 2.0, H-2'), 7.02 (1H, dd, J_{HH} 8.5, $^4J_{HF}$ 6.5 H-3), 6.97 (2H, AA'XX', *J* 8.5, 3.0, 2.0, H-3'), 6.49 (1H, ddd, $^3J_{HF}$ 8.5, J_{HH} 7.5, J_{HH} 2.5, H-4), 6.45 (1H, dd, $^3J_{HF}$ 10.5, 2.5, H-6), 3.84 (3H, s, OMe). **^{13}C NMR** (151 MHz, $CDCl_3$) δ 162.9 (d, $^1J_{CF}$ 243, CF), 158.8 (C), 145.1 (d, $^3J_{CF}$ 11, C), 131.6 (d, $^3J_{CF}$ 10, CH), 130.8 (C), 130.3 (CH), 123.3 (d, $^4J_{CF}$ 3, C), 114.3 (CH), 105.1 (d, $^2J_{CF}$ 21, CH), 102.0 (d, $^2J_{CF}$ 25, CH), 55.3 (OCH_3).

2-(2',4'-Difluorophenyl)-5-fluoroaniline (2.33). Prepared according to General Procedure A using a solution of 2-bromo-5-fluoroaniline (380 mg, 2.0 mmol, 1.0 equiv.), 2,4-difluorophenylboronic acid (411 mg, 2.6 mmol, 1.3 equiv.), Na_2CO_3 (848 mg, 8.0 mmol, 4.0 equiv.) and $Pd(PPh_3)_4$ (115 mg, 5 mol%) in dioxane-water (1:1) (14 mL) in a pressure-rated sealed tube (35 mL). Purification by flash column chromatography on SiO_2 (12 g), eluting with hexane-EtOAc (9:1) gave the *title compound* (0.12 g, 46%) as a colourless solid.

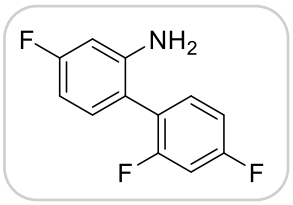

Mp: 77-78 °C. **Purity (LCMS):** 98%. **Found [ESI]:** MH^+, 224.0672. $C_{12}H_9F_3N$ [MH] requires 224.0687. **IR** (neat) *v*/cm^{-1} 3468, 3382 (NH_2), 2970 (C-H), 1606 (C-C), 1099 (C-F), 809 (C-H). **^{1}H NMR** (600 MHz, $CDCl_3$) δ 7.31 (1H, dd, J_{HF} 9.0, J_{HH} 8.5, J_{HF} 6.5, H-6'), 7.02 (1H, dd, J_{HH} 8.5, J_{HF} 7.0, H-3), 6.97 (1H, ddd, J_{HH} 8.5, J_{HF} 8.0, J_{HH} 2.5, H-5'), 6.94 (1H, ddd, J_{HF} 9.5, J_{HF} 9.0, J_{HH} 2.5, H-3'), 6.52 (1H, ddd, J_{HH} 8.5, J_{HF} 8.5, J_{HH} 2.5, H-4), 6.49 (1H, dd, J_{HF} 10.5, J_{HH} 2.5, H-6), 3.72 (2H, s, NH_2). **^{13}C NMR** (151 MHz, $CDCl_3$) δ 163.6 (d, $^1J_{CF}$ 245, CF), 162.6 (dd, $^1J_{CF}$ 249, $^3J_{CF}$ 12, CF), 160.0 (dd, $^1J_{CF}$ 249, $^3J_{CF}$ 12, CF), 145.9 (d, $^3J_{CF}$ 11, C), 132.8 (dd, $^3J_{CF}$ 10, $^3J_{CF}$ 5, CH), 132.4 (d, $^3J_{CF}$ 10), 121.7 (dd, $^2J_{CF}$ 17, $^4J_{CF}$ 4, C), 116.3 (d, $^4J_{CF}$ 3, C), 111.9 (dd, $^2J_{CF}$ 21, $^4J_{CF}$ 4, CH), 105.3 (d, $^2J_{CF}$ 22, CH), 104.5 (dd, $^2J_{CF}$ 26, $^2J_{CF}$ 26, CH), 102.3 (d, $^2J_{CF}$ 25, CH).

2-(2'-Fluoro-4'-methylphenyl)-5-fluoroaniline (2.34). Prepared according to General Procedure A using a solution of 2-bromo-5-fluoroaniline (380 mg, 2.0 mmol, 1.0 equiv.), 2-fluoro-4-methylphenylboronic acid (400 mg, 2.6 mmol, 1.3 equiv.), Na_2CO_3 (848 mg, 8.0 mmol, 4.0 equiv.) and $Pd(PPh_3)_4$ (115 mg, 5 mol%) in dioxane-water (1:1) (14 mL) in a pressure-rated sealed tube (35 mL). Purification by flash column chromatography on SiO_2 (12 g), eluting with hexane-EtOAc (9:1) gave the *title compound* (0.34 g, 76%) as a beige solid.

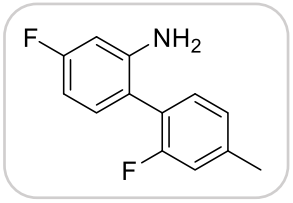

Mp: 45-46 °C. **Purity (LCMS):** 96%. **Found [ESI]:** MH^+, 220.0942. $C_{13}H_{12}F_2N$ [MH] requires 220.0938. **IR** (neat) *v*/cm^{-1} 3707, 3681 (NH_2), 2982 (C-H), 1616 (C-C), 1055 (C-F), 823, 808 (C-H). **^{1}H NMR** (600 MHz, $CDCl_3$) δ 7.20 (1H, dd, J_{HH} 8.0, J_{HF} 7.5, H-6'), 7.06 – 7.01 (2H, m, H-5', H-3), 6.99 (1H, d, $^3J_{HF}$ 11.0, H-3'), 6.52 (1H, ddd, J_{HF} 8.5, J_{HH} 8.5, 2.5, H-4), 6.49 (1 H, dd, J_{HF} 11.0, J_{HH} 2.5, H-6), 3.81 (2H, s, NH_2), 2.40 (3H, s, Me). **^{13}C NMR** (151 MHz, $CDCl_3$) δ 163.5 (d, $^1J_{CF}$ 244, CF), 159.7 (d, $^1J_{CF}$ 246, CF), 145.8 (d, $^3J_{CF}$ 11, C), 140.2 (d, $^3J_{CF}$ 8, C), 132.3 (d, $^3J_{CF}$ 10, CH), 131.6 (d, $^4J_{CF}$ 4, CH), 125.4 (CH), 122.5 (d, $^2J_{CF}$ 17, C), 117.4 (d, $^4J_{CF}$ 3, C), 116.6 (d, $^2J_{CF}$ 22, CH), 105.1 (d, $^2J_{CF}$ 22,CH), 102.2 (d, $^2J_{CF}$ 25, CH), 21.1 (CH_3).

2-(4'-Fluoro-2'-methoxyphenyl)-5-fluoroaniline (2.35). Prepared according to General Procedure A using a solution of 2-bromo-5-fluoroaniline (570 mg, 3.0 mmol, 1.0 equiv.), 4-fluoro-2-methoxyphenylboronic acid (663 mg, 3.9 mmol, 1.3 equiv.), Na_2CO_3 (1.27 g, 12.0 mmol, 4.0 equiv.) and $Pd(PPh_3)_2Cl_2$ (167 mg, 5 mol%) in dioxane-water (1:1) (14 mL) in a pressure-rated sealed tube (35 mL). Purification by flash column chromatography on SiO_2 (12 g), eluting with hexane-EtOAc (9:1) gave the *title compound* (0.55 g, 77%) as a yellow solid.

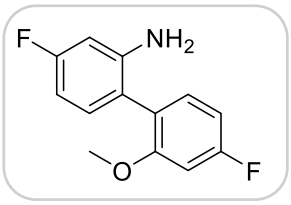

Mp: 66-67 °C. **Purity (LCMS):** 95%. **Found [ESI]:** MH^+, 236.0810. $C_{13}H_{12}F_2NO$ [MH] requires 236.0887 **IR** (neat) *v*/cm^{-1} 3465, 3380 (NH_2), 2940 (C-H), 1618 (C-C), 1150 (C-O), 1106 (C-F), 837 (C-H). **^{1}H NMR** (600 MHz, $CDCl_3$) δ 7.16 (1H, dd, J_{HH} 8.5, J_{HF} 7.0, H-6'), 6.97 (1H, dd, J_{HH} 8.5, J_{HF} 6.5, H-3), 6.77 – 6.69 (2H, m, H-3', H-5'), 6.50 (1H, ddd, J_{HF} 8.5, J_{HH} 8.5, J_{HH} 2.5, H-4), 6.45 (1H, dd, J_{HF} 10.5, J_{HH} 2.5, H-6), 3.79 (3H, s, OMe), 3.70 (2H, s, NH_2). **^{13}C NMR** (151 MHz, $CDCl_3$) δ 163.4 (d, $^1J_{CF}$ 246, CF), 163.2 (d, $^1J_{CF}$ 244), 157.9 (d, $^3J_{CF}$ 10, C), 146.0 (d, $^3J_{CF}$ 11, C), 132.6 (d, $^3J_{CF}$ 10, CH), 132.3 (d, $^3J_{CF}$ 10, CH), 122.9 (d, $^4J_{CF}$ 3, C), 119.6 (d, $^4J_{CF}$ 3, C), 107.5 (d, $^2J_{CF}$ 21, CH), 105.1 (d, $^2J_{CF}$ 21, CH), 102.2 (d, $^2J_{CF}$ 25, CH), 99.5 (d, $^2J_{CF}$ 26, CH), 55.9 (OMe).

2.10.2 Synthesis of azides

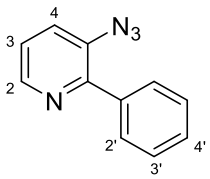

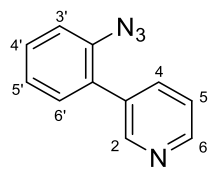

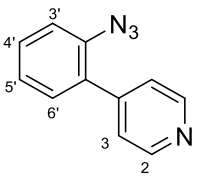

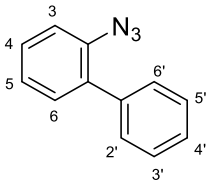

3-Azidopyridine (2.39). A solution of 3-Aminopyridine (97 mg, 1 mmol, 1 eq) in diluted H_2SO_4 (0.85 mL in 5 mL H_2O) was cooled to 0 °C. Then, a solution of $NaNO_2$ (82 mg, 1.2 mmol, 1.2 eq) in H_2O (3.6 mL) was added dropwise and the mixture was stirred for 20 min. After this time, urea (16 mg, 0.2 mmol, 0.2 eq)was added. The mixture was stirred for 20 min and then a solution of NaN_3 (110 mg, 1.7 mmol, 1.7 eq) in water (2.9 mL) was added. The reaction mixture was stirred for 1 h at 0 °C, and then it was stirred overnight at room temperature. The reaction was quenched with a saturated aqueous solution of $NaHCO_3$ (15 mL) and extracted with Et_2O (3 x 15 mL). The combined organic phases were dried over Na_2SO_4, filtered and concentrated under pressure. The *tittle compound* was obtained without further purification (102 mg, 85% yield) as a brown solid.

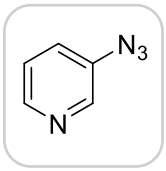

IR (neat) *v*/cm^{-1} 2895 (C-H), 3106 (N_3), 1597 (C-C), 737, 691 (C-H).**^{1}H NMR** (600 MHz, Chloroform-*d*) δ 8.39 (1H, dd, *J* 5.0, 1.5 Hz, H-6), 8.36 (1H, d, *J* 2.5 Hz, H-2), 7.35 (1H, m, H-4), 7.29 (1H, dd, *J* 8.5, 5.0 Hz, H-5).

3-Azido-2-Phenylpyridine (2.40). A solution of 3-Amino-2-Phenylpyridine (172 mg, 1 mmol, 1 eq) in diluted H_2SO_4 (0.85 mL in 5 mL H_2O) was cooled to 0 °C. Then, a solution of $NaNO_2$ (82 mg, 1.2 mmol, 1.2 eq) in H_2O (3.6 mL) was added dropwise and the mixture was stirred for 20 min. After this time, urea (15 mg, 0.2 mmol, 0.2 eq)was added. The mixture was stirred for 20 min and then a solution of NaN_3 (112 mg, 1.7 mmol, 1.7 eq) in water (2.9 mL) was added. The reaction mixture was stirred for 1 h at 0 °C, and then it was stirred overnight at room temperature. The reaction was quenched with a saturated aqueous solution of $NaHCO_3$ (20 mL) and extracted with Et_2O (3 x 20 mL). The combined organic phases were washed with water (20 mL), dried over Na_2SO_4, filtered and concentrated under pressure. The *tittle compound* was obtained without further purification (176 mg, 90% yield) as a brown solid.

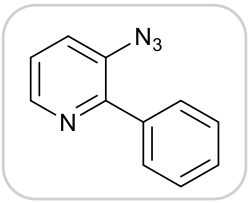

IR (neat) *v*/cm^{-1} 2895, 2106 cm^{-1} (N_3) **^{1}H NMR** (600 MHz, DMSO-d_6) δ 8.08 (1H, dd, *J* 5.0, 1.5, H-2), 7.83 – 7.79 (2H, m, H-2'), 7.42 (2H, m, H-3'), 7.36 (1H, tt, *J* 7.2, 1.2, H-4'), 7.32 (1H, dd, *J* 8.0, 1.5, H-4), 7.21 (1H, dd, *J* 8.0, 5.0, H-3).

2-Azido-1,1'-biphenyl (2.41). A solution of Biphenyl amine (338 mg, 2 mmol, 1 eq) in diluted H_2SO_4 (1.7 mL in 10 mL H_2O) was cooled to 0 °C. Then, a solution of $NaNO_2$ (171 mg, 2.4 mmol, 1.2 eq) in H_2O (7.2 mL) was added dropwise and the mixture was stirred for 20 min. After this time, urea (28 mg, 0.4 mmol, 0.2 eq) was added. The mixture was stirred for 20 min and then a solution of NaN_3 (224 mg, 3.4 mmol, 1.7 eq) in water (5.8 mL) was added. The reaction mixture was stirred for 1 h at 0 °C, and then it was stirred overnight at room temperature. The reaction was quenched with a saturated aqueous solution of $NaHCO_3$ (20 mL) and extracted with Et_2O (3 x 20 mL). The combined organic phases were

washed with water (20 mL), dried over Na_2SO_4, filtered and concentrated under pressure. The *tittle compound* was obtained without further purification (377 mg, 97% yield) as a brown solid.

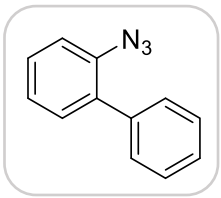

^{1}H NMR (600 MHz, Chloroform-*d*) δ 7.46 – 7.35 (6H), 7.34 (1H, dd, *J* 8.0, 1.0 H-3 or H-6), 7.26 (1H, dd, *J* 8.0, 1.0, H-3 or H-6), 7.21 (1H, td, *J* 8.0, 1.0, H-4 or H-5). (lit[196])

3-(2-Azidophenyl)pyridine (2.42). A solution of 2-(pyridin-3-yl)aniline (327 mg, 2 mmol, 1 eq) in diluted H_2SO_4 (1.7 mL in 10 mL H_2O) was cooled to 0 °C. Then, a solution of $NaNO_2$ (165 mg, 2.4 mmol, 1.2 eq) in H_2O (7.2 mL) was added dropwise and the mixture was stirred for 20 min. After this time, urea (26 mg, 0.4 mmol, 0.2 eq) was added. The mixture was stirred for 20 min and then a solution of NaN_3 (224 mg, 3.4 mmol, 1.7 eq) in water (5.8 mL) was added. The reaction mixture was stirred for 1 h at 0 °C, and then it was stirred overnight at room temperature. The reaction was quenched with a saturated aqueous solution of $NaHCO_3$ (50 mL) and extracted with Et_2O (3 x 20 mL). The combined organic phases were washed with water (20 mL), dried over Na_2SO_4, filtered and concentrated under pressure. The *tittle compound* was obtained without further purification (347 mg, 89%) as a brown solid.

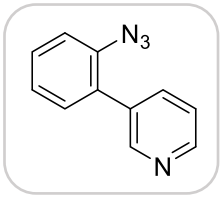

^{1}H NMR (600 MHz, Chloroform-*d*) δ 8.69 (1H, s, H-2), 8.59 (1H, d, *J* 5.0, H-6), 7.80 (1H, dt, *J* 8.0, 2.0, H-4), 7.44 (1H, td, *J* 8.0, 8.0, 1.5, H-4'), 7.36 (1H, dd, *J* 8.0, 5.0, H-5), 7.34 (1H, dd, *J* 7.5, 1.5, H-6'), 7.28 (1H, d, *J* 8.0, 7.5, H-3'), 7.24 (1H, td, *J* 7.5, 1.0, H-5').

4-(2-Azidophenyl)pyridine (2.43). A solution of Biphenyl amine (236 mg, 1.4 mmol, 1 eq) in diluted H_2SO_4 (1.2 mL in 7 mL H_2O) was cooled to 0 °C. Then, a solution of $NaNO_2$ (117 mg, 1.66 mmol, 1.2 eq) in H_2O (5 mL) was added dropwise and the mixture was stirred for 20 min. After this time, urea (17 mg, 0.28 mmol, 0.2 eq) was added. The mixture was stirred for 20 min and then a solution of NaN_3 (157 mg, 2.38 mmol, 1.7 eq) in water (4 mL) was added. The reaction mixture was stirred for 1 h at 0 °C, and then it was stirred overnight at room temperature. The reaction was quenched with a saturated aqueous solution of $NaHCO_3$ (30 mL) and extracted with Et_2O (3 x 20 mL). The combined organic phases were washed with water (20 mL), dried over Na_2SO_4, filtered and concentrated under pressure. The *tittle compound* was obtained without further purification (250 mg, 91%) as a brown solid.

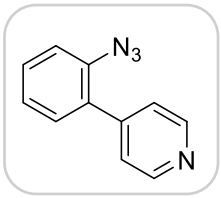

^{1}H NMR (600 MHz, Chloroform-*d*) δ 8.65 (2H, d, *J* 5.0, H-2), 7.46 (1H, td, *J* 8.0, 8.0, 1.5, H-4'), 7.39 (2H, dd, *J* 5.0, 1.5), 7.34 (1H, dd, *J* 7.5, 1.5, H-6'), 7.28 (1H, dd, *J* 8.0, 1.0, H-3'), 7.23 (1H, td, *J* 8.0, 7.5, 1.0, H-5')

2-Azido-4'-nitro-1,1'-biphenyl (2.44). A solution of 2-(4'-nitrophenyl)aniline (288 mg, 1.3 mmol, 1 eq) in diluted H_2SO_4 (1.7 mL in 10 mL H_2O) was cooled to 0 °C. Then, a solution of $NaNO_2$ (108 mg, 1.6 mmol, 1.2 eq) in H_2O (3.6 mL) was added dropwise and the mixture was stirred for 20 min. After this time, urea (36 mg, 0.6 mmol, 0.2 eq) was added. The mixture was stirred for 20 min and then a solution of NaN_3 (144 mg, 2.2 mmol, 1.7 eq) in water (2.9 mL) was added. The reaction mixture was stirred for 1 h at 0 °C, and then it was stirred overnight at room temperature. The reaction was quenched with a saturated aqueous solution of $NaHCO_3$ (20 mL) and extracted with Et_2O (3 x 20 mL). The combined organic phases were washed with water (20 mL), dried over Na_2SO_4, filtered and concentrated under pressure. The *tittle compound* was obtained without further purification (285 mg, 95%) as a brown solid.

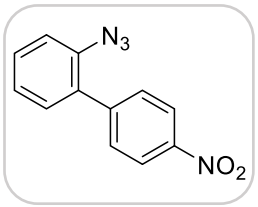

^{1}H NMR (600 MHz, Chloroform-*d*) δ 8.27 (2H, AA'XX', *J* 9.0, 2.5, 2.0, H-3'), 7.62 (2H, AA'XX', *J* 9.0, 2.5, 2.0, H-2'), 7.47 (1H, td, *J* 8.0, 8.0, 1.5, H-4), 7.34 (1 H, dd, *J* 7.5, 1.5, H-6), 7.29 (1 H, dd, *J* 8.0, 1.0, H-3), 7.23 (2 H, td, *J* 8.0, 7.5, 1.0, H-5).

2-Azido-4'-methoxy-1,1'-biphenyl (2.45). A solution of 2-(4'-methoxyphenyl)aniline (160 mg, 0.8 mmol, 1 eq) in diluted H_2SO_4 (1.7 mL in 10 mL of 2:3 H_2O:dioxane) was cooled to 0 °C. Then, a solution of $NaNO_2$ (69 mg, 1 mmol, 1.2 eq) in H_2O (3.6 mL) was added dropwise and the mixture was stirred for 20 min. After this time, urea (12 mg, 0.2 mmol, 0.2 eq) was added. The mixture was stirred for 20 min and then a solution of NaN_3 (88 mg, 1.4 mmol, 1.7 eq) in water (2.9 mL) was added. The reaction mixture was stirred for 1 h at 0 °C, and then it was stirred overnight at room temperature. The reaction was quenched with a saturated aqueous solution of $NaHCO_3$ (20 mL) and extracted with Et_2O (3 x 20 mL). The combined organic phases were washed with water (20 mL), dried over Na_2SO_4, filtered and concentrated under pressure. The *tittle compound* was obtained without further purification (171 mg, 99%) as a brown solid.

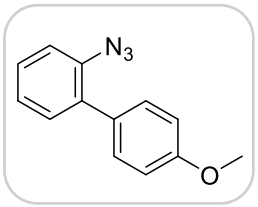

^{1}H NMR (600 MHz, Chloroform-*d*) δ 7.38 (2H, AA'XX', *J* 9.0, 3.0, 2.0, H-2'), 7.35 (1H, td, *J* 8.0, 7.5, 1.5, H-5), 7.31 (1H, dd, *J* 7.5, 1.5, H-3), 7.23 (1H, dd, *J* 8.0, 1.0, H-6), 7.18 (H, td, *J* 7.5, 7.5, 1.0, H-4), 6.96 (2H, AA'XX', *J* 9.0, 3.0, 2.0, H-3').

2'-Azido-2,4-difluoro-1,1'-biphenyl (2.46). A solution of 2-(2',4'-difluorophenyl)aniline (160 mg, 0.8 mmol, 1 eq) in diluted H_2SO_4 (1.7 mL in 10 mL of 2:3 H_2O:dioxane) was cooled to 0 °C. Then, a solution of $NaNO_2$ (69 mg, 1 mmol, 1.2 eq) in H_2O (3.6 mL) was added dropwise and the mixture was stirred for 20 min. After this time, urea (12 mg, 0.2 mmol, 0.2 eq) was added. The mixture was stirred for 20 min and then a solution of NaN_3 (88 mg, 1.4 mmol, 1.7 eq) in water (2.9 mL) was added. The reaction mixture was stirred for 1 h at 0 °C, and then it was stirred overnight at room temperature. The reaction was

quenched with a saturated aqueous solution of $NaHCO_3$ (20 mL) and extracted with Et_2O (3 x 20 mL). The combined organic phases were washed with water (20 mL), dried over Na_2SO_4, filtered and concentrated under pressure. The *tittle compound* was obtained without further purification (171 mg, 99%) as a brown solid.

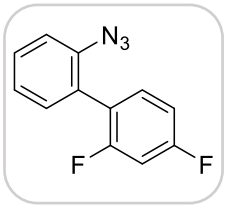

^{1}H NMR (600 MHz, Chloroform-*d*) δ 7.44 (1H, ddd, *J* 8.0, 7.5, 1.5, H-5'), 7.31 – 7.24 (3H, m, H-3', H-6, H-6'), 7.22 (1H, td, *J* 7.5, 7.5, 1.0, H-4'), 6.95 (1H, td, J_{HF} 8.5, J_{HH} 8.0, 2.5, H-5), 6.91 (1H, td, J_{HF} 9.5, 9.0, J_{HH} 2.5, H-3)

2'-Azido-4-bromo-2-fluoro-1,1'-biphenyl (2.47). A solution of 2-(4'-bromo-2'-fluorophenyl)aniline (289 mg, 1.1 mmol, 1 eq) in diluted H_2SO_4 (1.7 mL in 10 mL of 2:3 H_2O:dioxane) was cooled to 0 °C. Then, a solution of $NaNO_2$ (91 mg, 1.3 mmol, 1.2 eq) in H_2O (3.6 mL) was added dropwise and the mixture was stirred for 20 min. After this time, urea (18 mg, 0.3 mmol, 0.2 eq) was added. The mixture was stirred for 20 min and then a solution of NaN_3 (122 mg, 1.9 mmol, 1.7 eq) in water (2.9 mL) was added. The reaction mixture was stirred for 1 h at 0 °C, and then it was stirred overnight at room temperature. The reaction was quenched with a saturated aqueous solution of $NaHCO_3$ (20 mL) and extracted with Et_2O (3 x 20 mL). The combined organic phases were washed with water (20 mL), dried over Na_2SO_4, filtered and concentrated under pressure. The *tittle compound* was obtained without further purification (289 mg, 90%) as a brown solid.

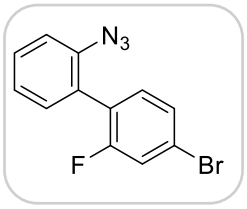

^{1}H NMR (600 MHz, Chloroform-*d*) δ 7.44 (1H, ddd, *J* 8.0, 7.5, 1.5, H-5'), 7.37 – 7.28 (2 H, m, H-3' H-6'), 7.28 – 7.23 (2 H, m, H-2, H-5), 7.21 (1H, td, *J* 7.5, 7.5, 1.0, H-4'), 7.16 (1 H, t, J_{HH} 8.5, J_{HF} 7.0, H-6).

2.10.3 Synthesis of carbazoles

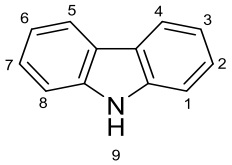

2-Methoxy-9*H*-carbazole (2.51). A solution (A) of 2-(4'-methoxyphenyl)aniline (409 mg, 2.1 mmol, 1.0 equiv.; 0.2 M) and $TMSN_3$ (0.27 mL, 2.1 mmol, 1.0 equiv.; 0.2 M) in dioxane (12 mL) and a solution (B) of *t*-BuONO (0.25 mL, 2.1 mmol, 0.2 M) in dioxane (12 mL) were mixed, heated in a PFA coil reactor at 80 °C for 50 min and then irradiated with 300 to 400 nm at 80 °C for 50 min using a UV-150 Photochemical Flow Reactor connected in-series. Purification by flash column chromatography on SiO_2, eluting with hexane-CH_2Cl_2, (4:1) and recrystallization with EtOAc gave the *title compound* (0.12 g, 28%) as a colourless solid.

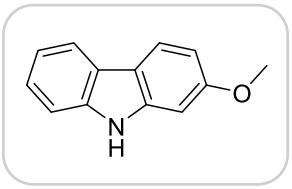

Mp: 238-240 °C (lit:[197] 237-238 °C). **Found [ESI]:** MH^+, 198.0917. $C_{13}H_{12}NO$ [MH] requires 198.0919. **IR** (neat) *v*/cm^{-1} 3387 (NH), 3011 (C-H), 1606 (C-C), 1161 (C-O). **^{1}H NMR** (600 MHz, d_6-DMSO) δ 11.11 (1H, s, H-9), 8.00 (1H, d, *J* 7.5, H-5), 7.97 (1H, d, *J* 8.5, H-4), 7.43 (1H, d, *J* 8.0, H-8), 7.30 (1H, ddd, *J* 8.0, 7.0, 1.2, H-7), 7.12 (1H, ddd, *J* 7.5, 7.0, H-6), 6.98 (1H, d, *J* 2.5, H-1), 6.78 (1H, dd, *J* 8.5, 2.5, H-3), 3.86 (3H, s, Me). **^{13}C NMR** (151 MHz, d_6-DMSO) 158.92 (C), 141.5 (C), 140.1 (C), 124.5 (CH), 123.1 (C), 121.3 (CH), 119.7 (CH), 119.0 (CH), 116.6 (C), 111.0 (CH), 108.1 (CH), 94.9 (CH), 55.7 (OMe).

2,4-Difluoro-9*H*-carbazole (2.52). A solution (A) of 2-(2',4'-difluorophenyl)aniline (491 mg, 2.4 mmol, 1.0 equiv.; 0.1 M) and $TMSN_3$ (0.31 mL, 2.4 mmol, 1.0 equiv.; 0.2 M) in dioxane (12 mL) and a solution (B) of *t*-BuONO (0.29 mL, 2.4 mmol, 0.15 M) in dioxane were mixed, heated in a PFA coil reactor at 80 °C for 50 min and then irradiated with 300 to 400 nm at 80 °C for 50 min using a UV-150 Photochemical Flow Reactor connected in-series. Purification by flash column chromatography on SiO_2, eluting with hexane-CH_2Cl_2, (4:1) gave the *title compound* (0.24 g, 22%) as a colourless solid.

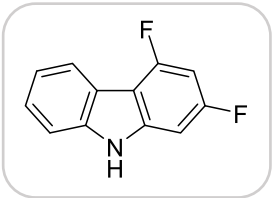

Mp: 206-207 °C (lit:[198] mp 101-102 °C). **Purity (by LCMS):** 96%. **Found [ESI]:** MH^+, 204.0628. $C_{12}H_8NF_2$ [MH] requires 204.0625. **IR** (neat) *v*/cm^{-1} 3392 (NH), 3038 (C-H), 1591 (C-C), 1118 (C-F). **^{1}H NMR** (600 MHz, d_6-DMSO) δ 11.67 (1H, s, 9-H), 7.98 (1H, d, *J* 7.5, H-5), 7.51 (1H, dd, *J* 8.0, 1.0, H-8), 7.40 (1H, ddd, *J* 8.0, 7.0, 1.0, H-7), 7.20 (1H, ddd, *J* 7.5, 7.0, 1.0, H-6), 7.14 (1H, dd, J_{HF} 9.5, J_{HH} 2.0, H-1), 6.93 (1H, ddd, J_{HF} 10.5, J_{HH} 2.0, H-3). **^{13}C NMR** (151 MHz, d_6-DMSO) 161.2 (dd, $^1J_{CF}$ 240, $^3J_{CF}$ 13, CF), 157.6 (dd, $^1J_{CF}$ 248, $^3J_{CF}$ 16, CF), 1412.0 (dd, $^3J_{CF}$ 15, $^3J_{CF}$ 13, C), 140.3 (d, $^4J_{CF}$ 2, C), 126.1 (CH), 121.9 (d, $^4J_{CF}$ 3, CH), 120.3 (CH), 119.6 (d, $^4J_{CF}$ 2, C), 111.6 (CH), 107.7 (d, $^3J_{CF}$ 19, C), 94.8 (CH), 94.7 – 94.2 (m, CH).

2-Fluoro-4-methyl-9*H*-carbazole (2.53). A solution (A) of 2-(2'-fluoro-4'-methylphenyl)aniline (400 mg, 1.6 mmol, 1.0 equiv.; 0.1 M) and $TMSN_3$ (0.2 mL, 1.7 mmol, 1.1 equiv.; 0.11 M) in dioxane (15 mL) and a solution (B) of *t*-BuONO (0.3 mL, 2.3 mmol, 1.15 equiv.; 0.15 M) in dioxane (15 mL) were mixed, heated in a PFA coil reactor at 80 °C for 50 min and then irradiated with 300 to 400 nm at 80 °C for 50 min using a UV-150 Photochemical Flow Reactor connected in-series. Purification by flash column chromatography on SiO_2, eluting with hexane-CH_2Cl_2, (9:1) gave the *title compound* (99 mg, 25%) as a colourless solid.

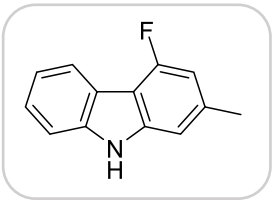

M p: 136-137 °C. **Purity (LCMS):** 97%. **Found [ESI]:** MH+, 200.0880. $C_{13}H_{11}FN$ [MH] requires 200.0876. **IR** (neat) *v*/cm^{-1} 3390 (N-H), 3060 (C-H), 1641 (C-C), 1118 (C-F), 746, 722 (C-H). **^{1}H NMR** (600 MHz, d_6-DMSO) δ 11.41 (1H, s, NH), 7.94 (1H, d, *J* 8.0, H-5), 7.45 (1H, d, *J* 8.0, H-8), 7.36 (1H, ddd, *J* 8.0, 7.0, 1.0, H-7), 7.15 (1H, ddd, *J* 8.0, 7.0, 1.0, H-6), 7.09 (1H, s, H-1), 6.75 (1H, d, $^3J_{HF}$ 11.5, H-3), 2.44 (3H, s, Me). **^{13}C NMR** (151 MHz, d_6-DMSO) 157.7 (d, $^1J_{CF}$ 246, CF), 142.7 (d, $^3J_{CF}$ 11, C), 139.8 (CH), 137.2 (d, $^3J_{CF}$ 8, C), 125.8 (CH), 121.9 (d, $^4J_{CF}$ 3., CH), 120.0 (d, $^4J_{CF}$ 2, C), 119.6 (CH), 111.42 (CH), 108.5 (d, $^2J_{CF}$ 21, C), 107.7 (d, $^4J_{CF}$ 3, C), 105.9 (d, $^2J_{CF}$ 18, CH), 22.0 (Me).

9-Ethyl-9*H*-carbazole (2.69). Prepared according to General Procedure C using a solution (A) of 2-biphenylamine (254 mg, 1.5 mmol, 1.0 equiv.; 0.1 M) and $TMSN_3$ (0.23 mL, 1.7 mmol, 1.1 equiv.; 0.11 M) in dioxane (15 mL), a solution (B) of *t*-BuONO (0.31 mL, 2.7 mmol, 1.5 equiv.; 0.15 M) in dioxane (17 mL), and KOH (168 mg, 3.0 mmol, 2.0 equiv.) and iodoethane (0.24 mL, 3.0 mmol, 2.0 equiv.) in 3 mL of DMSO. Purification by flash column chromatography on SiO_2 (12 g), eluting with hexane-CH_2Cl_2, (0 to 10%) gave the *title compound* (0.16 g, 56%) as a colourless solid.

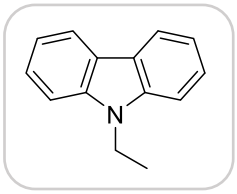

Purity (LCMS): 90%. **^{1}H NMR** (600 MHz, d_6-DMSO) δ 8.12 (2H, d, *J* 7.5, H-4), 7.58 (2H, d, *J* 8.0, H-1), 7.42 (2H, dd, *J* 8.0, 7.5, H-2), 7.16 (2H, dd, *J* 7.5, 7.5, H-3), 4.42 (2H, q, *J* 7.0, CH_2CH_3), 1.28 (3H, t, *J* 7.0, CH_2CH_3). **^{13}C NMR** (151 MHz, $CDCl_3$) δ 139.9 (C), 126.1 (CH), 122.5 (C), 120.8 (CH), 119.1 (CH), 109.5 (CH), 37.3 (CH_2), 14.1 (CH_3).

4-Fluoro-2-methyl-9-ethyl-9*H*-carbazole (2.70). Prepared according to General Procedure C using a solution (A) of 2-(2'-fluoro-4'-methylphenyl)aniline (288 mg, 1.4 mmol, 1.0 equiv.; 0.1 M) and $TMSN_3$ (0.23 mL, 1.6 mmol, 1.1 equiv.; 0.11 M) in dioxane (12 mL), a solution (B) of *t*-BuONO (0.31 mL, 2.7 mmol, 1.5 equiv.; 0.15 M) in dioxane (15 mL), and KOH (160 mg, 2.9 mmol, 2.0 equiv.) and iodoethane (0.23 mL, 2.9 mmol, 2.0 equiv.) in 3 mL of DMSO. Purification by flash column chromatography on SiO_2 (12 g), eluting with hexane-CH_2Cl_2, (0 to 10%) gave the *title compound* (0.15 g, 45%) as a colourless solid.

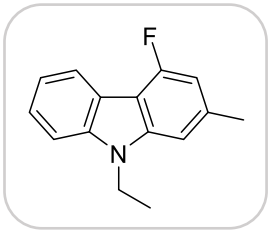

Mp: 83-84 °C. **Purity (LCMS):** 96%. **Found [ESI]:** MH^+, 228.1200. $C_{15}H_{15}FN$ [MH] requires 228.1189. **IR** (neat) *v*/cm^{-1} 2980 (C-H), 1640 (C-C), 1179 (C-F), 744, 720 (C-H). **^{1}H NMR** (600 MHz, d_6-DMSO) δ 7.98 (1H, d, *J* 7.5, H-5), 7.59 (1H, d, *J* 8.5, H-8), 7.43 (1H, ddd, *J* 8.5, 7.0, 1.0, H-7), 7.25 (1H, s, H-1), 7.19 (1H, ddd, *J* 7.5, 7.0, 0.4, H-6), 6.81 (1H, d, $^3J_{HF}$ 11.2, H-3), 4.39 (2H, q, *J* 7.0, CH_2CH_3), 2.48 (s, 3H, Me), 1.27 (3H, t, *J* 7.0, CH_2CH_3). **^{13}C NMR** (151 MHz, d_6-DMSO) δ 157.8 (d, $^1J_{CF}$ 246, CF), 142.4 (d, $^3J_{CF}$ 11, C), 139.6 (C), 137.5 (d, $^3J_{CF}$ 8, C), 126.0 (CH), 122.1 (d, $^4J_{CF}$ 3, CH), 119.9 (CH), 119.8 (d, $^4J_{CF}$ 2, C), 109.7 (CH), 108.2 (d, $^2J_{CF}$ 21, C), 106.1 (d, $^2J_{CF}$ 18, CH), 106.0 (d, $^4J_{CF}$ 3, CH), 37.7 (CH_2), 22.1 (CH_3), 14.1 (CH_3).

2,4-Fluoro-9-ethyl-9*H*-carbazole (2.71). Prepared according to General Procedure C using a solution (A) of 2-(2',4'-difluorophenyl)aniline (602 mg, 2.9 mmol, 1.0 equiv.; 0.1 M) and $TMSN_3$ (0.43 mL, 3.2 mmol, 1.1 equiv.; 0.11 M) in dioxane (30 mL), a solution (B) of *t*-BuONO (0.63 mL, 5.2 mmol, 1.5 equiv.; 0.15 M) in dioxane (35 mL), and solid KOH (330 mg, 5.9 mmol, 2.0 equiv.) and iodoethane (0.46 mL, 3.1 mmol, 2.0 equiv.) in 5 mL DMSO. Purification by flash column chromatography on SiO_2 (24 g), eluting with hexane-CH_2Cl_2, (0 to 10%) gave the *title compound* (0.20 g, 29%) as a colourless solid.

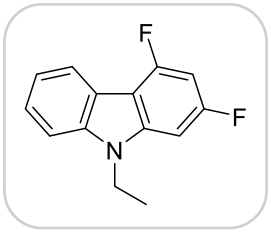

Mp: 64-65 °C. **Purity (LCMS):** 97%. **Found [ESI]:** MH^+, 232.0949. $C_{14}H_{12}NF$ [MH] requires 232.0938. **IR** (neat) *v*/cm^{-1} 2974 (C-H), 1605 (C-C), 1204 (C-O-C), 1103 (C-F), 818, 747 (C-H) **^{1}H NMR** (600 MHz, d_6-DMSO) δ 8.03 (1H, d, *J* 7.5, H-5), 7.66 (1H, d, *J* 8.5, H-8), 7.50 (1H, ddd, *J* 8.5, 7.0, 1.0, H-7), 7.45 (1H, dd, $^3J_{HF}$ 10.0, J_{HH} 2.0, H-1), 7.27 (1H, ddd, *J* 7.5, 7.0, 1.0, H-6), 7.01 (1H, ddd, $^3J_{HF}$ 10.5, 10.5, J_{HH} 2.0, H-3), 4.44 (2H, q, *J* 7.0, CH_2CH_3), 1.29 (3H, t, *J* 7.0, CH_2CH_3). **^{13}C NMR** (151 MHz, d_6-DMSO) δ 161.4 (dd, $^1J_{CF}$ 240, $^3J_{CF}$ 13, CF), 157.6 (dd, $^1J_{CF}$ 248, $^3J_{CF}$ 16, CF), 141.9 (dd, $^3J_{CF}$ 15, $^3J_{CF}$ 13, C), 140.1 (d, $^4J_{CF}$ 2, C), 126.3 (CH), 122.2 (d, $^4J_{CF}$ 3, CH), 120.5 (CH), 119.5 (d, $^4J_{CF}$ 2, C), 110.0 (CH), 107.1 (dd, $^2J_{CF}$ 20, $^4J_{CF}$ 2, C), 94.7 (dd, $^2J_{CF}$ 29, 23, CH), 93.3 (dd, $^2J_{CF}$ 27, 4, CH), 38.0 (CH_2), 14.0 (CH_3).

2-Methoxy-9-ethyl-9*H*-carbazole (2.72). Prepared according to General Procedure C using a solution (A) of 2-(4'-methoxyphenyl)aniline (213 mg, 1.1 mmol, 1.0 equiv.; 0.1 M) and $TMSN_3$ (0.16 mL, 1.2 mmol, 1.1 equiv.; 0.11 M) in dioxane (11 mL), a solution (B) of *t*-BuONO (0.23 mL, 1.4 mmol, 1.5 equiv.; 0.15 M) in dioxane (13 mL), and KOH (217 mg, 2.2 mmol, 2.0 equiv.) and iodoethane (0.17 mL, 2.2 mmol, 2.0 equiv.) in 3 mL of DMSO. Purification by flash column chromatography on SiO_2 (12 g), eluting with hexane-CH_2Cl_2, (0 to 10%) gave the *title compound* (0.15 g, 60%) as a colourless solid.

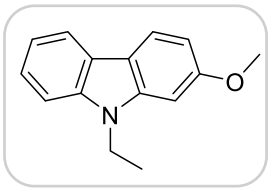

Mp: 63-64 °C. **Purity (by LCMS):** 92%. **Found [ESI]:** MH^+, 226.1227. $C_{15}H_{16}NO$ [MH] requires 226.1232. **IR** (neat) *v*/cm^{-1} 2953 (C-H), 1595 (C-C), 1198 (C-O), 814 (C-H). **^{1}H NMR** (600 MHz, d_6-DMSO) δ 7.99 (1H, d, *J* 7.5, H-5), 7.97 (1H, d, *J* 8.5, H-4), 7.50 (1H, d, *J* 8.0, H-8), 7.32 (1H, ddd, *J* 8.0, 7.0, 1.0, H-7), 7.11 (1H, dd, *J* 7.5, 7.0, 0.6, H-6), 7.10 (1H, d, *J* 2.0, H-1), 6.77 (1H, dd, *J* 8.5, 2.0, H-3), 4.37 (2H, q, *J* 7.0, CH_2CH_3), 3.85 (3H, s, OMe), 1.27 (3H, t, *J* 7.0, CH_2CH_3). **^{13}C NMR** (151 MHz, $CDCl_3$) δ 159.2 (C), 141.4 (C), 140.0 (C), 124.7 (CH), 122.9 (C), 121.5 (CH), 119.8 (CH), 119.2 (CH), 116.2 (C), 109.2 (CH), 108.0 (CH), 93.5 (CH), 55.9 (OMe), 37.3 (CH_2), 14.0 (CH_3).

2-Trifluoromethyl-9-ethyl-9*H*-carbazole (2.73). Prepared according to General Procedure C using a (A) of 2-(4'-trifluoromethylphenyl)aniline (504 mg, 2.1 mmol, 1.0 equiv.; 0.1 M) and $TMSN_3$ (0.30 mL, 2.3 mmol, 1.1 equiv.; 0.11 M) in dioxane (21 mL), a solution (B) of *t*-BuONO (0.45 mL, 3.75 mmol, 1.5 equiv.; 0.15 M) in dioxane (25 mL), and KOH (235 mg, 4.2 mmol, 2.0 equiv.) and iodoethane (0.33 mL, 4.2 mmol, 2.0 equiv.) in 3 mL of DMSO. Purification by flash column chromatography on SiO_2 (12 g), eluting with hexane-CH_2Cl_2, (0 to 10%) gave the *title compound* (0.24 g, 43%) as a colourless solid.

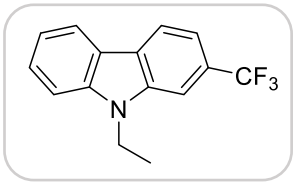

Mp: 89-91 °C. **Purity (LCMS):** 96%. **Found [ESI]:** MH^+, 264.0999. $C_{15}H_{13}F_3N$ [MH] requires 264.1000. **IR** (neat) *v*/cm^{-1} 2985 (C-H), 1576 (C-C), 1054 (C-F), 749, 722 (C-H) **^{1}H NMR** (600 MHz, d_6-DMSO) δ 8.34 (1H, d, *J* 8.0, H-5), 8.24 (1H, d, *J* 8.0, H-4), 8.02 – 7.99 (1H, m, H-1), 7.66 (1H, d, *J* 8.5, H-8), 7.53 (1H, ddd, *J* 8.5, 7.0, 1.0, H-7), 7.47 (1H, dd, *J* 8.0, 1.5, H-3), 7.25 (1H, ddd, *J* 8.0, 7.0, 0.9, H-6), 4.52 (2H, q, *J* 7.0, CH_2CH_3), 1.28 (3H, t, *J* 7.0, CH_2CH_3). **^{13}C NMR** (151 MHz, d_6-DMSO) δ 141.1 (C), 139.1 (C), 127.6 (CH), 126.3 (d, $^2J_{CF}$ 31, C), 125.6 (q, $^1J_{CF}$ 272, CF), 125.5 (C), 121.7 (CH), 121.6 (C), 121.6 (CH), 119.9 (CH), 115.4 (q, $^3J_{CF}$ 4, CH), 110.1 (CH), 106.9 (q, $^3J_{CF}$ 4, CH), 37.6 (CH_2), 14.1 (CH_3).

2-Trifluoromtehyl-4-fluoro-9-ethyl-9*H*-carbazole (2.74). Prepared according to General Procedure C using a solution (A) of 2-(2'-fluoro-4'-trifluoromethylphenyl)aniline (730 mg, 2.9 mmol, 1.0 equiv.; 0.1 M) and $TMSN_3$ (0.56 mL, 3.1 mmol, 1.1 equiv.; 0.11 M) in dioxane (29 mL), a solution (B) of *t*-BuONO (0.63 mL, 5.3 mmol, 1.5 equiv.; 0.15 M) in dioxane (35 mL), and solid KOH (320 mg, 5.7 mmol, 2.0 equiv.) and iodoethane (0.45 mL, 5.7 mmol, 2 equiv.) in 5 mL of DMSO. Purification by flash column chromatography on SiO_2 (24 g), eluting with hexane-CH_2Cl_2, (0 to 10%) gave the *title compound* (0.41 g, 50%) as a colourless solid.

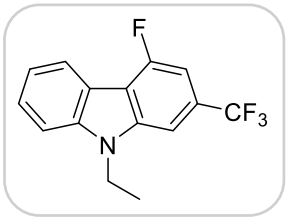

Mp: 72-73 °C. **Purity (LCMS):** 96%. **Found [ESI]:** MH^+, 282.0915. $C_{15}H_{12}F_4N$ [MH] requires 282.0906. **IR** (neat) *v*/cm^{-1} 2981 (C-H), 1587 (C-C), 1076 (C-F), 745, 715 (C-H). **^{1}H NMR** (600 MHz, *d*$_6$-DMSO) δ 8.13 (1H, d, *J* 8.0, H-5), 7.94 (1H, s, H-1), 7.74 (1H, d, *J* 8.5, H-8), 7.59 (1H, ddd, *J* 8.5, 7.5, 1.0, H-7), 7.35 (1H, d, $^3J_{HF}$ 10.5, H-3), 7.31 (1H, dd, *J* 8.0, 7.5, H-6), 4.55 (2H, q, *J* 7.0, CH_2CH_3), 1.29 (3H, t, *J* 7.0, CH_2CH_3). **^{13}C NMR** (151 MHz, *d*$_6$-DMSO) δ 157.7 (d, $^1J_{CF}$ 249, CF), 141.5 (d, $^3J_{CF}$ 11, C), 140.6 (C), 127.9 (C), 127.1 (qd, $^2J_{CF}$ 33, $^3J_{CF}$ 9, C), 124.7 (qd, $^1J_{CF}$ 273, $^4J_{CF}$ 3, CF_3), 123.2 (d, $^4J_{CF}$ 3, CH), 120.9 (CH), 118.8 (d, $^4J_{CF}$ 1, CH), 113.0 (d, $^2J_{CF}$ 20, C), 110.5 (CH), 103.9 (p, $^4J_{CF}$ 4, CH), 101.8 (dq, $^2J_{CF}$ 23, $^4J_{CF}$ 4, CH), 38.1 (CH_2), 14.2 (CH_3)

2-Fluoro-4-methoxy-9-ethyl-9*H*-carbazole (2.75). Prepared according to General Procedure C using a solution (A) of 2-(4'-fluoro-2'-methoxyphenyl)aniline (1.9 g, 8.7 mmol, 1.0 equiv.; 0.1 M) and $TMSN_3$ (1.26 mL, 9.6 mmol, 1.1 equiv.; 0.11 M) in dioxane (87 mL), a solution (B) of *t*-BuONO (1.61 mL, 13.5 mmol, 1.5 equiv.; 0.15 M) in dioxane (90 mL), and solid KOH (974 mg, 17.4 mmol, 2.0 equiv.) and iodoethane (1.4 mL, 17.4 mmol, 2.0 equiv.) in 10 mL of DMSO. The reaction mixture was dilluted with water and extracted with CH_2CL_2. The organic layers were combined and washed with brine, dried over $MgSO_4$ and concentrated under pressure. Purification by flash column chromatography on SiO_2 (24 g), eluting with hexane-CH_2Cl_2, (0 to 10%) gave the *title compound* (1.21 g, 57%) as a colourless solid.

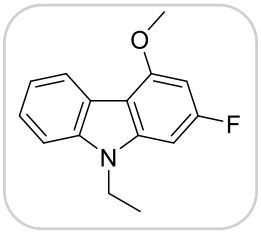

Mp: 94-96 °C. **Purity (LCMS):** 95%. **Found [ESI]:** MH^+, 244.1158. $C_{15}H_{15}NOF$ [MH] requires 244.1138. **IR** (neat) *v*/cm^{-1} 2974 (C-H), 1630 (C-C), 1186 (C-O), 1033 (C-F), 805 (C-H).**^{1}H NMR** (600 MHz, $CDCl_3$) δ 8.09 (1H, d, *J* 7.5, H-5), 7.54 (1H, d, *J* 8.0, H-8), 7.37 (1H, ddd, *J* 8.0, 7.5, 1.0, H-7), 7.16 (1 H, dd, *J* 7.5, 7.5, H-6), 7.08 (1 H, dd, J_{HF} 10.0, J_{HH} 1.5, H-1), 6.65 (1 H, dd, J_{HF} 12.0, J_{HH} 1.5, H-3), 4.36 (2H, q, *J* 7.0, CH_2CH_3), 4.00 (3H, s, OMe), 1.25 (3H, t, *J* 7.0, CH_2CH_3). **^{13}C NMR** (151 MHz, *d*$_6$-DMSO) δ 162.7 (d, $^1J_{CF}$ 238, CF), 156.7 (d, $^3J_{CF}$ 13, C), 141.2 (d, $^3J_{CF}$ 16, C), 139.6 (d, $^4J_{CF}$ 2, C), 124.8 (CH), 122.3 (CH), 121.7 (C), 119.8 (CH), 109.2 (CH), 107.8 (C), 90.5 (d, $^2J_{CF}$ 29, CH), 89.3 (d, $^2J_{CF}$ 27, CH), 56.4 (OMe), 37.7 (CH_2), 14.1 (CH_3).

2,4-Bis(trifluoromethyl)-9-ethyl-9*H*-carbazole (2.76). Prepared according to General Procedure C using a solution (A) of 2-(2',4'-Bis(trifluoromethylphenyl)aniline (590 mg, 1.9 mmol, 1.0 equiv.; 0.1 M) and $TMSN_3$ (0.31 mL, 2.2 mmol, 1.1 equiv.; 0.11 M) in dioxane (20 mL), a solution (B) of *t*-BuONO (0.45 mL, 3.6 mmol, 1.5 equiv.; 0.15 M) in dioxane (25 mL), and solid KOH (224 mg, 3.8 mmol, 2.0 equiv.) and iodoethane (0.33 mL, 3.8 mmol, 2.0 equiv.) in 5 mL DMSO. Purification by flash column chromatography on SiO_2 (24 g), eluting with hexane-CH_2Cl_2, (0 to 10%) gave the *title compound* (0.23 g, 36%) as a colourless solid.

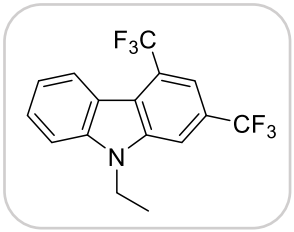

Mp: 88-89 °C. **Purity (LCMS):** 97%. **IR** (neat) *v*/cm^{-1} 2970 (C-H), 1740 (C-C), 1088 (C-F), 878, 867 (C-H). **^{1}H NMR** (600 MHz, d_6-DMSO) δ 8.48 (1H, s, H-3), 8.20 (1H, d, *J* 8.0, H-5), 7.83 (1H, d, *J* 8.5, H-8), 7.77 (1H, s, H-1), 7.66 (1H, ddd, *J* 8.5, 7.5, 1.0, H-7), 7.36 (1H, ddd, *J* 8.0, 7.5, H-6), 4.65 (2H, q, *J* 7.0, CH_2CH_3), 1.30 (3H, t, *J* 7.0, CH_2CH_3). **^{13}C NMR** (151 MHz, d_6-DMSO) δ 141.7 (C), 140.1 (C), 128.9 (CH), 125.8 (q, $^2J_{CF}$ 32, C), 124.7 (d, $^1J_{CF}$ 273, CF_3), 124.6 (d, $^1J_{CF}$ 272, CF_3), 123.4 (q, $^3J_{CF}$ 5, CH), 122.4 (q, $^2J_{CF}$ 33, C), 121.1 (CH), 120.7 (C), 118.5 (C), 112.7 (m, CH), 112.0 (q, $^3J_{CF}$ 4, CH), 111.0 (CH), 37.9 (CH_2), 14.1 (CH_3).

2,4-Dimethoxy-9-ethyl-9*H*-carbazole (2.77). Prepared according to General Procedure C using a solution (A) of 2-(2',4'-dimethoxyphenyl)aniline (350 mg, 1.5 mmol, 1.0 equiv.; 0.1 M) and $TMSN_3$ (0.22 mL, 1.7 mmol, 1.1 equiv.; 0.11 M) in dioxane (16 mL), a solution (B) of *t*-BuONO (0.35 mL, 3.0 mmol, 1.5 equiv.; 0.15 M) in dioxane (20 mL), and solid KOH (177 mg, 3.2 mmol, 2.0 equiv.) and iodoethane (0.25 mL, 3.2 mmol, 2.0 equiv.) in 3 mL of DMSO. Purification by flash column chromatography on SiO_2 (12 g), eluting with hexane-CH_2Cl_2, (0 to 10%) gave the *title compound* (0.13 g, 31%) as a yellow solid.

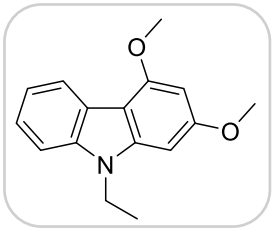

Mp: 101-102 °C. **Purity (LCMS):** 95%. **Found [ESI]:** MH^+, 256.1344. $C_{16}H_{18}NO_2$ [MH] requires 256.1338. **IR** (neat) *v*/cm^{-1} 2970 (C-H), 1626 (C-C), 1207 (C-O), 799, 743 (C-H). **^{1}H NMR** (600 MHz, d_6-DMSO) δ 7.99 (1H, d, *J* 7.5, H-5), 7.47 (1H, d, *J* 8.0, H-8), 7.27 (1H, ddd, *J* 8.0, 7.5, 1.0, H-7), 7.09 (1H, ddd, *J* 7.5, 7.5, 1.0, H-6), 6.72 (1H, d, *J* 2.0, H-1), 6.33 (1H, d, *J* 2.0, H-3), 4.35 (2H, q, *J* 7.0, CH_2CH_3), 3.95 (3H, s, OMe), 3.85 (3H, s, OMe), 1.26 (3H, t, *J* 7.0, CH_2CH_3). **^{13}C NMR** (151 MHz, d_6-DMSO) δ 160.5 (C), 156.5 (C), 142.1 (C), 139.1 (C), 123.7 (CH), 122.2 (C), 121.6 (CH), 119.3 (CH), 108.8 (CH), 105.4 (C), 91.1 (CH), 86.1 (CH), 56.0 (OMe), 55.9 (OMe), 37.4 (CH_2), 14.1 (CH_3).

4-Methoxy-2-trifluoromethyl-9-ethyl-9*H*-carbazole (2.78). Prepared according to General Procedure C using a solution (A) of 2-(2',4'-dimethoxyphenyl)aniline (350 mg, 1.5 mmol, 1.0 equiv.; 0.1 M) and $TMSN_3$ (0.22 mL, 1.7 mmol, 1.1 equiv.; 0.11 M) in dioxane (16 mL), a solution (B) of *t*-BuONO (0.35 mL, 3.0 mmol, 1.5 equiv.; 0.15 M) in dioxane (20 mL), and solid KOH (177 mg, 3.2 mmol, 2.0 equiv.) and iodoethane (0.25 mL, 3.2 mmol, 2.0 equiv.) in 3 mL of DMSO. Purification by flash column chromatography on SiO_2 (12 g), eluting with hexane-CH_2Cl_2, (0 to 10%) gave the *title compound* (0.13 g, 31%) as a yellow solid.

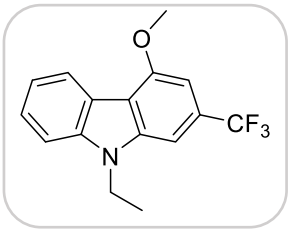

Mp: 86-87 °C. **Purity (LCMS):** 94%. **Found [ESI]:** MH^+, 293.1027. $C_{16}H_{14}NOF_3$ [MH] requires 293.1027. **IR** (neat) *v*/cm^{-1} 2974 (C-H), 1630 (C-C), 1102 (C-O), 1033 (C-F), 829 (C-H). **^{1}H NMR** (600 MHz, d_6-DMSO) δ 8.22 (1H, d, *J* 7.5, H-5), 7.63 (2H, m, H-1, H-8), 7.48 (1H, dd, *J* 8.0, 7.5, H-7), 7.24 (1H, dd, *J* 7.5, 7.5, H-6), 6.98 (1H, s, H-3), 4.49 (2H, q, *J* 7.0, CH_2CH_3), 4.08 (3 H, s, OMe), 1.27 (3H, t, *J* 7.0, CH_2CH_3). **^{13}C NMR** (151 MHz, d_6-DMSO) δ 156.3 (C), 140.4 (C), 140.1 (C), 127.4 (q, $^2J_{CF}$ 32, C), 126.5 (CH), 125.4 (q, $^1J_{CF}$ 273, CF), 123.5 (CH), 121.0 (C), 120.1 (CH), 113.9 (C), 109.7 (CH), 100.3 (d, $^3J_{CF}$ 5, CH), 97.0 (q, $^3J_{CF}$ 4, CH), 56.4 (OMe), 37.7 (CH_2), 14.2 (CH_3).

4-Fluoro-7-methoxy-2-methyl-9-ethyl-9*H*-carbazole (2.79). Prepared according to General Procedure C using a solution (A) of 2-(2'-fluoro-4'-methylphenyl)-5-methoxyaniline (360 mg, 1.6 mmol, 1.0 equiv.; 0.1 M) and $TMSN_3$ (0.22 mL, 1.7 mmol, 1.1 equiv.; 0.11 M) in dioxane (16 mL), a solution (B) of t-BuONO (0.36 mL, 3.0 mmol, 1.5 equiv.; 0.15 M) in dioxane (20mL), and solid KOH (175mg, 3.1 mmol, 2.0 equiv.) and iodoethane (0.25 mL, 3.1 mmol, 2.0 equiv.) in 3 mL of DMSO. Purification by flash column chromatography on SiO_2 (12 g), eluting with hexane-CH_2Cl_2, (0 to 10%) gave the *title compound* (0.16 g, 41%) as a yellow solid.

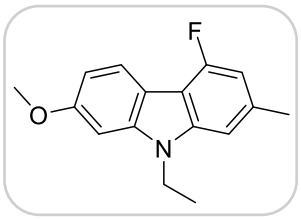

Mp: 142-144 °C. **Purity (LCMS):** 96%. **Found [ESI]:** MH^+, 258.1288. $C_{16}H_{17}FNO$ [MH] requires 258.1294. **IR** (neat) *v*/cm^{-1} 2936 (C-H), 1616 (C-C), 1205 (C-O), 1033 (C-F), 811 (C-H). **^{1}H NMR** (600 MHz, d_6-DMSO) δ 7.82 (1H, d, *J* 8.5, H-5), 7.18 (1H, s, H-1), 7.12 (1H, d, *J* 2.0, H-8), 6.79 (1H, dd, *J* 8.5, 2.0, H-6), 6.76 (1H, d, $^3J_{HF}$ 11.0, H-3), 4.35 (2H, q, *J* 7.0, CH_3CH_2), 3.85 (3H, s, OMe), 2.45 (3H, s, Me), 1.26 (3H, t, *J* 7.0, CH_3CH_2). **^{13}C NMR** (151 MHz, d_6-DMSO) δ 159.0 (C), 157.2 (d, $^1J_{CF}$ 244, CF), 142.6 (d, $^3J_{CF}$ 12, C), 141.2 (CH), 135.9 (d, $^3J_{CF}$ 8, C), 122.8 (d, $^4J_{CF}$ 3, C), 113.4 (C), 108.7 (CH), 108.3 (d, $^2J_{CF}$ 21, C), 106.2 (d, $^2J_{CF}$ 19, CH), 105.8 (d, $^4J_{CF}$ 3, CH), 93.9 (CH), 55.9 (CH), 37.6 (CH), 22.0 (CH), 14.0 (CH).

2-Fluoro-4,7-dimethoxy-9-ethyl-9*H*-carbazole (2.80). Prepared according to General Procedure C using a solution (A) of 2-(4'-fluoro-2'-methoxyphenyl)-5-methoxyaniline (420 mg, 1.7 mmol, 1.0 equiv.; 0.1 M) and $TMSN_3$ (0.25 mL, 1.9 mmol, 1.1 equiv.; 0.11 M) in dioxane (17 mL), a solution (B) of t-BuONO(0.36 mL, 3.0 mmol, 1.5 equiv.; 0.15 M) in dioxane (20 mL), and solid KOH (190 mg, 3.4 mmol, 2.0 equiv.) and iodoethane (0.27 mL, 3.4 mmol, 2.0 equiv.) in 3 mL of DMSO. Purification by flash column chromatography on SiO_2 (12 g), eluting with hexane-CH_2Cl_2, (0 to 10%) gave the *title compound* (0.23 g, 50%) as a yellow solid.

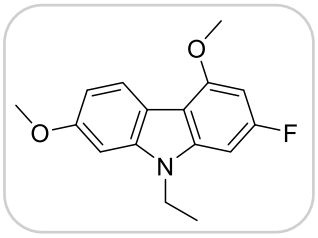

Mp: 116-119 °C. **Purity (LCMS):** 96%. **Found [ESI]:** MH^+, 274.1248. $C_{16}H_{17}FNO_2$ [MH] requires 274.1243. **IR** (neat) *v*/cm^{-1} 3008 (C-H), 1614 (C-C), 1164 (C-O), 1033 (C-F), 801 (C-H). **^{1}H NMR** (600 MHz, d_6-DMSO) δ 7.94 (1H, d, *J* 8.5, H-5), 7.11 (1H, d, *J* 2.0, H-8), 7.05 (1H, dd, $^3J_{HF}$ 10.0, J_{HH} 2.0, H-1), 6.79 (1H, dd, *J* 8.5, 2.0, H-6), 6.64 (1H, dd, $^3J_{HF}$ 12.0, J_{HH} 2.0, H-3), 4.35 (2H, q, *J* 7.0, CH_2CH_3), 3.99 (3H, s, OMe), 3.86 (3H, s, OMe), 1.26 (3H, t, *J* 7.0, CH_2CH_3). **^{13}C NMR** (151 MHz, d_6-DMSO) δ 161.8 (d, $^1J_{CF}$ 237, CF), 158.2 (C), 155.7 (d, $^3J_{CF}$ 13, C), 141.1 (d, $^3J_{CF}$ 15, C), 140.9 (d, $^4J_{CF}$ 2, C), 122.9 (CH), 115.3 (C), 108.3 (CH), 107.9 (C), 93.7 (CH), 90.5 (d, $^2J_{CF}$ 29, CH), 89.3 (d, $^2J_{CF}$ 27, CH), 56.3 (CH), 55.7 (CH), 37.6 (CH), 14.0 (CH).

2,4-Difluoro-7-methoxy-9-ethyl-9*H*-carbazole (2.81). Prepared according to General Procedure C using a solution (A) of 2-(2',4'-difluorophenyl)-5-methoxyaniline (370 mg, 1.6 mmol, 1.0 equiv.; 0.1 M) and $TMSN_3$ (0.22 mL, 1.7 mmol, 1.1 equiv.; 0.11 M) in dioxane (16 mL), a solution (B) of t-BuONO (0.36 mL, 3.0 mmol, 1.5 equiv.; 0.15 M) in dioxane (20 mL) and solid KOH (175 mg, 3.1 mmol, 2.0 equiv.) and iodoethane (0.25 mL, 3.1 mmol, 2.0 equiv.) in 3 mL of DMSO. Purification by flash column chromatography on SiO_2 (12 g), eluting with hexane-CH_2Cl_2, (0 to 10%) gave the *title compound* (0.11 g, 27%) as a colourless solid.

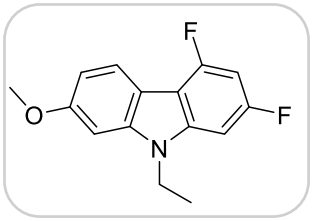

Mp: 90-92 °C. **Purity (LCMS):** 95%. **Found [ESI]:** MH^+, 262.1058. $C_{15}H_{14}FNO$ [MH] requires 252.1043. **IR** (neat) *v*/cm^{-1} 2981 (C-H), 1619 (C-C), 1217 (C-O), 1055 (C-F), 813, 798 (C-H). **^{1}H NMR** (600 MHz, d_6-DMSO) δ 7.85 (1H, d, *J* 8.5, H-5), 7.35 (1H, dd, J_{HF} 10.0, J_{HH} 2.0, H-1), 7.17 (1H, d, *J* 2.0, H-8), 6.93 (1H, ddd, J_{HF} 10.5, J_{HH} 2.0, H-3), 6.84 (1H, dd, *J* 8.5, 2.0, H-6), 4.37 (2H, q, *J* 7.0, CH_2CH_3), 3.86 (3H, s, OMe), 1.25 (3H, t, *J* 7.0, CH_2CH_3). **^{13}C NMR** (151 MHz, d_6-DMSO) δ 160.5 (dd, $^1J_{CF}$ 239, $^3J_{CF}$ 13, CF), 159.2 (C), 156.8 (dd, $^1J_{CF}$ 247, $^3J_{CF}$ 16, CF), 142.0 (dd, $^3J_{CF}$ 16, $^3J_{CF}$ 14, C), 141.7 (d, $^4J_{CF}$ 2, C), 122.8 (d, $^4J_{CF}$ 3, CH), 112.99 (C), 109.3 (CH), 107.3 (dd, $^2J_{CF}$ 21, $^4J_{CF}$ 2, C), 94.7 (dd, $^2J_{CF}$ 26, $^2J_{CF}$ 22, CH), 94.1 (CH), 93.2 (dd, $^2J_{CF}$ 27, $^4J_{CF}$ 4, CH), 56.0 (OCH_3), 37.9 (CH_2), 13.8 (CH_3).

2,7-Difluoro-4-methoxy-9-ethyl-9*H*-carbazole (2.82). Prepared according to General Procedure C and a solution (A) of 2-(4'-methoxyphenyl)-5-fluoroaniline (370 mg, 1.8 mmol, 1.0 equiv.; 0.1 M) and $TMSN_3$ (0.25 mL, 1.9 mmol, 1.1 equiv.; 0.11 M) in dioxane (18 mL), a solution (B) of t-BuONO (0.35 mL, 3.0 mmol, 1.5 equiv.; 0.15 M) in dioxane (20 mL), and solid KOH (370 mg, 1.8 mmol, 2.0 equiv.) and iodoethane (0.28 mL, 3.5 mmol, 2.0 equiv.) in 3 mL of DMSO. Purification by flash column chromatography on SiO_2 (12 g), eluting with hexane-CH_2Cl_2, (0 to 10%) gave the *title compound* (0.17 g, 40%) as a yellow solid.

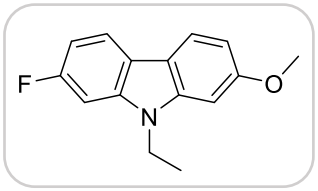

Mp: 104-106 °C. **Purity (LCMS):** 98%. **Found [ESI]:** MH^+, 244.1139. $C_{15}H_{15}FNO$ [MH] requires 244.1139. **IR** (neat) *v*/cm^{-1} 2980 (C-H), 1601 (C-C), 1206 (C-O), 1050 (C-F), 820, 798 (C-H). **^{1}H NMR** (600 MHz, *d*$_6$-DMSO) δ 7.98 (1H, dd, J_{HH} 8.5, $^4J_{HF}$ 5.5, H-4), 7.95 (1H, d, *J* 8.5, H-5), 7.40 (1H, dd, $^3J_{HF}$ 10.5, 2.5, H-1), 7.10 (1H, d, *J* 2.0, H-8), 6.94 (1H, ddd, $^3J_{HF}$ 10.0, 8.5, 2.5, H-3), 6.78 (1H, dd, *J* 8.5, 2.0, H-6), 4.35 (2H, q, *J* 7.0, CH_2CH_3), 3.85 (3H, s), 1.25 (3H, t, *J* 7.0, CH_2CH_3). **^{13}C NMR** (151 MHz, *d*$_6$-DMSO) δ 161.1 (d, $^1J_{CF}$ 237, CF), 159.0 (C), 142.0 (d, $^4J_{CF}$ 2, C), 140.8 (d, $^3J_{CF}$ 13, C), 121.30 (CH), 120.9 (d, $^3J_{CF}$ 10, CH), 119.5 (C), 116.0 (C), 108.4 (CH), 106.7 (d, $^2J_{CF}$ 24, CH), 96.3 (d, $^2J_{CF}$ 27, CH), 93.8 (CH), 55.9 (OCH_3), 37.5 (CH_2), 13.9 (CH_3).

4,7-Difluoro-2-methyl-9-ethyl-9*H*-carbazole (2.83). Prepared according to General Procedure C using a solution (A) o 2-(2'-fluoro-4'-methylphenyl)-5-fluoroaniline (477 mg, 2.2 mmol, 1.0 equiv.; 0.1 M) and $TMSN_3$ (0.32 mL, 2.4 mmol, 1.1 equiv.; 0.11 M) in dioxane (22 mL), a solution (B) of t-BuONO (0.45 mL, 3.8 mmol, 1.5 equiv.; 0.15 M) in dioxane (25 mL), and solid KOH (246 mg, 4.4 mmol, 2.0 equiv.) and iodoethane (0.35 mL, 4.4 mmol, 2.0 equiv.) in 3 mL of DMSO. Purification by flash column chromatography on SiO_2 (12 g), eluting with hexane-CH_2Cl_2, (0 to 10%) gave the *title compound* (0.31 g, 57%) as a colourless solid.

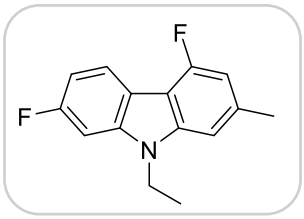

Mp: 92-93 °C. **Purity (LCMS):** 96%. **Found [ESI]:** MH+, 246.1106. $C_{15}H_{14}F_2N$ [MH] requires 246.1094. **IR** (neat) *v*/cm^{-1} 2974 (C-H), 1614 (C-C), 1055 (C-F), 820 (C-H). **^{1}H NMR** (600 MHz, *d*$_6$-DMSO) δ 7.94 (1H, dd, J_{HH} 8.5, $^4J_{HF}$ 5.5, H-5), 7.50 (1H, dd, $^3J_{HF}$ 10.5, J_{HH} 2.5, H-8), 7.23 (1H, s, H-1), 7.01 (1H, ddd, $^3J_{HF}$ 10.0, J_{HH} 8.5, J_{HH} 2.5, H-6), 6.81 (1H, d, $^3J_{HF}$ 11.0, H-3), 4.35 (2H, d, *J* 7.0, CH_2CH_3), 2.46 (3H, s, Me), 1.25 (3H, t, *J* 7.0, CH_2CH_3). **^{13}C NMR** (151 MHz, *d*$_6$-DMSO) δ 161.6 (d, $^1J_{CF}$ 239, CF), 157.4 (d, $^1J_{CF}$ 246, CF), 143.0 (dd, $^3J_{CF}$ 11, $^4J_{CF}$ 2, C), 140.6 (d, $^3J_{CF}$ 13, C), 137.3 (d, $^3J_{CF}$ 8, C), 123.2 (dd, $^3J_{CF}$ 11, $^4J_{CF}$ 3, CH), 116.4 (C), 107.9 (d, $^2J_{CF}$ 21, C), 107.7 (d, $^2J_{CF}$ 24, CH), 106.6 (d, $^2J_{CF}$ 18,CH), 106.1 (d, $^4J_{CF}$ 3, CH), 96.8 (d, $^2J_{CF}$ 27, CH), 37.9 (CH_2), 22.1 (CH_3), 13.9 (CH_3).

2,4,7-Trifluoro-9-ethyl-9*H*-carbazole (2.84). Prepared according to General Procedure C using a solution (A) of 2-(2',4'-difluorophenyl)-5-fluoroaniline (250 mg, 1.2 mmol, 1.0 equiv.; 0.1 M) and $TMSN_3$ (0.17 mL, 1.3 mmol, 1.1 equiv.; 0.11 M) in dioxane (12 mL), a solution (B) of t-BuONO (0.27 mL, 2.6 mmol, 1.5 equiv.; 0.15 M) in dioxane (15 mL), and solid KOH (134 mg, 2.4 mmol, 2.0 equiv.) and iodoethane (0.19 mL, 2.4 mmol, 2.0 equiv.) in 3 mL of DMSO. Purification by flash column chromatography on SiO_2 (12 g), eluting with hexane-CH_2Cl_2, (0 to 10%) gave the *title compound* (0.14 g, 49%) as a colourless solid.

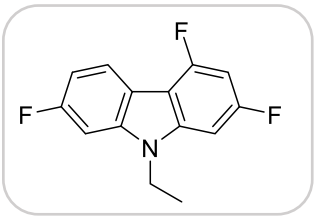

Mp: 124-125 °C. **Purity (LCMS):** 95%. **Found [ESI]:** MH^+, 250.0844. $C_{14}H_{11}F_3N$ [MH] requires 250.0844. **IR** (neat) *v*/cm^{-1} 2981 (C-H), 1615 (C-C), 1055 (C-F), 804 (C-H). **^{1}H NMR** (600 MHz, d_6-DMSO) δ 7.96 (1H, dd, J_{HH} 8.5, $^4J_{HF}$ 5.5, H-5), 7.56 (1H, dd, $^3J_{HF}$ 10.5, J_{HH} 2.5, H-8), 7.42 (1H, dd, $^3J_{HF}$ 10.0, J_{HH} 2.0, H-1), 7.06 (1H, ddd, $^3J_{HF}$ 9.5, J_{HH} 8.5, J_{HH} 2.5, H-6), 7.00 (1H, ddd, $^3J_{HF}$ 10.5, $^3J_{HF}$ 10.0, J_{HH} 2.0, H-3), 4.38 (2H, q, *J* 7.0, CH_2CH_3), 1.25 (3H, t, *J* 7.0, CH_2CH_3). **^{13}C NMR** (151 MHz, d_6-DMSO) δ 161.7 (d, $^1J_{CF}$ 243, CF), 161.2 (dd, $^1J_{CF}$ 240, $^3J_{CF}$ 13, CF), 157.2 (dd, $^1J_{CF}$ 248, $^3J_{CF}$ 16, CF), 142.6 (ddd, $^3J_{CF}$ 13, $^3J_{CF}$ 123 $^4J_{CF}$ 2, C), 141.1 (dd, $^3J_{CF}$ 13, $^4J_{CF}$ 2,C), 123.3 (dd, $^3J_{CF}$ 11, $^4J_{CF}$ 3, CH), 116.1, (C), 108.4 (d, $^2J_{CF}$ 24, CH), 106.9 (d, $^2J_{CF}$ 20, C), 97.2 (d, $^2J_{CF}$ 27, CH), 95.2 (dd, $^2J_{CF}$ 29, $^2J_{CF}$ 23.3, CH), 93.6 (dd, $^2J_{CF}$ 27, $^4J_{CF}$ 4, CH), 38.2 (CH_2), 13.8 (CH_3).

2,7-Difluoro-4-methoxy-9-ethyl-9*H*-carbazole (2.85). Prepared according to General Procedure C using a solution (A) of 2-(4'-fluoro-2'-methoxyphenyl)-5-fluoroaniline (330 mg, 1.4 mmol, 1.0 equiv.; 0.1 M) and $TMSN_3$ (0.20 mL, 1.5 mmol, 1.1 equiv.; 0.11 M) in dioxane (14 mL), a solution (B) of *t*-BuONO (0.29 mL, 2.4 mmol, 1.5 equiv.; 0.15 M) in dioxane (35 mL), and solid KOH (157 mg, 2.8 mmol, 2.0 equiv.) and iodoethane (0.22 mL, 2.8 mmol, 2.0 equiv.) in 3 mL of DMSO. Purification by flash column chromatography on SiO_2 (12 g), eluting with hexane-CH_2Cl_2, (0 to 10%) gave the *title compound* (0.20 g, 55%) as a colourless solid.

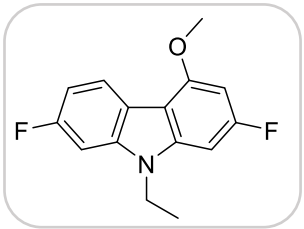

Mp: 112-114 °C. **Purity (LCMS):** 97%. **Found [ESI]:** MH^+, 262.1031. $C_{15}H_{14}NOF_2$ [MH] requires 262.1043. **IR** (neat) *v*/cm^{-1} 2982 (C-H), 1607 (C-C), 1213 (C-O), 1101 (C-F), 827, 800 (C-H). **^{1}H NMR** (600 MHz, d_6-DMSO) δ 8.03 (1H, dd, $^3J_{HH}$ 8.5, $^4J_{HF}$ 5.5, H-5), 7.46 (1H, dd, $^3J_{HF}$ 10.5, $^5J_{HH}$ 2.5, H-8), 7.09 (1H, ddd, $^3J_{HF}$ 10, $^5J_{HH}$ 2.0, H-1), 6.99 (1 H, ddd, $^3J_{HF}$ 9.5, $^3J_{HH}$ 8.5, $^5J_{HH}$ 2.5, H-6), 6.67 (1H, dd, $^3J_{HF}$ 12.0, $^5J_{HH}$ 2.0, H-3), 4.33 (2H, q, *J* 7.0, CH_2CH_3), 3.99 (3H, s), 1.24 (3H, t, *J* 7.0, CH_2CH_3).**^{13}C NMR** (151 MHz, d_6-DMSO) δ 162.5 (d, $^1J_{CF}$ 232, CF), 160.9 (d, $^1J_{CF}$ 232, CF), 156.3 (d, $^3J_{CF}$ 13, C), 141.8 (d, $^3J_{CF}$ 15, C), 140.4 (d, $^3J_{CF}$ 12, C), 123.2 (d, $^3J_{CF}$ 10, CH), 118.3 (C), 107.5 (d, $^2J_{CFJ}$ 24, CH), 107.5 (C), 96.4 (d, $^2J_{CF}$ 27, CH), 91.0 (d, $^2J_{CF}$ 29, CH), 89.5 (d, $^2J_{CF}$ 28, CH), 56.5 (CH_2), 38.0 (OMe), 14.0 (CH_3).

CHAPTER 3: Synthesis of new chemical binders to a p53 mutant

Tumour protein p53, also known as p53, is any isoform of a protein encoded by homologous genes in various organisms, such as *TP53* (humans) and *Trp53* (mice). This homologue (originally thought to be a single protein) is crucial in multicellular vertebrates as a tumour suppressor gene, and it has been described as "the guardian of the genome" because of its role in conserving stability by preventing genome mutation. The name p53 was given in 1979 describing the apparent molecular mass; SDS-PAGE analysis that indicated it was a 53-kilodalton (kDa) protein. However, the actual mass of the full-length p53 protein (p53α) based on the sum of masses of the residues is only 43.7 kDa. In addition to the full-length protein, the human *TP53* gene encodes at least 15 protein isoforms, called the p53 isoforms.[199,200]

The p53 protein can be divided into three major regions or domains based on function. The acidic amino-terminal transactivation domain (TAD), which can be further subdivided into the subdomains TAD1 and TAD2 and contains a binding site for the product of the MDM2 gene. The central domain is necessary for sequence specific DNA binding and contains the binding sites for SV40 large T-antigen. The regulatory domain at the extreme carboxyl terminus (CTD) is necessary for p53 oligomerization, one primary and two secondary nuclear localization signal sequences, mediating non-specific DNA binding (**Figure 31**).[201]

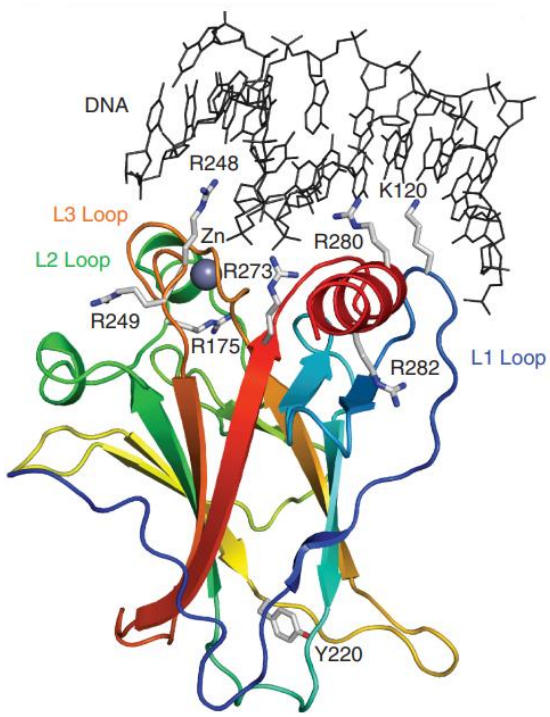

Figure 31. *Domain structure of p53. From Structures to Drug Discovery, Joerger et al. Copyright (2010) Cold Spring Harbor Laboratory Press, U.S.A.*[201]

The p53 gene has a prominent role in cancer and much of human biology. The 'guardian of the genome' continues to fascinate investigators because of its many functions. The p53 tumour suppressor can be induced by a range of stresses through transcriptional, post-transcriptional and post-translational control mechanisms.[202–205]. Although many functions have been attributed to p53, including direct roles in repair and recombination, association with proteins involved in genome stability, and chromatin modification[206] its main cellular effect is that of a transcription factor. The many roles of p53 as a tumour suppressor include DNA metabolism, apoptosis, cell cycle regulation, senescence, energy metabolism, angiogenesis, immune response, cell differentiation, motility and migration and cell–cell communication.[207–214]

Despite massive research efforts and the very impressive progress made over the past several decades, full molecular understanding of cancer still remains a major challenge to the biomedical community. The evolution of a normal cell towards a cancerous one is a complex process, accompanied by multiple steps of genetic and epigenetic alterations that confer selective advantages upon the altered cells. The alterations underlying tumourigenesis are considered to endow the evolving tumour with self-sufficiency of growth signals, insensitivity to antigrowth signals, evasion from programmed cell death, unlimited replicative potential, sustained angiogenesis, and finally, the ability to invade and metastasize. The notion that mutations in TP53 may occur at different stages along the process of malignant

transformation raises the possibility that mutated p53 may contribute differently to various steps of this process. Therefore, it is still an open question whether TP53 mutations are involved in the initiation of malignant transformation or perhaps only at more advanced stages of cancer, leading to additional growth and aggressiveness/survival advantages. It appears, however, that the timing of the mutation during tumourigenesis is extremely variable from one cancer to another. Although mutations and loss-of-function take place in most of the cancers, in many other cancers, where p53 is not mutated, the wild-type function is, however, compromised through various inhibitory mechanisms.[215]

P53 is found mutated in all of the major histogenetic groups, including cancers of the colon, stomach, breast, ovary, lung, brain, and esophagus. It is estimated that p53 mutations are the most frequent genetic events in human cancers and account for more than 50% of all cases.[216] The concept that mutant p53 proteins gain tumour-promoting functions was established over two decades ago by showing that mutant p53 has oncogenic effects in the absence of wild-type p53 in tissue culture systems.[217] However, the most compelling support for gain-of-function comes from mice engineered to harbour some of the most frequently occurring tumour-associated p53 mutations.[218,219] Mutant-p53-driven cancers also showed increased metastasis and genomic instability. Many other oncogenic functions of mutant p53 have been characterized in cell culture models, including an ability to promote invasion, migration, scattering, angiogenesis, stem cell expansion, survival, proliferation, tissue remodelling, enhanced chemo-resistance, mitogenic defects and genomic instability. This wide range of different responses is reflected by increasing evidence that mutant p53 can function through multiple different pathways.

In most human cancers, p53 retains wild-type status but its function is inhibited by its primary cellular chaperone. An example of these inhibitory mechanisms is the overexpression of E3 ubiquitin ligase mouse double minute 2 homolog (MDM2; HDM2 in humans). MDM2 is an important negative regulator of p53 in normal cells' functions both as an E3 ubiquitin ligase that recognizes the *N*-terminal trans-activation domain (TAD) of the p53 tumour suppressor and as an inhibitor of p53 transcriptional activation, but when deregulated provides growth advantage to cells.[220] Hence, p53 transcribes the MDM2 gene and, in turn, the MDM2 protein inhibits p53 activity.

Unlike the majority of tumour suppressor genes, the TP53 gene in human tumours is often found to undergo missense mutations, in which a single nucleotide is substituted by another.[221] Consequently, a full-length protein containing only a single amino acid substitution is produced. The vast majority of the mutations, nearly account for 70%,[222] result in loss of p53's ability to bind DNA in a sequence-specific manner and activate transcription of canonical p53 target genes. This results in its wide range of cellular effects which controls diverse group of biological activities.

Y220C is the ninth most frequent p53 cancer mutation, which accounts for an estimated 100,000 new cancer cases per year worldwide.[223] It is located at the far end of the *β*-sandwich, at the start of the loop connecting *β*-strands S7 and S8 and destabilizes the p53 core domain with the protein >80% unfolded at body temperature. The Y220C mutation is the mutation of a tyrosine-220 on the surface of the protein to a smaller cysteine (Cys-220) residue (**Figure 32**). The benzene moiety of Tyr-220 forms part of the hydrophobic core of the *β*-sandwich, whereas the hydroxyl group points toward the solvent. The Y220C mutation creates a solvent-accessible cavity at the surface of the protein, which decreases the melting point of the protein by around 8 °C and contributes to unfolding and aggregation.[224]

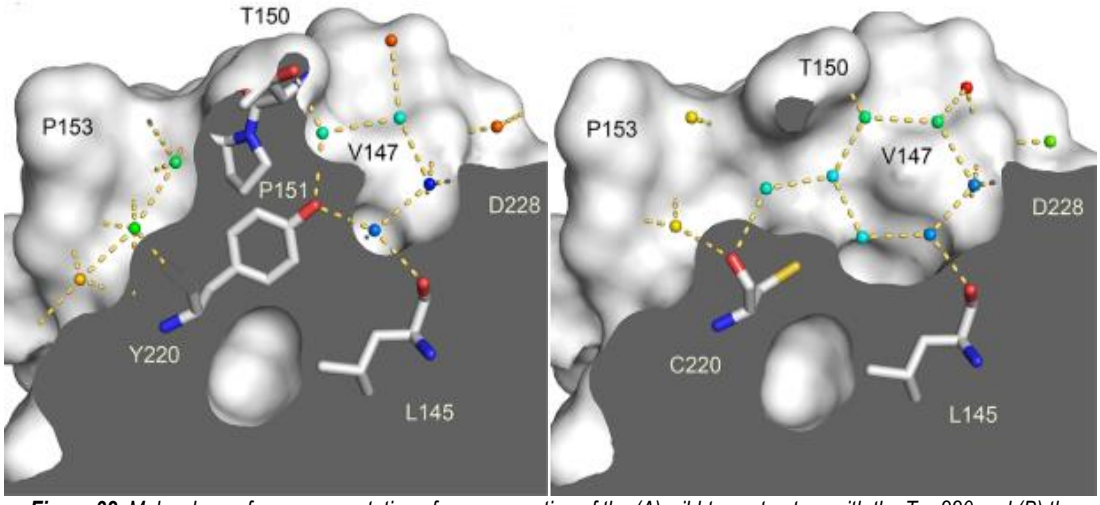

Figure 32. *Molecular surface representation of a cross-section of the (A) wild-type structure with the Tyr-220 and (B) the mutation-induced surface crevice with a Cys220 in mutant Y220C, from ACS Chemical Biology 2020, 15 (3), 659.*

The Y220C mutant is an ideal test case for a small-molecule stabilization approach, as a surface crevice created by the tyrosine-to-cysteine mutation can be targeted by small-molecule stabilizers. The cavity binders are designed to selectively interact with the native form of the target protein and not with unfolded or misfolded forms.

This crevice is flanked by two proline-rich loops, S3/S4 and S7/S8, and has its greatest depth at the mutation site. The binding site can formally be subdivided into a central cavity and three subsites, I, II, and III. In the central cavity there are several prolines (Pro151, Pro222, and Pro223) plus Thr150 and Val147. Subsite I is a highly polar solvent-exposed subsite with the backbone oxygen of Asp228 acting as a hydrogen bond acceptor, but its targeting by small molecules is difficult due to its narrow depth. A narrow channel on the opposite end of the central cavity leads into subsite II, where several prolines, including Pro153, provide a hydrophobic interaction surface, with several backbone oxygens lining this hydrophobic patch (Cys220, Pro151, and Pro152). Subsite III is at the bottom of the central cavity, which is essentially modulated by the conformational state of Cys220. A representation of the binding site is shown in **Figure 33**.

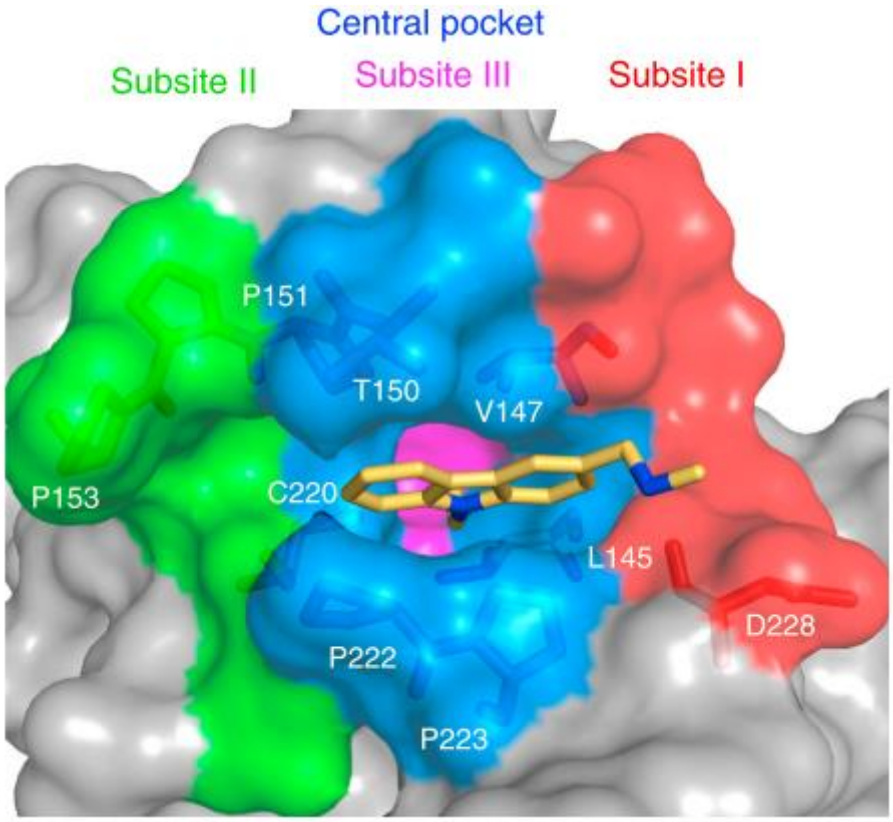

Figure 33. *Molecular surface representation of the binding pocket with the carbazole derivative PK083 (**3.1**). Displayed with permission from Structure 2015, 23 (12), 2247*

PhiKan083, or PK083 (**3.1**), was the first structurally characterized Y220C binder. Binding affinity depends on enthalpic and entropic components. Enthalpic contributions come from specific molecular interactions, and entropic binding is related to nonspecific interactions, such as hydrophobic and Van der Waals interactions.[225] The carbazole derived compound binds to the cavity of the Y220C mutated protein and stabilizes its structure by supporting the S7/ S8 loop, increasing its half-life from 3.8 to 15.7 min and raising the melting temperature by 0.55 °C.[222] It is located between the prolines in the central cavity, with the ethyl group serving as a hydrophobic anchor; it forms a hydrogen bond with the oxygen of Asp228 (D228) using the methylamine chain.[226] PK083 acts by binding to Y220C p53 with K_D ~150 μM, increasing its apparent melting temperature (T_m), slowing its rates of unfolding and aggregation, and partially restoring its apoptotic activity in cultured cells.[227–229]A drug that binds with a low K_D value is doubly important here, not only for minimizing the dosage but also because higher affinity provides the ability to refold more destabilized mutants.

In collaboration with biologists and crystallographers, John Spencer's group have synthesised and tested a range of PK083 analogues with differential scanning fluorimetry (DSF), also known as thermal shift assays. The DSF technique consists of comparing the changes in the thermal denaturation temperature (and therefore the stability) of a protein with and without the drug (ΔT_m), thus proving a

protein-ligand interaction that may increase/decrease protein stability. The dissociation constant (K_D) can be obtained by isothermal calorimetry (ITC) and the value is the concentration of ligand at which half the ligand binding sites on the protein are occupied in the system equilibrium.[227] Previous results are shown in **Table 14**.

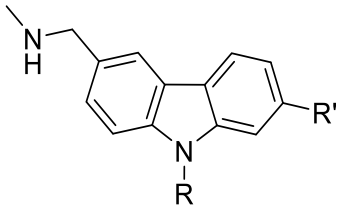

Table 14. *Thermostabilization and Dissociation Constants of Carbazole-Based Y220C Binders.*

Entry	Compound	R	R'	ΔT_m(°C)[a]	K_D (μM)
1	PK083 (**3.1**)	Et	H	0.5 ± 0.1[b]	125 ± 10[c]
2	PK9284 (**3.2**)	Et	Br	2.4 ± 0.1[b]	14 ± 2[c]
3	PK9295 (**3.3**)	Et		1.2 ± 0.1[b]	62 ± 7[c]
4	PK9318 (**3.4**)	Et		4.4 ± 0.1[b]	2.6 ± 0.4[c]
5	PK9320 (**3.5**)	Et		3.4 ± 0.0[b]	41 ± 0.2[c]
6	PK9322 (**3.6**)	Et		3.4 ± 0.0[b]	8.3 ± 2.6[c]
7	PK9323 (**3.7**)	Et		3.1 ± 0.1[b]	5.3 ± 1.4[c]
8	PK9424 (**3.8**)	Et		2.3 ± 0.1[b]	-
9	PK9327 (**3.9**)	Et		3.7 ± 0.2[b]	-
10	PK9328 (**3.10**)	Et	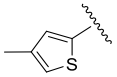	3.7 ± 0.0[b]	1.7 ± 0.2[c]
11	PK9331 (**3.11**)	Et		2.1 ± 0.1[b]	-
12	PK9255 (**3.12**)	CH_2CF_3	H	1.7 ± 0.1[b]	28[d]
13	PK9301 (**3.13**)	CH_2CF_3	Br	3.5 ± 0.1[b]	6.0 ± 0.3[b]

a) Measured at a compound concentration of 250 μM. Mean values of quadruplicate measurements ± SEM are shown.
b) Data taken from Bauer et al.[227]
c) Data taken from Bauer et al.[228]
d) Data taken from Bauer et al.[229]

All the molecules gave better results than PK083 (**3.1**), but the largest improvements in affinity were observed when R' was a thiophene (entries 4, 9 and 10), although a methyl on position 4 of the heterocycle decreased the activity (entry 11). Simpler functional groups such as bromine (entry 2) or an ethoxy chain (entry 3) also improved the activity but did not provide the same results. Moreover, changing from sulphur to oxygen as in a furan (entry 5) or to nitrogen (entries 6-8) heterocycles did not improve activity compared with the thiophene analogue. Furthermore, PK9255 (**3.12**) and PK9301 (**3.13**) (entries 12 and 13), the analogues of PK083 (**3.1**) and PK9284 (**3.2**) with a 2,2,2-trifluoroethyl chain attached to the central nitrogen, showed an additive improvement in affinity. The binding mode of all carbazoles were almost identical to PK083 (**3.1**), where the benzylic amine formed a hydrogen bond with the backbone carbonyl of Asp228. A slight shift of the carbazole in PK9318 (**3.4**) (entry 4) and PK9320 (**3.5**) (entry 5) compared to PK083 was observed in order to accommodate the 5-membered ring in subsite II (**Figure 34**).[225]

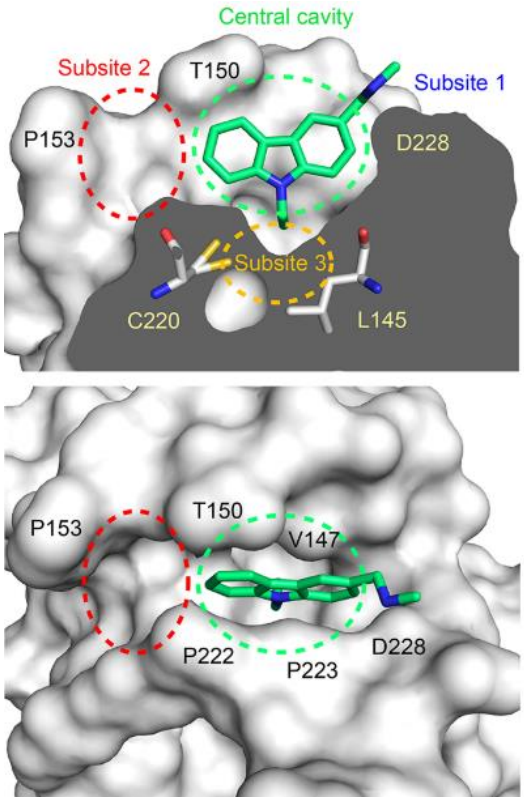

Figure 34. *Mutation-induced surface crevice in the p53 cancer mutant Y220C with bound molecule PK083 (**3.1**) as a stick molecule (PDB ID: 2VUK). Represented in cross section and top view of the mutation-induced surface crevice representation with the potential regions to be studied, being the subsite two the one discussed in this thesis. Reproduced with permission from ACS Chem. Biol. 2020, 15, 3, 657–668.*

Following previous work, the effect of the CF_3 moiety on position 2 with the hydrophobic interaction surface provided by the Pro153 in subsite II, and additional interactions with different substituents on position 4 with Thr150 were aimed to be studied. For this purpose, PK083 analogues containing these functional groups needed to be synthesised from the *N*-ethylated carbazoles previously prepared in Chapter 2, displayed in **Table 15** (reproduced from **Table 12** and **Table 13** in Chapter 2).

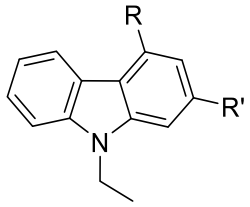

Table 15. *Carbazole scaffolds synthetised using reagentless techniques.*

Entry	R	R'	Suzuki yield (%)[a]	3-step yield (%)[a,b]	Total Yield (%)[a]	Compound	Purity (%)[c]
1	H	CF_3	80	40	32	**2.73**	96
2	F	CF_3	85	43	37	**2.70**	95
3	CF_3	CF_3	68	44	29	**2.73**	95
4	OCH_3	F	80	57	46	**2.75**	95
5	OCH_3	CF_3	85	65	55	**2.78**	93

a) Isolated yield after purification by flash chromatography.
b) Isolated yield after the flow process and following ultrasound N-ethylation.
c) Purity determined by LCMS analysis.

After achieving the synthesis of these *N*-ethylated carbazoles in good yields, which allowed full characterization, and with purities suitable for future biological purposes, the next step was to pursue the synthesis of fluorine rich PK083 analogues. The methylamino chain is crucial to form a hydrogen bond with the oxygen of Asp228 and increase the affinity of the molecule, and the ethyl group will act as a hydrophobic anchor**.** In order to introduce the requisite aliphatic chain containing the secondary amine, the approach was initially planned in two steps, starting with a formylation followed by reductive amination on selected compounds (**Scheme 61**).

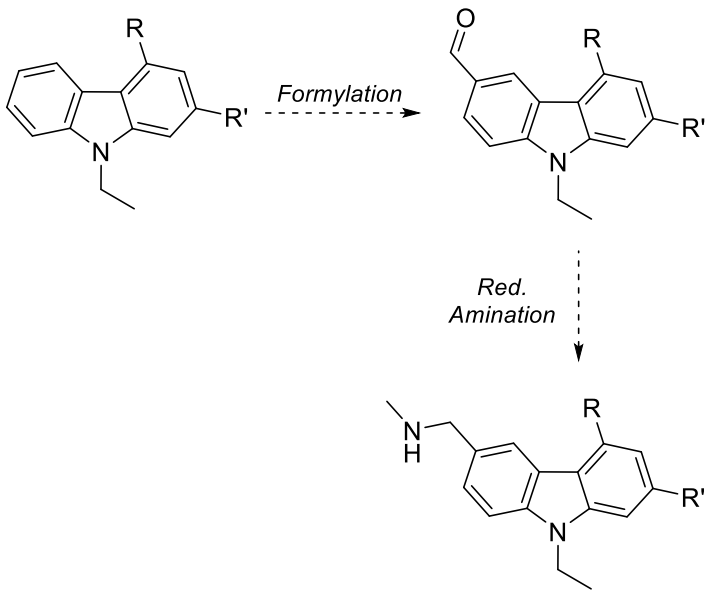

Scheme 61. *Synthetic approach to PK083 (**3.1**) analogues from N-ethylated carbazoles.*

3.1 Synthesis of p53 binders

3.1.1. Vilsmeier-Haack reaction

As stated before, the required initial reaction was a regioselective formylation of the *N*-ethylated carbazole. This step was investigated using a Vilsmeier-Haack reaction.[230] The widely known conditions for this reaction, shown in **Scheme 62**, were the addition of the carbazole to a solution of phosphorus(V) oxychloride in *N,N*-dimethylformamide (DMF), at reflux overnight. The first substrate investigated was **2.76**.

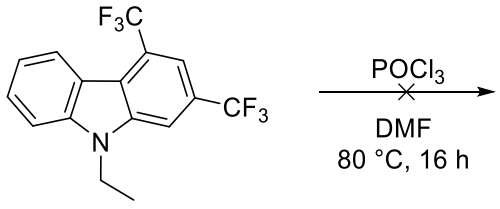

2.76

Scheme 62. *Vilsmeier-Haack conditions for formylation of carbazole **2.76**.*

This reaction was previously studied in the group and had been successful for more electron-rich carbazoles, but yields were known to decrease significantly when fluorine atoms were present in the substrate. In this case, the presence of the two trifluoromethyl groups excessively decreased the nucleophilicity of the aromatic compound, and no expected product was observed. The reaction was also carried out under microwave irradiation on a small scale, as a test to see if forcing conditions would

lead to product formation. An excess of pressure and lack of product formation led to this approach being discarded. Given the poor reactivity of bis-trifluoromethyl substrate **2.76** and, as all of the target structures possessed a trifluoromethyl group, an electron withdrawing group that would reduce the reactivity of the π-system, it was decided to change the reagent and make the intermediate more reactive, increasing its electrophilicity by adding electron withdrawing groups to the formylating agent. The same reaction conditions were employed using diphenylformamide **3.14** in 1,2-dichloroethane and this led to an improvement in the results (**Scheme 63**). Although some of the yields were high enough to proceed with the synthesis of the final product sufficient for biological testing, some alternative routes were investigated with the aim of optimising the yield.

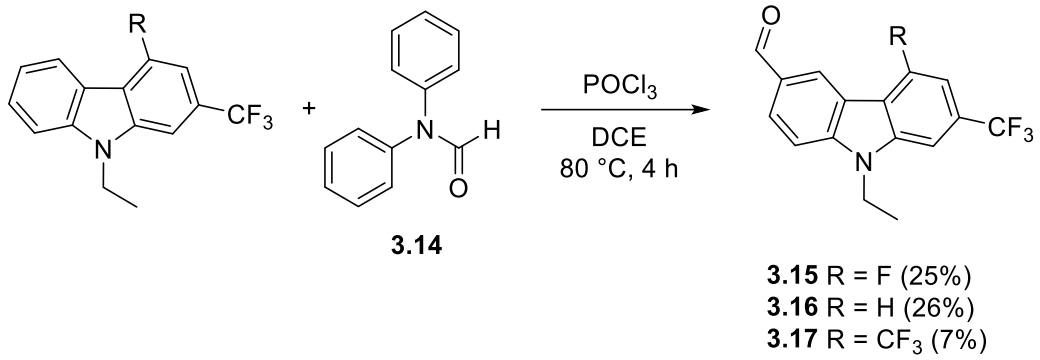

Scheme 63. *Vilsmeier-Haack formylation reaction using diphenylformamide.*

^{1}H-NMR spectroscopy proved to be a convenient method for reaction monitoring. An example is shown in **Figure 35**, where the ^{1}H-NMR spectrum of **3.15** is displayed. The appearance of the aldehyde peak is a definitive proof of the transformation, but also the change in the aromatic signals. In addition to a change in chemical shifts, the disappearance of the H-3 signal and the change of the multiplicities of H-2 and H-4 (from triplet and doublet to doublet and singlet respectively) left no doubt as to the progress of the transformation. Besides, the LCMS and the HRMS confirmed the mass of the corresponding product with a difference of 28 Daltons (for compound **3.15**: MH^+, 310.0854).

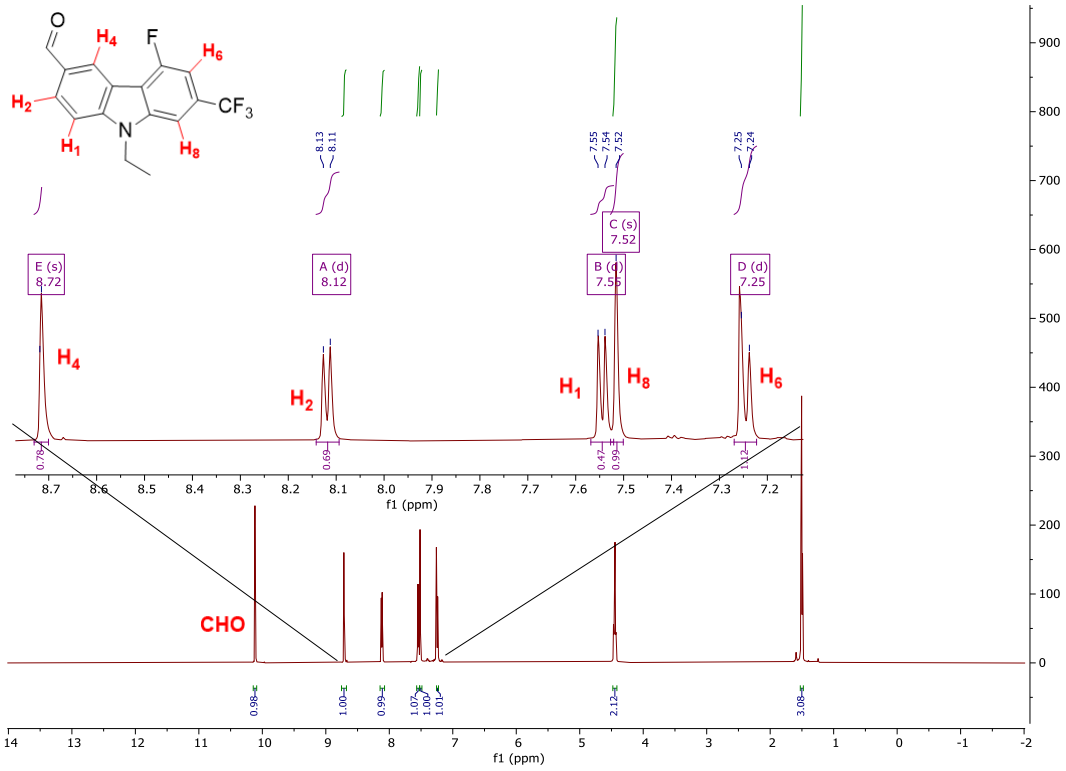

Figure 35. *^{1}H-NMR spectrum of compound* ***3.15****.*

The mechanism for this reaction is displayed in **Scheme 64**. It begins with the reaction of the disubstituted formamide with the phosphorus oxychloride to form an iminium salt **3.18** known as the "Vilsmeier reagent".

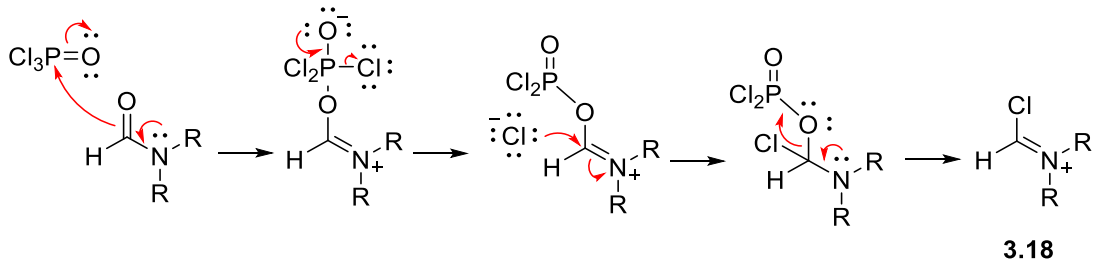

Scheme 64. *Vilsmeier reagent formation mechanism.*

This Vilsmeier reagent is sufficiently electrophilic to be attacked by the carbazole species at position-6 (the *para* position to the nitrogen) (**Scheme 65**). Once the Vilsmeier reagent has reacted, the hydrolysis of the iminium salt produced by electrophilic aromatic substitution provides the final aldehyde compound **3.19**.

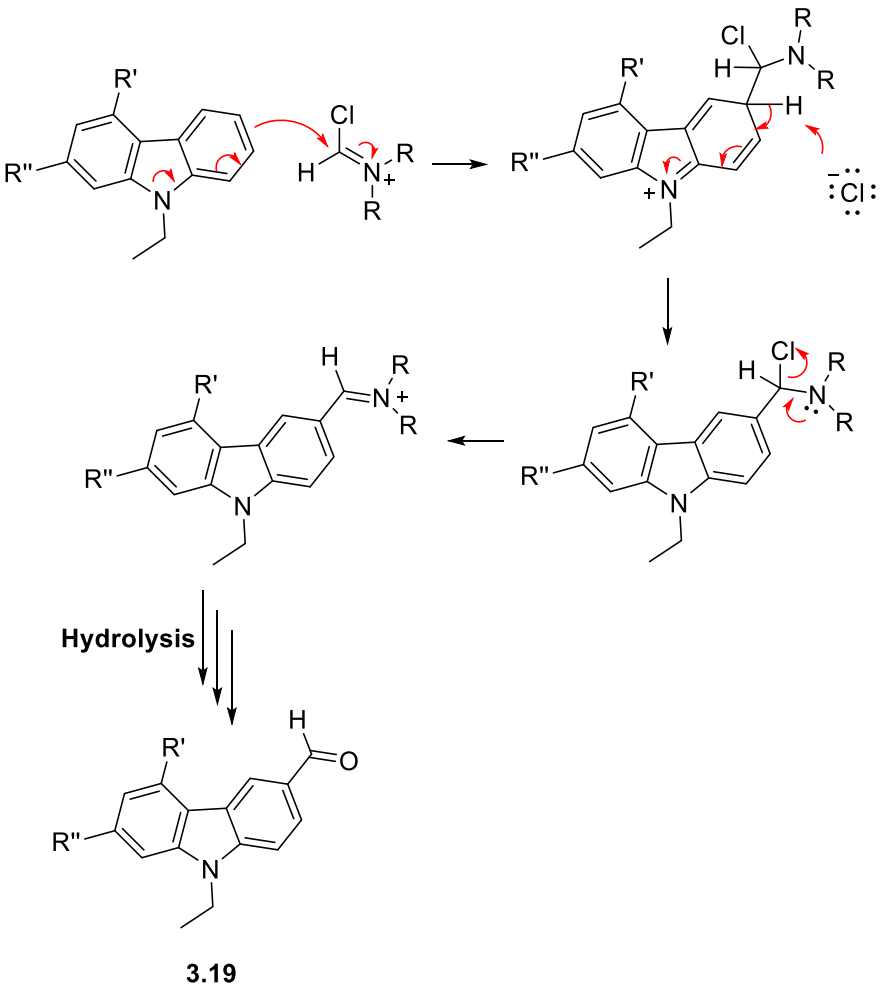

3.19

Scheme 65. *Aldehyde formation through electrophilic aromatic substitution.*

For biological purposes, an oxy-group at position 4 of the carbazole could have a positive effect on the activity of the molecule, and the presence of an electron-donating group should activate the π-system making it more reactive towards the electrophilic Vilsmeier-Haack reagent. Thus, 2-fluoro-7-methoxy-9-ethyl-9*H*-carbazole (**2.75**) was chosen as a suitable substrate to investigate the formylation reaction, although it would need an additional protodemethylation step to liberate a free hydroxyl group.

However, the presence of the methoxy group activated the right-hand ring of the carbazole towards electrophilic aromatic substitution, resulted in formylation at the positions *ortho* and *para* to the methoxy substituent and gave two additional regioisomers, as shown in **Scheme 66**. The target compound **3.20** was, besides, the minor product.

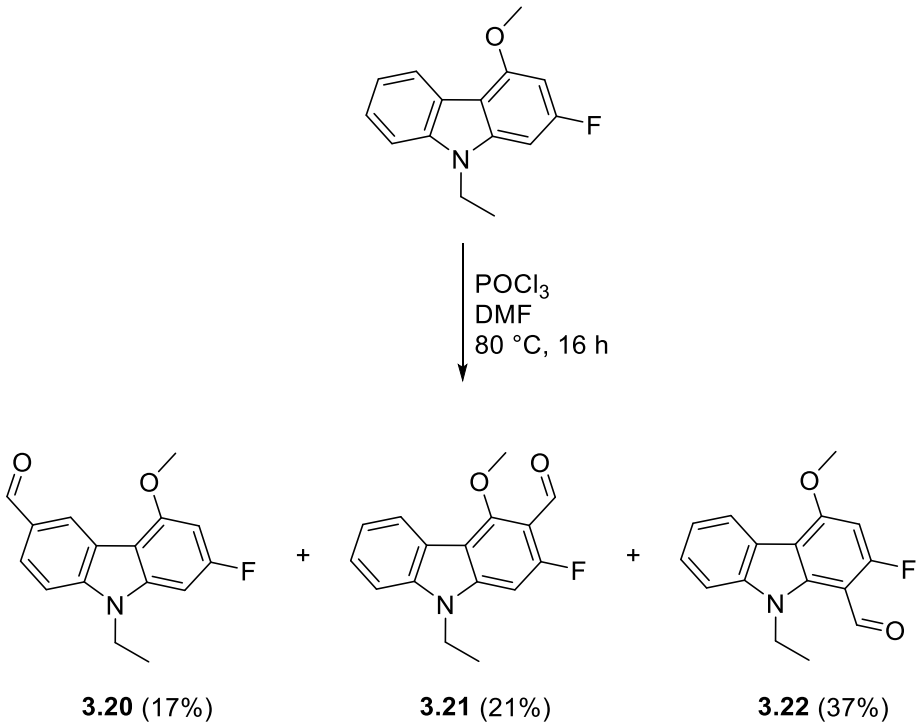

Scheme 66. *Formylation of carbazole* ***2.75*** *resulted in the formation of regioisomers* ***3.20****,* ***3.21*** *and* ***3.22****.*

The assignment of each compound was carried out by analysis of the ^{1}H-NMR spectra of fractions after purification by column chromatography. As stated before, the target product was identified, by the appearance of the aldehyde peak, by the disappearance of the H-3 signal and the change in the multiplicities of H-2 and H-4, as explained before (from triplet and doublet to doublet and singlet, respectively). The two other regioisomers were similar and distinguishing them was not trivial. They both had the same number of signals, and same multiplicities, with the only main difference being the shift of the proton on the methoxy and fluorine ring, which could be easily identified due to the high value of the J_{HF} *coupling constant* (~14 and ~12 Hz respectively). All these phenomena can be observed in **Figure 36**, where an expansion of the aromatic region of the ^{1}H-NMR spectra of the three regioisomers is displayed.

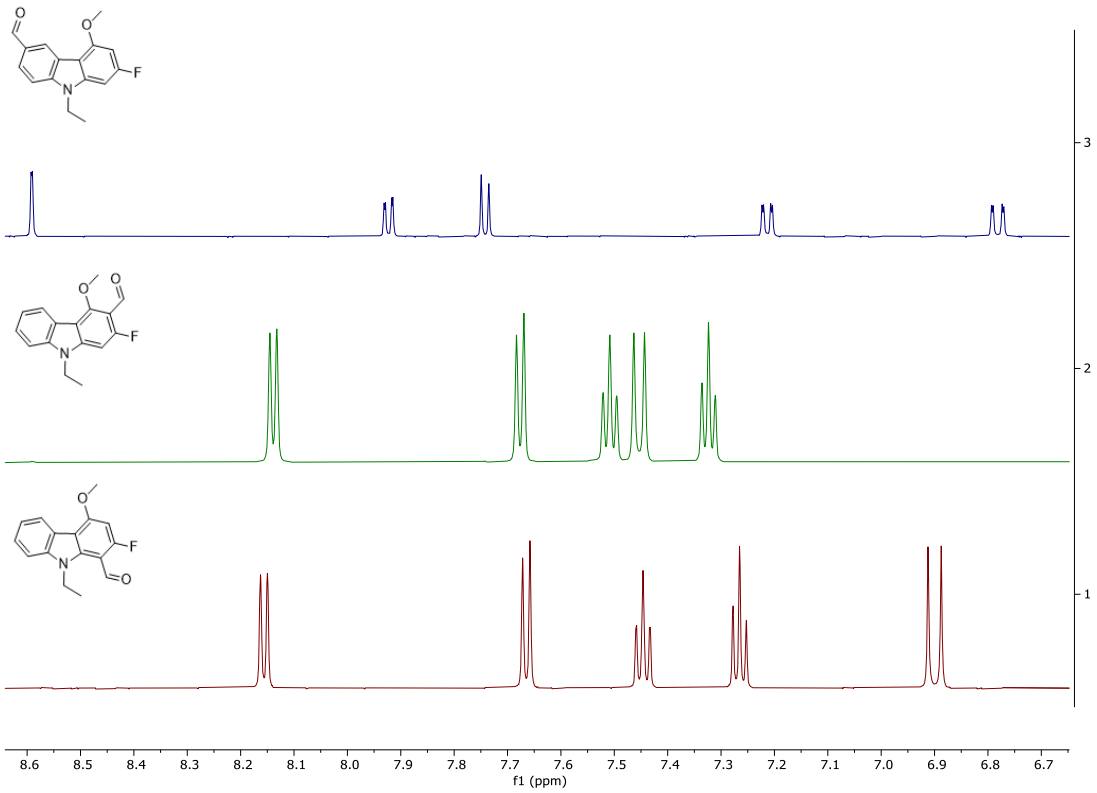

Figure 36. *Expansion of the aromatic region of the ^{1}H-NMR spectra of compounds* ***3.20****,* ***3.21*** *and* ***3.22*** *for comparison.*

Following the data in the literature,[231] the signal at δ~6.9 ppm was attributed to a proton at position 3, as this position on the carbazole ring plus the *ortho* position in regard to the methoxy group implies less dishielding. Hence, the proton on position 1 should be more dishielded, as the signals at this position appear at lower field, and the deshielding at the *para* position of the methoxy group is slightly lower to the *ortho* position. However, an extra NOESY experiment of the side products was carried out in order to confirm this hypothesis by analysing the interactions of the proximal protons. As displayed in **Figure 37a**, proton H3 of compound **3.22** is close in space to the 3 protons on the methoxy group and not with the ethyl chain, which only interacts with H8. On the other hand, in **Figure 37b**, it is observed that for compound **3.21**, proton H1 and proton H8, are close in space to the CH_2 of the ethyl group attached to the nitrogen and not close to the protons on the methoxy group. These attributions confirmed the position of each proton and therefore the identity of each regioisomer.

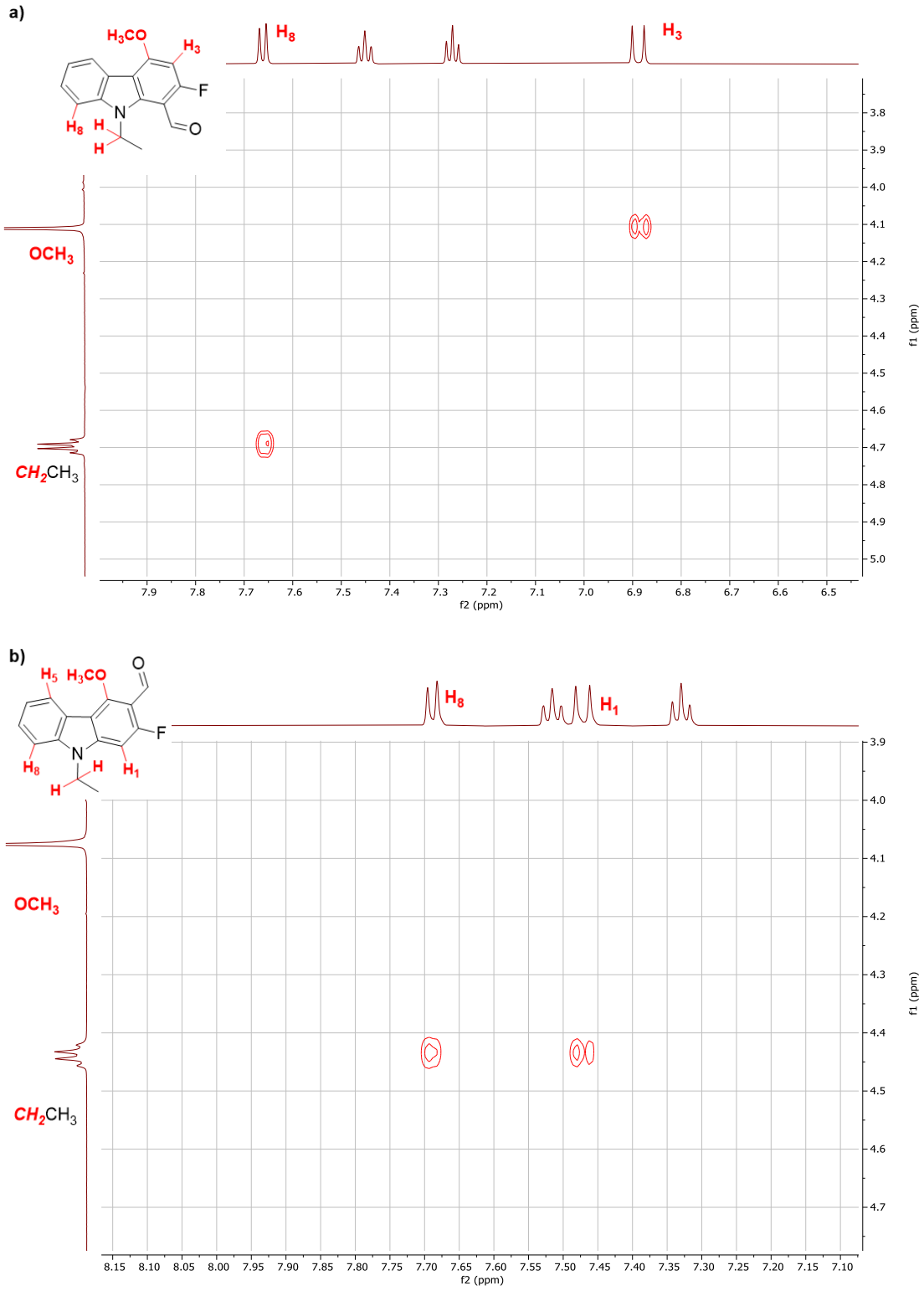

Figure 37. *NOESY spectra for compounds a)* ***3.22*** *and b)* ***3.21****.*

Encapsulating the results, the first approach to improve the formylation reaction of the fluorinated carbazoles consisted of increasing the reactivity of the formylating agent by introducing electron withdrawing groups to the amide, but it did not prove satisfactory. The second approach consisted of activating the carbazole skeleton to make it more reactive towards the Vilsmeier-Haack intermediate, but it was found that adding an electron donating group to the carbazole skeleton led to a compromise in the regioselectivity. Given the poor yields, the difficulty of separation and the loss of material, the decision was taken to investigate alternative, more efficient routes.

3.1.2. Alternative routes to the Vilsmeier-Haack reaction

An initial alternative route was planned to attempt the whole procedure with the aliphatic chain already in place. Thus, as the corresponding bromoaniline was not commercially available, starting with *N*-(4-aminobenzyl)-*N*-methylamine (**3.23**), an additional bromination reaction, would give the bromoaniline **3.24** needed for a Suzuki-Miyaura cross-coupling reaction and, after the flow process and subsequent *N*-ethylation, the PK083 analogues would be synthesised without the necessity of further functionalization (**Scheme 67**).

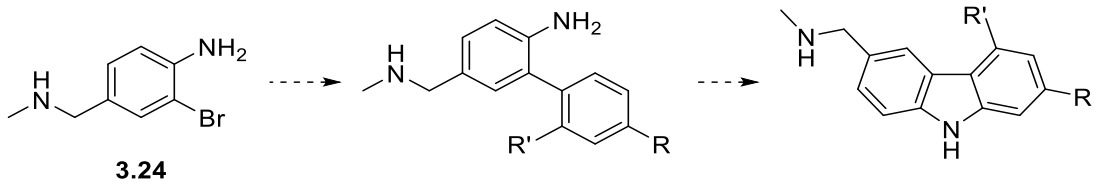

Scheme 67. *Synthetic proposal for the synthesis of carbazole analogues with the amine chain in place.*

The bromination reaction was attempted by slowly adding a solution of *N*-bromosuccinimide (NBS) dropwise using an addition funnel to a solution of the aniline **3.23** in an ice bath, to ensure monobromination, and the mixture was left stirring overnight at room temperature (**Scheme 68**). This reaction did not provide the target compound, although no starting material remained. After ^{1}H-NMR and LCMS analysis of the crude material, it was suspected that the formation of a salt with the secondary amine prevented the ring bromination. The poor solubility of the product in organic solvents and its ready solubility in water supported this hypothesis.

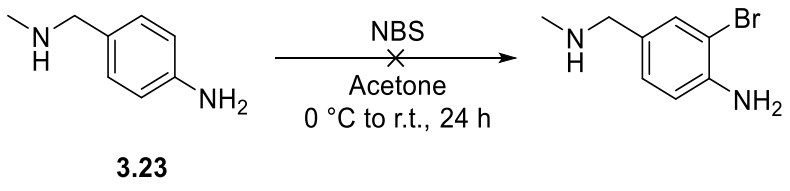

Scheme 68. *Bromination reaction of the N-(4-Aminobenzyl)-N-methylamine.*

The second alternative was to introduce bromine at the desired position to direct the late-stage introduction of the formyl group, improving the reactivity of the carbazole and avoiding the regioselectivity problems (**Scheme 69**). This bromination reaction would be conducted on the biphenyl species **3.24**, to avoid the presence of two halides in the cross-coupling reaction, which might cause regioselectivity issues and decrease the yield of the first step. Once the corresponding biphenyl had been brominated, the flow process should provide the brominated carbazole **3.25**. In the *N*-ethylation step there was the possibility of a side reaction with the nitrogen of the carbazole reacting with the arylbromide of another carbazole molecule, but the excess of iodoethane and its superior electrophilicity should allow the reaction to take place as desired.

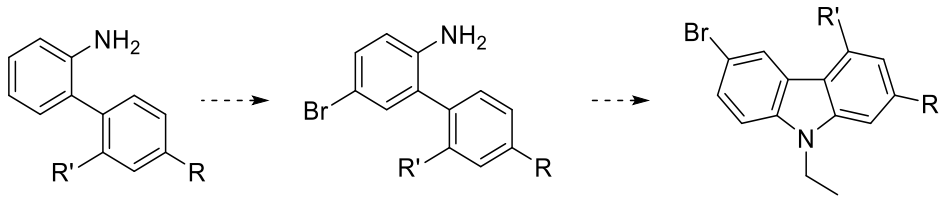

3.24 **3.25**

Scheme 69. *Synthetic proposal for the synthesis of 6-bromocarbazole (**3.25**).*

Thus, the bromination reaction was carried out using the same conditions previously described for the bromination of the alkylated aniline. After stirring overnight at room temperature, the desired brominated intermediate **3.26** was isolated in good yield, to facilitate study of the flow procedure. The compound was identified by ^{1}H-NMR spectroscopy, as the multiplicities on the aniline ring changed and matched the previously reported in the literature.[232] Nevertheless, when the brominated biphenyl was used in the flow azide formation-photocyclization procedure, the carbazole cyclisation was successfully achieved but after analysing the ^{1}H-NMR and LCMS data of the reaction crude the bromine was lost and only the unsubstituted 9*H*-carbazole was identified (comparing the data to the known compound) (**Scheme 70**).

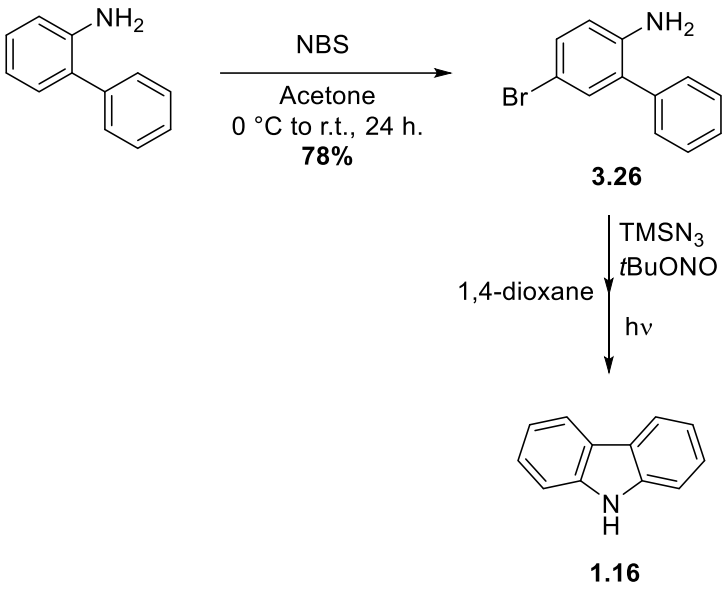

Scheme 70. *Attempted synthesis of 3-bromo-9H-carbazole* ***3.25a*** *(R = R' = H) resulting in 9H-carbazole (****1.16****).*

After reviewing the UV-spectrum of the bromine in the literature, it was observed that bromine absorbs at wavelengths around λ 400 nm,[233] and there could be a secondary excitation range even in the presence of the wavelength filters that had been used. This may have caused an excitation and further elimination of the bromine.

The next approach was to investigate was the formylation of the biphenyl amine. Previous experiments with aldehydes present in the Suzuki-Miyaura cross-coupling reaction under microwave irradiation carried out in the group were conducted using nitro biphenyls, but the presence of the amine group induced the formation of the corresponding amide between the aldehyde and the amine group instead of formation of a C-C bond. Since the aldehyde could not be present in the cross-coupling step, it was hypothesised that the aniline substrate (**2.40**) would be more nucleophilic to attack the Vilsmeier-Haack reagent than the carbazole species, and the presence of a carbonyl group should not affect the progress of the flow process or the *N*-ethylation step (**Scheme 71**).

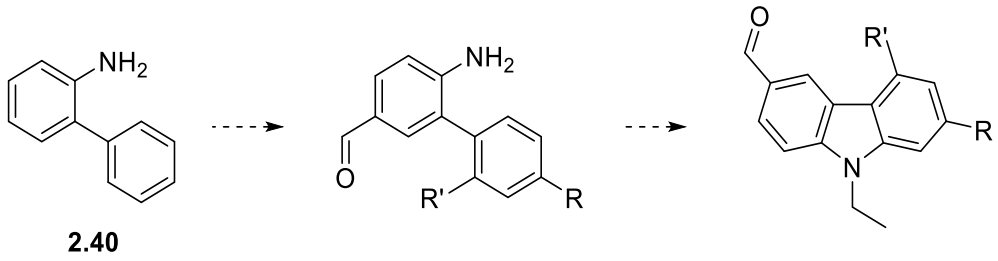

Scheme 71. *Synthetic proposal for the synthesis of carbazole analogues with the formylation step before the cyclization.*

The same conditions used for the formylation of carbazoles were chosen, under the hypothesis that the aniline might be more reactive than the carbazole which was inefficient in this process, and the possibility of using again more electrophilic reagents was kept in mind. However, the presence of the primary amine intervened this reaction as well, reacting with the Vilsmeier-Haack reagent giving formamidine **3.27** (**Scheme 72**).

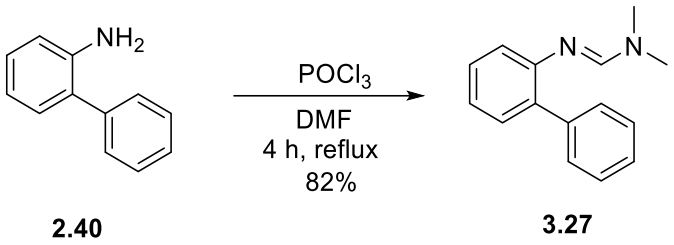

2.40 **3.27**

Scheme 72. *Formylation of 2-biphenylamine (**2.40**) gave formamidine **3.27**.*

Compound **3.27** was identified via ^{1}H-NMR spectroscopic analysis and LCMS. As shown in **Figure 38**, the presence of 9 protons in the aromatic region and the multiplicity of signals led us to discard the potential formylation reaction outcome, as well as the absence of the aldehyde peak. Once the formylation was discarded, there were two key signals that led us to speculate about the structure of the reaction product. The most obvious signal was a singlet at δ ~2.9 ppm integrating to 6H, which was interpreted as two methyl groups attached to the N,N-dimethylformamide. In addition, an extra singlet, integrating to 1H, appeared at δ ~7.37 ppm, which did not match with any of the positions of the biphenyl structure. To support this hypothesis, LCMS analysis was carried out, which provided a mass MH^{+} at m/z 225, matching with the theoretical mass of the proposed structure. As the product was not the target, it was no longer characterised or studied.

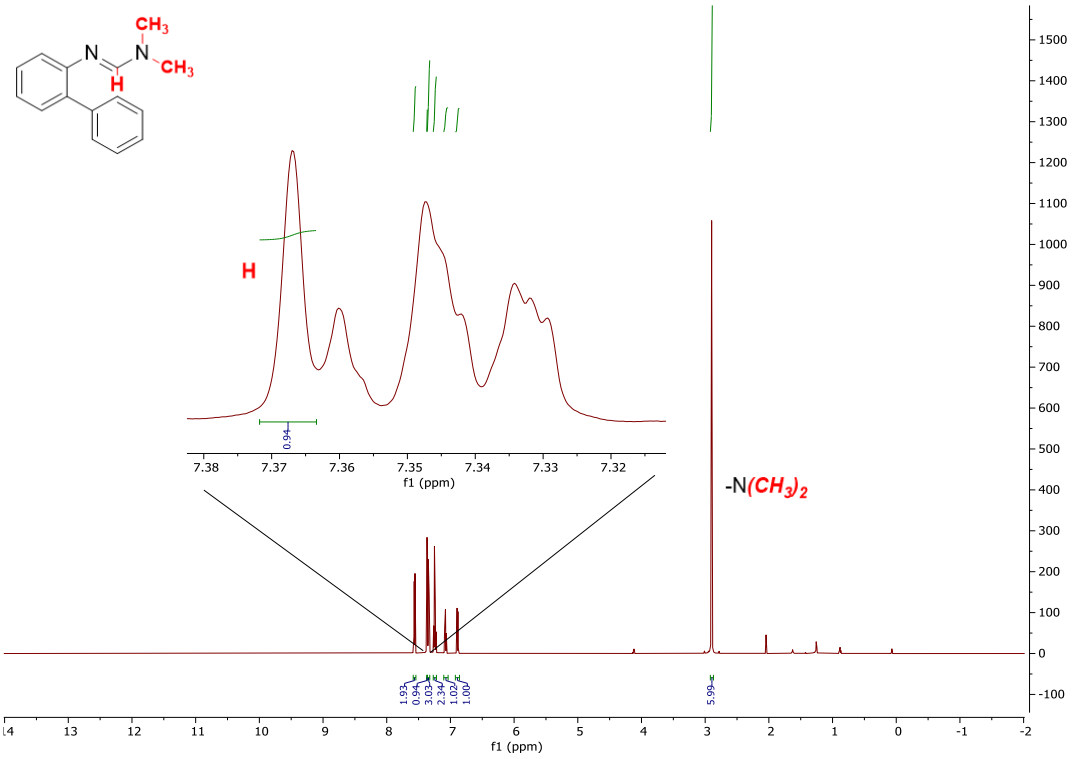

Figure 38. *^{1}H-NMR spectra of formamidine* ***3.27****.*

Two proposed mechanisms for this transformation are displayed in **Scheme 73**. In the first case (**Scheme 73a**) the amine attacks the formamide directly (presumably under acidic catalysis), and the diamino alcohol resulting from the proton transfer gives the formamidine by elimination of water. However, this mechanism was dismissed immediately as it would indicate that every reaction involving amines in DMF could lead to that compound, and that has not been observed to be the case. The second proposed mechanism, which looks much more plausible, would be the attack of the amine to the Vilsmeier-Haack reagent, which would be more electrophilic than the free formamide, and after elimination of hydrochloric acid would provide the formamidine (**Scheme 73b**).

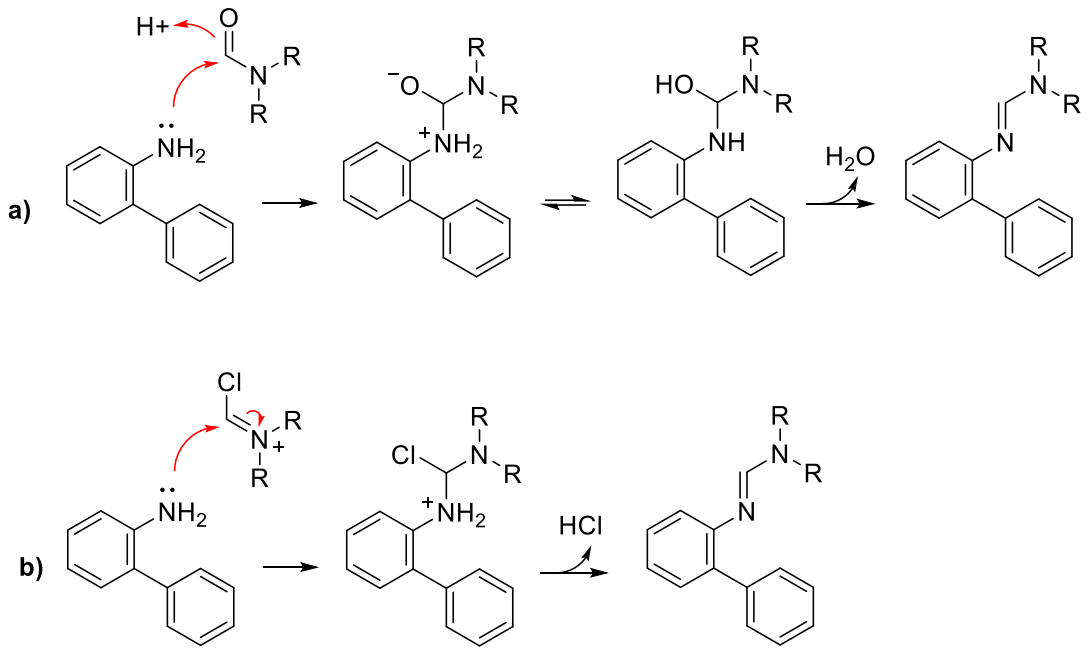

Scheme 73. *Two proposed mechanisms for the formation of the formamidine* ***3.27****.*

The direct formylation of the carbazole gave poor results and introducing the aldehyde or alkylamino group before carbazole formation was not a feasible approach to the PK083 analogues. However, the idea of having a suitable group in place at the desired position before carbazole formation had not yet been rejected. Introducing a group that could be oxidised or reduced in an additional step after carbazole formation appeared to be a promising strategy to follow.

Two possibilities were contemplated as groups suitable for oxidation. Firstly, according to a patent from Bayern Pharma, published in 2016,[234] and the work published by Joaquín Tamariz,[235] the oxidation of a methyl group to an aldehyde could be achieved using 2,3-dichloro-5,6-dicyanobenzoquinone (DDQ) in a mixture of methanol and water. A previous attempt with the 4,7-difluoro-2-methyl-9-ethyl-9*H*-carbazole already synthesised (**2.83**) gave poor conversion but led us to believe that the reaction could be optimized. Thus, 4-fluoro-6-methyl-2-trifluoromethyl-9-ethyl-9*H*-carbazole (**3.28**) was synthesised in 30% yield (for the four steps) using the method previously described in Chapter II. (**Scheme 74**).

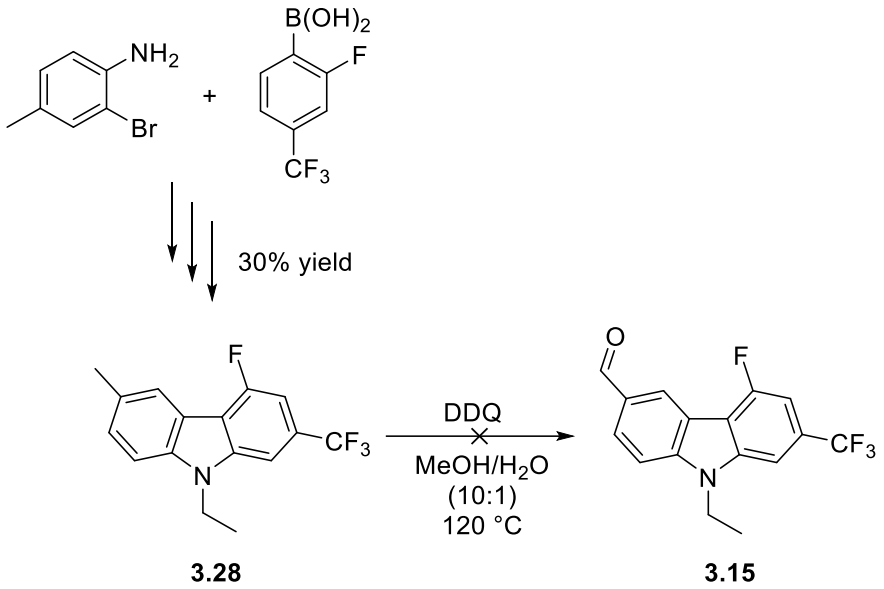

Scheme 74. *Methyl (**3.28**) oxidation to aldehyde **3.15** mediated by DDQ.*

The attempted DDQ oxidation was carried out using conventional heating in batch and in the microwave reactor in a sealed vessel, and in both cases provided poor conversion (less than 5%). As the conditions, especially in the microwave reactor, had been reasonably forcing, it was assumed that the reaction could not be improved significantly. As the oxidation seemed to not be feasible it was hypothesised that placing a group which could be reduced could be a better approach.

3.1.3. Ester route

Work published by the Denton group,[236,237] on the catalytic reductive amination of carboxylic acids, appeared to be a feasible approach to PK083 analogues (**Scheme 75**). The target compounds would be synthesised by the reduction of an amide analogue prepared from of the corresponding carboxylic acid, which could be obtained by hydrolysis of a carbazole-6-carboxylate derivative.

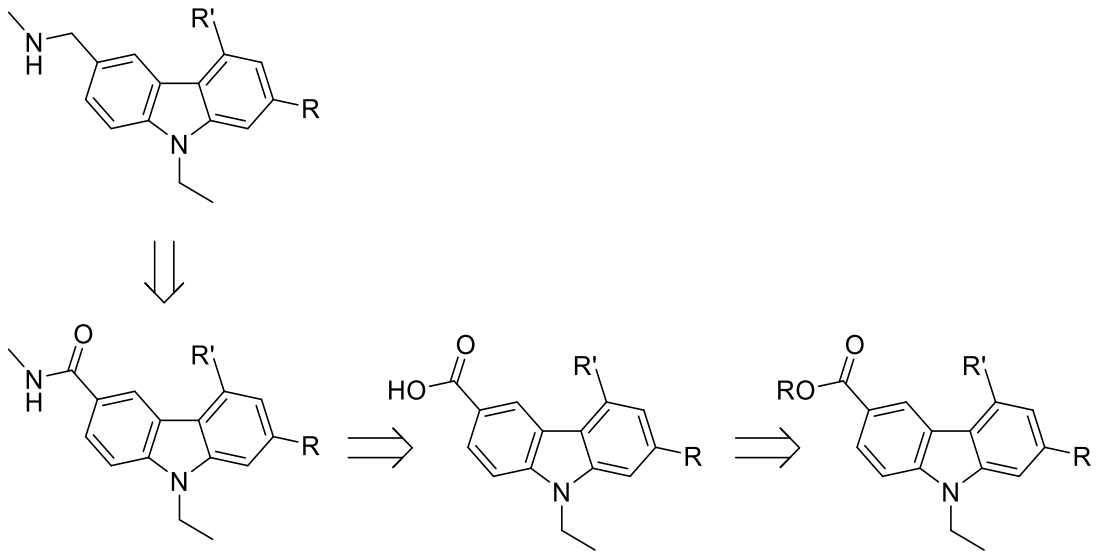

Scheme 75. *Retrosynthesis of the PK083 analogues through Denton's catalytic reductive amination.*[236,237]

As shown in **Scheme 76**, the synthesis would proceed in a similar manner to the successful route described before but starting with the corresponding boronic acid and an aniline bearing an ester group *para* to the anilino amine. The presence of an ester group was not studied in previous examples, but had the potential of being compatible with the whole process, without side reactions or undesired interactions between the ester and the reagents presents in each step.

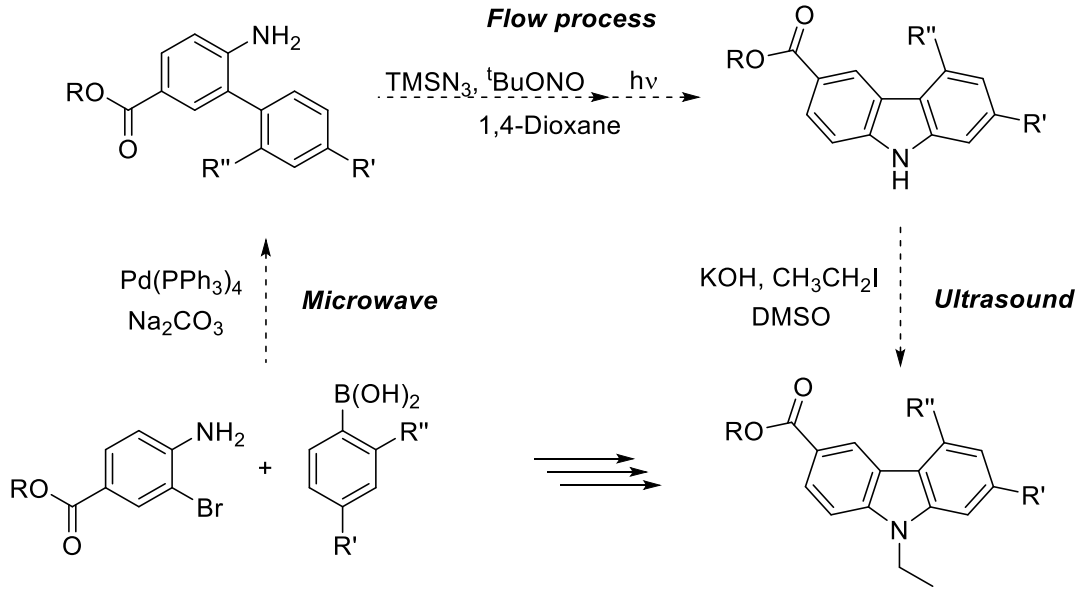

Scheme 76. *Synthetic scheme for the synthesis of carbazoles with an ester group on position 6.*

3.1.3.1 Suzuki-Miyaura cross-coupling reaction

Following the methodology described in Chapter II, a range of aminoesters were initially tested for the Suzuki-Miyaura cross-coupling in the first step of reaction with the fluorinated boronic esters of

interest. The ester group caused some new difficulties in the approach, demonstrated in the results shown in **Table 16**.

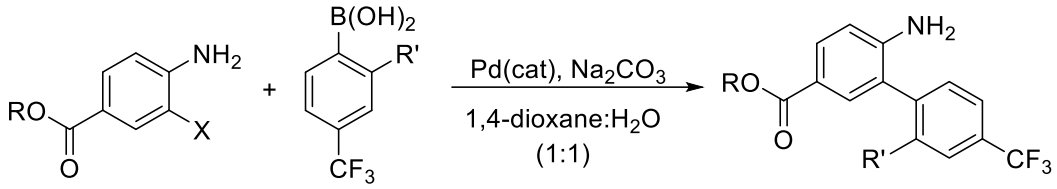

Table 16. *Results for the Suzuki-Miyaura coupling of an aniline containing an ester group on position 4.*

Entry	R	R'	X	Cat.	Compound	Yield (%)[a]
1	Me	H	I	$Pd(dppf)Cl_2$	**3.28**	40
2	Et	H	Br	$Pd(dppf)Cl_2$	**3.29**	85
3	Et	F	Br	$Pd(PPh_3)_4$	**3.30**	53
4	Et	F	Br	$Pd(PPh_3)_2Cl_2$	**3.30**	70

a) *Isolated yield after purification by flash chromatography.*

Methyl 4-amino-3-iodobenzoate was the first aniline investigated (entry 1). It gave an unexpectedly low yield for the formation of **3.28**, which was attributed to the hydrolysis of the methoxycarbonyl group under microwave irradiation in the presence of aqueous base. Although the corresponding carboxylic acid was not identified, this theory was reinforced when changing the methyl chain for an ethyl group, which improved the yield to the previously reported efficiency for this reaction. Hence, **3.29** was synthesised in high yield (entry 2). For **3.30**, the use of of tetrakis(triphenylphosphine)palladium(0), did not provide the expected yield (entry 3), so bis(triphenylphosphine)palladium(II) chloride was used and provided better results (entry 4).

The conditions for the cross-coupling reaction had been improved and the required biphenyls were synthesised in good yields following the same methodology used for the non- ester containing anilines. These favourable results enabled the continuation of the route and the submission of the synthesised compounds to the flow process for carbazole formation.

3.1.3.2 Flow process

Given the success in synthesising biphenyls **3.29** and **3.30** in good yield, these two compounds were submitted to the flow process for the photocyclisation towards the carbazole scaffold. The conditions used for these experiments were exactly the same as reported previously, with azide formation followed by photocyclization. No major changes or issues were observed in the reactor when

conducting the reactions, but, after ^{1}H-NMR spectroscopic analysis, essentially full conversion of starting material was observed, however, to an unusual side product, shown in **Scheme 77**.

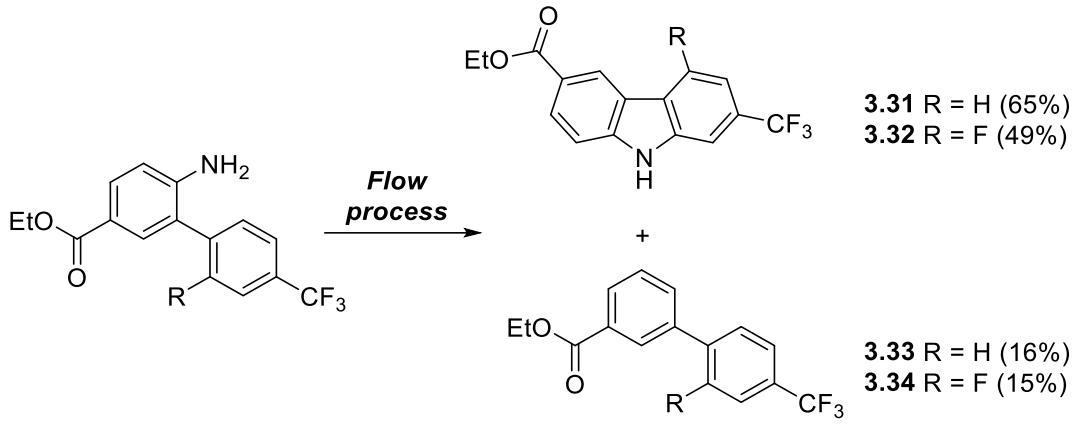

Scheme 77. *Reaction scheme of the flow process for the biphenyl carboxylates.*

The photocyclization mechanism is discussed in **Scheme 32** (section 1.4.3.3 in Chapter II). The mechanism of these new compounds, however, remains uncertain. Following the work published by Catherine J. Smith *et al.*, azide formation is tolerant of ester groups present in the azidobenzene ring,[170] which ruled out a different rearrangement or elimination during the diazonium salt formation. The product would, then, be formed under photochemical conditions in the photoreactor. There are many examples in the literature of photoactivation of carbonyls, and a more detailed explanation of the effect of the photo-induced electron transfer to esters and carboxylic acids was published by Ralf Kijppe and Paul H. Kasai.[238] However, a plausible mechanism for a rearrangement of a radical species with elimination of the nitrogen group could not be described. Eventually, as it is well known that diazonium species can be reduced in the presence of a wide range of reagents and even electrochemically,[239–241] the most plausible explanation would be the reduction of the diazonium salt due to photochemical activation, probably induced by the presence of an activated carbonyl, or the presence of this EWG in the para position of the leaving group.

The target products, which were present as major products, were identified as previously described for the analogues, via ^{1}H and ^{13}C-NMR spectroscopy and HRMS. The side products were also identified by ^{1}H-NMR spectroscopic and ESI spectrometric analyses. The ^{1}H-NMR spectrum of compound **3.33** is displayed in **Figure 39** as an example. The first observation was the presence of the two doublets integrating to 2 protons corresponding to the AA'XX' system of the CF_3 containing ring, which should disappear if cyclisation occurs. This suggested that the cyclisation did not happen, and the biphenyl skeleton was still present. Moreover, in the aromatic region there was an extra proton which was not observed before. These two facts, plus the presence of the ethyl ester, appeared to confirm the

structure of the product. HRMS confirmed the structure by matching with the theoretical mass: MH^+, 295.0937.

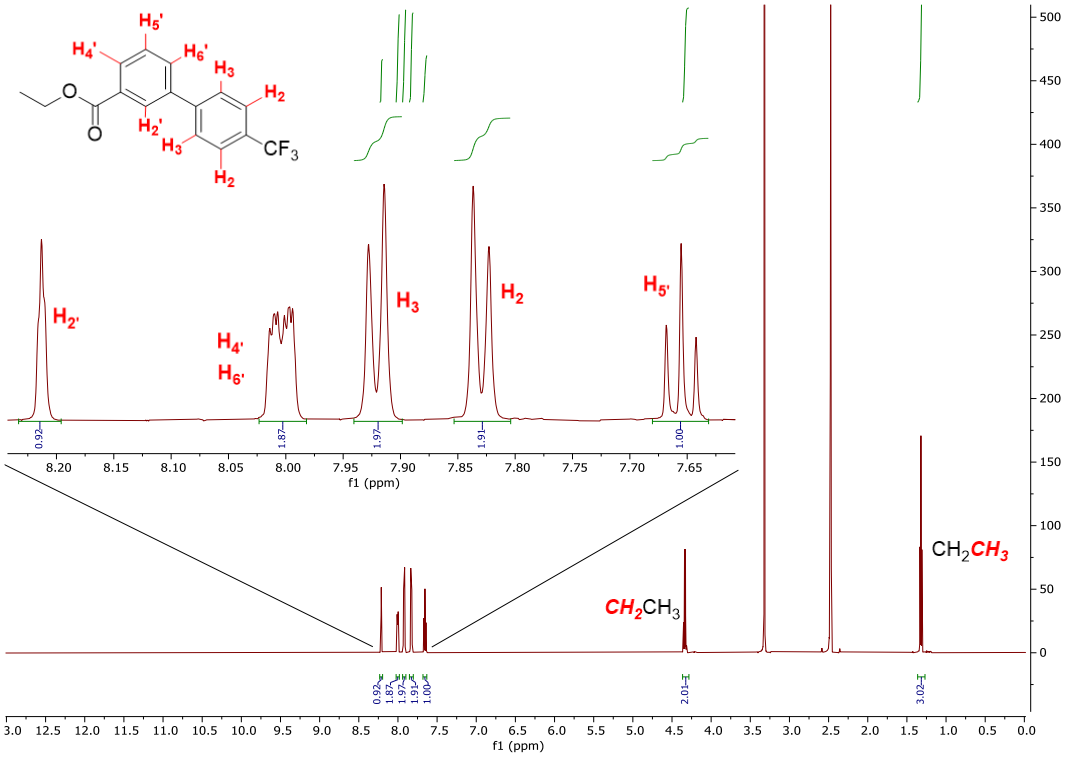

Figure 39. *^{1}H-NMR spectra of side product* ***3.33.***

Despite this setback, the yields for this step were not dramatically lower than the previous attempts and the two products could be separated without major problems by flash column chromatography for both analogues. Thus, both biphenyls, **3.29** and **3.30**, were successfully converted into the carbazole analogues **3.31** and **3.32** in good yields, and although purification was needed before the *N*-ethylation step, it did not compromise the viability of the synthetic pathway.

3.1.3.3 *N*-ethylation and hydrolysis

The following *N*-ethylation step, using the pure carbazole product, provided full conversion for both compounds and a high isolated yield for **3.36**, although the isolated yield for compound **3.35** was slightly lower than expected (**Scheme 78**). The last step, also shown in **Scheme 77**, was the hydrolysis of the ester group to give the corresponding carboxylic acid. Although most of the examples in the literature suggested ethanol would be suitable as a solvent,[242,243] the carbazoles were heated to reflux in the presence of base and water in dioxane, to avoid potential transesterification. The reaction was monitored by TLC analysis, after 2 and 4 hours, and, as it did not show full conversion, the process was

left overnight. Acids **3.37** and **3.38** were obtained essentially pure in quantitative yield after acidifying the solution and extracting with ethyl acetate.

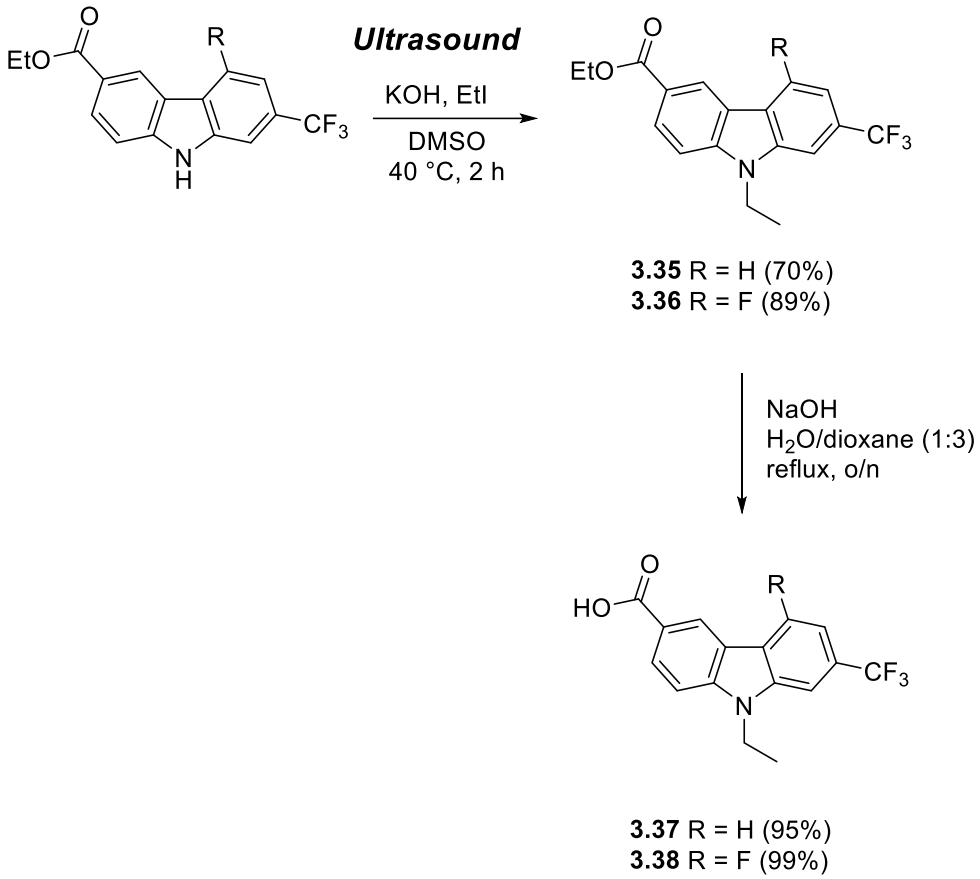

Scheme 78. *N-ethylation of the ethyl 9H-carbazole-3-carboxylates and hydrolysis of the ester group.*

The analysis of these compound was not complicated, as the only modified signals related to the disappearance of the quartet and triplet from the ethyl chain of the ester. The ^{1}H-NMR spectrum was conducted in acetone due to insolubility of the carboxylic acid in *d*-chloroform. In this solvent the intermolecular rate of exchange was slow enough that a peak due to HDO is usually also observed around δ 3 ppm, and the COOH proton was observed at δ ~ 2.86 ppm. Once again, the theoretical mass was confirmed by LCMS and HRMS analysis, being MH^{+}: 308.0890 for **3.37** and MH^{+}: 326.0800 for **3.38**.

The *N*-ethylation step provided the expected results and the additional hydrolysis step gave almost a quantitative conversion to the corresponding carboxylic acids, also in high purity. Hence, the overall synthesis of the carbazole was not affected by the presence of the ester group, and the formation of the acid gave noticeably higher yields than the formylation approach. The reductive amination of these two acids was the only step required for the procurement of the PK083 analogues.

3.1.3.4 Reductive amination

After obtaining the carbazole 6-carboxylic acids in high yield, the new approach seemed to be more efficient that previous studies, keeping in mind the poor efficiency of the formylation step due to an inefficient Vilsmeier-Haack reaction. Thus, the last step, the catalytic reductive amination reported by R.M. Denton's group,[236,237] should provide the methylmethanamine group following amide formation and reduction, as shown in **Scheme 79**.

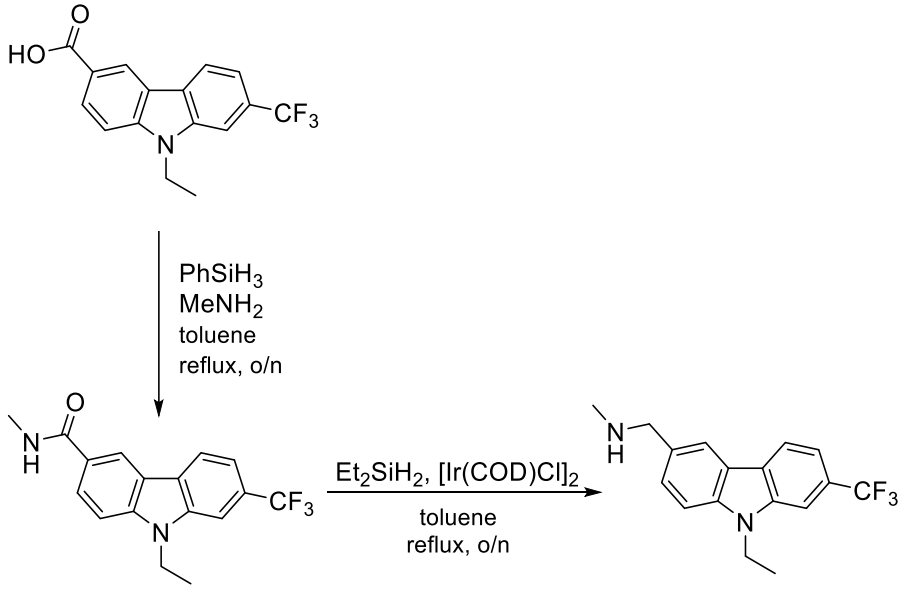

Scheme 79. *Catalytic reductive N-alkylation of amines using carboxylic acids.*[236,237]

The two-phase process was conducted in one pot. Firstly, the phenylsilane-mediated amidation was carried out in toluene stirring at reflux overnight. Then, 1 mol% of $[Ir(COD)Cl]_2$ was added along with Et_2SiH_2 and the reaction mixture was stirred, again, overnight at reflux. Initial studies of the ^{1}H-NMR spectrum of the reaction crude using **3.37** showed a mixture of compounds, in which the aliphatic signals of the reduced methylamine chain were not observed. Thus, a last attempt was carried out by interrupting the reaction after the first step, in order to check if the amide formation had taken place. The ^{1}H-NMR spectrum of the crude reaction mixture showed only starting material was present. The amide formation step was not occurring, and thus the subsequent reduction step was being carried out on the carboxylic acid. Therefore, a new methodology for the amide formation was proposed to be studied, using 1-ethyl-3-(3-dimethylaminopropyl)carbodiimide (EDC) as an activating agent in the presence of *N*-methylmorpholine (NMM) and catalytic 1-hydroxy benzotriazole (HOBt) (**Scheme 80**).[244]

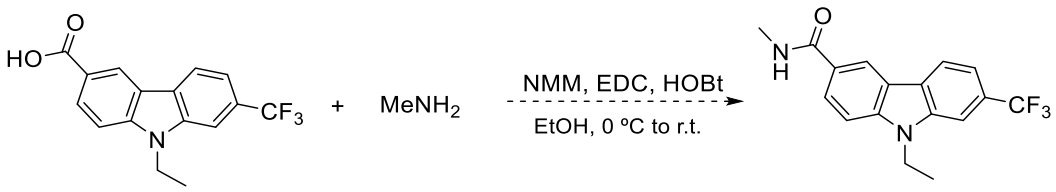

Scheme 80. *EDC-mediated amide formation.*

The corresponding carbazole carboxylic acid was dissolved in ethanol with methylamine, NMM and HOBt and the solution was cooled to 0 °C before EDC was added. The solution was then allowed to warm up to room temperature and stirred overnight. The ^{1}H-NMR spectra of the crude reaction only showed starting materials. The amine bond could not be made using this method, but it was hypothesised that the carboxylic acid could also act as a hydrogen bond donor and interact with the Asp228 in p53-Y220C increasing the stability. Hence, compounds **3.37** and **3.38** were synthesised in good overall yields of 37% and 30%, respectively, and were also tested as potential reactivators of the mutated p53.

3.1.4. Rieche formylation

The difficulties found in the ester route and the necessity of adding two additional steps, although the yields were not low, suggested that this route was far from ideal. Therefore, new alternatives were investigated in the literature and the Rieche formylation, using dichloromethyl methylether in the presence of titanium(IV) chloride, appeared a good candidate for further study. The method, first reported by A. Rieche, H. Gross, and E. Höft[245] and further developed by T. M. Cresp and M. V. Sargent[246] and more recently studied by E. Nicolás's group[247,248] on electron-rich phenols. The intermediate **3.39** involved in the process (**Scheme 81**) had the potential to be more electrophilic than the Vilsmeier-Haack reagent formed in the previously described approach.

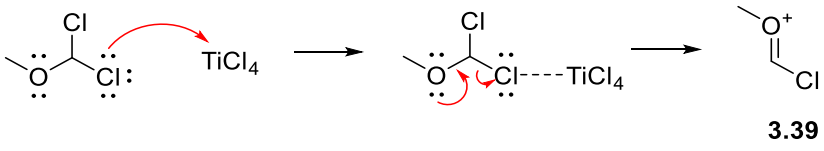

Scheme 81. *Rieche formylation intermediate **3.39** formation mechanism.*

Margaret A. Brimble's group published the use of this reaction on fluorinated carbazoles with prominent results,[249] so similar methodology was adapted for the formylation of our target compounds due to the similarity of the substrates. The reaction was carried out at room temperature, monitored by TLC analysis, and it was stirred overnight. As shown in **Scheme 82**, the reaction provided excellent results for both compounds, standing out as the most efficient formylation method for this step of the synthesis on any precursor.

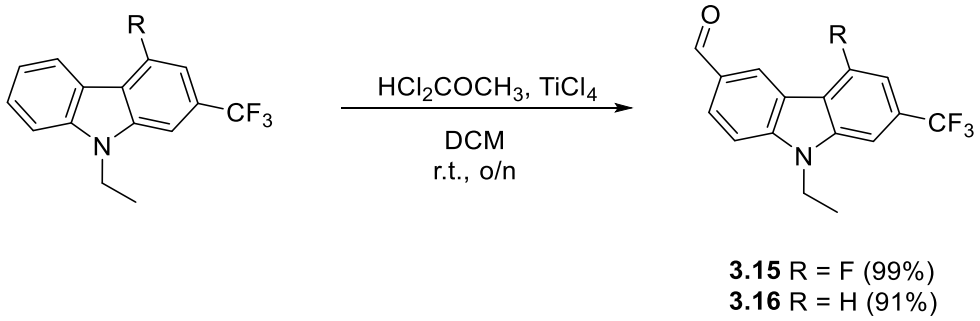

3.15 R = F (99%)
3.16 R = H (91%)

Scheme 82. *Rieche formylation reaction scheme.*

Structural verification of the identity of the products was carried out as explained before for the Vilsmeier-Hack reaction, with the change in the signals of the protons on the aldehyde-containing ring and the appearance of an aldehyde resonance. The mechanism for this reaction consists of two simple steps, starting with the attack of the carbazole on the chlorooxonium ion intermediate, followed by hydrolysis to furnish the aldehyde (**Scheme 83**).

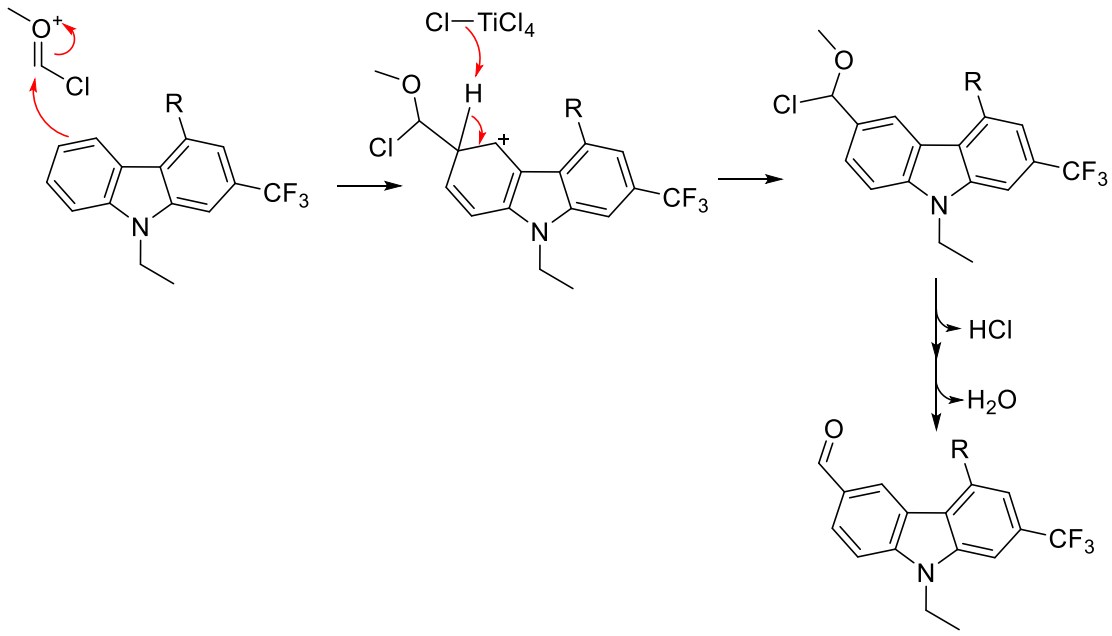

Scheme 83. *Proposed mechanism for the Rieche formylation.*

The application of these new conditions provided a powerful method for the formylation of electron poor carbazoles which could be extrapolated to the bis(trifluoromethyl) analogue **2.54** providing the resulting aldehyde **3.17** in a moderate yield of 54%. The three analogues, obtained in high purities, were used in the final reductive amination step to obtain the corresponding p53 reactivator scaffolds.

3.1.5 Reductive amination

The reductive amination (or reductive alkylation) reaction was previously studied in the group and provided good results when investigated on previous analogues.[225] Following the same procedure, the carbazole aldehydes were stirred for up to 72 h at room temperature in the presence of methylamine and sodium triacetoxyborohydride (STAB) for imine formation and subsequent reduction with a view to obtaining the corresponding methylmethanamine derivative (**Scheme 84**).

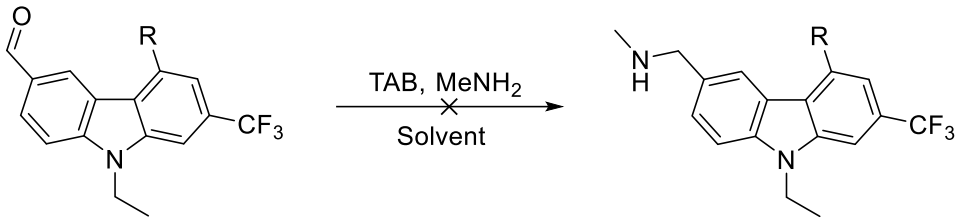

3.40 R = H
3.41 R = F
3.42 R = CF_3

Scheme 84. *Reductive amination using sodium triacetoxyborohydride.*

The corresponding aldehyde, methylamine and STAB were dissolved in anhydrous THF (or CH_2Cl_2) and stirred at room temperature over the weekend. After concentrating under pressure, the crude ^{1}H-NMR spectrum showed full conversion to a new compound for all the substrates. However, instead of the signals corresponding to the two new resonances that was expected (2 protons for the –CH_2 and 3 protons for the –CH_3 of the aminated chain), two different signals, one integrating to 3 protons at around δ 3.5 ppm and an additional singlet in the aromatic region (~8.5 ppm) was observed. After purification by flash column chromatography, using either a SiO_2 or basic alumina stationary phase, the species obtained was the starting material. These results suggested that the new compound was the imine analogue, which would have hydrolysed back to the aldehyde in the presence of aqueous acid (SiO_2) or base (alumina). The ^{1}H-NMR spectrum of the imine intermediate **3.43** is shown in **Figure 40** as an example.

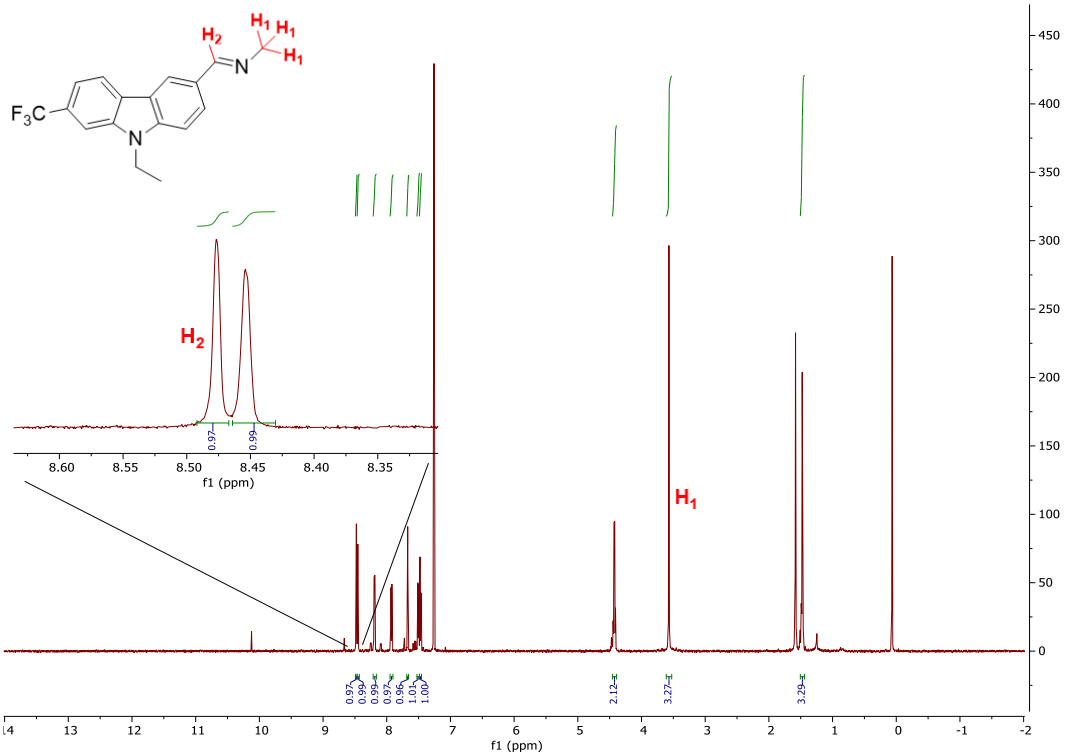

Figure 40. *^{1}H-NMR spectra of the imine intermediate* ***3.43****.*

The well-known imine formation mechanism is shown in **Scheme 85**. It starts with the nucleophilic addition of the primary amine to the carbonyl group of the aldehyde. Next, a proton transfer forms a neutral amino alcohol called a carbinolamine **3.44**. Then, the hydroxyl is protonated, and elimination of water provides the imine group in an equilibrium process. The absence of an acid catalyst is the reason why the reaction is slow and must be left overnight.

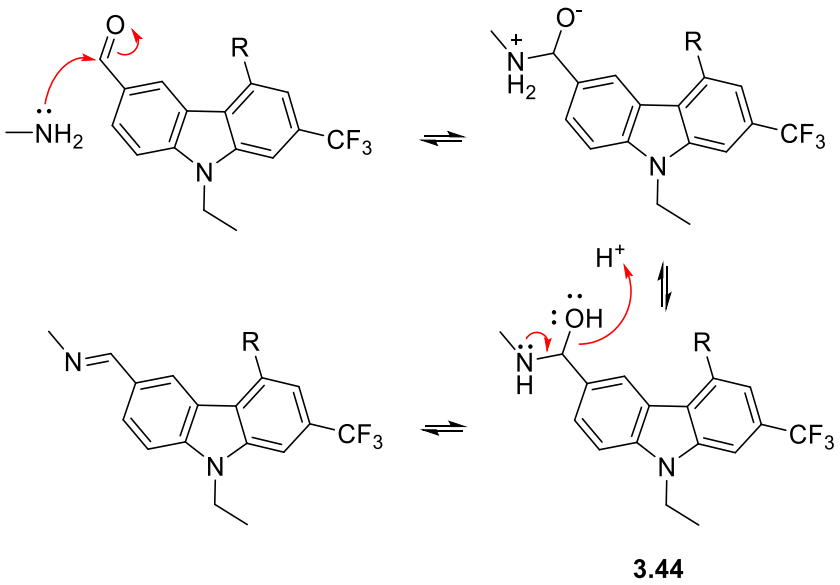

3.44

Scheme 85. *Imine formation reaction mechanism.*

The low solubility of the borohydride in THF led to a scope of alternative solvents, such as dichloromethane or *N*-methyl-2-pyrrolidone (NMP). The former did not provide any improvement and, although the solubility of the borohydride was increased in NMP, only starting material was obtained. An extra test using benzaldehyde under the same conditions but adding an equimolar amount of acetic acid was also studied but no change in outcome was observed.

Thus, the reducing agent was changed to sodium borohydride. The reaction was left overnight and after sampling the reaction, the crude ^{1}H-NMR spectrum showed the appearance of one new major compound, with a new signal integrating to 2 protons at δ 3.8 ppm. From the new signals, the target product or the imine were not identified, so it was assumed that the reduction step had taken place before imine formation, and the main compound in the reaction mixture was the hydroxy analogue, reduced from the aldehyde. The reaction was repeated, isolating the two steps and adding the sodium borohydride once the first step was complete. Although again there was good evidence that the imine formation had taken place successfully, the reduction step did not work as well, and the crude reaction mixture showed a mixture of products, in which the target compound could not be identified.

Sodium cyanoborohydride was the last reducing agent to investigate from the borohydride group, but although its solubility was higher, it was not able to facilitate the reduction of the imine group. Eventually, a reductive amination method reported by Feng Han *et al.*[250] using a solution of $NaBH_4$ in THF/MeOH added in portions to the solution provided full conversion to the desired product and enabled the isolation of compounds **3.40**, **3.41** and **3.42** (**Scheme 86**).

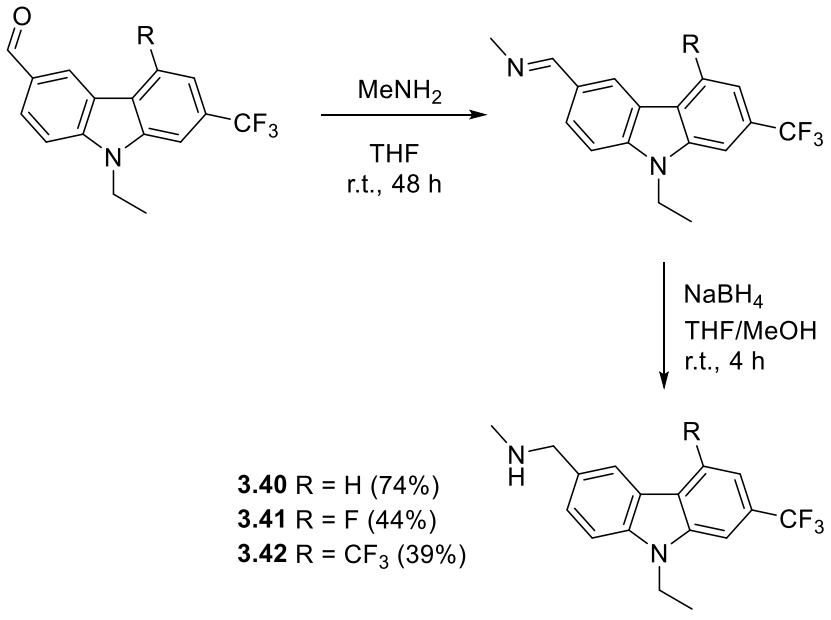

Scheme 86. *Reductive amination reaction scheme.*

In this case, the two signals corresponding to the CH_3 (integrating 3H) and the CH_2 (integrating 2H) of the amine chain were clearly observed in the ^{1}H-NMR spectrum, as shown in **Figure 41** for the ^{1}H-NMR spectrum of **3.40**. The rest of the signals were consistent with the expected for the N-ethylated carbazole skeleton, and although LCMS could not be carried out due to degradation of the molecule in the analysis, HRMS confirmed the mass of each compound (for compound **3.40**, MH^+, m/z 307.1436).

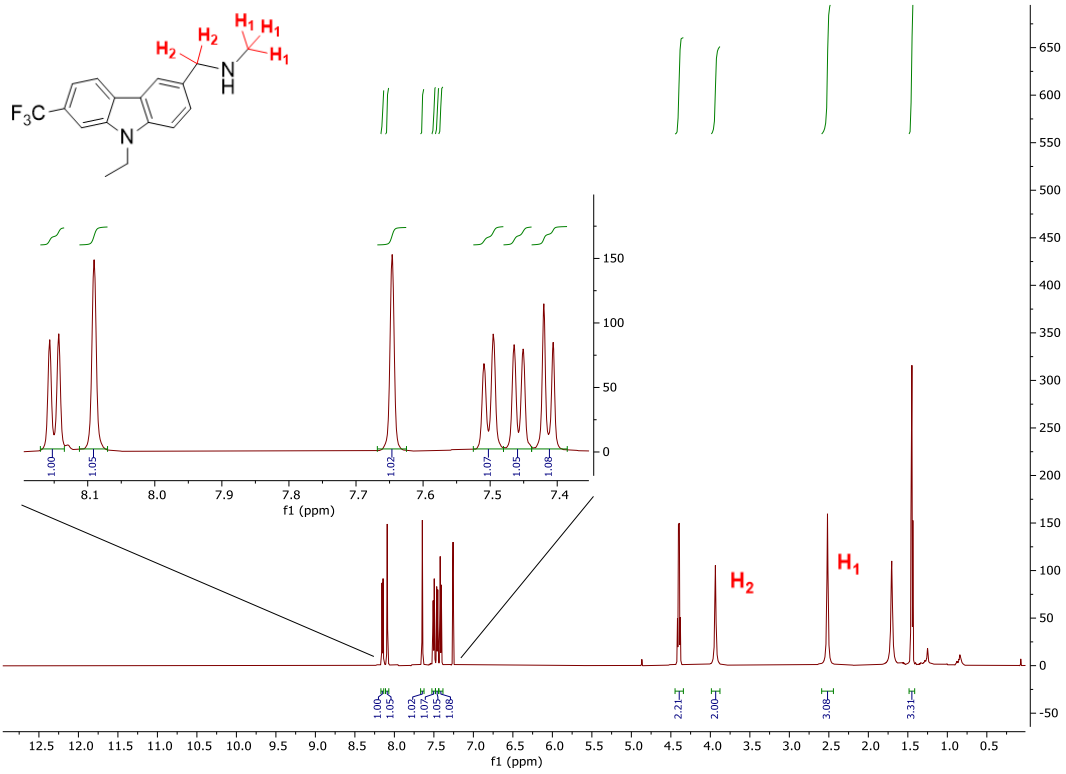

Figure 41. *^{1}H-NMR spectrum of compound **3.40**.*

Scheme 87 shows the proposed mechanism of the $NaBH_4$ in methanol mediated reduction. In the first step, one H^- detaches from the BH_4^- and adds to the carbon adjacent to the nitrogen, while the nitrogen is attached to the remaining BF_3 (an example of [1,2]-addition). This forms the C-H bond. Then, the BH_3 gets eliminated when the nitrogen gets protonated by the proton of the methanol. That is why a protic solvent helps the reaction at this step.

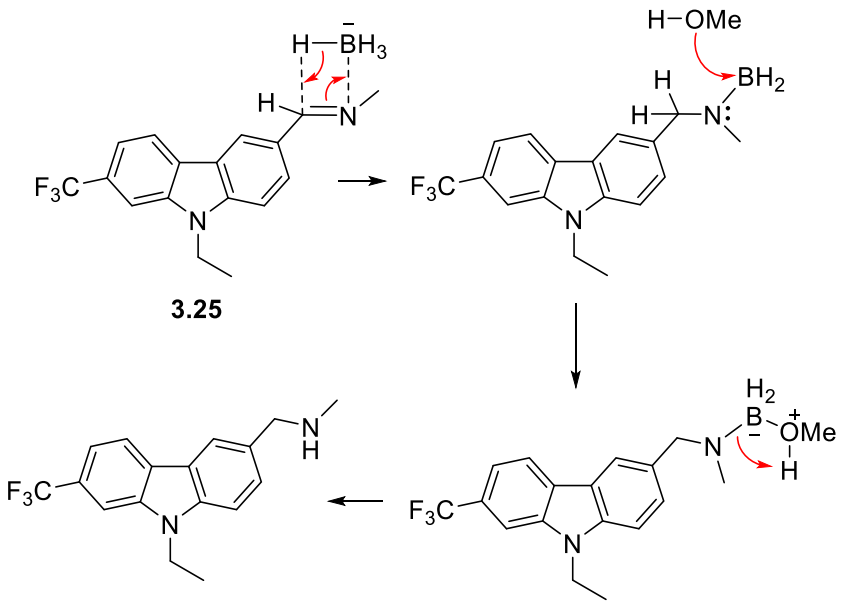

Scheme 87. *Mechanism for the $NaBH_4$ mediated reduction of the imine* ***3.43****.*

Although the conversions were almost quantitative, the purification of the three analogues was more challenging than expected. Following previous investigations in John Spencer's group, the amino chain appeared to be susceptible to elimination from the molecule promoted by the electron donating properties of the ethyl attached to the central carbazole nitrogen. Although the hypothetical product could not be isolated, in previous investigations of the mass spectra of PK083 (**3.1**) analogues, species with a reduced mass that would be consistent with the loss of the methylamine side group.[251] Hence, as shown in **Scheme 88**, this part of the molecule turned out to be sensitive and broke down in presence of an acid source: in SiO_2 when submitted for flash column chromatography, or when heated on recrystallization.

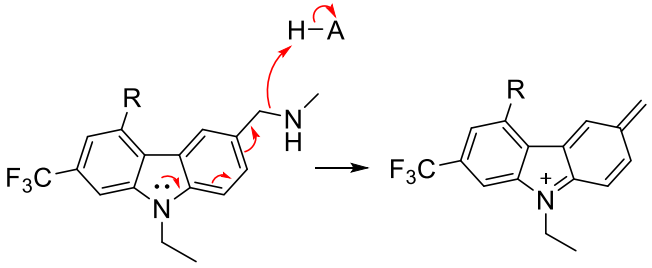

Scheme 88. *Potential amine loss in carbazoles observed in ESI-HRMS.*

Eventually, flash column chromatography using alumina columns became the most reliable purification method, and although the yields could not be optimized, the three compounds could be synthesised, isolated and tested as potential reactivators of the p53 gene.

3.2 Biological results

The potency of the p53 reactivators was initially determined by differential scanning fluorimetry (DSF), a technique that measures protein unfolding by monitoring changes in fluorescence during an increasing temperature gradient, using a hydrophobic fluorescent dye that binds to the protein as it unfolds. If a ligand is able to create a stable interaction with the protein, the stability of this structure will increase, thus the temperature needed to unfold it will rise (generating a positive ΔT_m value). These biological studies were conducted by Dr Andreas Joerger's group (SGC, Institute of Pharmaceutical Chemistry, Goethe University, Frankfurt). The results using each compound at 250 μM concentration with the protein at 8 μM are shown in **Table 17**. Entry 1 shows the apparent melting temperature (T_m) of the protein for the WT and the Y220C mutation measured by DSF. This entry will be used as a reference to calculate the ΔT_m as the difference between the T_m of the protein with the corresponding binder and the T_m of the protein in the apo form, for the WT and the Y220C mutation. Entry 2 shows the thermostabilization by the lead compound PK083, calculated as ΔT_m. This entry will be used to compare the activity of each compound of the series.

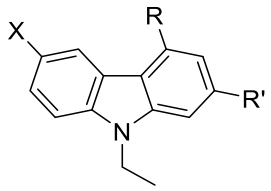

Table 17. *Thermostabilization of carbazole-based WT and Y220C binders.*

Entry	Compound	X	R	R'	Wild type protein		Y220C mutation	
					T_m[a]	ΔT_m (°C)[b]	T_m[a]	ΔT_m (°C)[b]
1	Protein	-	-	-	51.61 ± 0.13	-	43.30 ± 0.04	**-**
2	PK083 (**3.1**)	$-CH_2NHCH_3$	H	H	51.18 ± 0.10	-0.43	43.85 ± 0.04	**0.55**
3	**3.37**	-COOH	H	CF_3	50.97 ± 0.18	-0.64	42.72 ± 0.03	**-0.58**
4	**3.38**	-COOH	F	CF_3	51.42 ± 0.17	-0.19	43.20 ± 0.08	**-0.10**
5	**3.40**	$-CH_2NHCH_3$	H	CF_3	50.80 ± 0.08	-0.80	44.34 ± 0.02	**1.04**
6	**3.41**	$-CH_2NHCH_3$	F	CF_3	50.92 ± 0.02	-0.69	43.35 ± 0.10	**0.05**
7	**3.42**	$-CH_2NHCH_3$	CF_3	CF_3	49.77 ± 0.16	-1.84	43.28 ± 0.13	**-0.02**

a) Measured at a compound concentration of 250 μM. Mean values ± SEM are given
b) ΔT_m values were calculated as $\Delta T_m = T_m$ (protein +compound) − T_m (protein)

Firstly, the fact that ΔT_m values are negative for the wild type and positive in the mutant indicate that the binder is specific for the mutant protein, and only interacts in the cavity formed by the mutation, which is not present in the protein in its natural state. If ΔT_m values were positive for the wild type and the mutated protein the compound would be interacting with the protein, but not with the cavity generated by the mutation, and if it did, it would mean that it would be binding to more than one site, which would demand an increase of the concentration. As shown in **Table 17**, then, all the compounds are specific for the mutated protein and interact (if they do) only with the cavity. Compounds **3.37** and **3.38**, containing a carboxylic acid in position X (**Figure 41**), did not improve the stability of the protein in DSF (entries 3 and 4) as the amino chain appeared to be crucial to form a hydrogen bond with the oxygen of Asp228 and increase the affinity of the molecule**.** With the amino chain in place for compounds **3.40**, **3.41** and **3.42** (**Figure 41**), the CF_3 moiety in position R' was found to increase affinity with the protein, with compound **3.40** increasing the stability by 1.04 °C at a concentration of 250 μM (entry 5), being a better result than the parent compound PK083, whose shift is 0.55 °C at the same concentration. However, further modification at position R negatively affected the result (entries 6 and 7), especially with a CF_3 present (**Figure 42**).

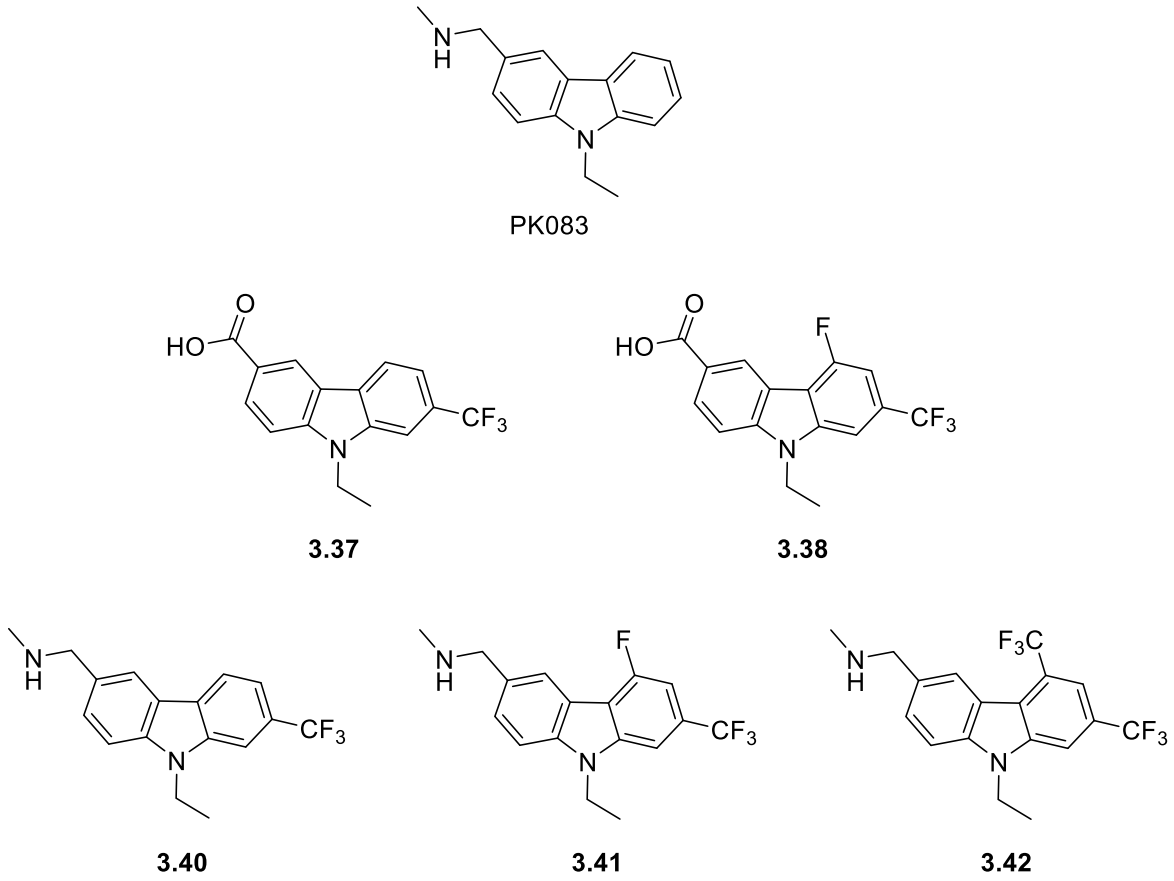

Figure 42. *Structures of PK083 (**3.1**) and fluorinated analogues **3.37**, **3.38**, **3.40**, **3.41** and **3.42**.*

Compound **3.40** was the only compound of the series for which a crystal structure in the protein was determined (**Figure 43**) as it was the only one that showed an increase in melting temperature in the thermoshift assay by DSF at a compound concentration of 250 μM. Observing **Figure 42**, all the values displayed in **Table 17** are easier to explain in modelling terms. The poor results for compounds containing the carboxylic acid show that the carboxylate seems to clash with the Asp228 (D228) of the protein in the subsite II. Also, although the CF_3 moiety proved to increase activity, further modification on that ring that appeared to be incompatible with the binding, clashing with Thr150 (T150) of the central cavity, which could have been expected for entry 7 as compound **3.42** has a CF_3 group in position 4. However, the results indicate that even the fluorine atom of **3.41** abolishes activity at this position (entry 6).

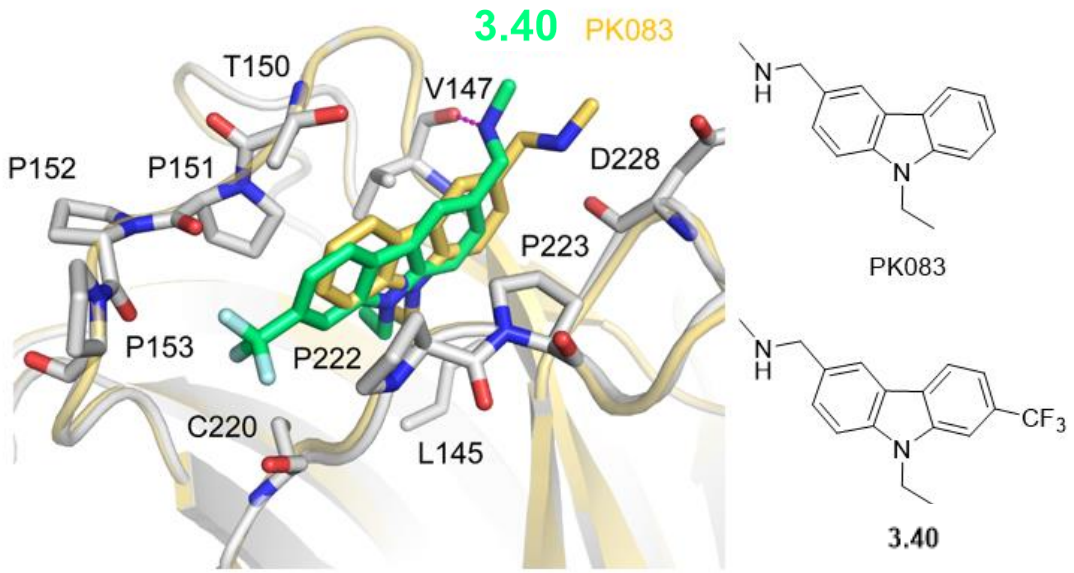

Figure 43. *Superposition of **3.40** (green) and PK083 (yellow) in the Y220C cavity of p53. The crystal structure was determined at 1.48 Å. The hydrogen bond of the **3.40**-Y202C complex with the backbone oxygen of V147 is highlighted (purple) so it can be observed the change in the H-bond from D228 for PK083 (yellow).*

Thus, a figure of the superposition of **3.40** and PK083 in the Y220C cavity of p53 is shown in **Figure 43**. The crystal structure was determined at 1.48 Å in the same space group as Y220C apo and the Y220C-PK083 complex. There are two molecules in the asymmetric unit in that crystal form. The shown model is chain B, as the electron density is much better in this chain. Boeckler *et al.* previously observed that the electron density for weakly binding carbazoles is usually better in chain B.[252] As displayed in **Figure 43**, the CF_3 moiety sterically induces a shift of the carbazole inside the subsite III cavity towards subsite II, which consequently induces a flip of the Cys220 (C220) side chain, with the sulphur pointing towards the interior of the protein instead of being solvent-facing as in the apo structure or the PK083 complex. This occurrence had been observed before with other compounds, such as the iodophenol series published by Matthias Baud *et al.*[225] Another characteristic feature is the hydrogen bond formed by the amine group in subsite I. In the PK083-Y220C complex, the NHMe interacts with the NH-C=O of Asp228 (D228), while in the **3.40**-Y202C complex, this amino group forms a hydrogen bond with the backbone oxygen of Val147 (V147). Any attempts of adding an extra methyl group in the amino chain (NMe_2 analogue) results in the loss of the hydrogen bond with this methylamino group nestling into a hydrophobic pocket, which causes a decrease in affinity, but for the **3.40**-Y200C complex, the H bond is retained but to the backbone carbonyl of a different amino acid (Val147).

Isothermal calorimetry (ITC) is a technique that allows the determination of the affinity between two molecules. The technique consists of two chambers, one with a solution containing the protein and the other with only the buffer. The addition of microinjections of the ligand cause a change in the

temperature because of the interactions between the ligand and the protein, and the energy invested to maintain the two chambers at the same temperature results in the first peaks of the graph[253] (**Figure 43**, top). As these are exothermic reactions, the values in the graph are negative, because the system has to cool the temperature of the chambers. Since nearly all proteins are initially ligand-free, temperature changes are higher in the first additions, but as the system starts to saturate, less free p53 Y220C remain, which means less interactions and therefore less thermal difference, until the differences are not noticeable. A linear regression of the data converted from µcal/s to Kcal/mol (**Figure 44**, bottom) provides the value of K_D and the stoichiometry (n). In this case, a value of n = 1 indicates that only one molecule of **3.40** binds each protein. A higher value would indicate that **3.40** could bind with different affinity in other sites of the protein, meaning that the molecule would be unspecific. Thus, it is very likely that the only interaction occurs in the cavity. The calculated K_D is 4.7 ± 7.8 µM for **3.40** (with two repetitions of the experiment), while PK083 (**3.1**) has a reported K_D of = 125 ± 10.[228] As for the biological significance, a lower K_D means that **3.40** binds more efficiently. In case of using this drug in a treatment, the same results could be obtained with a lower dose of this compound, minimizing side effects or the development of tolerance due to prolonged consumption of the drug.

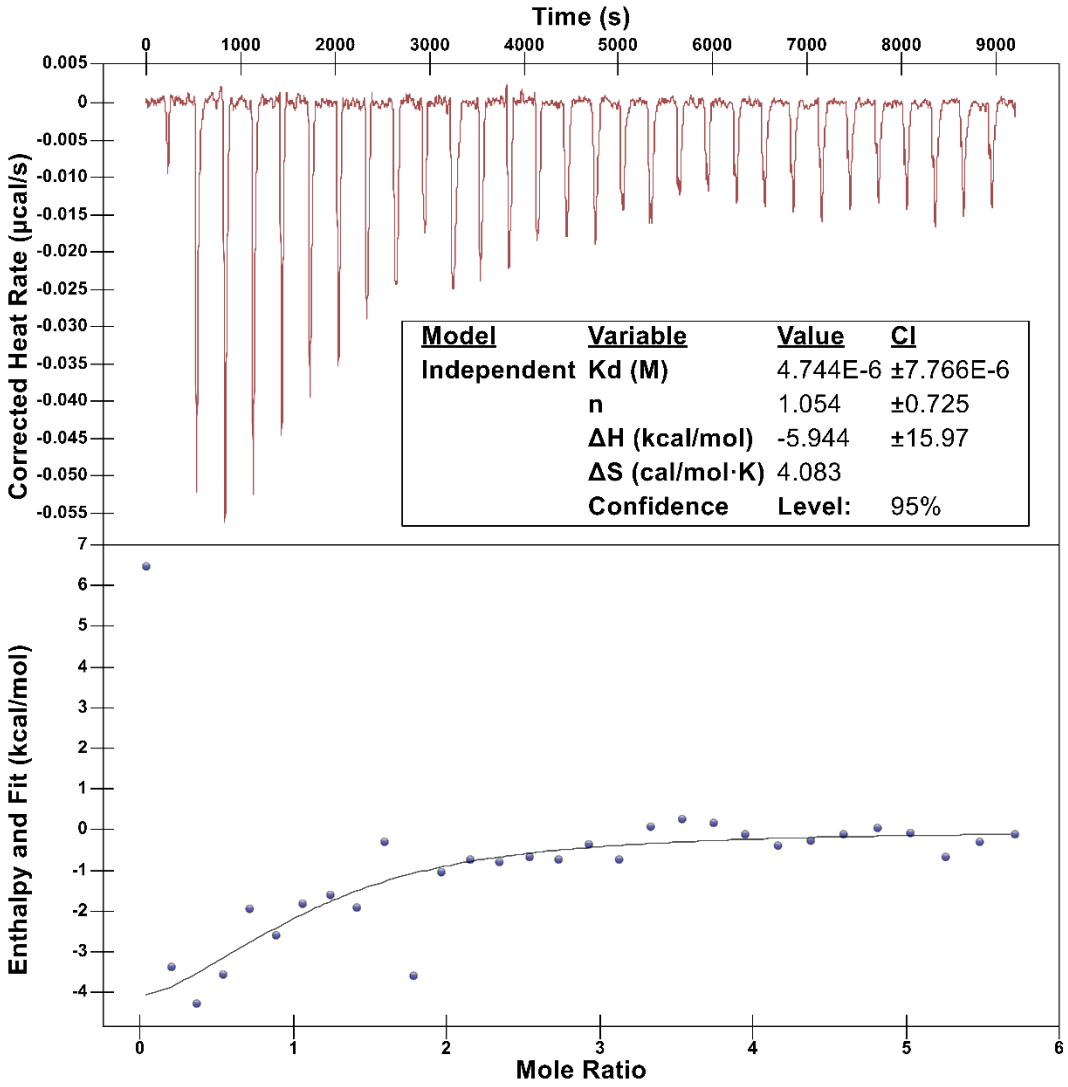

Figure 44. *ITC curve of* ***3.40****.*

3.3 Schrödinger calculations

Schrödinger is a physics-based computational platform that integrates differentiated solutions for predictive modelling, data analytics, and collaboration to enable rapid exploration of chemical space. It can be used for lead discovery and lead optimization in the context of drug discovery, atomic-scale simulation of chemical systems, modelling biologics, antibodies, and proteins, and production of stunning high-performance molecular graphics for communicating structural results. The majority of these applications can be accessed via a single graphical interface called Maestro.[254] Some compounds were submitted for docking studies at early stages of the project, and although the active compound **3.40** was not included, as it had not been planned at that point, more examples apart from the fluorinated ones were also docked for comparison.

Glide Score is an empirical scoring function that approximates the ligand binding free energy. Its terms include force field contributions such as electrostatic or van der Waals interactions, rewarding or penalizing interactions known to influence ligand binding. It has been optimized for docking accuracy, database enrichment, and binding affinity prediction. As it simulates a binding free energy, more negative values represent tighter binders. Emodel has a more significant weighting of the force field components, which makes it well-suited for comparing conformers, but less so for comparing chemically distinct species. Therefore, Glide uses Emodel to pick the best pose of a ligand, and then ranks these best poses against the best poses of other compounds with Glide Score.[255] The Glide Score and Glide Emodel values calculated by Schrodinger are shown in **Table 18**.

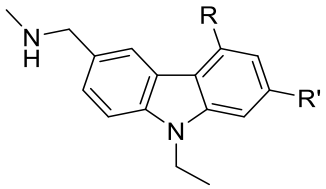

Table 18. *Schrodinger calculations.*

Entry	Compound	R	R'	Glide score	Glide emodel
1	**3.1**	H	H	-8.995	-65.110
2	**3.45**	F	CH_3	-8.477	-59.825
3	**3.46**	F	F	-8.498	-60.658
4	**3.47**	H	OCH_3	-7.690	-56.167
5	**3.48**	H	OH	-9.575	-69.750
6	**3.41**	F	CF_3	-7.023	-47.786
7	**3.49**	OCH_3	F	-8.537	-62.300
8	**3.50**	OH	F	-9.274	-67.353
9	**3.42**	CF_3	CF_3	-5.475	-39.777
10	**3.51**	OCH_3	OCH_3	-7.592	-55.144
11	**3.52**	OH	OH	-9.963	-74.119
12	**3.53**	OCH_3	CF_3	-5.667	-42.791
13	**3.54**	OH	CF_3	-7.740	-53.962

Entry 1 shows the docking score for PK083 (**3.1**), and it can be used as comparison for evaluating the predicted activity of the rest of the binders. As stated before, more negative values represent tighter binders. The first conclusion that could be extracted from the table is that fluorine does not have a great impact on activity on its own (entry 3) and the value of the fluorine containing binders will be mainly conditioned by the other groups present (entries 6, 7 and 8). Compound **3.25** containing a fluorine and a methyl group did not have a significant difference to PK083 (**3.1**) either, suggesting that the methyl group does also not have a great impact on the affinity of the molecule with the protein. The hydroxy group, however, appeared to be the most suitable for binding with the protein exhibiting the best values (entries 5, 8 and 11), while the methoxy or trifluoromethyl were less suitable with lower activities than the lead compound (entries 4, 6, 10 and 13). The presence of two CF_3 groups or the combination of methoxy and trifluoromethyl increased the free energy considerably as observed in entries 9 and 12, making them the worst candidates.

These occurrences can be explained with a visual representation of the CF_3 containing binders in the protein. **Figure 45** shows **3.41** in the Y220C binding pocket as an example, docked using Schrodinger Maestro. The first feature that stands out is that Schrödinger suggests a change in the ligand position induced by the CF_3 group in position R', flipping and rotating the ligand through 45° inside the protein, displacing the binder outside of the pocket. This rotation would also suggest that the CF_3 point towards the mutated Cys220. This phenomenon is not observed for other functionality like fluoro, methyl, methoxy or hydroxy groups. Therefore, the interactions between each ligand and the binding pocket are different. In the PK083 (**3.1**)-Y220C complex, the NHMe interacts with the NH-C=O of Asp228, while in the **3.41**-Y202C complex, this amino group does not form a hydrogen bond.

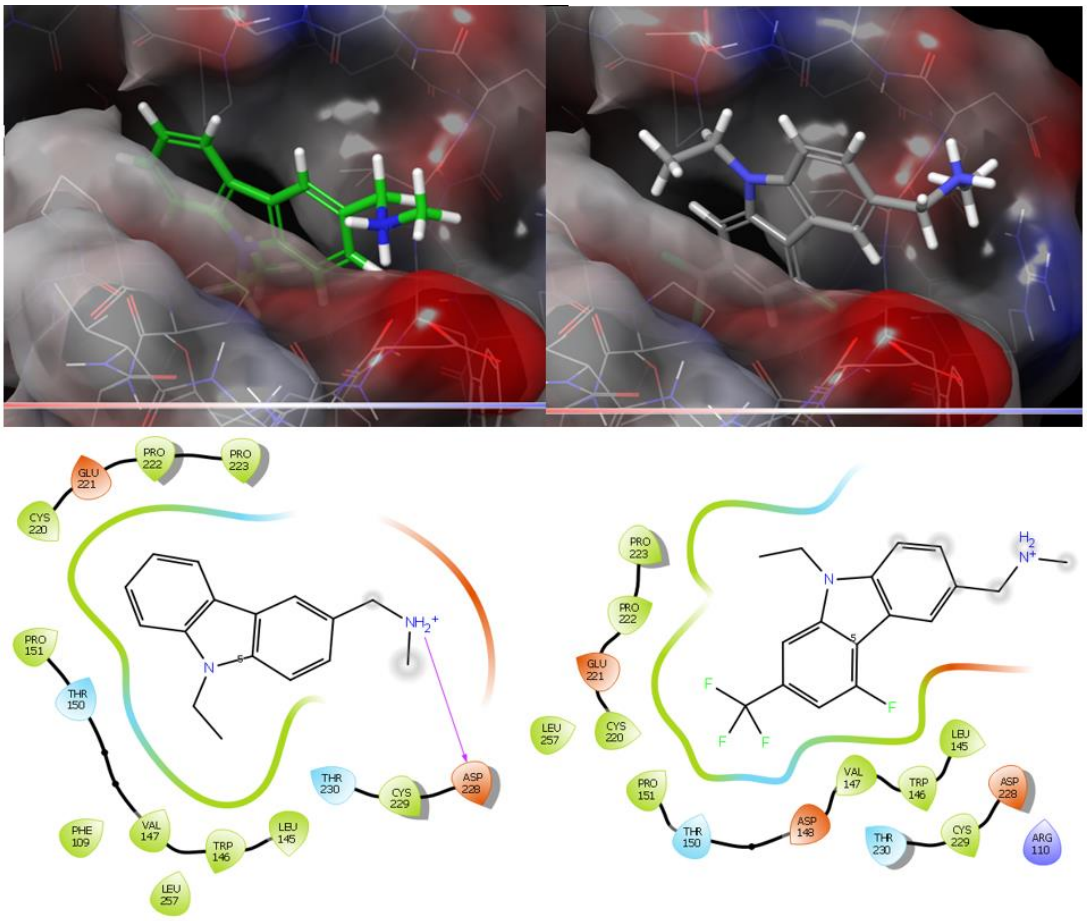

Figure 45. *Comparison between the calculated position of PK083 (**3.1**) (left) and **3.41** (right) in the Y220C cavity by Schrödinger.*

This steric effect is even more pronounced in compound **3.42**, in which the CF_3 group is present in both positions R and R'. In this case, the molecule is completely upside down, with the CF_3 in position R' pointing towards Asp228, and the amino group of the side chain forms an unexpected hydrogen bond with the glutamic acid Glu221 (**Figure 46**).

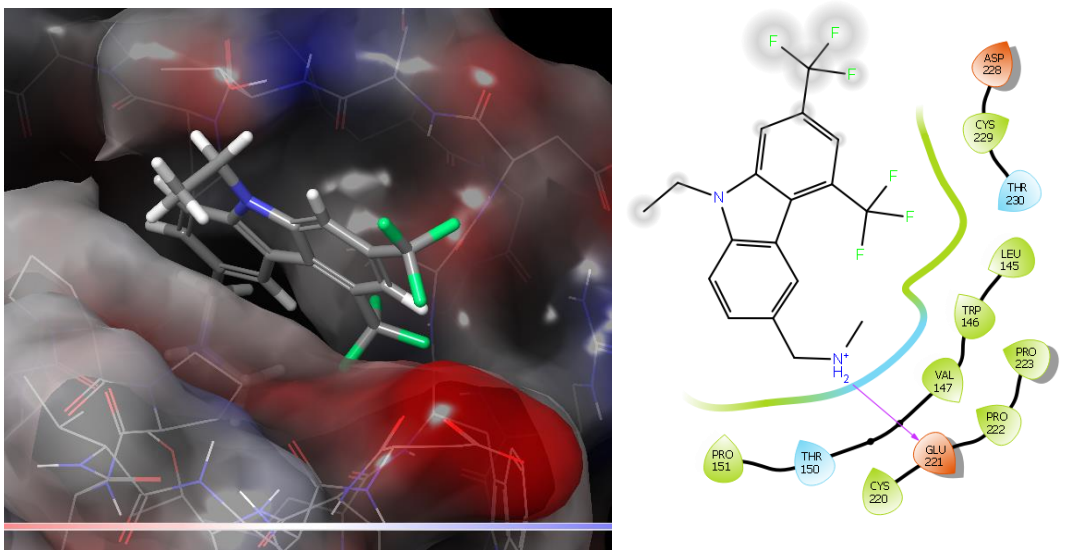

Figure 46. *Calculated position* ***3.24*** *in the Y220C cavity by Schrödinger.*

In conclusion, twelve new PK083 analogues, precursors that had been synthesised in Chapter II, were submitted for predictive modelling using Schrödinger graphical interface Maestro. Although the active compound **3.40** was not evaluated, its analogue **3.41** served to compare the experimental results with the ones predicted by the software. The computational platform, then, helped to predict a change in the binder position inside the cavity and a decrease in the affinity for compounds **3.41** and **3.42**, a phenomenon that was observed experimentally (**Table 18**, section 3.2).

3.4 Conclusions

Five analogues of PK083 (**3.1**) have been synthesised to test the effect of the CF_3 moiety on the potency of these molecules. The CF_3-containing *N*-ethylated carbazoles previously synthesised in Chapter 2 have been further functionalized, providing two alternative routes to ones previously reported, as those proved to be unsuitable for electron-poor carbazoles. Compounds **3.37** and **3.38**, containing a carboxylic acid, were obtained by hydrolysis of the carbazolyl-6-carboxylate derivatives synthesised using the methodology described in Chapter 2 with good overall yields (37 and 30%, respectively). On the other hand, compounds **3.40**, **3.41** and **3.42** were synthesised by a titanium(IV) chloride mediated formylation, that provided exceptional results, and subsequent reductive amination using a solution of $NaBH_4$ in MeOH, added in portions to the imine intermediate.

The potency of these five compounds as reactivators of the p53 Y220C mutated gene was tested by DSF try to compare changes in the thermal denaturation temperature. Compound **3.40** was the only compound of the series that showed an increase in melting temperature (+ 1.04 °C), and its crystal

structure in the protein was determined. The dissociation constant (K_D) for this compound was obtained by ITC and found to be K_D = 4.7 ± 7.8 μM. Hence, compound **3.40** proved to be a promising candidate for further development as an cancer treatment.

Additionally, twelve new PK083 analogues were submitted for predictive modelling using Schrödinger graphical interface Maestro. Although the active compound **3.40** was not evaluated, its analogue **3.41** served to compare the experimental results with ones predicted by the software, which helped to predict a change in the binder position inside the cavity and a decrease in the affinity for compounds **3.41** and **3.42**.

3.5 Experimental

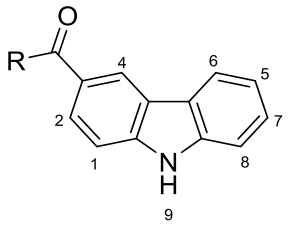

4-Fluoro-2-trifluoromethyl-9-ethyl-9*H*-3-carbazolealdehyde (3.15). A solution of 2-trifluoromtehyl-4-fluoro-9-ethyl-9*H*-carbazole (190 mg, 0.7 mmol, 1.0 equiv) and dichloromethyl methyl ether (0.06 mL, 0.7 mmol, 1.0 equiv.) was cooled to 0 °C in an ice bath. Then, a solution of $TiCl_4$ 1M in CH_2Cl_2 (0.82 mL, 0.8 mmol, 1.2 equiv) was added and the reaction mixture was allowed to warm up to room temperature and stirred overnight. The reaction mixture was poured into ice, stirred vigorously during 5 minutes and extractd with CH_2Cl_2. The crude solid was loaded to a column and purified by flash column chromatography on SiO_2 (12 g), eluting with hexane-CH_2Cl_2 (0 to 100% CH_2Cl_2), using a Teledyne ISCO Combiflash Rf instrument to give the title compound (0.22 g, 99% yield) as a beige solid.

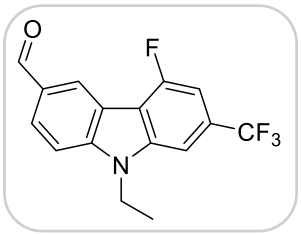

Mp: 172-174 °C **Purity (LCMS):** 90%. **Found [ESI]:** MH^+, 310.0854. $C_{16}H_{12}F_4NO$ [MH] requires 310.0855 .**IR** (neat) *v*/cm^{-1} 2970 (C-H), 1739 (C=O), 1685 (C-C), 1111 (C-F), 896, 740 (C-H). **^{1}H NMR** (600 MHz, $CDCl_3$) δ 10.13 (1H, s, CHO), 8.75 (1H, d, *J* 1.5, H-4), 8.14 (1H, dd, *J* 8.5, *J* 1.5, H-2), 7.56 (1H, d, *J* 8.5, H-1), 7.53 (1H, s, H-8), 7.26 (1H, d, $^2J_{HF}$ 8.5, H-6), 4.47 (2H, q, *J* 7.5, CH_2CH_3), 1.51 (3H, t, *J* 7.5, CH_2CH_3).**^{13}C NMR** (151 MHz, $CDCl_3$) δ 191.4 (CHO), 158.0 (d, $^1J_{CF}$ 252, CF), 143.8 (CH), 142.0 (d, $^3J_{CF}$ 11, C), 129.8 (C), 129.5 (qd, $^2J_{CF}$ 33, $^3J_{CF}$ 8, C-2), 127.7 (CH), 127.7 (C), 123.9 (qd, $^1J_{CF}$ 270, $^4J_{CF}$ 2, CF_3), 119.7 (C), 113.8 (d, $^2J_{CF}$ 20, C), 109.3 (CH), 103.6 (dq, $^2J_{CF}$ 23, $^3J_{CF}$ 4, CH), 102.6 (app p, $^3J_{CF}$ 4, $^4J_{CF}$ 4, CH), 38.6 (CH), 13.9 (CH).

2-Trifluoromtehyl-9-ethyl-9*H*-3-carbazolealdehyde (3.16). A solution of 2-trifluoromtehyl-9-ethyl-9*H*-carbazole (240 mg, 1 mmol, 1 equiv) and dichloromethyl methyl ether (0.12 mL, 1.0 mmol, 1.0 equiv.) was cooled to 0 °C in an ice bath. Then, a solution of $TiCl_4$ 1M in CH_2Cl_2 (1.2 mL, 1.2 mmol, 1.2 equiv) was added and the reaction mixture was allowed to warm up to room temperature and stirred overnight. The reaction mixture was poured into ice, stirred vigorously for 5 minutes and extractd with CH_2Cl_2. The crude solid was loaded to a column and purified by flash column chromatography on SiO_2 (12 g), eluting with hexane-CH_2Cl_2 (0 to 100% CH_2Cl_2), using a Teledyne ISCO Combiflash Rf instrument to give the title compound (0.24 g, 92% yield) as a beige solid.

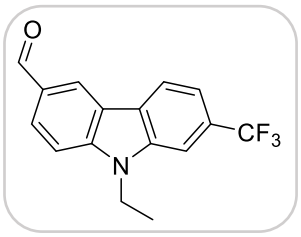

Mp: 130-133 °C. **Purity (LCMS):** 95%. **Found [ESI]:** MH^+, 292.0968. $C_{14}H_{12}NF$ [MH] requires 292.0949. **IR** (neat) *v*/cm^{-1} 3063 (C-H), 1683 (C=O), 1595 (C-C), 1170 (C-F), 798, 719 (C-H). **^{1}H NMR** (600 MHz, $CDCl_3$) δ 10.12 (1H, s, CHO), 8.66 (1H, s, H-4), 8.25 (1H, d, *J* 8.0, H-5), 8.09 (1H, d, *J* 8.5, H-2), 7.72 (1H, s, H-8), 7.58 (1H, d, *J* 8.0, H-6), 7.55 (1H, d, *J* 8.5, H-1), 4.46 (2H, q, *J* 7.5, CH_2CH_3), 1.51 (3H, t, *J* 7.5, CH_2CH_3). **^{13}C NMR** (151 MHz, $CDCl_3$) δ 191.5 (CHO), 144.4 (C), 139.9 (C), 129.1 (C), 128.6 (q, $^2J_{CF}$ 33, C), 128.2 (CH), 125.6 (C), 124.7 (CH), 124.6 (q, $^1J_{CF}$ 273, CF_3), 122.3, 121.2 (CH), 117.0 (q, $^3J_{CF}$ 4, CH), 109.2 (CH), 106.4 (q, $^3J_{CF}$ 4, CH), 38.2 (CH), 13.9 (CH).

2,4-Bis(trifluoromtehyl)-9-ethyl-9*H*-3-carbazolealdehyde (3.17). A solution of 2,4-bis(trifluoromethyl)-9-ethyl-9*H*-carbazole (334 mg, 1.0 mmol, 1.0 equiv) and dichloromethyl methyl ether (0.1 mL, 1.0 mmol, 1.0 equiv.) was cooled to 0 °C in an ice bath. Then, a solution of $TiCl_4$ 1M in CH_2Cl_2 (1.2 mL, 1.2 mmol, 1.2 equiv) was added and the reaction mixture was allowed to warm up to room temperature and stirred overnight. The reaction mixture was poured into ice, stirred vigorously during 5 minutes and extractd with CH_2Cl_2. The crude solid was loaded to a column and purified by flash column chromatography on SiO_2 (12 g), eluting with hexane-CH_2Cl_2 (0 to 100% CH_2Cl_2), using a Teledyne ISCO Combiflash Rf instrument to give the *title compound* (0.20 g, 54% yield) as a beige solid.

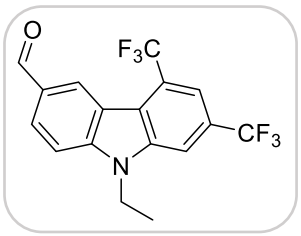

Mp: 189-191. **Purity (LCMS):** 91%. **Found [ESI]:** MH^+, 360.0808. $C_{17}H_{12}NF_6O$ [MH] requires 360.0823. **IR** (neat) *v*/cm^{-1} 3075 (C-H), 1684 (C=O), 1582 (C-C), 1099 (C-F), 759 (C-H). **^{1}H NMR** (600 MHz, $CDCl_3$) δ 10.14 (1H, s, CHO), 8.83 (1H, s, H-4), 8.21 (1H, d, *J* 8.5, H-2), 7.94 (1H, s, H-8), 7.88 (1H, s, H-6), 7.63 (1H, d, *J* 8.5, H-1), 4.54 (1 H, q, *J* 7.5, CH_2CH_3), 1.53 (1 H, t, *J* 7.5, CH_2CH_3). **^{13}C NMR** (151 MHz, $CDCl_3$) δ 191.5, 144.6, 140.7, 130.0, 129.4 (q, $^4J_{CF}$ 5), 128.0 (q, $^2J_{CF}$ 34), 127.8, 124.3 (q, $^2J_{CF}$ 34), 123.9 (q, $^1J_{CF}$ 272) 121.8, 119.4, 114.7 – 114.5 (m, CH), 110.1 (q, $^4J_{CF}$ 4), 109.8, 38.5, 13.9. One CF_3 not observed or overlapped with the other one (big peak).

9-Ethyl-7-fluoro-5-methoxycarbazole-3-carbaldehyde (3.20). $POCl_3$ (0.28 mL, 3.0 mmol, 3.0 equiv.) was added to DMF 5 mL at 0 °C. Then a solution of 2-fluoro-4-methoxy-9-ethyl-9*H*-carbazole (243 mg, 1.0 mmol, 1.0 equiv) in DMF (5 mL) also at 0 °C was added and the resulting solution was stirred at 80 0 °C overnight. Then, the reaction mixture was poured into ice, neutralized with NaOH 0.1 M and extracted with EtOAc (3 x 50 mL). The organic extracts were dried over anhydrous $MgSO_4$, filtered and concentrated under a reduced pressure to afford crude product that was purified by flash column chromatography on SiO_2 (24 g), eluting with hexane-CH_2Cl_2 (0 to 80%), using a Teledyne ISCO Combiflash Rf instrument to give the *title compound* (0.45 g, 17% yield) as a beige solid.

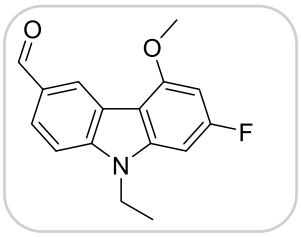

Mp: 130-133 °C. **Purity (LCMS):** 90%. **Found [ESI]:** MH^+, 272.1091. $C_{16}H_{15}NO_2F$ [MH] requires 272.1087. **IR** (neat) *v*/cm^{-1} 2981 (C-H), 1682 (C=O), 1589 (C-C), 1051 (C-F), 790 (C-H). **^{1}H NMR** (600 MHz, $CDCl_3$) δ 10.09 (1H, s, CHO), 8.72 (1H, s, H-4), 7.95 (1H, dd, *J* 8.5, 1.5, H-2), 7.41 (1H, d, *J* 8.5, H-1), 6.74 (1H, dd, *J* 9.0, 2.0, H-8), 6.52 (1H, dd, J_{HF} 11.5, J_{HH} 2.0, H-6), 4.30 (2H, q, *J* 7.5, CH_2CH_3), 4.08 (3H, s, OMe), 1.43 (3H, t, *J* 7.5, CH_2CH_3). **^{13}C NMR** (151 MHz, $CDCl_3$) δ 192.1 (C=O), 163.4 (d, $^1J_{CF}$ 242.3, CF), 156.9 (d, $^3J_{CF}$ 12.7, C), 143.2 (C), 141.9 (d, $^3J_{CF}$ 14.9, C), 129.2 (CH), 126.4 (C), 125.8 (CH), 122.3 (C), 108.4 (C), 108.2 (CH), 91.2 (d, $^2J_{CF}$ 28.7, CH), 88.9 (d, $^2J_{CF}$ 27.3, CH), 55.9 (OMe), 38.27 (CH_2), 13.77 (CH_3).

9-Ethyl-2-fluoro-4-methoxycarbazole-3-carbaldehyde (3.21). $POCl_3$ (0.28 mL, 3.0 mmol, 3.0 equiv.) was added to DMF 5 mL at 0 °C. Then a solution of 2-fluoro-4-methoxy-9-ethyl-9*H*-carbazole (243 mg, 1.0 mmol, 1.0 equiv) in DMF (5 mL) also at 0 °C was added and the resulting solution was stirred at 80 0 °C overnight. Then, the reaction mixture was poured into ice, neutralized with NaOH 0.1 M and extracted with EtOAc (3 x 50 mL). The organic extracts were dried over anhydrous $MgSO_4$, filtered and concentrated under a reduced pressure to afford crude product that was purified by flash column chromatography on SiO_2 (24 g), eluting with hexane-CH_2Cl_2 (0 to 80%), using a Teledyne ISCO Combiflash Rf instrument to give the *title compound* (0.56 g, 21% yield) as a beige solid.

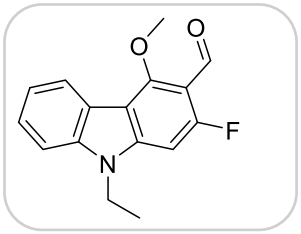

Mp: 118-120 °C. **Purity (LCMS):** 92%. **Found [ESI]:** MH^+, 272.1078. $C_{16}H_{15}NO_2F$ [MH] requires 272.1087. **IR** (neat) *v*/cm^{-1} 2984 (C-H), 1681 (C=O), 1597 (C-C), 1121 (C-F), 748. **^{1}H NMR** (600 MHz, $CDCl_3$) δ 10.30 (1 H, s, CHO), 8.14 (1H, d, *J* 7.5, H-5), 7.68 (1H, d, *J* 8.0, H-8), 7.51 (1H, dd, *J* 8.0, 7.5, H-7), 7.45 (1H, d, J_{HF} 12.0, H-1), 7.32 (1H, dd, *J* 7.5, 7.5, H-6), 4.43 (2H, q, *J* 7.0, CH_2CH_3), 4.07 (3H, s, OMe), 1.28 (3H, t, *J* 7.0, CH_2CH_3). **^{13}C NMR** (151 MHz, d_6-DMSO) δ 186.1 (CHO), 162.1 (d, $^1J_{CF}$ 255, CF), 159.3 (d, $^3J_{CF}$ 6.8, C), 144.7 (d, $^2J_{CF}$ 16.3, C), 140.5 (C), 126.7 (CH), 122.7 (CH), 121.5 (CH), 120.9 (C), 112.2 (C), 110.7 (d, $^3J_{CF}$ 9.8, C), 110.4 (CH), 93.9 (d, $^2J_{CF}$ 26.6, CH), 63.4 (OMe), 38.1 (CH_2), 14.1 (CH_3).

9-Ethyl-2-fluoro-4-methoxycarbazole-1-carbaldehyde (3.22). $POCl_3$ (0.28 mL, 3.0 mmol, 3.0 equiv.) was added to DMF 5 mL at 0 °C. Then a solution of 2-fluoro-4-methoxy-9-ethyl-9*H*-carbazole (243 mg, 1.0 mmol, 1.0 equiv) in DMF (5 mL) also at 0 °C was added and the resulting solution was stirred at 80 0 °C overnight. Then, the reaction mixture was poured into ice, neutralized with NaOH 0.1 M and extracted with EtOAc (3 x 50 mL). The organic extracts were dried over anhydrous $MgSO_4$, filtered and concentrated under a reduced pressure to afford crude product that was purified by flash column chromatography on SiO_2 (24 g), eluting with hexane-CH_2Cl_2 (0 to 80%), using a Teledyne ISCO Combiflash Rf instrument to give the *title compound* (0.10 g, 37% yield) as a beige solid.

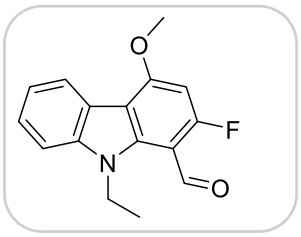

Mp: 110-112 °C. **Purity (LCMS):** 96%. **Found [ESI]:** MH^+, 272.1086. $C_{16}H_{15}NO_2F$ [MH] requires 272.2087. **IR** (neat) *v*/cm^{-1} 3076 (C-H), 1673 (C=O), 1551 (C-C), 1205 (C-F), 747 (C-H). **^{1}H NMR** (600 MHz, d_6-DMSO) δ 10.35 (1H, s, CHO), 8.15 (1H, d, *J* 7.5, H-5), 7.66 (1H, d, *J* 8.5, H-8), 7.45 (1H, ddd, *J* 8.5, 7.0, 1.5, H-7), 7.27 (1H, ddd, *J* 7.5, 7.0, 1.0, H-6), 6.90 (1H, d, J_{HF} 14.5, H-3), 4.70 (2H, q, *J* 7.0, CH_2CH_3), 4.11 (3H, s, OMe), 1.19 (3H, t, *J* 7.0, CH_2CH_3). **^{13}C NMR** (151 MHz, d_6-DMSO) δ 186.0 – 185.8 (m, CHO), 167.6 (d, $^1J_{CF}$ 253), 161.5 (d, $^2J_{CF}$ 15, C), 140.8 (C), 138.5 ($^3J_{CF}$, *J* 7, C), 125.8 (CH), 122.5 (CH), 121.4 (CH), 110.6 (CH), 109.7 (C), 105.3 (d, $^3J_{CF}$ 7, C), 91.6 (d, $^2J_{CF}$ 29, CH), 57.3 (OMe), 41.6 (CH_2), 14.7 (CH_3).

5-bromo-[1,1'-biphenyl]-2-amine. 2-Biphenylamine (338 mg, 2.0 mmol, 1.0 equiv. was dissolved in DMF (2 mL) and the solution was cooled to 0 °C. Then, a solution of NBS (356 mg, 2.0 mmol, 1.0 equiv.) in DMF (2 mL) was added dropwise using an addition funnel and the reaction mixture was allowed to warm up to room temperature and stirred overnight. Then, water (5 mL) was added, and the resulting mixture was extracted with EtOAc (3 x 10 mL). The crude product that was purified by flash column chromatography on SiO_2 (24 g), eluting with hexane-EtOAC (0 to 20%), using a Teledyne ISCO Combiflash Rf instrument to give the *title compound* (0.38 g, 78% yield) as a brown oil.

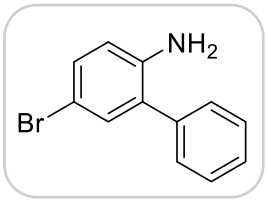

^{1}H NMR (600 MHz, $CDCl_3$) δ 7.47-7.39 (4H, m), 7.39 – 7.33 (1H, m), 7.27 – 7.20 (2H, m), 6.64 (1H, d, *J* 8.0), 3.75 (1H, s, NH_2).

***N*'-([1,1'-biphenyl]-2-yl)-*N*,*N*-dimethylformimidamide (3.27).** To a solution of $POCl_3$ (0.56 mL, 6 mmol, 3 equiv.) in DMF (5 mL) cooled to 0 °C was added a solution of biphenylamine (338 mg, 2.0 mmol, 1.0 equiv.) in DMF (5 mL). The reaction mixture was stirred at reflux for 4 h and monitored by TLC until completion. Then, the reaction mixture was poured into ice and neutralized with NaOH (1

M). The resulting mixture was extracted with EtOAc (3 x 10 mL) and after concentration under pressure the crude product that was purified by flash column chromatography on SiO_2 (24 g), eluting with hexane-EtOAC (0 to 20%), using a Teledyne ISCO Combiflash Rf instrument to give the *title compound* (0.37 g, 82% yield) as a beige solid.

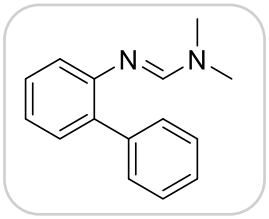

Purity (LCMS): 90%. **^{1}H NMR** (600 MHz, $CDCl_3$) δ 7.56 (2H, d, *J* 7.5, H-2'), 7.37 (1H, s, N=CH), 7.36 – 7.32 (3H), 7.28 – 7.21 (2H), 7.08 (1H, td, *J* 7.5, 1.5, H-5), 6.89 (1H, dd, *J* 8.0, 1.5, H-3), 2.90 (6H, s, NMe_2). **LRMS** (CI) *m/z* (relative intensity) 225 (100, MH^+).

2-(2'-Fluoro-4'-trifluoromethylphenyl)-4-methylaniline. Prepared according to General Procedure A using a solution of 2-bromo-4-methylaniline (372 mg, 2.0 mmol, 1.0 equiv.), 2-fluoro-4-trifluoromethylphenylboronic acid (541 mg, 2.6 mmol, 1.3 equiv.), Na_2CO_3 (848 mg, 8.0 mmol, 4.0 equiv.) and $Pd(PPh)_2Cl_2$ (115 mg, 5 mol%) in dioxane-water (1:1) (14 mL) in a pressure-rated sealed tube (35 mL). Purification by flash column chromatography on SiO_2 (12 g), eluting with hexane-EtOAc (9:1) gave the *title compound* (0.48 g, 88%) as a yellow solid.

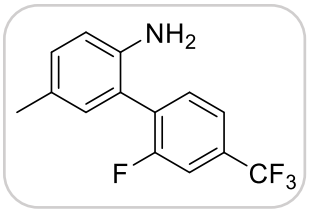

Mp: 83-85 °C. **Purity (LCMS):** 95%. **Found [ESI]:** MH^+, 270.0904. $C_{14}H_{12}F_4N$ [MH] requires 270.0906. **IR** (neat) *v*/cm^{-1} 3457, 3371 (NH_2), 2922 (C-H), 1623 (C-C), 1119 (C-F), 744 (C-H). **^{1}H NMR** (600 MHz, $CDCl_3$) δ 7.55 – 7.48 (2H, m, H-6', H-5'), 7.45 (1H, d, $^3J_{HF}$ 9.5, H-3'), 7.05 (1H, dd, *J* 8.0, 2.0, H-5), 6.93 (1H, s, H-3), 6.74 (1H, d, *J* 8.0, H-6), 3.53 (2H, s, NH_2), 2.29 (3H, s, Me). **^{13}C NMR** (151 MHz, $CDCl_3$) δ 159.5 (d, $^1J_{CF}$ 249, CF), 141.4 (C), 132.77 (d, $^4J_{CF}$ 4, CH), 131.6 (qd, $^2J_{CF}$ 34, $^3J_{CF}$ 8, C), 131.2 (CH), 130.8 (d, $^2J_{CF}$ 17, C), 130.5 (CH), 128.1 (C), 123.30 (qd, $^1J_{CF}$ 272, $^4J_{CF}$ 3, CF_3), 121.4 (p, $^4J_{CF}$ 4, CH), 120.1 (C), 116.30 (CH), 113.5 (dq, $^2J_{CF}$ 26, $^4J_{CF}$ 4, CH), 20.4 (Me).

4-Fluoro-6-methyl-2-trifluoromethyl-9-ethyl-9*H*-carbazole (3.28). Prepared according to General Procedure C using a solution (A) of 2-(2'-fluoro-4'-trifluoromethylphenyl)-4-methylaniline (490 mg, 1.8 mmol, 1.0 equiv.; 0.1 M) and $TMSN_3$ (0.26 mL, 2.0 mmol, 1.1 equiv.; 0.11 M) in dioxane (18 mL), a solution (B) of *t*-BuONO (0.36 mL, 3.0 mmol, 1.5 equiv.; 0.15 M) in dioxane (20 mL), and solid KOH (201 mg, 3.6 mmol, 2 equiv.) and iodoethane (0.28 mL, 3.6 mmol, 2.0 equiv.) in 3 mL of DMSO. Purification by flash column chromatography on SiO_2 (12 g), eluting with hexane-CH_2Cl_2, (0 to 10%) gave the *title compound* (0.18 g, 34%) as a colourless solid.

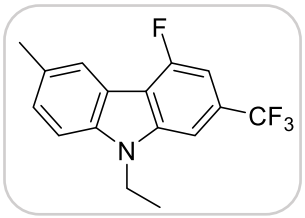

Mp: 98-99 °C. **Purity (LCMS):** 96%. **Found [ESI]:** MH^+, 296.1061. $C_{16}H_{14}F_4N$ [MH] requires 296.1062. **IR** (neat) *v*/cm^{-1} 2982 (C-H), 1585 (C-C), 1074 (C-F), 838, 799 (C-H). **^{1}H NMR** (600 MHz, d_6-DMSO) δ 7.90 (1H, s, H-5), 7.88 (1H, s, H-1), 7.60 (1H, d, *J* 8.5, H-8), 7.40 (1H, dd, *J* 8.5, 1.5, H-7), 7.29 (1H, dd, $^3J_{HF}$ 10.5, J_{HH} 1.0, H-3), 4.50 (2H, q, *J* 7.0, CH_2CH_3), 2.46 (3H, s, Me) 1.26 (3H, t, *J* 7.0, CH_2CH_3). **^{13}C NMR** (151 MHz, d_6-DMSO) δ 157.7 (d, $^1J_{CF}$ 248, CF), 141.6 (d, $^3J_{CF}$ 11), 139.0 (CH), 129.8 (CH), 129.3 (CH), 126.9 (dd, $^2J_{CF}$ 32, $^3J_{CF}$ 8, C), 124.7 (qd, $^1J_{CF}$ 272, $^4J_{CF}$ 3, CF_3), 122.8 (d, $^4J_{CF}$ 3, C), 118.9 (d, $^4J_{CF}$ 2, C), 112.7 (d, $^2J_{CF}$ 20, C), 103.8 (p, $^3J_{CF}$, $^4J_{CF}$ 4, CH), 101.5 (dq, $^2J_{CF}$ 23, $^4J_{CF}$ 4, CH), 38.0 (CH_2), 21.3 (CH_3), 14.2 (CH_3).

Methyl 6-amino-4'-(trifluoromethyl)-[1,1'-biphenyl]-3-carboxylate (3.28). Prepared according to General Procedure A using a solution of methyl 3-iodo-4-aminobenzonate (554 mg, 2.0 mmol, 1.0 equiv.), 4-trifluoromethylphenylboronic acid (494 mg, 2.6 mmol, 1.3 equiv.), Na_2CO_3 (848 mg, 8.0 mmol, 4.0 equiv.) and Pd(dppf)Cl_2 (74 mg, 5 mol%) in dioxane-water (1:1) (14 mL) in a pressure-rated sealed tube (35 mL). Purification by flash column chromatography on SiO_2 (12 g), eluting with hexane-EtOAc (9:1) gave the *title compound* (0.26 g, 44%) as a colourless solid.

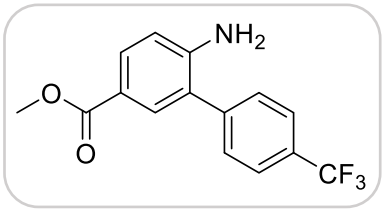

Mp: 130-132 °C. **Purity (LCMS):** 97%. **Found [ESI]:** MH^+, 296.0847. $C_{15}H_{13}NO_2F_3$ [MH] requires 296.0898. **IR** (neat) *v*/cm^{-1} 3464, 3399 (NH_2), 2994 (C-H), 1738 (C=O), 1620 (C-C), 1296 (C-O), 1067 (C-F), 769 (C-H). **^{1}H NMR** (600 MHz, $CDCl_3$) δ 7.87 (1H, dd, *J* 8.5, 2.0, H-5), 7.81 (1H, d, *J* 2.0, H-3), 7.72 (2H, d, AA'XX', *J* 8.0, H-3'), 7.58 (2H, AA'XX', d, *J* 8.0, H-2'), 6.75 (1H, d, *J* 8.5, H-6), 4.14 (2H, s, NH_2), 3.86 (3H, s, OMe). **^{13}C NMR** (151 MHz, $CDCl_3$) δ 167.0 (C=O), 147.7 (C), 142.1 (C), 132.4 (CH), 131.1 (CH), 129.8 (q, $^2J_{CF}$ 32, C), 129.4 (CH), 126.0 (q, $^3J_{CF}$ 4, CH), 124.9 (C), 124.1 (q, $^1J_{CF}$ 272, CF_3), 120.1 (C), 114.8 (CH), 51.8 (OMe).

Ethyl 6-amino-4'-(trifluoromethyl)-[1,1'-biphenyl]-3-carboxylate (3.29). Prepared according to General Procedure A using a solution of methyl 3-bromo-4-aminobenzonate (488 mg, 2.0 mmol, 1.0 equiv.), 4-trifluoromethylphenylboronic acid (494 mg, 2.6 mmol, 1.3 equiv.), Na_2CO_3 (848 mg, 8.0 mmol, 4.0 equiv.) and Pd(dppf)Cl_2 (74 mg, 5 mol%) in dioxane-water (1:1) (14 mL) in a pressure-rated sealed tube (35 mL). Purification by flash column chromatography on SiO_2 (12 g), eluting with hexane-EtOAc (9:1) gave the *title compound* (0.53 g, 85%) as a colourless solid.

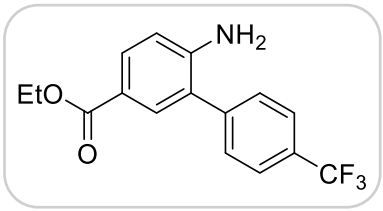

Mp: 118-119 °C. **Purity (LCMS):** 93%. **Found [ESI]:** MH^+, 310.1090. $C_{16}H_{15}NO_2F_3$ [MH] requires 310.1055. **IR** (neat) *v*/cm^{-1} 3441, 3349 (NH_2), 2994 (C-H), 1672 (C=O), 1620 (C-C), 1246 (C-O), 1129 (C-F), 773 (C-H). **^{1}H NMR** (600 MHz, $CDCl_3$) δ 7.87 (1H, dd, *J* 8.5, 2.0, H-5), 7.81 (1H, d, *J* 2.0, H-3), 7.72 (2H, d, AA'XX', *J* 8.0, H-3'), 7.58 (2H, AA'XX', d, *J* 8.0, H-2'), 6.75 (1H, d, *J* 8.5, H-6), 4.14 (2H, s, NH_2), 3.86 (3H, s, OMe). **^{13}C NMR** (151 MHz, $CDCl_3$) δ 167.0 (C=O), 147.7 (C), 142.1 (C), 132.4 (CH), 131.1 (CH), 129.8 (q, $^2J_{CF}$ 32, C), 129.4 (CH), 126.0 (q, $^3J_{CF}$ 4, CH), 124.9 (C), 124.1 (q, $^1J_{CF}$ 272, CF_3), 120.1 (C), 114.8 (CH), 51.8 (OMe).

Ethyl 6-amino-2'-fluoro-4'-(trifluoromethyl)-[1,1'-biphenyl]-3-carboxylate (3.30). Prepared according to General Procedure A using a solution of 3-iodo-4-aminobenzonate (554 mg, 2.0 mmol, 1.0 equiv.), 2-fluoro-4-trifluoromethylphenylboronic acid (541 mg, 2.6 mmol, 1.3 equiv.), Na_2CO_3 (848 mg, 8.0 mmol, 4.0 equiv.) and $Pd(PPh)_2Cl_2$ (71 mg, 5 mol%) in dioxane-water (1:1) (14 mL) in a pressure-rated sealed tube (35 mL). Purification by flash column chromatography on SiO_2 (12 g), eluting with hexane-EtOAc (4:1) gave the *title compound* (0.42 g, 68%) as a colourless solid.

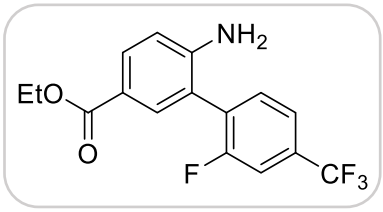

Mp: 125-126 °C. **Purity (LCMS):** 96%. **Found [ESI]:** MH^+, 328.0947. $C_{16}H_{14}NO_2F_4$ [MH] requires. **IR** (neat) *v*/cm^{-1} 3470, 3356 (NH_2), 2989 (C-H), 1708 (C=O), 1627 (C-C), 1228 (C-O), 1102 (C-F), 770 (C-H). **^{1}H NMR** (600 MHz, $CDCl_3$) δ 7.91 (1H, dd, *J* 8.5, 2.0, H-5), 7.81 (1H, d, *J* 2.0, H-3), 7.55 – 7.49 (2H, m, H-5', H-6'), 7.46 (1H, d, J_{HF} 9.5, H-3'), 6.77 (1H, d, *J* 8.5, H-6), 4.32 (2H, q, *J* 7.1, CH_2CH_3), 4.04 (2H, s, NH_2), 1.35 (3H, t, *J* 7.1, CH_2CH_3). **^{13}C NMR** (151 MHz, $CDCl_3$) δ 166.3 (C=O), 159.5 (d, $^1J_{CF}$ 250, CF), 148.1 (C), 132.9 (CH), 132.8 (d, $^3J_{CF}$ 4, CH), 132.2 (qd, $^2J_{CF}$ 34, $^3J_{CF}$ 8, C), 131.7 (CH), 129.5 (d, $^2J_{CF}$ 17, C), 123.2 (dd, $^1J_{CF}$ 272, $^3J_{CF}$ 4, CF_3), 121.7 (p, $^3J_{CF}$ 4, CH), 120.35 (C), 118.8 (C), 114.8 (CH), 113.7 (dq, $^2J_{CF}$ 26, $^3J_{CF}$ 4, CH), 60.5 (CH_2), 14.4 (CH_3).

Methyl 7-trifluoro-9*H*-carbazole-3-carboxylate. A solution (A) of (4'-trifluoromethylphenyl)aniline (881 mg, 3.0 mmol, 1.0 equiv.; 0.1 M) and $TMSN_3$ (0.43 mL, 3.3 mmol, 1.1 equiv.; 0.1 M) in dioxane (30 mL) and a solution (B) of *t*-BuONO (0.62 mL, 5.3 mmol, 1.5 equiv.; 0.2 M) in dioxane (35 mL) were mixed, heated in a PFA coil reactor at 80 °C for 50 min and then irradiated with 300 to 400 nm at 80 °C for 50 min using a UV-150 Photochemical Flow Reactor connected in-series.. Purification by flash column chromatography on SiO_2 (24 g), eluting with hexane-CH_2Cl_2, (4:1) gave the *title compound* (0.45 g, 51%) as a yellow solid.

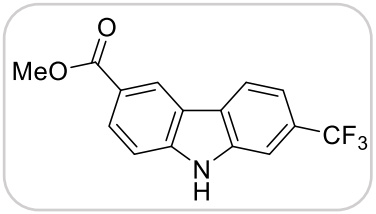

Mp: 222-224 °C. **Purity (LCMS):** 89%. **Found [ESI]:** MH^+, 294.0743. $C_{15}H_{11}F_3NO_2$ [MH] requires 294.0742. **IR** (neat) *v*/cm^{-1} 3291 (N-H), 2960 (C-H), 1687 (C=O), 1611 (C-C), 1258 (C-F), 730 (C-H). **^{1}H NMR** (600 MHz, d_6-DMSO) δ 12.05 (1H, s, N-H), 8.90 (1H, d, *J* 2.0, H-4), 8.49 (1H, d, *J* 8.0, H-5), 8.08 (1H, dd, *J* 8.5, 2.0, H-2), 7.86 (1H, s, H-8), 7.65 (1H, d, *J* 8.5, H-1), 7.51 (1H, d, *J* 8.0, H-6), 3.88 (3H, s, OMe).**^{13}C NMR** (151 MHz, d_6-DMSO) δ 167.2 (C=O), 144.0 (C), 139.9 (C), 128.4 (CH), 126.9 (q, $^2J_{CF}$ 31), 125.8 (C), 125.3 (q, $^1J_{CF}$ 272), 123.8 (CH), 122.2 (CH), 121.7 (C), 121.1 (C), 116.2 (q, $^3J_{CF}$ 4, CH), 111.9 (C), 108.9 (q, $^3J_{CF}$ 4, CH), 52.3 (OMe).

Ethyl 7-trifluoro-9*H*-carbazole-3-carboxylate (3.31). A solution (A) of (4'-trifluoromethylphenyl)aniline (520 mg, 1.7 mmol, 1.0 equiv.; 0.1 M) and $TMSN_3$ (0.24 mL, 1.9 mmol, 1.1 equiv.; 0.1 M) in dioxane (30 mL) and a solution (B) of *t*-BuONO (0.36 mL, 3.0 mmol, 1.5 equiv.; 0.2 M) in dioxane (17 mL) were mixed, heated in a PFA coil reactor at 80 °C for 50 min and then irradiated with 300 to 400 nm at 80 °C for 50 min using a UV-150 Photochemical Flow Reactor connected in-series. Purification by flash column chromatography on SiO_2 (24 g), eluting with hexane-CH_2Cl_2, (4:1) gave the *title compound* (0.27 g, 53%) as a yellow solid.

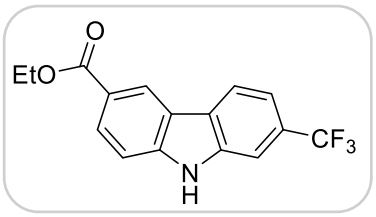

Purity (LCMS): 85%. **Found [ESI]:** MH+, 308.0903. $C_{16}H_{13}NO_2F_3$ [MH] requires. **IR** (neat) *v*/cm^{-f1} 3426 (N-H), 3001 (C-H), 1599 (C=O), 1026 (C-F), 698 (C-H). **^{1}H NMR** (600 MHz, d_6-DMSO) δ 12.03 (1H, s, NH_2), 8.89 (1H, d, *J* 1.5, H-4), 8.50 (1H, d, *J* 8.0, H-5), 8.07 (1H, dd, *J* 8.5, 1.5, H-2), 7.85 (1H, s, H-8), 7.64 (1H, d, *J* 8.5, H-1), 7.51 (1H, dd, *J* 8.0, 1.5, H-6),4.34 (2H, q, *J* 7.0, CH_2CH_3), 1.35 (3H, t, *J* 7.0, CH_2CH_3). **^{13}C NMR** (151 MHz, d_6-DMSO) δ 166.7 (C=O), 144.0 (C), 139.9 (C), 128.4 (CH), 127.8 (q $^2J_{CF}$ 26, C), 125.9 (C), 125.3 (q, $^1J_{CF}$ 271, CF_3), 123.8 (CH), 122.2 (CH), 121.7 (C), 121.5 (C), 116.2 (q, $^3J_{CF}$ 4, CH), 111.9 (CH), 109.0 (q, $^3J_{CF}$ 5, CH), 60.9 (CH_2), 14.8 (CH_3).

Ethyl 5-fluoro-7-trifluoro-9*H*-carbazole-3-carboxylate (3.32). A solution (A) of (2'- fluoro-4'-trifluoromethylphenyl)aniline (715 mg, 2.3 mmol, 1.0 equiv.; 0.1 M) and $TMSN_3$ (0.33 mL, 2.5 mmol, 1.1 equiv.; 0.1 M) in dioxane (23 mL) and a solution (B) of *t*-BuONO (0.45 mL, 3.8 mmol, 1.5 equiv.; 0.2 M) in dioxane (17 mL) were mixed, heated in a PFA coil reactor at 80 °C for 50 min and then irradiated with 300 to 400 nm at 80 °C for 50 min using a UV-150 Photochemical Flow Reactor connected in-series. Purification by flash column chromatography on SiO_2 (24 g), eluting with hexane-CH_2Cl_2, (4:1) gave the *title compound* (0.46 g, 65%) as a yellow solid.

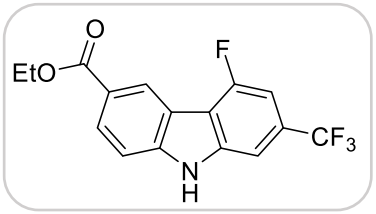

Mp: 259-262 °C. **Purity (LCMS):** 94%. **Found [ESI]:** MH+, 326.0799. $C_{16}H_{12}NO_2F_4$ [MH] requires 326.0804. **IR** (neat) *v*/cm^{-1} 3269 (N-H), 2993 (C-H), 1684 (C=O), 1610 (C-C), 1255 (C-F), 726 (C-H). **^{1}H NMR** (600 MHz, d_6-DMSO) δ 12.36 (1H, s, NH), 8.69 (1H, d, *J* 1.5, H-4), 8.12 (1H, dd, *J* 8.5, 1.5, H-2), 7.76 (1H, s, H-8), 7.71 (1H, d, *J* 8.5, H-1), 7.43 (1H, d, J_{HF} 10.2, H-6), 4.34 (2H, q, *J* 7.0, CH_2CH_3), 1.34 (3H, t, *J* 7.0, CH_2CH_3). **^{13}C NMR** (151 MHz, d_6-DMSO) δ 166.4 (C=O), 157.7 (d, $^1J_{CF}$ 249, CF), 143.5 (C), 142.3 (d, $^3J_{CF}$ 11, C), 128.6 (CH), 127.8 (qd, $^2J_{CF}$ 41, $^3J_{CF}$ 9, C), 124.7 (d, $^4J_{CF}$ 3, CH), 124.5 (qd, $^1J_{CF}$ 272, $^4J_{CF}$ 4, CF_3), 122.2 (C), 118.8 (C), 113.52 (d, $^2J_{CF}$ 20.1, C) 112.3 (CH), 105.9 (p, $^4J_{CF}$ 3.4, CH), 102.7 (dq, $^2J_{CF}$ 23, $^3J_{CF}$ 4, CH), 61.1 (CH_2), 14.7 (CH_3).

Methyl 7-trifluoro-9-ethyl-9*H*-carbazole-3-carboxylate. A solution of methyl 7-trifluoro-9*H*-carbazole-3-carboxylate (120 mg, 0.4 mmol, 1 equiv.) and KOH (46 mg, 0.8 mmol, 2 equiv.) in DMSO (3 mL) was sonicated at 40 °C for 20 min. Then, iodoethane (0.1 mL, 0.8 mmol, 2 equiv.) was added and the reaction mixture was further sonicated for 2 h min at the same temperature. The reaction mixture loaded to a column and purified by flash column chromatography on SiO_2 (12 g), eluting with hexane-CH_2Cl_2 (4:1), using a Teledyne ISCO Combiflash Rf instrument to yield the *tittle compound* (0.11 g, 85% yield) as a yellow compound.

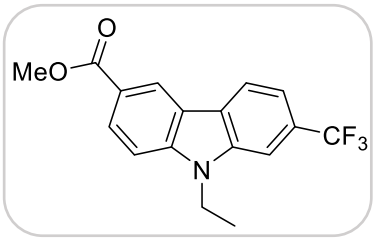

Mp: 140-141 °C. **Purity (LCMS):** 89 %. **Found [ESI]:** MH+, 322.1054. $C_{17}H_{15}F_3NO_2$ [MH] requires 322.1055. **IR** (neat) *v*/cm^{-1} 2983 (C-H), 1707 (C=O), 1603 (C-C), 1311 (C-F), 764 (C-H) . **^{1}H NMR** (600 MHz, d_6-DMSO) δ 8.90 (1H, s, H-4), 8.50 (1H, d, J 8.0, H-5), 8.12 (1H, d, J 8.5, H-2), 8.08 (1H, s, H-8), 7.76 (1H, d, J 8.5, H-1), 7.54 (1H, d, J 8.0, H-6), 4.56 (2H, q, *J* 7.0, CH_2CH_3), 3.88 (3H, s, OMe), 1.30 (3H, t, *J* 7.0, CH_2CH_3). **^{13}C NMR** (151 MHz, d_6-DMSO) δ 167.1 (C=O), 143.7 (C), 139.9 (C), 128.5 (CH), 127.2 (q, $^2J_{CF}$ 32, C),125.6 (C), 125.4 (q, $^1J_{CF}$ 272, CF_3), 123.9 (CH), 122.3 (CH), 121.5 (C), 121.3 (C), 116.5 (q, $^3J_{CF}$ 4, CH), 110.1 (CH), 107.5 (q, $^3J_{CF}$ 4, CH), 52.4 (CH_2), 37.9 (OCH_3), 14.2 (CH_3).

Ethyl 7-trifluoro-9-ethyl-9*H*-carbazole-3-carboxylate (3.35). A solution of ethyl 7-trifluoro-9*H*-carbazole-3-carboxylate (440 mg, 1.4 mmol, 1.0 equiv.) and KOH (157 mg, 2.8 mmol, 2.0 equiv.) in DMSO (5 mL) was sonicated at 40 °C for 20 min. Then, iodoethane (0.20 mL, 2.8 mmol, 2.0 equiv.) was added and the reaction mixture was further sonicated for 2 h min at the same temperature. The reaction mixture loaded to a column and purified by flash column chromatography on SiO_2 (12 g), eluting with hexane-CH_2Cl_2 (4:1), using a Teledyne ISCO Combiflash Rf instrument to yield the *tittle compound* (0.30 g, 68% yield) as a yellow compound.

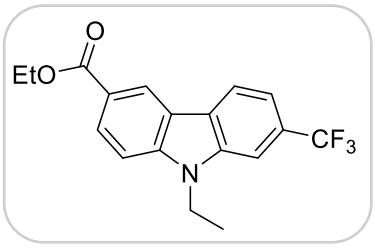

Mp: 252-254 °C. **Purity (LCMS):** 91%. **Found [ESI]:** MH+, 336.1210. $C_{18}H_{17}F_3NO_2$ [MH] requires 336.1211. **IR** (neat) *v*/cm^{-1} 2979 (C-H), 1674 (C=O), 1603 (C-C), 1271 (C-F), 813 (C-H) **^{1}H NMR** (600 MHz, d_6-DMSO) δ 8.90 (1H, d, *J* 1.5, H-4), 8.52 (1H, d, *J* 8.0, H-5), 8.13 (1H, dd, *J* 8.5, 1.5, H-2), 8.09 (1H, s, H-8), 7.77 (1H, d, *J* 8.5, H-1), 7.54 (1 H, d, *J* 8.0, H-6), 4.57 (2H, q, *J* 7.0, CH_2CH_3), 4.34 (2H, q, *J* 7.0, CH_2CH_3), 1.35 (3H, t, *J* 7.0, CH_2CH_3), 1.31 (3H, t, *J* 7.0, CH_2CH_3). **^{13}C NMR** (151 MHz, d_6-DMSO) δ 166.6 (C=O), 143.7 (C), 139.9 (C), 128.5 (CH), 127.1 (q, $^2J_{CF}$ 31, C), 125.6 (C), 125.4 (q, $^1J_{CF}$ 272, CF_3), 123.8 (CH), 122.3 (CH), 121.6 (C), 121.5 (C), 116.5 (d, $^3J_{CF}$ 4, CH), 110.1 (CH), 107.5 (d, $^3J_{CF}$ 4, CH), 60.9 (CH_2), 38.0 (CH_2), 14.8 (CH_3), 14.2 (CH_3).

Ethyl 5-fluoro-7-trifluoro9-ethyl-9*H*-carbazole-3-carboxylate (3.36). A solution of ethyl 5-fluoro-7-trifluoro-9*H*-carbazole-3-carboxylate (365 g, 1.1 mmol, 1.0 equiv.) and KOH (125 mg, 2.2 mmol, 2.0 equiv.) in DMSO (3 mL) was sonicated at 40 °C for 20 min. Then, iodoethane (0.20 mL, 2.2 mmol, 2.0 equiv.) was added and the reaction mixture was further sonicated for 2 h min at the same temperature. The reaction mixture loaded to a column and purified by flash column chromatography on SiO_2 (12 g), eluting with hexane-CH_2Cl_2 (4:1), using a Teledyne ISCO Combiflash Rf instrument to yield the *tittle compound* (0.35 g, 89% yield) as a yellow compound.

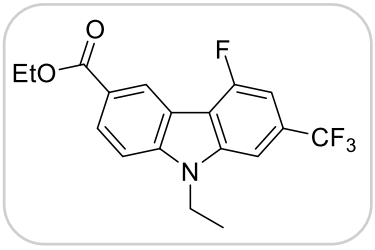

Mp: 116-118°C. **Purity (LCMS):** 85 %. **Found [ESI]:** MH+, 354.1115. $C_{13}H_{11}FN$ [MH] requires 354.1117. **IR** (neat) *v*/cm^{-1} 2984 (C-H), 1698 (C=O), 1610 (C-C), 1289 (C-F), 769 (C-H) **^{1}H NMR** (600 MHz, d_6-DMSO) δ 8.66 (1H, s, H-4), 8.15 (1H, dd, *J* 8.5, 1.5, H-2), 8.02 (1H, s, H-8), 7.83 (1H, d, *J* 8.5, H-1), 7.45 (1H, d, J_{HF} 10.0, H-6), 4.58 (2H, q, *J* 7.0, CH_2CH_3), 4.34 (2H, q, *J* 7.0, CH_2CH_3), 1.35 (3H, t, *J* 7.0, CH_2CH_3), 1.31 (3H, t, *J* 7.0, CH_2CH_3). **^{13}C NMR** (151 MHz, d_6-DMSO) δ 166.3, (C=O), 157.7 (d, $^1J_{CF}$ 249, CF), 143.2 (CH), 142.3 (d, $^3J_{CF}$ 11, C), 128.7 (CH), 128.1 (dq, $^2J_{CF}$ 33, $^3J_{CF}$ 8, C), 124.8 (d, $^4J_{CF}$ 3, C), 124.5 (qd, $^1J_{CF}$ 275, $^4J_{CF}$ 3, CF_3), 122.3 (CH), 118.5 (C), 113.1 (d, $^2J_{CF}$ 20, C), 110.6 (CH), 104.8 – 104.5 (m, C), 103.0 (dq, $^2J_{CF}$ 23, $^4J_{CF}$ 4, CH), 61.1 (CH_2), 38.5 (CH_2), 14.7 (CH_3), 14.2 (CH_3).

5-Fluoro-7-trifluoro9-ethyl-9*H*-carbazole-3-carboxylic acid (3.37). A solution of ethyl 7-trifluoro-9-ethyl-9*H*-carbazole-3-carboxylate (320 mg, 1.1 mmol, 1.0 equiv.) and NaOH (168 mg, 4.2 mmol, 4 equiv.) in 1,4-dioxane:water (3:1) (10 mL) was stirred at reflux overnight. Then, the reaction was allowed to cool down to room temperature and was acidified to pH 3 with HCl (1M). Extraction with EtOAc gave the *tittle compound* (0.31 g, 95% yield) as a colourless solid.

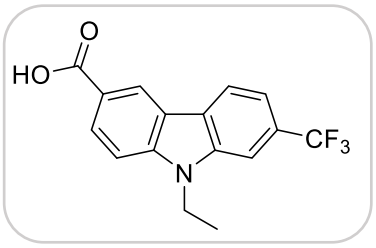

Mp: 264-267 °C. **Purity (LCMS):** 90 %. **Found [ESI]:** MH+, 308.0890. $C_{16}H_{13}F_3NO_2$ [MH] requires 308.0898. **IR** (neat) *v*/cm^{-1} 2982 (C-H), 1678 (C=O), 1603 (C-C), 1272 (C-F), 869 (C-H) **^{1}H NMR** (600 MHz, Acetone-*d*$_6$) δ 11.09 (1H, s, COOH) 8.96 (1H, d, *J* 1.5, H-4), 8.52 (1H, d, *J* 8.0, H-5), 8.25 (1H, dd, *J* 8.5, 1.5, H-2), 8.04 (1H, s, H-8), 7.77 (1H, d, *J* 8.5, H-1), 7.60 (1H, dd, *J* 8.0, 1.5, H-6), 4.68 (2H, q, *J* 7.0, *CH*$_2$CH$_3$), 1.47 (3H, t, *J* 7.0, CH$_2$*CH*$_3$). **^{13}C NMR** (151 MHz, Acetone-*d*$_6$) δ 167.1 (C=O), 143.7 (C), 140.0 (C), 128.6 (CH), 127.6 (q, $^2J_{CF}$ 32, C), 125.8 (C), 125.1 (q, $^1J_{CF}$ 273, CF$_3$), 123.6 (CH), 121.9 (C), 121.6 (C), 121.4 (CH), 116.1 (q, $^3J_{CF}$ 4, CH), 109.1 (CH), 106.7 (q, $^3J_{CF}$ 4, CH), 37.7 (CH$_2$), 13.2 (CH$_3$).

5-Fluoro-7-trifluoro9-ethyl-9*H*-carbazole-3-carboxylic acid (3.38). A solution of ethyl 7-5-fluoro-trifluoro-9-ethyl-9*H*-carbazole-3-carboxylate (273 mg, 0.8 mmol, 1.0 equiv.) and NaOH (124 mg, 3.1 mmol, 4 equiv.) in 1,4-dioxane:water (3:1) (8 mL) was stirred at reflux overnight. Then, the reaction was allowed to cool down to room temperature and was acidified to pH 3 with HCl (1M). Extraction with EtOAc gave the *tittle compound* (0.25 g, 99% yield) as a colourless solid.

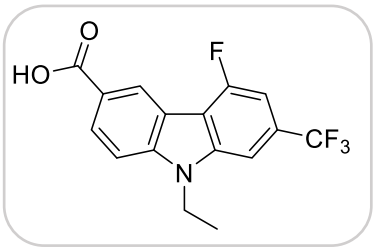

Mp: 295-298 °C. **Purity (LCMS):** 94 %. **Found [ESI]:** MH+, 326.0800. $C_{16}H_{12}F_4NO_2$ [MH] requires 326.0804. **IR** (neat) *v*/cm^{-1} 2989 (C-H), 1698 (C=O), 1679 (C-C), 1293 (C-F), 740 (C-H) **^{1}H NMR** (600 MHz, DMSO-*d6*) δ 8.70 (1H, s, H-4), 8.16 (0 H, d, *J* 8.5, H-2), 8.02 (1H, s, H-8), 7.82 (1H, d, *J* 8.5, H-1), 7.45 (1H, d, J_{HF} 10.0, H-6), 4.59 (1H, q, *J* 7.5, *CH*$_2$CH$_3$), 1.31 (1 H, t, *J* 7.5, *CH*$_2$CH$_3$). **^{13}C NMR** (151 MHz, DMSO-*d6*) δ 167.9 (C=O), 156.9 (d, $^1J_{CF}$ 249, CF), 143.1 (C), 142.2 (d, $^3J_{CF}$ 11, C), 129.0 (CH), 128.0 (qd, $^2J_{CF}$ 32, $^3J_{CF}$ 10, C), 125.0 (d, $^4J_{CF}$ 3, C), 124.5 (qd, $^1J_{CF}$ 271, $^4J_{CF}$ 4, CF$_3$), 123.4 (C), 118.5 (CH), 113.2 (d, $^2J_{CF}$ 19, C), 110.4 (CH), 104.7 – 103.9 (m, CH), 103.0 (dq, $^2J_{CF}$ 23, $^3J_{CF}$ 4, CH), 38.5 (CH$_2$), 14.2 (CH$_3$).

1-(2-Trifluoromtehyl-9-ethyl-9*H*-carbazol-3-yl)-*N*-methylmethanamine (3.40). A solution of methylamine 2 M in THF (1.7 mL, 3.3 mmol, 4.0 equiv.) was added to a solution of 4-fluoro-2-trifluoromtehyl-9-ethyl-9*H*-3-carbazolealdehyde (242 mg, 0.8 mmol, 1.0 equiv.) in anhydrous THF (10 mL) and the reaction mixture was stirred at room temperature for 48 h. Then, a solution $NaBH_4$ (157 mg, 4.2 mmol, 5.0 equiv) in MeOH (3 mL) was added and the reaction mixture stirred overnight for 4 h. The solvent was evaporated and the crude solid was extracted with CH_2Cl_2. Purification by flash column chromatography on basic alumina (24 g), eluting with hexane-CH_2Cl_2, (1:1) gave the *title compound* (0.19 g, 74%) as a beige solid.

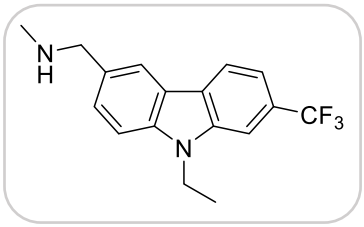

Mp: 56-58 °C. **Found [ESI]:** MH^+, 307.1436. $C_{17}H_{18}N_2F_3$ [MH] requires 307.1422. **IR** (neat) *v*/cm^{-1} 3701, 3681 (NH), 2974 (C-H), 1607 (C-C), 1105 (C-F), 818 (C-H). **^{1}H NMR** (600 MHz, d_6-DMSO) δ 8.15 (1H, d, *J* 8.0, H-5), 8.09 (1H, s, H-4), 7.65 (1H, s, H-8), 7.50 (1H, d, *J* 8.5, H-1), 7.46 (1H, d, *J* 8.0, H-6), 7.41 (1H, d, *J* 8.5, H-2), 4.40 (2H, q, *J* 7.5, CH_2CH_3), 3.94 (2H, s, CH_2NHCH_3), 2.52 (3H, s, CH_2NHCH_3), 1.45 (3H, t, *J* 7.5, CH_2CH_3). N-H not observed. **^{13}C NMR** (151 MHz, d_6-DMSO) δ140.2 (C), 139.3 (C), 131.4 (C), 127.6 (CH), 127.4 (d, $^2J_{CF}$ 32, C), 125.4 (C), 124.9 (d, $^1J_{CF}$ 272, CF_3), 122.1 (C), 120.7 (CH), 120.7 (CH), 115.4 (q, $^3J_{CF}$ 4, CH), 108.8 (CH), 105.7 (q, $^3J_{CF}$ 4, CH), 56.3 (CH_2), 37.8 (CH_2), 36.0 (CH_3), 13.9 (CH_3).

X crystallography:

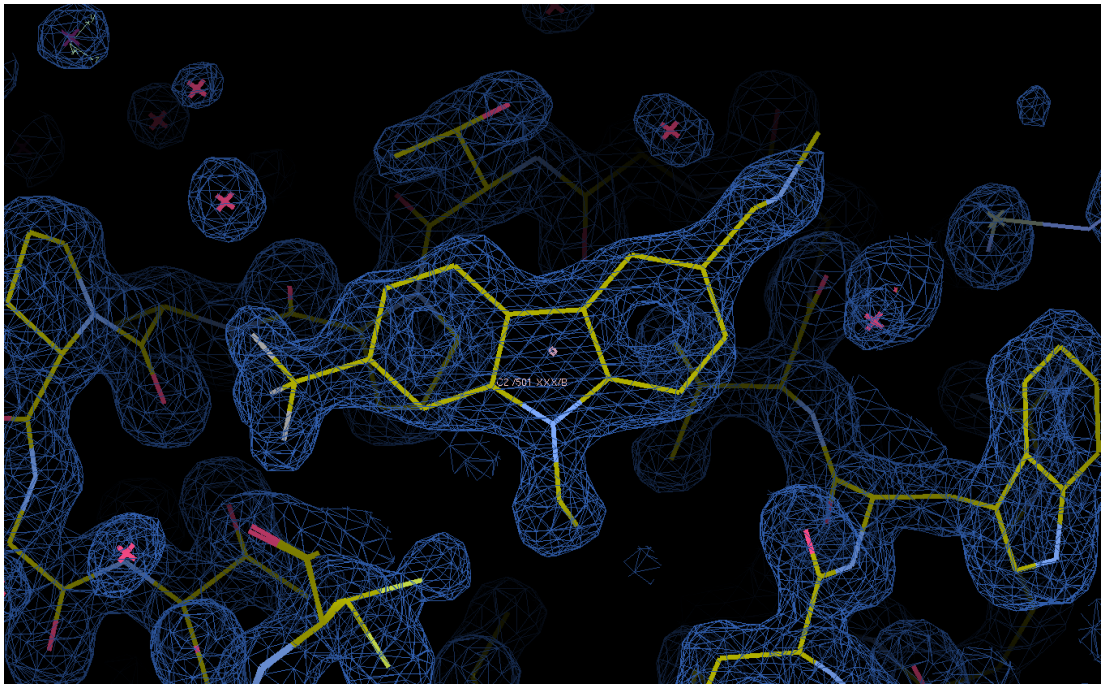

1-(4-Fluoro-2-trifluoromtehyl-9-ethyl-9*H*-carbazol-3-yl)-*N*-methylmethanamine (3.41). A solution of methylamine 2 M in THF (1.1 mL, 2.2 mmol, 4.0 equiv.) was added to a solution of 4-fluoro-2-trifluoromtehyl-9-ethyl-9*H*-3-carbazolealdehyde (170 mg, 0.7 mmol, 1 equiv.) in anhydrous THF (5 mL) and the reaction mixture was stirred at room temperature for 48 h. Then, a solution $NaBH_4$ (123 mg, 3.3 mmol, 5 equiv.) in MeOH (2 mL) was added and the reaction mixture stirred overnight at room temperature. The solvent was evaporated and the crude solid was extracted with CH_2Cl_2. Purification by flash column chromatography on basic alumina (24 g), eluting with hexane-CH_2Cl_2, (1:1) gave the *title compound* (92 mg, 44%) as a beige solid.

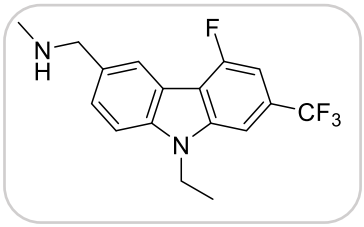

Mp: 77-80 °C. **Found [ESI]:** MH^+, 325.1324. $C_{17}H_{17}N_2F_4$ [MH] requires 325.1328. **IR** (neat) *v*/cm^{-1} 3839, 3802 (NH), 2931 (C-H), 1611 (C-C), 1111 (C-F), 844 (C-H).**^{1}H NMR** (600 MHz, d_6-DMSO) δ 8.16 (1H, s, H-4), 7.53 (1H, dd, *J* 8.5, 1.5, H-2), 7.43 (1H, s, H-8), 7.40 (1H, d, *J* 8.5, H-1), 7.13 (1H, d, *J* 10.0, H-6), 4.36 (2H, q, *J* 7.5, CH_2CH_3), 3.92 (2H, s, CH_2NHCH_3), 2.51 (3H, s, CH_2NHCH_3), 1.44 (3 H, t, *J* 7.5, CH_2CH_3). **^{13}C NMR** (151 MHz, d_6-DMSO) δ 158.1 (d, $^1J_{CF}$ 251, CF), 141.5 (d, $^3J_{CF}$ 11, C), 139.6 (C), 132.4 (CH), 128.1 (qd, $^2J_{CF}$ 33, $^3J_{CF}$ 8, C), 127.8 (CH), 124.3 (qd, $^1J_{CF}$ 272, $^3J_{CF}$ 3, CF_3), 123.1 (d, $^3J_{CF}$ 3.5, CH), 119.6 (C), 113.44 (d, $^2J_{CF}$ 20, C), 108.7 (CH), 102.0 (dq, $^2J_{CF}$ 27, $^3J_{CF}$ 4, CH), 101.8 (p, $^3J_{CF}$ 4, $^4J_{CF}$ 4, CH), 56.3 (CH_2), 38.2 (CH_2), 36.0 (CH_3), 13.8 (CH_3).

1-(5,7-Bis(trifluoromethyl)-9-ethyl-9*H*-carbazol-3-yl)-*N*-methylmethanamine (3.42). A solution of methylamine 2 M in THF (1.2 mL, 2.5 mmol, 4.0 equiv.) was added to a solution of 2,4-bis(trifluoromtehyl)-9-ethyl-9H-3-carbazolealdehyde (213 mg, 0.6 mmol, 1.0 equiv.) in anhydrous THF (5 mL) and the reaction mixture was stirred at room temperature for 48 h. Then, a solution $NaBH_4$ (117 mg, 3.1 mmol, 5.0 equiv.) in MeOH (2 mL) was added and the reaction mixture stirred overnight for 4 h. The solvent was evaporated and the crude solid was extracted with CH_2Cl_2. Purification by flash column chromatography on basic alumina (24 g), eluting with hexane-CH_2Cl_2, (1:1) gave the *title compound* (90 mg, 39%) as a colourless solid.

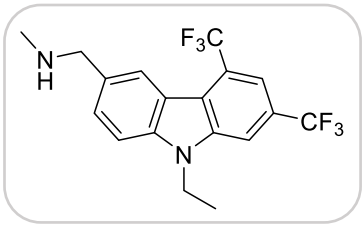

Mp: 99-101 °C. **Purity (LCMS):** %. **Found [ESI]:** MH^+, 375.1295. $C_{18}H_{17}N_2F_6$ [MH] requires 375.1296. **IR** (neat) *v*/cm^{-1} 3707, 3681 (N-H), 2923 (C-H), 1635 (C-C), 1033 (C-F), 803, (C-H). **^{1}H NMR** (600 MHz, $CDCl_3$) δ 8.25 (1H, s, H-4), 7.85 (1H, s, H-6), 7.77 (1H, s, H-8), 7.63 (1 H, dd, *J* 8.4, 1.6, H-2), 7.49 (1 H, d, *J* 8.4, H-1), 4.46 (2 H, q, *J* 7.3, CH_2CH_3), 3.95 (2 H, s, $NHCH_2$), 2.52 (3H, s, CH_3NH), 1.47 (3 H, t, *J* 7.3, CH_2CH_3). **^{13}C NMR** (151 MHz, d_6-DMSO) δ 140.6 (C), 140.0 (C), 132.6 (C), 128.9 (CH), 126.7 (q, $^2J_{CF}$ 32.9, C), 126.6 (q, $^2J_{CF}$ 32.9, C), 124.2 (q, $^1J_{CF}$ 272.2, CF_3), 123.6 (q, $^2J_{CF}$ 34.6, C), 123.3 (q, $^3J_{CF}$ 272.6, CF_3), 121.4 (m, C) , 119.2 (CH), 113.2 (m, CH), 109.3 (q, $^3J_{CF}$ 4.5, CH), 109.1 (CH), 56.5 (CH_2), 38.0 (CH_2), 36.0 (CH_3), 13.8 (CH_3).

CHAPTER 4: Applications in natural product and carboline synthesis

4.1 Natural products

Historically, natural products from plants and animals were the source of nearly all medicines, especially as active components of herbal remedies. More recently, natural products have been used in the clinic and many more feature as leads for compounds that have entered clinical trials. Natural products are structurally optimized by evolution over millions of years to serve particular biological functions and have acquired a unique chemical diversity, which consequently results in the diversity of their biological activities and drug-like properties, which makes them highly relevant in drug discovery.[256] The discipline of natural product synthesis, which consists of the study and synthesis of substances produced by living organisms and their structural analogues, is always an important field of investigation and one of the prominent activities of organic synthesis. Research can help improve the understanding of biological processes or identify compounds that may lead to the development of new drugs, improving chemical synthesis by attempting to push its frontiers to higher molecular complexity, diversity, and efficiency. Historically, natural products have been especially important for cancer and infectious diseases.[2]

There exist numerous natural products which are essentially substituted carbazoles. Apart from clausenine (**1.13**) and clausenol (**1.14**), previously described (**Figure 20,** section 1.4.1), other derivates extracted from *Clausena anisata* show promising biological activities, including different clausines and mukonidines, shown in **Figure 47**. This type of scaffold has attracted much interest due to its wide range of biological activity upon modification, including antibacterial, antimalarial, anticancer, and anti-Alzheimer properties, and compound libraries are being constantly designed to imitate as closely as possible the chemical properties of natural products, or even improve them.[258]

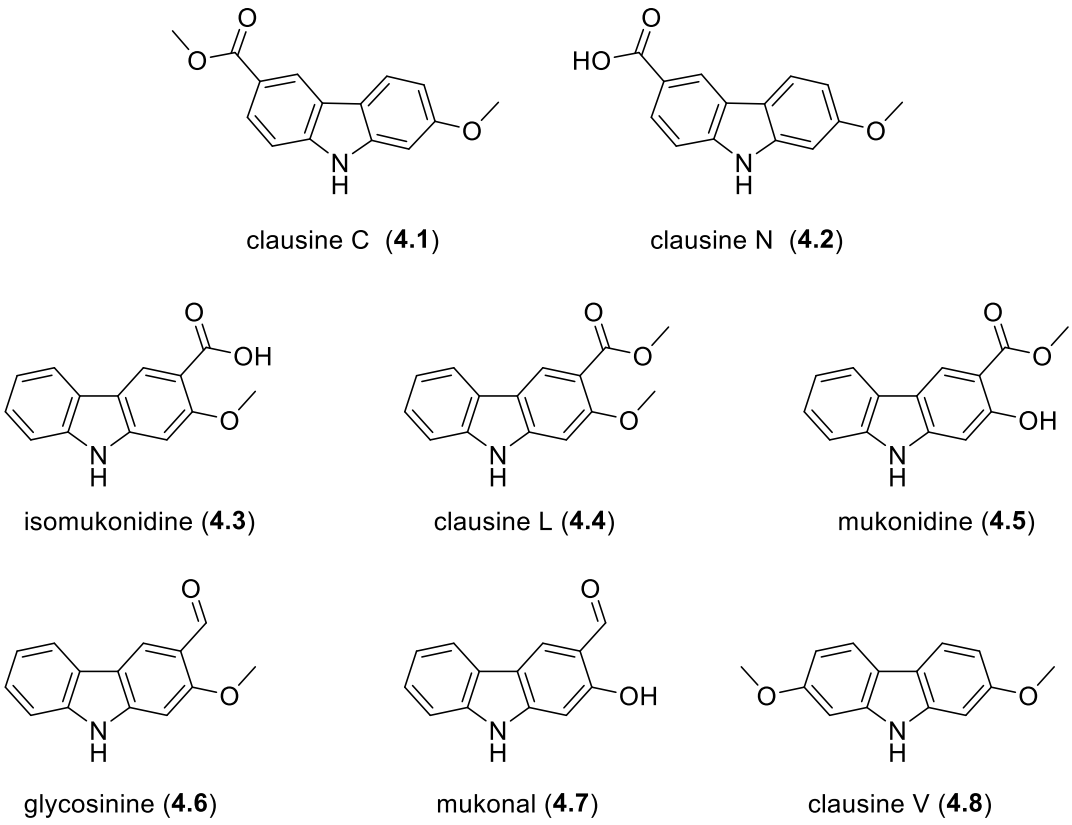

Figure 47. *A sample of naturally occurring carbazole alkaloids.*

Although natural products have been a rich provenance of compounds for drug discovery, they have received declining attention in the past two decades by the pharmaceutical industry because they present challenges such as unreliable access and supply, intellectual property,[259] cost, and profit concerns, technical barriers to screening products in high-throughput assays against molecular target, isolation, characterization and optimization. Consequently, the necessity of convenient access to natural products and their derivatives stands as an ongoing challenge. Given the structural similarity of the many reported examples of carbazole natural products to the structures and functional groups of the scaffolds previously synthesized in this thesis, the possibility of adapting the synthetic methodology developed to the synthesis of carbazole containing natural products arose as a feasible objective.

Hence, the aim of this chapter is to adapt the synthetic methods described in Chapter 2 to provide a highly efficient novel route to naturally occurring scaffolds, utilizing reagentless techniques to provide carbazole-based natural products in useful quantities for biological evaluation or additional functionalization and diversification, starting with those natural products that are essentially differently substituted carbazoles. The retrosynthesis, displayed in **Scheme 89**, will be the starting point for the synthesis of this scaffold.

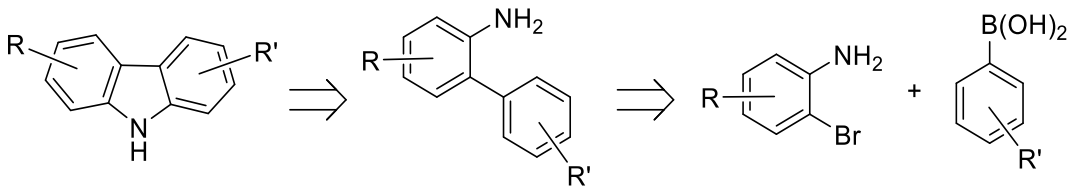

Scheme 89. *Retrosynthesis of natural product carbazoles.*

4.1.1 Clausines C, N and V

Using the developed method for the synthesis of the core 9*H*-carbazole skeleton could enable access to useful quantities of a valuable building block for the synthesis of these natural products in high yield and in a short period of time. In order to test this theory and provide some examples, natural products, which are essentially substituted carbazoles, were chosen to be synthesized. The synthetic proposal, shown in **Scheme 90**, uses the same conditions previously described for the synthesis of carbazole scaffolds, even those ones including esters, and a further hydrolysis, a reaction which had been studied as well for this type of compounds, to synthesize clausine C (**4.1**) and its analogue clausine N (**4.2**).

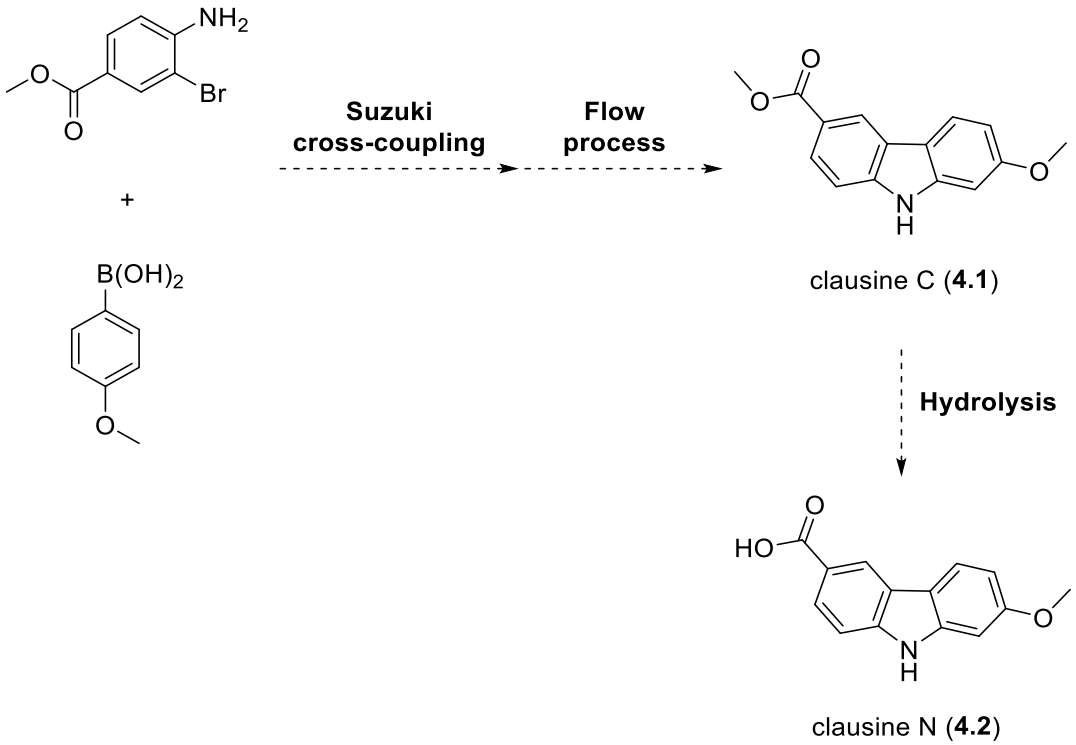

Scheme 90. *Synthetic proposal for the synthesis of clausine C (**3.1**) and clausine N (**3.2**).*

The synthesis, then, started with the Suzuki coupling reaction, submitting the corresponding haloaniline and boronic acid in a sealed vial with $Pd(dppf)Cl_2$ as a catalyst for microwave irradiation.

Although this reaction with the presence of a methyl ester implied some issues for electron poor carbazole, the presence of the methoxy group on the boronic acid seemed to facilitate the transformation and stabilize the ester, obtaining a superior yield in comparison to the CF_3 containing biphenyls studied earlier. The resulting biphenyl **4.9** was then submitted to the flow process described in Chapter II, with the azide formation and following photocyclization. The reaction provided the same biphenyl intermediate described in Chapter II, section 3.1.3.2, resulting from the hypothetical reduction of the diazonium salt, which in this case was not characterized, and the target product clausine C (**4.1**) that was obtained in a good yield of 65%. The following hydrolysis took place as expected and provided clausine N (**4.2**) in near quantitative yield (**Scheme 91**).

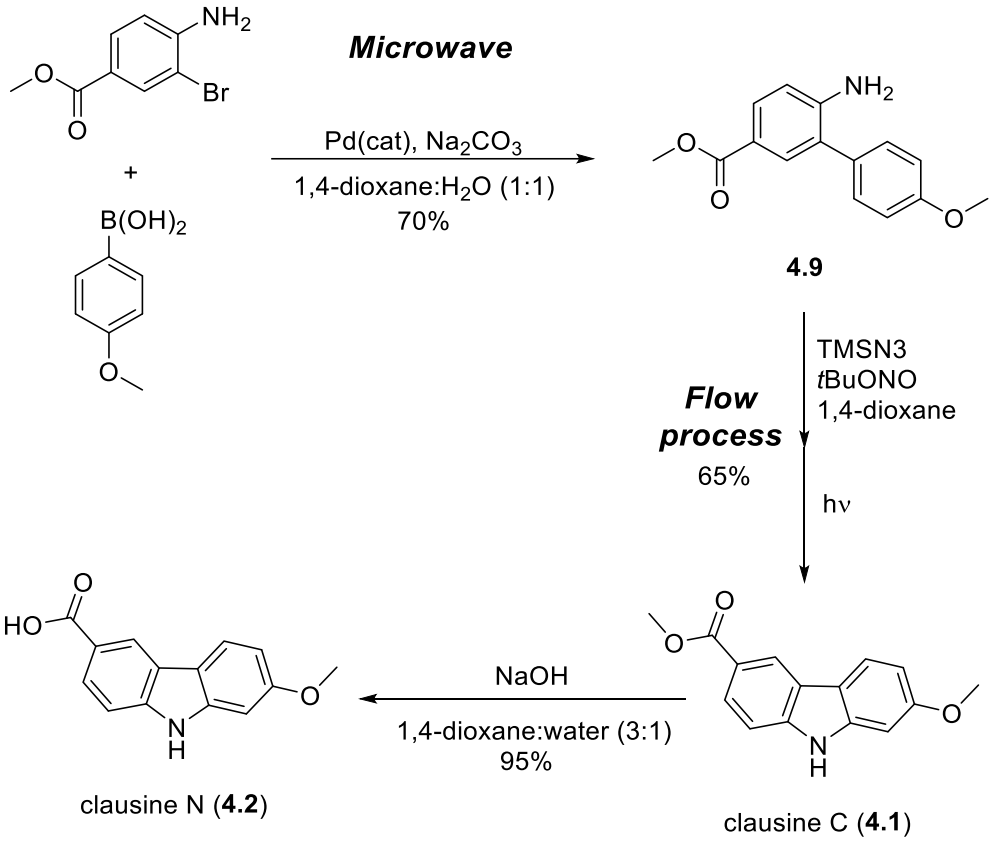

Scheme 91. *Synthetic route for the synthesis of clausine C (**4.1**) and clausine N (**4.2**).*

The two natural products were fully characterized via ^{1}H, ^{13}C-NMR, LCMS and HRMS. The ^{1}H NMR spectra of the two compounds, shown in **Figure 48**, are almost identical, and matched the literature data previously reported.[260,261] Apart from a slight difference in the chemical shifts, the two main differences between them were the disappearance of one of the methyl groups, and the appearance of a peak at δ ~ 2.9 ppm caused by the carboxylic acid, which appears in this area when the analysis is conducted in deuterated acetone due to the intermolecular exchange of HDO. For the assignment of each proton of the carbazole ring, the expected shift of each proton on these molecules was

considered,[231] accounting for the electronic effects of the carbonyl and methoxy groups (the signals on the ring with the methoxy group would be those higher fields and the ones in the ring with the ester at lower fields), and the multiplicities of each signal. The three protons of the methoxy (and the methyl ester) group of clausine C (**4.1**) (**Figure 48a**) were assigned by comparison to the spectrum of clausine N (**4.2**) (**Figure 48b**).

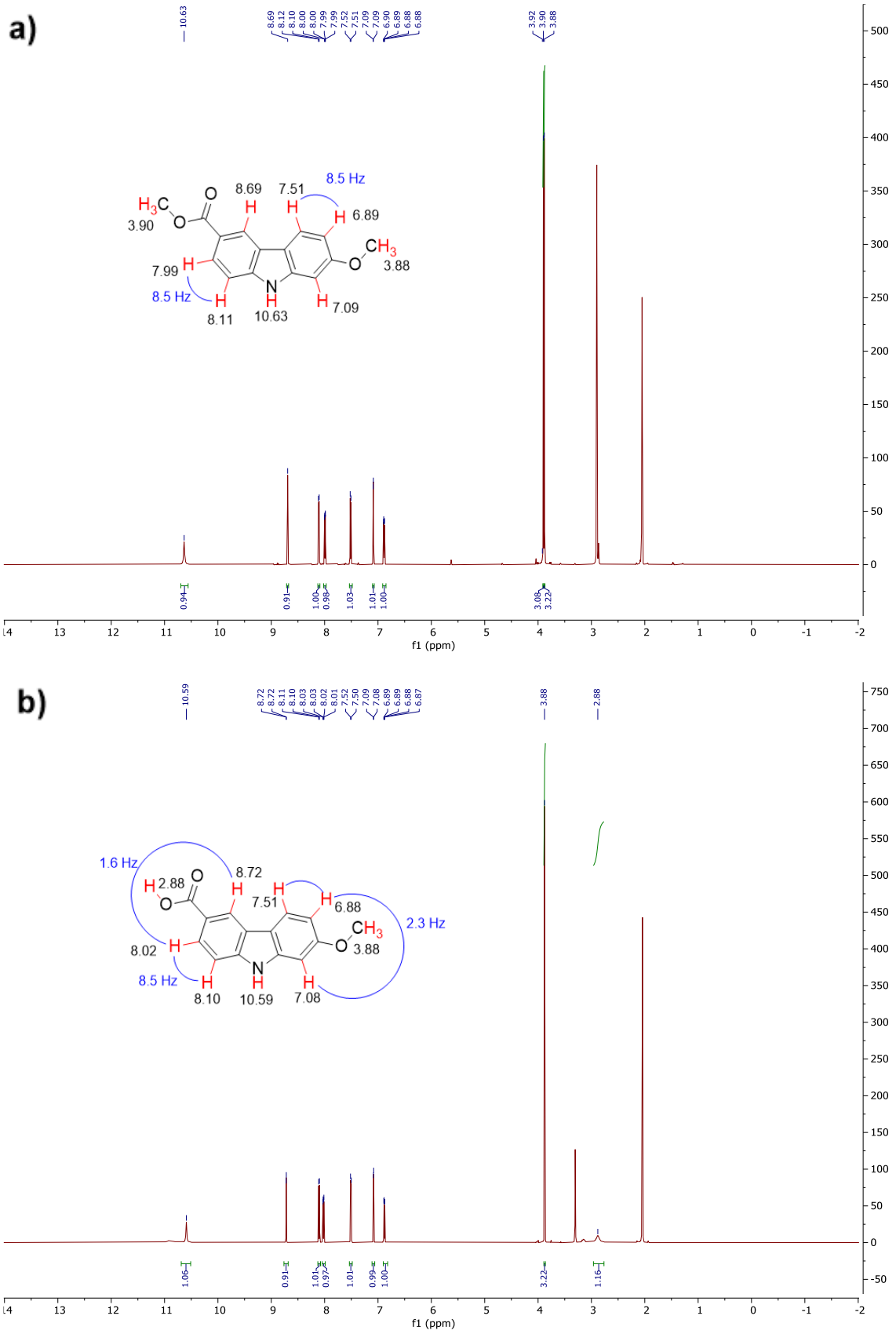

Figure 48. *^{1}H-NMR spectra of a) clausine C (**4.1**) and b) clausine N (**4.2**), showing all proton resonances δ/ppm.*

Clausine V (**4.8**), another analogue with similar structure, was also attempted to be synthesized. The synthetic proposal followed exactly the same approach as clausine C, with the Suzuki cross coupling reaction and subsequent flow photocyclization process. Some examples of methoxy and dimethoxycarbazole had been already synthesized, so the method should be adaptable to the new compound. Thus, the synthetic pathway proceeded as shown in **Scheme 92**.

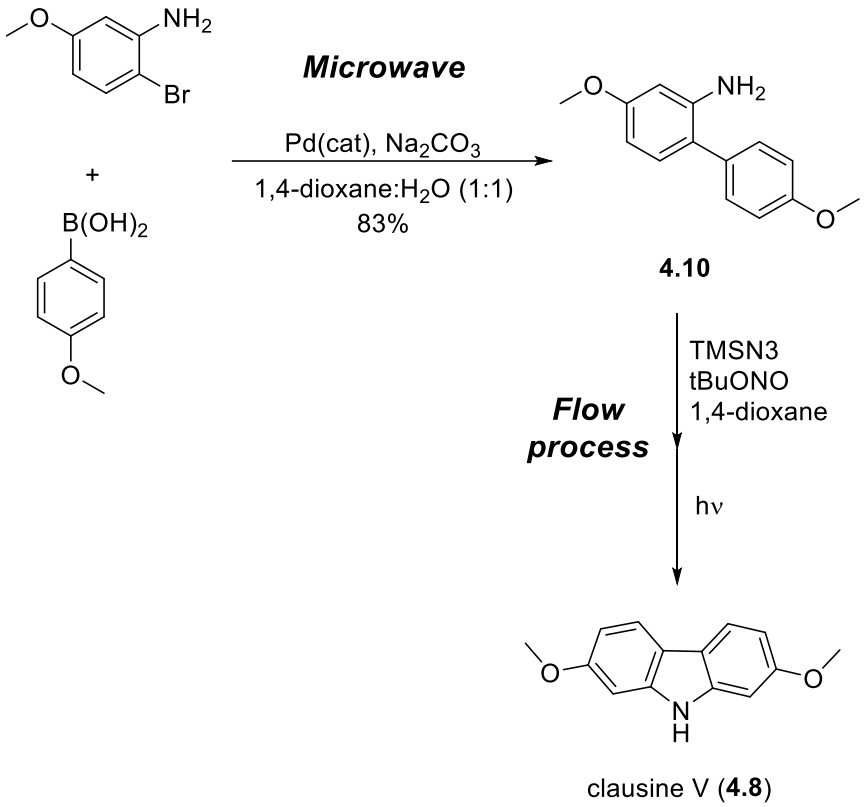

Scheme 92. *Clausine V (**4.8**) synthetic scheme.*

The cross-coupling step worked efficiently providing a high yield for the synthesis of the biphenyl intermediate **4.10**. The flow process was next carried out with the obtained compound, but although the conversion was around 90% the product was lost after attempting the purification by flash column chromatography. The compound could not be isolated, purified and fully characterized, but the ^{1}H-NMR spectrum of the crude reaction mixture, shown in **Figure 49**, proved the presence of the carbazole analogue with a very good conversion. As stated for the basic 9*H*-carbazole, the symmetry of the product made the identification clearer. Moreover, the proton signals matched the assignment reported in the literature.[262]

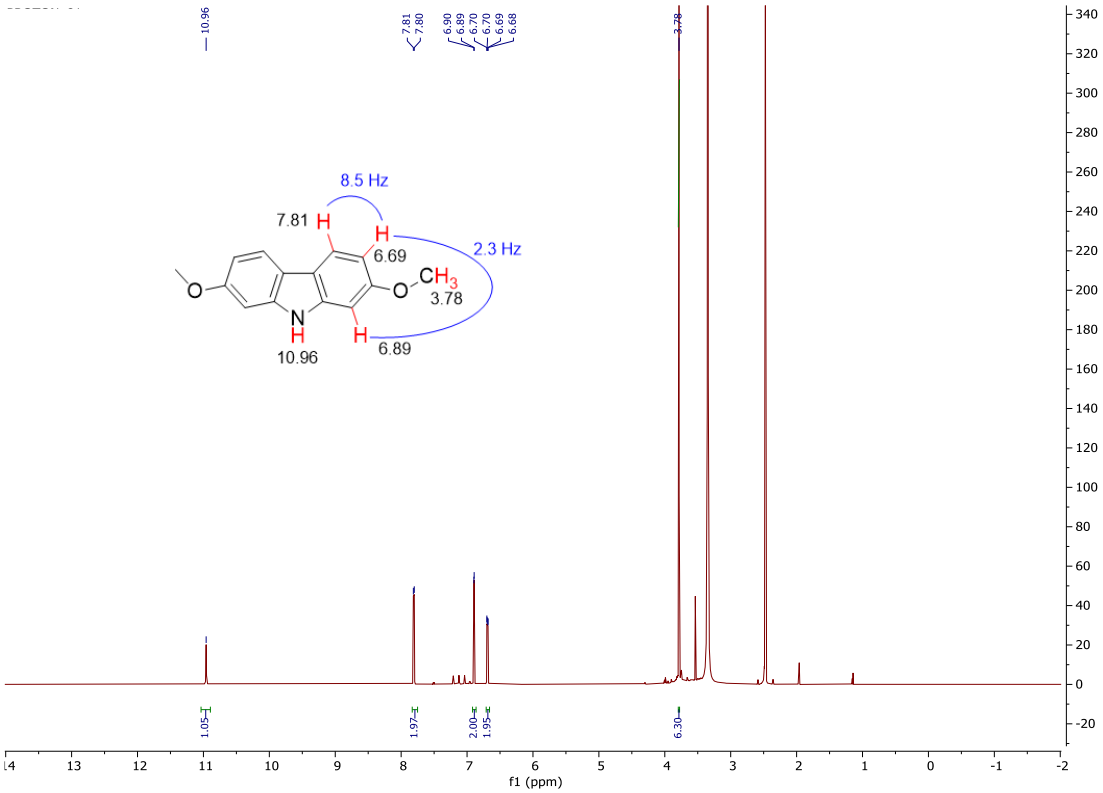

Figure 49. *^{1}H-NMR spectra of the crude of clausine V (**4.8**), showing chemical shift of proton resonances δ/ppm.*

Encapsulating the results, three natural products were synthesised used the methods described in Chapter 2. Clausine C (**4.1**) and clausine N (**4.2**) were synthesised in good yields, isolated and fully characterized, and Clausine V (**4.8**) was synthesised but could not be purified, although the ^{1}H-NMR spectrum of the reaction mixture gave evidence of the presence of the compound, indicating that the purification step was the actual issue, which could not be repeated or optimized due to time limitations. **Table 19** shows a comparison of the three compounds ^{1}H-NMR signals with those previously reported in the literature by Akiyama, T. *et al.*,[196] Tian, X. *et al.*[263] and Chatterjee, T. *et al.*,[264] confirming the identity of the 3 compounds. For clausine C (**4.1**) and clausine N (**4.2**), an additional comparison of the ^{13}C-NMR data to those reported by Akiyama, T. *et al.*[196] and Tian, X. *et al.*[263] is also displayed in **Table 20**.

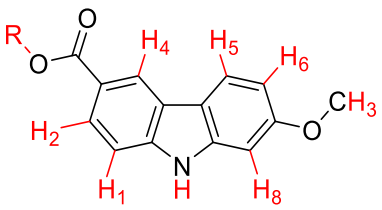

Table 19. *^{1}H-NMR signals for clausine C (**4.1**), clausine N (**4.2**) and clausine V (**4.8**) compared to previously reported data.*

Entry	Signal	Clausine C[a]		Clausine N[b]		Clausine V[c]	
		Exp δ (ppm)	Lit[196] δ (ppm)	Exp δ (ppm)	Lit[263] δ (ppm)	Exp δ (ppm)	Lit[264] δ (ppm)
1	H-1	8.11	8.10	8.10	7.97	-	-
2	H-2	7.99	8.00	8.02	7.90	-	-
3	H-4	8.69	8.69	8.72	8.63-8.57	-	-
4	H-5	7.51	7.51	7.51	7.38	7.81	7.83
5	H-6	6.89	6.89	6.88	6.75	6.69	6.72
6	H-8	7.09	7.09	7.08	6.95	6.89	6.92
7	NH	10.63	10.6	10.59	10.43	10.96	10.95
8	OCH_3	3.88	3.89	3.88	3.74	3.78	3.80
9	COOR	3.90	3.90	2.88	-	-	-

a) *Entry 9: R = CH_3.*
b) *Entry 9: R = H.*

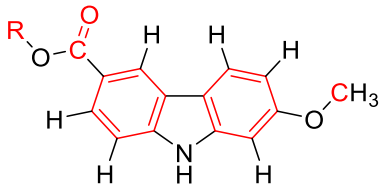

Table 20. *^{13}C-NMR signals for clausine C (**4.1**) and clausine N (**4.2**) compared to previously reported data.*

Entry	Signal	Clausine C[a]		Clausine N[b]	
		Exp δ (ppm)	Lit[196] δ (ppm)	Exp δ (ppm)	Lit[263] δ (ppm)
1	C	159.7	160.5	159.7	160.6
2	C	142.9	143.7	143.0	143.9
3	C	142.1	142.9	142.2	143.0
4	CH	125.7	126.5	126.0	127.0
5	C	123.1	123.9	123.0	124.0
6	CH	121.3	122.1	121.6	122.6
7	CH	121.2	122.0	121.2	122.0
8	C	120.9	121.7	121.1	122.0
9	C	116.6	117.5	116.7	117.6
10	CH	110.2	111.0	110.1	111.0
11	CH	108.9	107.7	108.8	109.8
12	CH	94.9	95.7	94.9	95.8
13	C=O	167.1	167.9	167.8	168.6
14	CO_2CH_3	51.0	51.9	-	-
15	OCH_3	54.9	55.7	54.9	55.8

a) *Entry 14: R = CH_3.*
b) *Entry 4: R = H.*

4.1.2. Clausine L and mukonidine.

After synthesising clausine C (**4.1**), clausine N (**4.2**) and clausine V (**4.8**), the next step was to synthesise a few more examples using the same methodology. As shown in **Figure 46**, mukonal (**4.7**), mukonidine (**4.5**), glycosinine (**4.6**) and clausine L (**4.4**) all have very similar structure, with the same main difference: the ester or carbonyl group and the methoxy or hydroxyl are on the same ring. These compounds have been previously synthesised using different methods such as an Au-catalysed[265] or Pd catalysed synthesis,[266] and even with a visible-light-promoted method.[144] However, this last method had reaction times of over 48 hours, which suggested that adapting the methodology developed in this synthesis could provide a more efficient synthetic route for which would potentially be eligible for scaling up to obtain the carbazole precursors on gram scale. Once the carbazole precursors are obtained, the formylation of the 2-hydroxy or the 2-methoxycarbazole would provide mukonal (**4.7**), and the methoxycarbonylation, or oxidation of mukonal (**4.7**) would give mukonidine (**4.5**). The same approach starting with 2-methoxycarbazole would yield glycosinine (**4.6**) and clausine L (**4.4**) (**Scheme 93**).

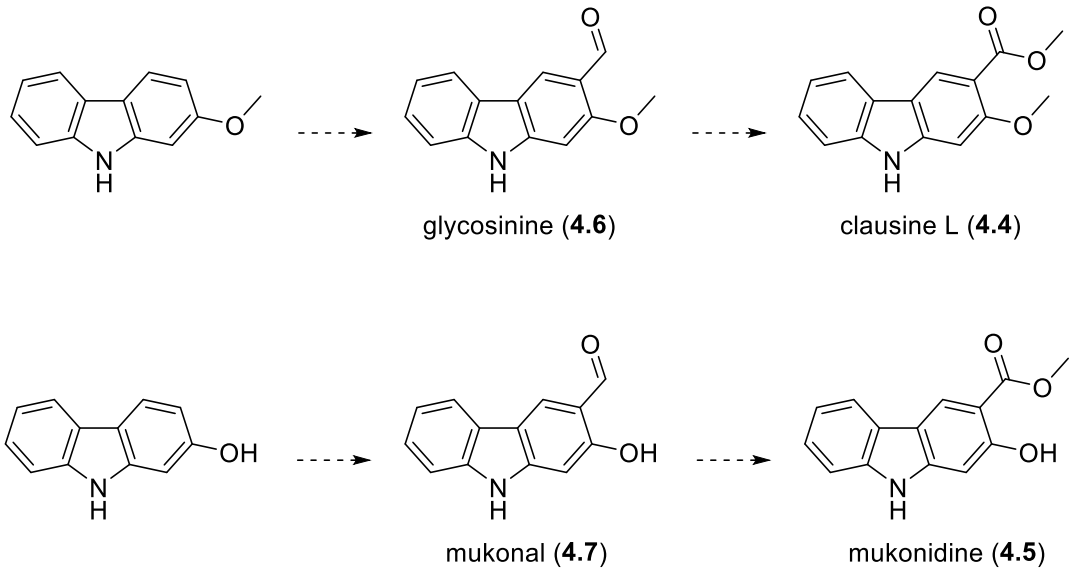

Scheme 93. *Potential approach to the synthesis of naturally occurring carbazoles.*

Since all of these series of natural products would begin with formylation from the carbazole scaffold, two different approaches were investigated for the formylation reaction. The first one, showed in **Scheme 94**, was using the conditions for the classic Vilsmeier-Haack reaction, which consists of the addition of the carbazole to a solution of phosphorus (V) oxychloride in *N,N*-dimethylformamide. Investigating this reaction, no functionalization of the carbazole was observed to take place and only starting materials were obtained. Hence, *N,N*-dimethylformamide was replaced with *N,N*-

diphenylformamide in 1,2-dichloroethane to increase the reactivity of the Vilsmeier-Haack reagent, but with the same results.

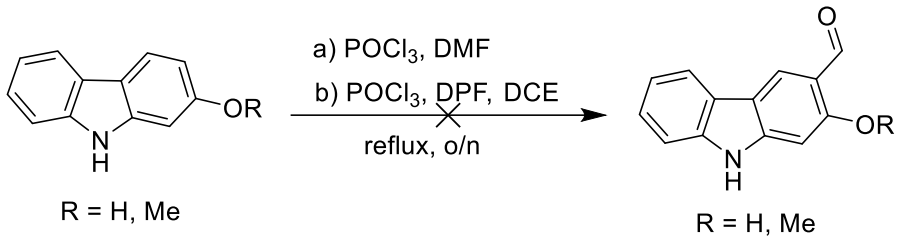

Scheme 94. *Vilsmeier-Haack conditions for formylation of mukonal (**4.7**) or glycosinine (**4.6**).*

An additional formylation method was attempted, the Rieche formylation, which utilizes dichloromethyl methylether in the presence of titanium(IV) chloride. This reaction, displayed in **Scheme 95**, did not provide good results either, as only starting materials with traces of other compounds were observed after ^{1}H-NMR spectroscopic analysis. It was assumed that the formylation of these species was not facile with the N-H group unprotected.

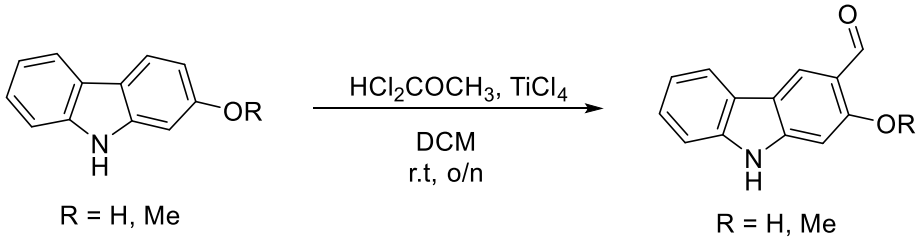

Scheme 95. *Rieche formylation conditions for the formation of mukonal (**4.7**) or glycosinine (**4.6**).*

A final approach was then investigated. The synthetic route would start with the methyl ester in place, an alternative that had been studied in the synthesis of the p53 reactivators. In this case, however, the carbazole product could be obtained as a mixture regioisomers since the cyclization could occur at positions 2' and 6' of the biphenyl anisole ring. After separation, if required, the process could lead to clausine L (**4.4**), and subsequent protodemethylation of this carbazole could provide the rest of the molecules of this family, displayed in **Scheme 96**.

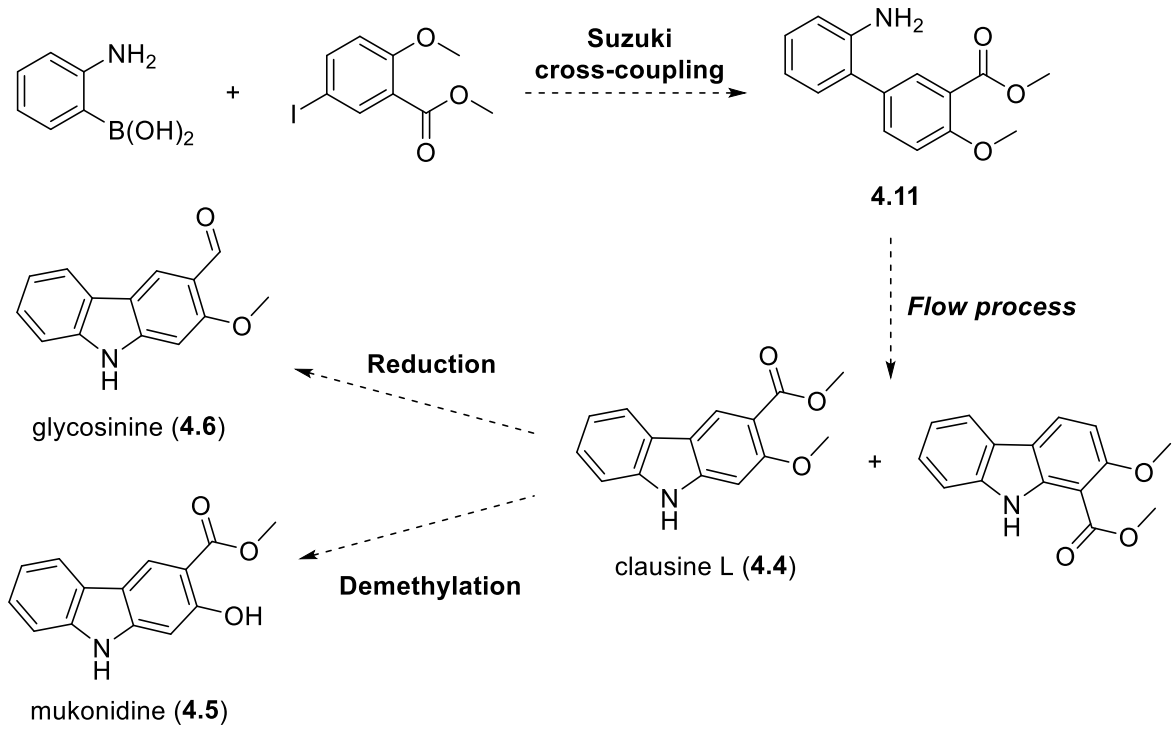

Scheme 96. *Possible approach for the synthesis of naturally occurring carbazoles.*

The first step took place efficiently although in this approach the boronic acid and the halide were present in different reagents, being an anilino boronic acid reacting with the aryl halide. After the success of this step, the obtained compound (**4.11**) was transferred to the flow reactor (**Scheme 97**). In this case, as the ester was not on the same ring as the aniline, it was hoped that the loss of the nitrogen to yield a biphenyl species described in **Chapter III** (section 3.1.3.2, conmpounds **3.16** and **3.17**) should not occur, but after analyzing the crude material by ^{1}H-NMR spectroscopy a complex mixture was observed, and the compound was not isolated.

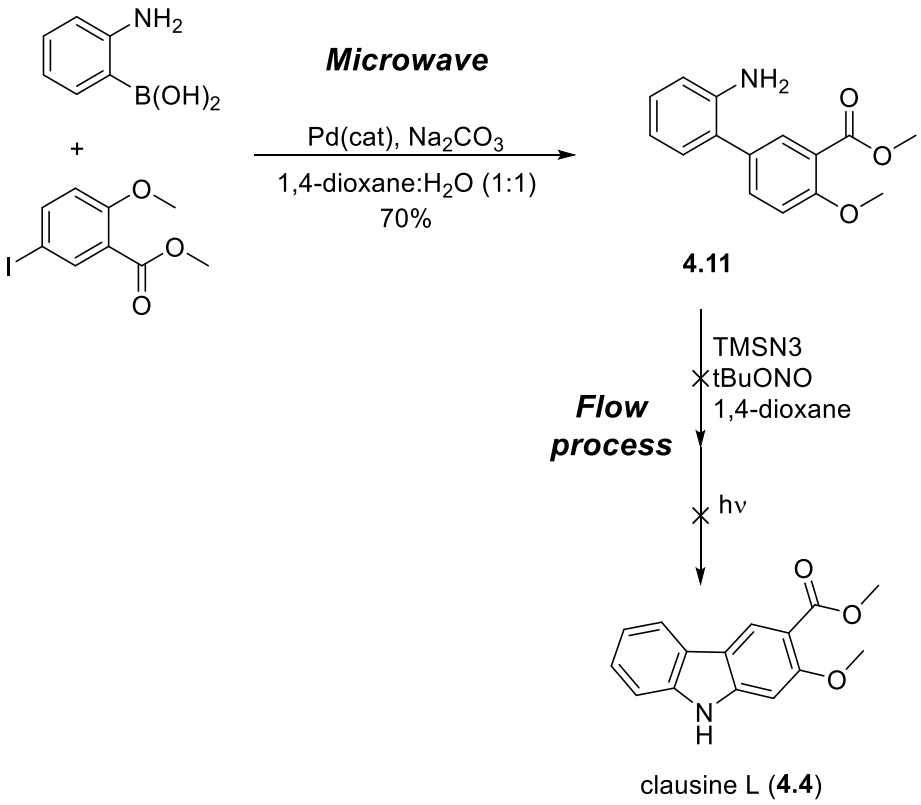

Scheme 97. *Synthetic route for the synthesis of clausine L (**4.4**).*

As previously discussed in section 3.1.3.2, carbonyl groups are susceptible to be activated under visible light irradiation. In this case, the presence of an ester group in the phenyl ring adjacent to the aniline appeared to present, similarly, a considerable obstacle to the synthesis of clausine L (**4.4**) and its analogues.

In conclusion, these studies suggest that the photocyclization approach can be frustrated by the presence of carbonyl groups, especially on the ring that reacts with the nitrene intermediate, and the absence of an *N*-alkyl prevented the formylation reaction with a range of formylating agents. Thus, it was assumed that this group of natural products could not be accessed by the methodology described in this thesis, without in-depth further studies.

4.2 Carbolines

β-Carbolines (9*H*-pyrido[3,4-*b*]indole) are a group of biologically active, naturally occurring plant-derived alkaloids which consist of a pyridine ring that is fused to an indole skeleton. It represents the basic chemical structure for more than a hundred alkaloids and synthetic compounds. The first isolated compound of this family from *Peganum harmala was* harmaline (**Figure 50**) obtained in 1841 by F. Goebel.[267] A few decades later, numerous aromatized analogues were isolated also from *Peganum harmala*, with different substituents especially in positions 1 and 7, but over the years these compounds have been also found in different plants, fungi, microbes, marine invertebrates, insects, and mammals.[268] The effects of *β*-carbolines depend on their respective substituents,[269] and the chemical structures of the most characteristic compounds of this group (showed in **Figure 50**) are related to the nonpolar heterocyclic aromatic amines, the products of pyrolysis of proteins and amino acids.

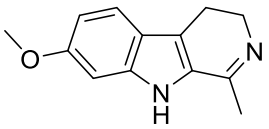

Harmaline (**4.12**)

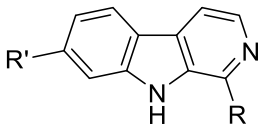

Norharmane; R = R' = H (**4.13**)
Harmane; R = CH_3, R' = H (**4.14**)
Harmine; R = CH_3, R' = OCH_3 (**4.15**)
Harmol; R = CH_3, R' = OH (**4.16**)

Figure 50. *Harmaline (**4.12**) and its analogues structures.*

Among the various structural analogues, harmine (**4.15**) is the *β*-carboline indole alkaloid which has found most widespread use in medicine. It is a privileged structure with a wide spectrum of biological activity,[268] including potent activity as an ATP-competitive inhibitor (IC_{50} 80 nM) of DYRK1A (Dual-specificity tyrosine-phosphorylation-regulated kinase 1A), a kinase implicated in Down's syndrome.[270] Excessive DYRK1A activity would also appear to contribute to the early onset of Alzheimer's disease and the development of a number of human malignancies.[269] Harmine also behaves as a potent (IC_{50} = 8.7 nM)[268] and selective inhibitor of type A MAO (monoamine oxidase), an enzyme that deaminates important bioactive amines such as dopamine, norepinephrine, and serotonin.[270] Moreover, harmine was reported to exhibit a diverse range of pharmacological properties such as hallucinogenic, antitumour, antiviral and antiparasitic activities.[270]

In recent years, many examples of synthetic *β*-carbolines have appeared in the literature with promising anticancer activities. The antitumour activities of *β*-carbolines have been attributed to several mechanisms including DNA intercalation and the inhibition of key enzymes, including monoamine

oxidase (MAO), cyclin-dependent kinases (CDKs), Polo-like kinases (PLKs), and topoisomerases I/II.[269] Besides, *N*- or ring-functionalisation can alter the kinase selectivity profile without adversely affecting potency in a number of commercial harmine analogues, mainly *δ*- and *β*-carbolines (**Figure 51**). Ishida *et al*. reported the incorporation of various substituents at different harmine positions and the evaluation of their biological activities as antitumour agents.[271] Analysis of structure-activity relationships demonstrated that introducing alkoxy substituents into position-7 of harmine (R' in **Figure 51**) led to enhanced cytotoxic activities, the length of the alkoxy chain affected both cytotoxicity and cell line specificity, N^9-alkylated harmine derivatives exhibited strong cytotoxic effects, and N^2-alkylated *β*-carboline derivatives (R'' in **Figure 51**) displayed specific cytotoxic activities.[268]

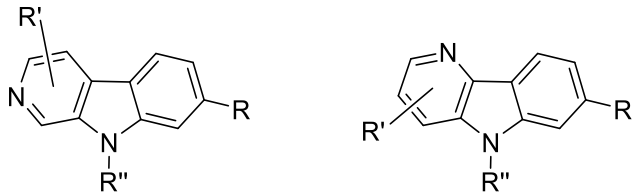

β–carboline *δ*–carboline

Figure 51. *Structures of β- and δ-carbolines.*

Understanding the biosynthesis of *β*-carbolines has always been a challenge of relevance. In 1982, R. B. Herbert and J. Mann described their experiments with *Passiflora edulis* and *Eleagnus angustiflora*, two species of plants capable of biosynthesising harmane and eleagnine (**Scheme 98**).[271] After the decarboxylation of 1-carboxy-tetrahydroharman that provides the intermediate harmalan, in *Passiflora edulis* the hydrogenation of the double bond adjacent to the pyridine nitrogen takes place in the biogenesis of eleagnine (**Scheme 98a**), while in *Eleagnus angustiflora* the aromatization of the pyridine ring leads to harman (**Scheme 98b**). Later, in 1993, J. Berlin's group established that harmaline and harmol served as precursos for the synthesis of harmine *in vivo,*[272] but they could only prove the *O*-methylation of harmol and harmalol *in vitro*,[273] and could not identify which enzymes were involved in the process. Furthermore, in mammals, tryptophan, tryptamine and serotonin could be involved in the biosynthesis of *β*-carbolines with variations of the Bischler-Napieralski reaction or the Pictet-Spengler reaction.[274]

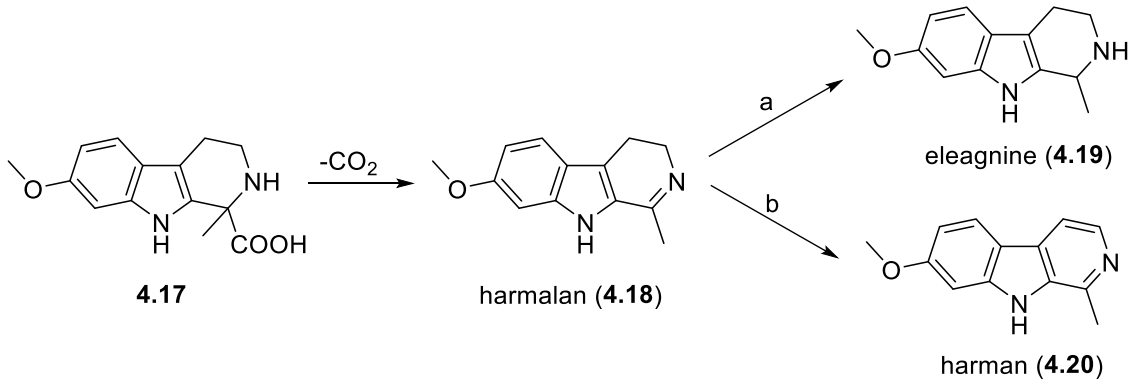

Scheme 98. *Biosynthetic pathways towards (a) eleagnine (**4.19**) in Passiflora edulis and (b) harman (**4.20**) in Eleagnus angustiflora.*

The most commonly employed method for the preparation of *β*-carbolines is the Pictet-Spengler reaction.[275] The reaction, first discovered in 1951, as shown in **Scheme 99**, proceeds through the imination of the amine group of a tryptamine derivate **4.21**, and further cyclisation with the electronic rearrangement and deprotonation to provide the tetrahydro-*β*-carbolines **4.22**. As *β*-carbolines are fully aromatic, an oxidation method is required, and the typical reagent for this purpose is palladium on carbon.

.

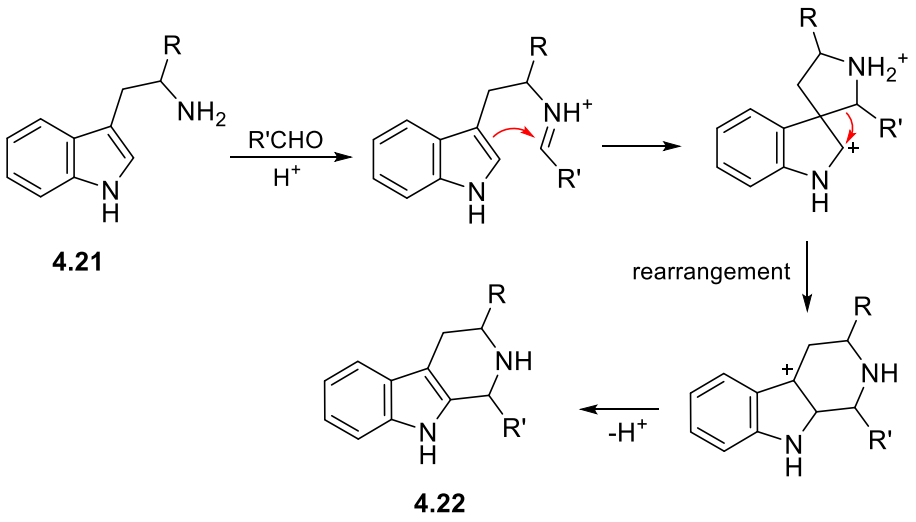

Scheme 99. *Pictet-Spengler reaction scheme for the synthesis of tetrahydro-β-carbolines.*

More recentrly, in 2017, Shashikant U. Dighe *et al.* described an efficient iodine-mediated oxidative Pictet-Spengler reaction using terminal alkynes **4.23** as the 2-oxoaldehyde surrogate for the synthesis of 1-aryl-*β*-carbolines **4.24**.[276] The suggested mechanism would be the previously described in **Scheme 97**, but with the previous transformation of the alkyne **4.23** into 2-iodo-1-phenylethan-1-one **4.25** which is oxidized in situ to afford the 2-oxoaldehyde (**Scheme 100**).

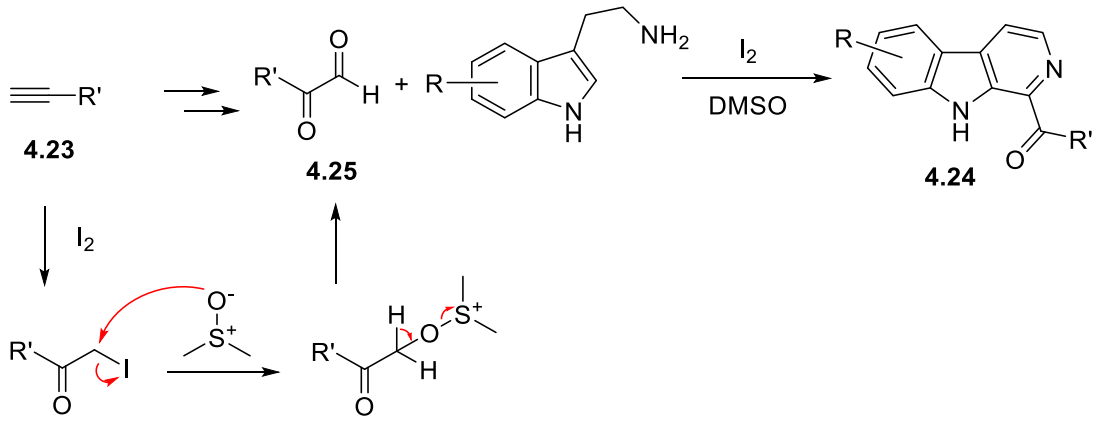

Scheme 100. *Iodine-mediated oxidative Pictet-Spengler reaction using terminal alkynes.*

Another classical method for the snynthesis of of *β*-carbolines is the Bischler-Napieralski reaction (**Scheme 101**). Discovered in 1893, this intramolecular electrophilic aromatic substitution reaction also starts with a tryptamine derivative **4.21**, like the Pictet-Spengler reaction, but for this reaction it needs to be acylated first.[277] The acylated substrate generated **4.26** is treated with phosphoryl chloride to induce the cyclodehydration that terminates on the dihydro-*β*-carboline specie **4.27**. As in the Pictet-Spengler, an additional oxidation step is required for the aromatization of the carboline, but the intermediates that the Bischler-Napieralski reaction produce are easier to oxidise.

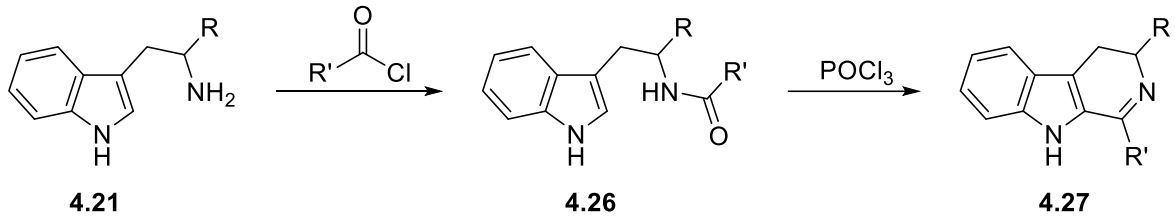

Scheme 101. *General scheme for the Bischler-Napieralski reaction.*

In 2016, T. P. Singh and O. M. Singha reported an adapted one-pot Bischler-Napieralski reaction of 1-substituted tetrahydro-*β*-carbolines **4.28** by cyclocondensation of ketene *S,S*–acetals **4.29** with tryptamine **4.21** in the presence of $InCl_3$ and TFA as co-catalysts by Bischler-Napieralski cyclization. The mechanism is similar to the reported process for the Bischler-Napieralski, starting with attack of the amine of tryptamine to the electrophilic carbon of the ketene *S,S*-acetal **4.29** in the presence of $InCl_3$ (**Scheme 102**).[278]

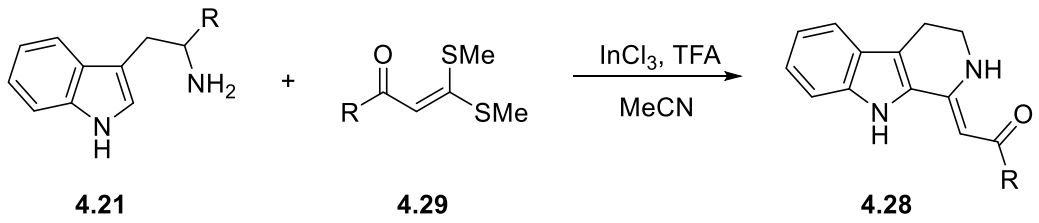

4.21 **4.29** **4.28**

Scheme 102. *One-pot Bischler-Napieralski reaction by T. P. Singh and O. M. Singha.*[23]

An alternative to the previous methods using tryptamine is the Cadogan cyclisation, providing *β*-carbolines from nitrophenylpyridines. T. Kametani and co-workers published details of the reaction between 4-(2-nitrophenyl)nicotinates **4.30** and triethyl phosphite. The pyridines obtained from a Hantzsch-type process, were heated in the presence of an excess of triethyl phosphite to provide the carboline species **4.31**, but in poor yields (**Scheme 103**).[279] The synthesis of carboline scaffolds using the Cadogan method with a triphenylphosphine-mediated cyclization of nitropyridines has been previously studied in the group.[7]

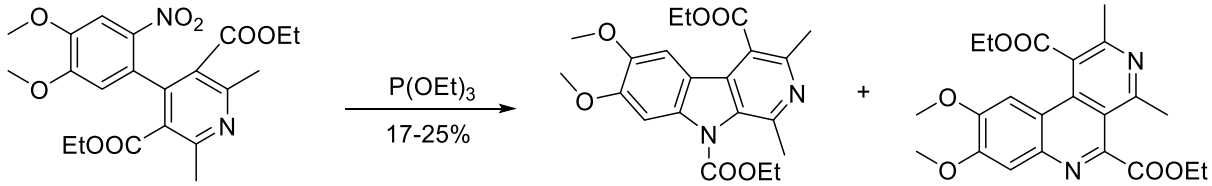

4.30 **4.31a** **4.31b**

Scheme 103. *Cadogan cyclisation reaction.*

Similar methods starting from pheylpyridines have been reported, such as the published route by Dhara's group. They developed an easy access to halocarbolines **4.32** under mild reaction conditions using $Pd(OAc)_2/Cu(OAc)_2$ as a catalytic system via C-H activation (**Scheme 104**). They also demonstrated that these halocarbolines **4.32** could be further modified with additional cross-coupling reactions.

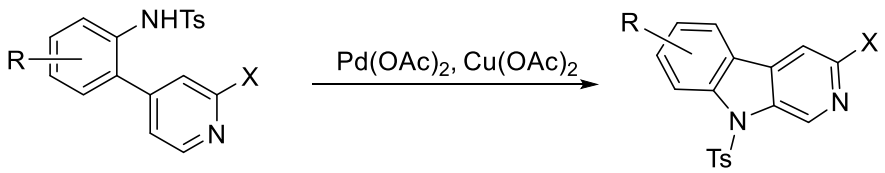

4.32

Scheme 104. *Synthetic approach to halo-β-carbolines using C-H activation chemistry.*

Tom G. Driver *et al.* used rhodium catalysis to access *N*-methylated *δ*-carbolines via ring closure of aryl azides (**Scheme 105**).[280] The azide precursors **4.33** were prepared from 2-bromoanilines

through a Suzuki cross coupling reaction, with subsequent azidation and methylation. The treatment of the azide **4.33** with $[Rh_2(esp)_2]$ in DCE at 70 °C produced the carbolinium ion intermediates **4.34**, which following deprotonation furnished the *N*-methylated *δ*-carbolines **4.35** in excellent yields. They also reported that this method was also amenable for the synthesis of *β*-carbolines, *α*-carbolines, and *γ*-carbolines.

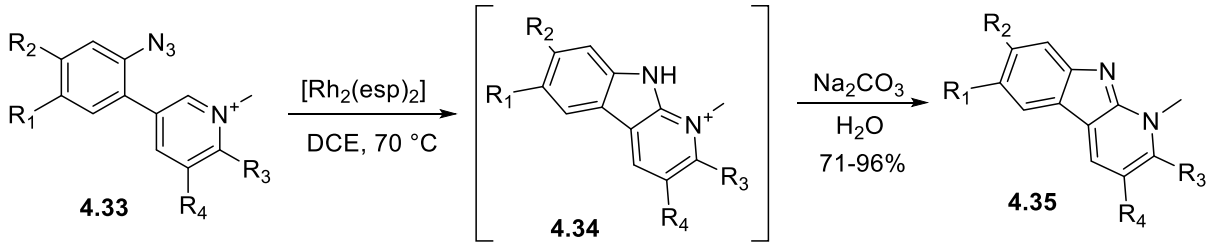

Scheme 105. *RhII-Catalyzed Synthesis of α-, β-, or δ- carbolines from aryl azides.*

Following these examples, it was hypothesised that a novel route to *β*-carbolines, with improved yield and without unwanted substitution in the pyridyl and phenyl rings could be achieved by adaptation of the synthetic pathway to carbazoles using reagentless technologies, as described previously. Thus, the aim was to synthesise different pyridoanilines from anilines and pyridyl boronic acids and submit them to the flow process for azide formation and photochemical cyclisation to allow the synthesis of a library of diverse substituted *β*-carbolines in useful quantities for biological evaluation (**Scheme 106**). If successful, the *N*-substitution of the obtained *β*-carbolines could also be explored in order to improve the potency or selectivity of desired compounds.

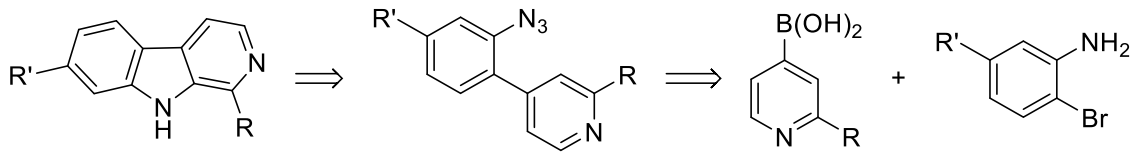

Scheme 106. *An approach for the synthesis of δ- and β-carbolines.*

4.2.1. Synthesis of carbolines

After the success of the developed method for the synthesis of *N*-ethylated carbazoles, and some natural occurring carbazoles, an attempt was made to adapt the route to the synthesis of carboline scaffolds, starting with *β*-carbolines. Thus, *β*-carbolines **4.36** could be generated by using a photochemical cyclization of the corresponding azidophenylpyridines originating from the pyridoaniline **4.37** species in flow, which would be obtained after the cross-coupling reaction of a pyridine boronic acid and a bromoaniline (**Scheme 107**).

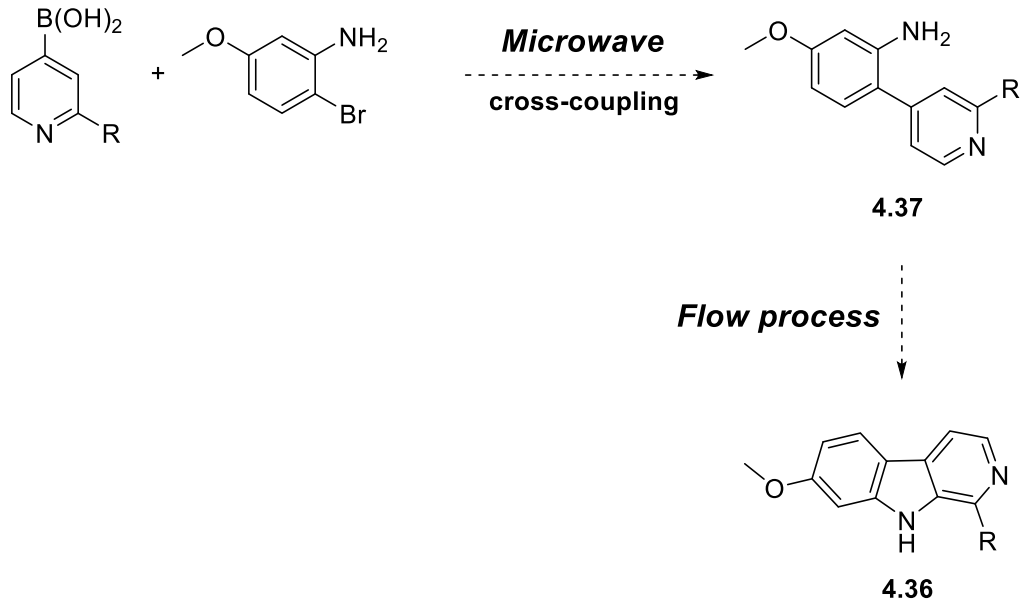

Scheme 107. *Synthetic proposal for the synthesis of β-carbolines.*

4.2.1.1 Suzuki-Miyaura cross-coupling reaction.

The synthesis of the pyridoaniline intermediates started, again, with the Suzuki cross coupling reaction. The investigation started with the simplified version of the pyridines, as a test for this reaction and the following steps. After proving the viability of the reaction for compounds **4.38** and **4.39**, the desired precursors for harmine (**4.15**) and two analogues were then investigated. The results of this study are shown in **Table 21**.

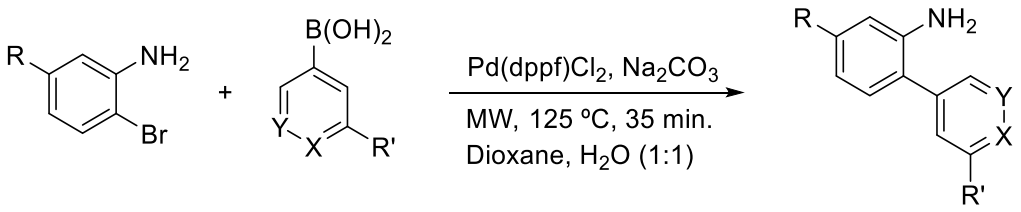

***Table 21**. Suzuki coupling reaction results.*

Entry	X	Y	R	R'	Compound	Yield (%)[a]
1	CH	N	H	H	**4.38**	96
2	N	CH	H	H	**4.39**	73
3	N	CH	OCH_3	H	**4.40**	97
4	N	CH	OCH_3	CH_3	**4.41**	66
5	N	CH	OCH_3	OCH_3	**4.42**	87

a) *Isolated yield after flash column chromatography.*

As shown in **Table 21**, this step did not cause any major issues when changing the nature of the boronic acid from phenyl to pyridinyl. For these molecules, $Pd(dppf)Cl_2$ was used as there were no substituents at the *ortho* position to the boronic acid, and so the same conditions used for the synthesis of biphenyls were applied. The reaction showed good results for the synthesis of 3-pyridinyl **4.38** (entry 1), and a slight decrease in yield for the synthesis of 4-pyridinyl derivative **4.39** (entry 2). This phenomenon could suggest that the presence the nitrogen closer to the boronic acid might help the reaction. The reaction also worked very well for compounds **4.40** and **4.42** (entries 3 and 5), which could mean that an electron donating group, such as the methoxy group, could improve the reactivity of the aniline, but a small reduction in yield was observed for the synthesis of compound **4.22** (entry 4). The reaction was repeated but the yield could not be improved. A potential reason for the lower efficiency could be the acidity of the methyl group at the α-position of the pyridine, which in basic media could have interfered with the reaction. The identification and characterization of these compounds was carried out in exactly the same way as for their biphenyl analogues. By ^{1}H-NMR spectroscopy the presence of the characteristic signals of the pyridine ring in addition to the aromatic aniline resonances indicated the presence of the product. The ^{1}H-NMR spectra of compound **4.42** is displayed in **Figure 52** as an example. This information was supported by HRMS confirming the exact mass of the product.

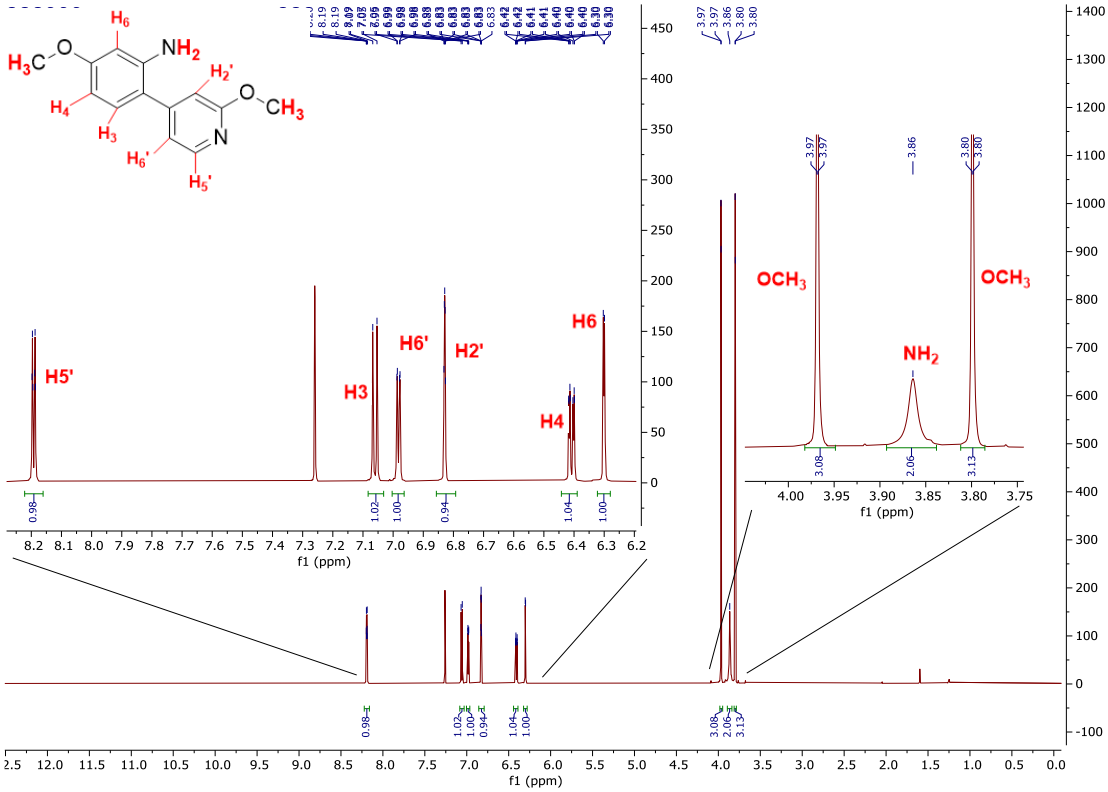

Figure 52. *^{1}H-NMR spectrum of 4-phenylpyridine* ***4.42****.*

The Suzuki-Miyaura cross-coupling reaction proved to be adaptable to the synthesis of pyridoanilines, and 5 compounds of this kind could be synthesised in good yields (66-96%) for study in the next step of the synthetic pathway.

4.2.1.2 Azide formation.

Following the success of synthesising different pyridoaniline scaffolds in good yield and useful quantities in the previous step, the synthetic pathway proceeded with the azide formation step, which had already been investigated in the early stages of method development (see Chapter 2). As mentioned in section 2.3.1, the azide formation reaction with pyridine functionality present could not be adapted and transferred from batch to a flow process, and so, for this method, this reaction and the following photocyclization had to be conducted separately. The investigation of the azide formation reaction started with 3-azidopyridine (**2.39**) as an electron poor substrate, assuming the success on optimizing this reaction should be applicable to biphenyls and pyridoanilines. After success in synthesising 3-azidopyridine (**2.39**) in a yield of 85%, 3-azido-2-phenylpyridine (**4.43**) was now investigated as a commercially available amine precursor that could facilitate azide formation and undergo cyclization to an *α*-carboline. The reaction conditions were the same employed for the synthesis of 3-azidopyridine and are displayed in **Scheme 108**.

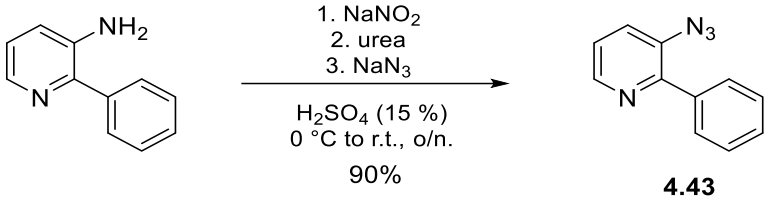

4.43

Scheme 108. *Synthesis of 3-azido-2-phenylpyridine (**4.43**).*

The reaction provided the same excellent results for the 2-phenyl analogue which was prepared in 90% yield (**Scheme 107**), suggesting that steric hindrance was not a problem in the azide forming process. After the two successful tests with commercially available aminopyridines, the next step was to study the reaction with the pyridoanilines previously synthesised. The results for azide formation using pyridoanilines **4.38-4.42** are reported in **Table 22.**

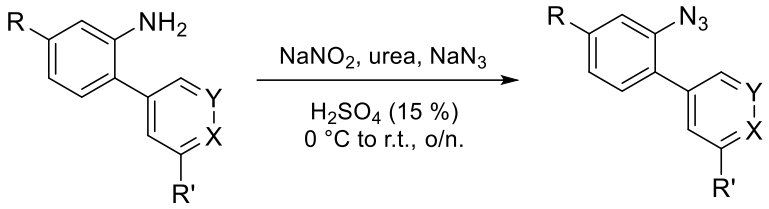

Table 22*. Azide formation under batch conditions.*

Entry	SM	X	Y	R	R'	Compound	Yield (%)[a]
1	**4.38**	H	N	H	H	**4.44**	89
2	**4.39**	N	H	H	H	**4.45**	91
3	**4.40**	N	H	OCH_3	H	**4.46**	97
4	**4.41**	N	H	OCH_3	CH_3	**4.47**	66
5	**4.42**	N	H	OCH_3	OCH_3	**4.48**	87

a) Isolated yield after neutralization with sat. $NaHCO_3$ and extraction with diethyl ether.

Although the reaction did not provide quite the same level of efficiency as it did for carbazoles, it provided good yields for the 5 compounds, with superior performance for the synthesis of compound **4.46** (entry 3). Interestingly, once again the compound containing a methyl group adjacent to the nitrogen of the pyridine ring provided the worst results, suggesting that the acidity of this methyl group could be a problem that deactivated the precursor making it less reactive. In any case, no side products were observed, and this success enabled the continuation of the synthesis with the photocyclization under flow conditions. As stated in Chapter 2, section 2.3.1, after confirming the azide formation by IR for a number of examples, this reaction was normally followed

by ^{1}H-NMR spectroscopy. Because these products were unstable intermediates and were used directly in the next step, no further characterization was carried out. Nonetheless, the ^{1}H-NMR spectra of the crude material not only appeared essentially pure and ready to use in the next step, but also provided good confirmation of successful transformation. The ^{1}H-NMR spectrum of compound **4.48** is displayed in **Figure 52** (red line) in superposition with the starting material spectrum (compound **4.42**, blue line) as an example. It can be clearly observed that, apart from the disappearance of the NH_2 peak observed on the corresponding pyridoaniline (which ^{1}H-NMR spectra is displayed in **Figure 53** and has been discussed previously), the shifts of most of the signals had changed in the product, especially the ones from the aniline ring, with signals for protons H4 and H6 appearing around δ 0.5 ppm downfield.

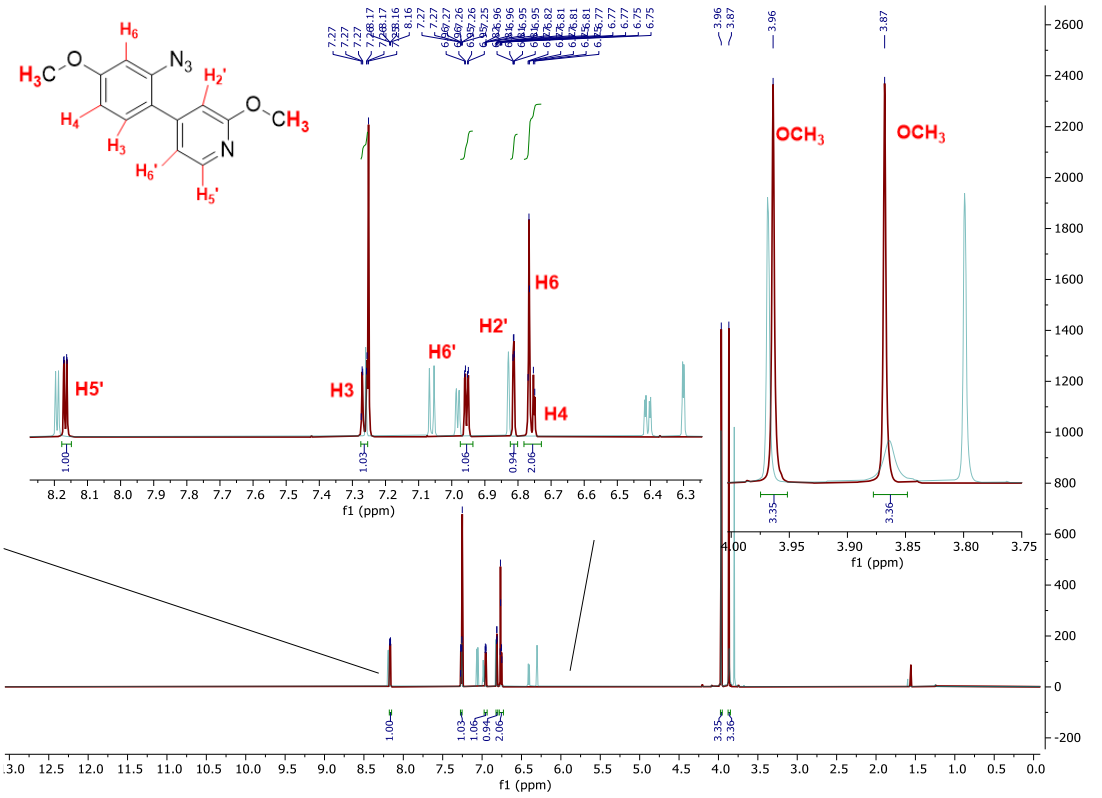

Figure 53. *^{1}H-NMR spectra of azide **4.48** (red line) superposed to the ^{1}H-NMR spectra of the amine precursor **4.42** (blue line) for comparison.*

In summary, despite of not being able to be adapted to flow processing, the azide formation reaction could be achieved in batch, providing good yields for most of the compounds and enabling the continuation of the synthesis. Thus, the azidophenyl pyridines synthesised herein were transferred to the flow reactor in order to be irradiated with visible light in the photochemical reactor.

4.2.1.3 Photocylization.

Once the azide intermediates needed for the photocyclization were synthesised, the following step was the photocyclization of the biaryl compounds to give the corresponding carboline skeleton. First attempts at this reaction, conducted at early stages of the investigation, were carried out using the 3-azido-2-phenylpyridine (**4.43**), previously synthesised, in DMF, but the ^{1}H-NMR spectrum of the crude reaction mixture indicated that only starting materials were present. However, a water-promoted method in the presence of silica (0.1 g / mmol azide) as solid surface support did appear to enable cyclization to carboline **4.49** (**Table 23**).[144]

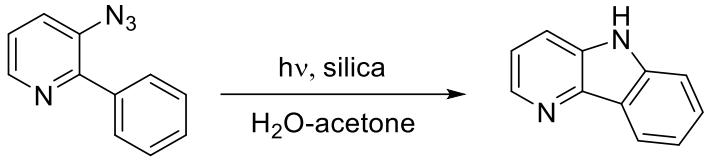

4.43 **4.49**

Table 23. *Results for the synthesis of α-carboline **4.49**.*

Entry	Technique	Time	Temperature	Conv. (%)[a]
1	Batch	3 days	rt	20
2	Flow	100 min	55	17

a) *Conversion calculated by integration of the ^{1}H -NMR signals of the crude material.*

The results displayed in **Table 23** were encouraging. The ^{1}H-NMR spectroscopic analysis showed a 20% conversion (1:4 ratio) in batch (entry 1). The reaction was then transferred to flow processing. As the desired amount of **4.43** was not soluble in 2 mL of H_2O-acetone (1:1), the ratio of acetone in the solvent mixture was increased to 1:5. Then, the reaction was conducted under similar conditions, and the conversion was found to be about 17% (1:5 ratio of conversion by ^{1}H-NMR spectroscopic analysis) in a noticeably reduced time (entry 2). Unfortunately, this yield could not be optimized further with longer reaction times or increasing the reaction temperature or pressure. The next step, then, was to investigate the reaction in dichloromethane and heating the mixture to 80 °C for 2 hours (**Scheme 109**). Azides **4.44** and **4.45** were used for these tests, and the results were not exceptional but led to some useful conclusions.

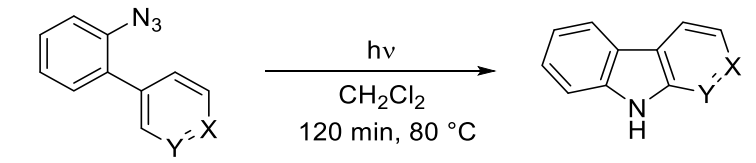

4.44 X = H, Y = N
4.45 X = N, Y = H

4.50 X = H, Y = N
4.51 X = N, Y = H

Scheme 109. *Synthesis of carbolines using photochemistry at elevated temperature.*

These two compounds caused a blockage in the flow reactor, suggesting that the resulting carbolines **4.50** and **4.51** might not be soluble in the selected solvent. For this reason, the reaction solvent was changed to 1,4-dioxane to avoid solubility issues. After analysis of ^{1}H-NMR spectra of the two crude reaction mixtures, carboline **4.50** exhibited the expected regioselectivity issue and provided a complex mixture with the presence of some starting material. This did not happen with compound **4.51**, although starting material could still be observed in a ratio 1:1 with a new formed product.

Given the success synthesising the carbazoles in dioxane, carbolines **4.50** and **4.51** were no longer studied and the efforts were focused in harmine (**4.15**) and its analogues. Thus, the three azidophenyl pyridines precursors synthesised in batch were irradiated in the photochemical reaction for 1 h in 1,4-dioxane. The results of this reaction are shown in **Table 24**.

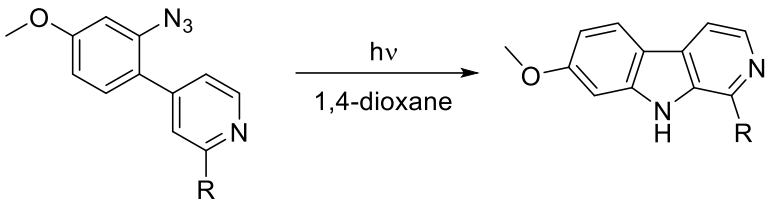

4.40 R = H
4.41 R = CH_3
4.42 R = OCH_3

4.52 R = H
4.15 R = CH_3
4.53 R = OCH_3

Table 24*. Azide formation under batch conditions.*

	Azide	R	Product	Yield (%)[a]
1	**4.40**	H	**4.52**	59
2	**4.41**	CH_3	Harmine (**4.15**)	-
3	**4.42**	OCH_3	**4.53**	45

a) *Isolated yield after flash column chromatography.*

The cyclization provided a good yield for the synthesis of carboline **4.52** (entry 1). However, as expected, the photocyclization of the azidophenylpyridine **4.47** provided a mixture of regioisomers, in a ratio of 2:3 **4.54**-harmine (**4.15**) (**Scheme 110**). The regioisomers could not be separated by flash column chromatography, as both eluted with the same retention time, and harmine thus could not be isolated. Interestingly, the harmine (**4.15**) regioisomer was favoured, and this was in contrast to the expected steric or electronic effects of the methyl group, but the comparison of the ^{1}H-NMR spectra clearly confirmed the excess of harmine in the crude reaction mixture, which was identified by comparison of data to pure material, which was commercially available.

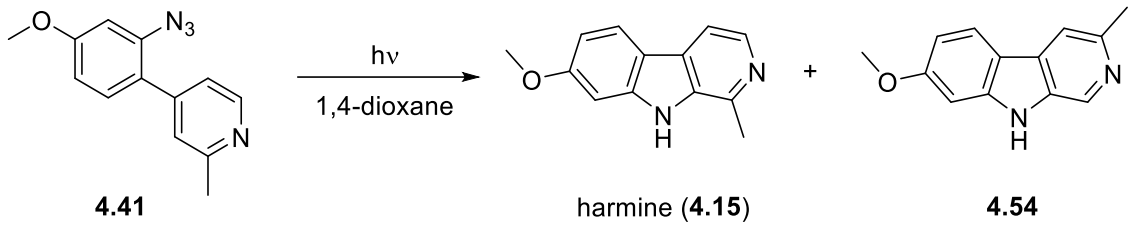

4.41 harmine (**4.15**) **4.54**

Scheme 110. *Photocyclization reaction for the synthesis of harmine (**4.15**) and regioisomer (**4.54**).*

The hypothesis relating to the regioselectivity was that the stability of the carbocation had more of an impact on the product forming steps of the reaction than steric hindrance, especially keeping in mind that the methyl group is not particualy bulky. Supporting this hypothesis was one reason to investigate the methoxy analogue, which should be even more favourable to react to give the analogue with a functional group in position 1. This theory was confirmed when the ^{1}H-NMR spectrum of the crude reaction mixture was analysed and it was observed that the desired regioisomer was the major product, enabling the isolation and characterization of this methoxy analogue **4.53** in moderate yield (entry 3). A comparison of the ^{1}H-NMR spectrum of harmine (**4.15**) and carboline **4.53** is shown in **Figure 54**, where the difference in the conversion for both reactions can be clearly observed.

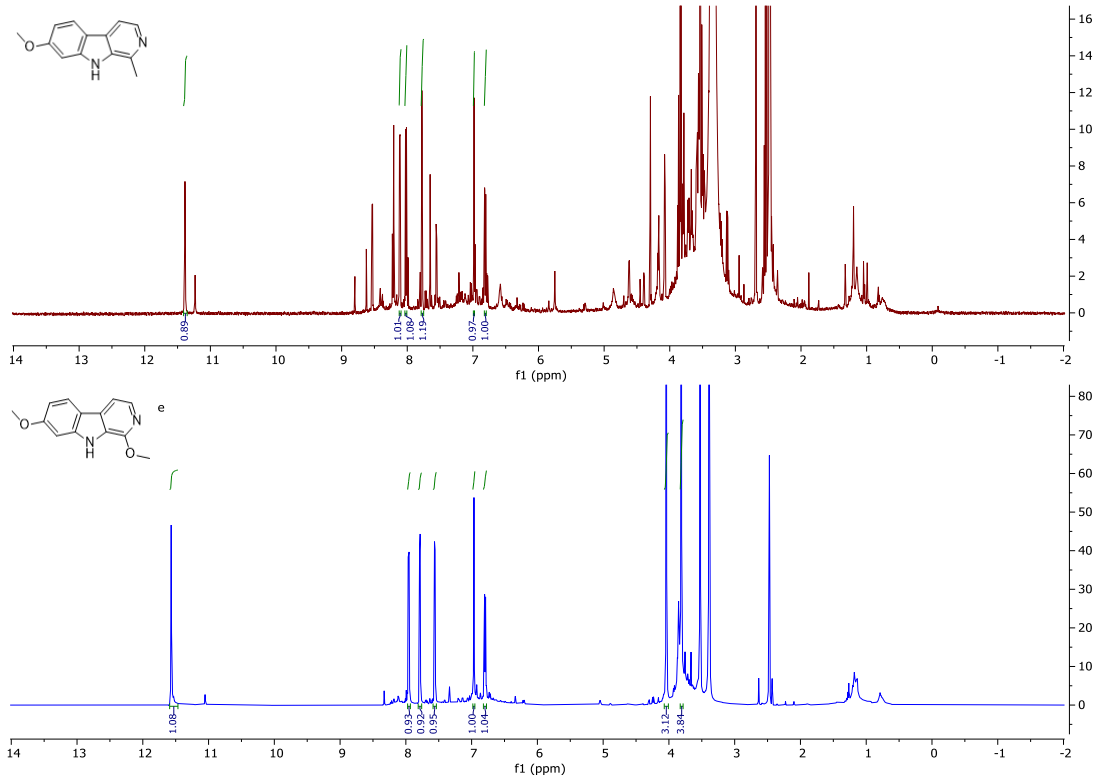

Figure 54. *Comparison between harmine (**4.15**) crude ^{1}H-NMR spectrum (top) and methoxy analogue **4.51** ^{1}H-NMR spectrum (bottom).*

Thus, carboline **4.52** and methoxy-analogue **4.53** were successfully synthesised in yields of 59 and 45%, respectively. The difference in yield can be attributed to the presence of a minor regioisomer that had to be removed. Nevertheless, harmine (**4.15**) could not be isolated due to regioselectivity issues of the reaction, which complicated the purification, as the two regioisomers could not be separated by flash column chromatography.

4.2.1.4 Summary table

A generic scheme for the global synthesis of carbolines plus the results for each of the three steps of the synthesis is shown in **Table 25**. The overall yields for the whole process are also indicated.

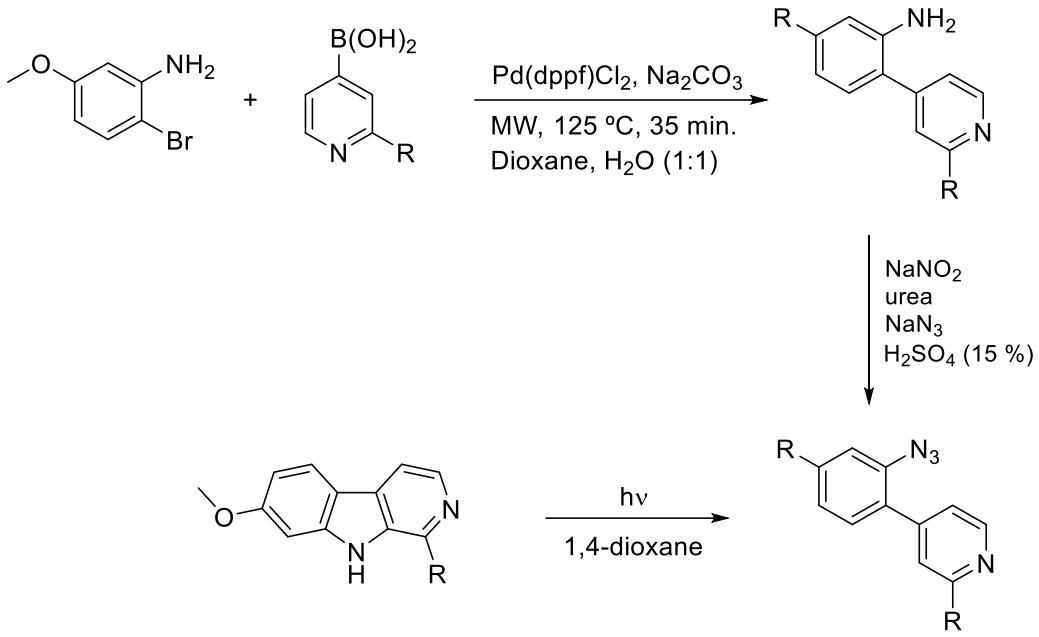

Table 25. *Summary table for the synthesis of β-carbolines.*

Entry	Compound	R	Cross-coupling yield (%)[a]	Azide formation yield (%)[a]	Photocylization yield (%)[a]	Overall yield (%)[a]
1	**4.52**	H	97	77	59	44
2	**4.15**	CH_3	66	88	-	-
3	**4.53**	OCH_3	87	79	45	31

a) Isolated yield after flash column chromatography.

β-Carbolines **4.52** and **4.53** were synthesised in moderate overall yield from the corresponding pyridineboronic acids. The higher yield for compound **4.52** was a combination of the exceptional yield in the cross-coupling step and the relatively efficient photocyclization reaction. On the other hand, the synthesis of **4.53** was shown to be more regioselective than the synthesis of harmine (**4.15**), eliminating almost completely the problem of regioselectivity that the natural product analogue presented. However, although the cross-coupling reaction yield was good, a moderate yield in the azide formation step and lower efficiency for photocyclization, probably caused by the presence of a regioisomer as stated above, reduced the efficiency of the route. The method was demonstrated to be adaptable but less efficient than the synthesis of carbazoles. Not only were the yields lower, for each step and for the total synthesis, even with one less step, but the necessity of separating the steps of the flow process and the difficulty of separating regioisomers suggested that this route was not as widely applicable as the approach for the synthesis of carbazoles.

4.2.1.4 Harmine *N*-functionalization

N-Functionalization of harmine can also lead to biologically interesting carbolines. The presence of a nitrile group in the N-ethyl chain appeared as a promising target to improve the selectivity of harmine. Although harmine could not be synthesised by the method developed, it is a readily available building block, which allowed us to continue our investigation on this type of compound. The first approach attempted to reproduce the conditions that were successful for the *N*-functionalization of carbazoles, but using bromoacetonitrile (**Scheme 111**).

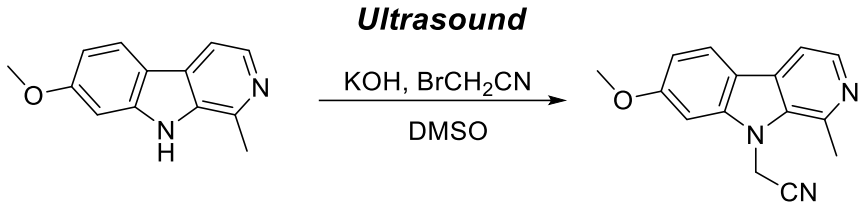

Scheme 111. *Harmine (**4.15**) N-functionalization reaction using sonochemistry.*

The reaction did not provide good results, and the conversions could not be improved to more than 20%. The reaction was attempted under microwave irradiation and under solvent free conditions in a mixer mill, but none of these methods provided the target compound. A last attempt was carried out using iodoethane, as it proved to be adequate for the *N*-functionalization of carbazoles and would open the possibility of exploring new groups to attach to the nitrogen (**Scheme 112**).

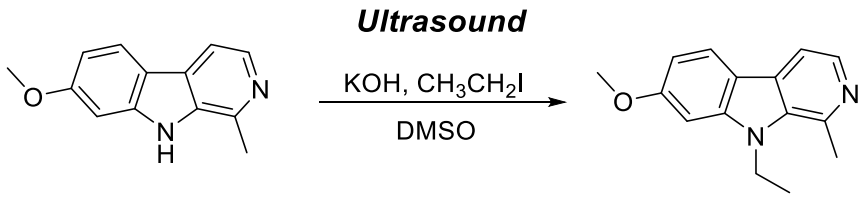

Scheme 112. *Harmine (**4.15**) N-functionalization reaction scheme using iodoethane.*

This reaction did not proceed either, and in the end it was assumed that carbolines were too electron poor to attach the electrophile or were reacting through the pyridine lone pair competitively, and a whole process of optimization would be necessary to establish the *N*-functionalization of this class of compounds, which was discarded due to time restrictions.

4.3 Conclusions

The synthetic method described in Chapter 2 has been adapted to provide a highly efficient novel route utilizing reagentless techniques for the synthesis of carbazole-based natural products in useful quantities. Clausine C (**4.1**) and clausine N (**4.2**) were synthesised in good yields (65% and 61% with an additional step, respectively). The two natural products were isolated and fully characterized, and the ^{1}H-NMR and ^{13}C-NMR spectroscopic data have been compared to those previously reported in the literature in order to confirm the identity of the products. Clausine V (**4.8**), was synthesised but could not be purified. However, the comparison of the ^{1}H-NMR spectroscopic data of the crude reaction mixture with the formerly published in the literature gave encouraging evidence of the presence of the compound, indicating that the chemistry was successful, but the purification still needed to be optimized.

Glycosinine (**4.6**) and mukonal (**4.7**) could not be synthesised from the 2-methoxy- and 2-hydroxy-9*H*-carbazole using the conditions for the Rieche formylation of *N*-ethylated carbazoles, as the free nitrogen appeared to impede this reaction. An alternative approach was studied for the synthesis of clausine L (**4.4**), utilizing the synthetic route described in Chapter 2 with a methyl ester in place (demonstrated for the synthesis of the p53 reactivators) could provide clausine L (**4.4**), which would serve as a starting material for the synthesis of glycosinine (**4.6**) and mukonidine (**4.5**). Nevertheless, the presence of carbonyl groups on the aromatic ring seemed to interfere in the photocyclization. Thus, the methodology developed proved not to be suitable for the synthesis of these natural products.

The synthetic method was proved to be adaptable, but less efficient, for the synthesis of *β*-carbolines. The main issue experienced was the inability to conduct the azide formation reaction in flow, which resulted in an additional step to the synthesis, the isolation and handling of organic azides, and a decrease in the yield of each step and the overall yield, even without the *N*-ethylation step. These facts combined with new difficulties introduced by issues of regioiselectivity in the cyclization suggested that this route was not as applicable to the synthesis of carbolines. Nonetheless, carbolines **4.50** and **4.51** were synthesised successfully in overall yields of 44 and 31% respectively. Harmine (**4.15**) could not be isolated due to the regioselectivity issues of reaction.

4.4 Experimental

4.4.1 Synthesis of carbazole-containing natural products

Methyl 6-amino-4'-(methoxy)-[1,1'-biphenyl]-3-carboxylate (4.9). Prepared according to General Procedure A using a solution of methyl 3-iodo-4-aminobenzonate (554 mg, 2.0 mmol, 1.0 equiv.), 4-methoxybenzeneboronic acid (395 mg, 2.6 mmol, 1.3 equiv.), Na_2CO_3 (848 mg, 8.0 mmol, 4.0 equiv.) and $Pd(dppf)Cl_2$ (75 mg, 5 mol%) in dioxane-water (1:1) (14 mL) n a pressure-rated sealed tube (35 mL). Purification by flash column chromatography on SiO_2 (12 g), eluting with hexane-EtOAc (4:1) gave the *title compound* (0.36 g, 70%) as a yellow solid.

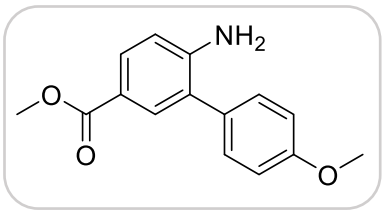

Mp: 52-55 °C. **Purity (LCMS):** 95%. **Found [ESI]:** MH^+, 258.1121. $C_{15}H_{16}NO_3$ [MH] requires 258.1130. **IR** (neat) *v*/cm^{-1} 3469, 3364 (NH_2), 2948 (C-H), 1737 (C=O), 1631 (C-C), 1234 (C-O), 770 (C-H). **^{1}H NMR** (600 MHz, $CDCl_3$) δ 7.80 (2H, m, H-3, H-5), 7.35 (2H, AA'XX', *J* 8.5, 3.0, 2.0, H-2'), 6.98 (2H, AA'XX', *J* 8.5, 3.0, 2.0, H-3'), 6.71 (1H, d, *J* 8.5, H-6), 4.15 (2H, s, NH_2), 3.85 (3H, s, OMe), 3.84 (3H, s, OMe). **^{13}C NMR** (151 MHz, $CDCl_3$) δ 167.3 (C=O), 159.0 (C), 148.2 (C), 132.4 (CH), 130.5 (C), 130.2 (CH), 130.2 (CH), 126.2 (C), 119.7 (C), 114.4 (CH), 114.3 (CH), 55.3 (OMe), 51.7 (OMe).

Clausine C (4.1). Prepared according to General Procedure C using a solution (A) of (2'- fluoro-4'-trifluoromethylphenyl)aniline (715 mg, 2.3 mmol, 1.0 equiv.; 0.1 M) and $TMSN_3$ (0.33 mL, 2.5 mmol, 1.1 equiv.; 0.1 M) in dioxane (23 mL) and a solution (B) of *t*-BuONO (0.45 mL, 3.8 mmol, 1.5 equiv.; 0.2 M) in dioxane (17 mL). Purification by flash column chromatography on SiO_2 (24 g), eluting with hexane-CH_2Cl_2, (4:1) gave the *title compound* (0.46 g, 65%) as a yellow solid.

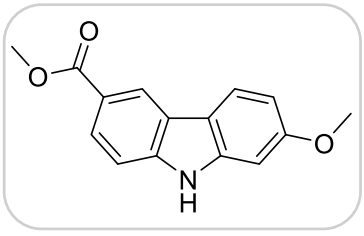

Mp: 195-196 °C (lit:[281] 193-195 °C). **Found [ESI]:** MH^+, 256.0977. $C_{15}H_{14}NO_3$ [MH] requires 256.0974. **^{1}H NMR** (600 MHz, Acetone-*d6*) δ 10.63 (1H, s, N-H), 8.69 (1H, s, H-4), 8.11 (1 H, d, *J* 8.5, H-5), 7.99 (1 H, d, *J* 8.5, H-2), 7.51 (1H, d, *J* 8.5, H-1), 7.09 (1H, s, H-8), 6.89 (1H, dd, *J* 8.5, 1.5, H-6), 3.90 (3H, s, OMe), 3.88 (3H, s, OMe). **^{13}C NMR** (151 MHz, Acetone-*d6*) δ 167.1 (C=O), 159.7 (C), 142.9 (C), 142.1 (C), 125.7 (CH), 123.1 (C), 121.3 (CH), 121.2 (CH), 120.9 (C), 116.6 (C), 110.2 (CH), 108.9 (CH), 94.9 (CH), 54.9 (OMe), 51.0 (OMe).

Clausine N (4.2). A solution of Clausine C (300 mg, 1.2 mmol, 1.0 equiv.) and NaOH (188 mg, 4.7 mmol, 4 equiv.) in 1,4-dioxane:water (3:1) (10 mL) was stirred at reflux overnight. The reaction was allowed to cool to room temperature and was acidified to pH 3 with HCl (1M). Extraction with EtOAc gave the *tittle compound* (0.26 g, 95% yield) as a yellow solid.

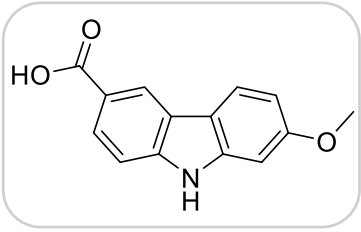

Mp: 280-282 °C (lit:[282] 282-284 °C). **Found [ESI]:** MH^+, 242.0834. $C_{14}H_{12}NO_3$ [MH] requires 242.0817. **^{1}H NMR** (600 MHz, Acetone-*d6*) δ 10.59 (1H, s, N-H), 8.72 (1H, s, H-4), 8.10 (1H, d, *J* 8.5, H-5), 8.02 (1H, dd, *J* 8.5, 1.5, H-2), 7.51 (1H, d, *J* 8.5, H-1), 7.08 (1H, d, *J* 2.5, H-8), 6.88 (1H, dd, *J* 8.5, 2.5, H-6), 3.88 (3H, s OMe), 3.30 (1H, s, OH). **^{13}C NMR** (151 MHz, Acetone-*d6*) δ 167.8 (C=O), 159.7 (C), 143.0 (C), 142.2 (C), 126.0 (CH), 123.0 (C), 121.6 (CH), 121.2 (C), 121.1 (CH), 116.7 (C) 110.1 (CH), 108.8 (CH), 94.9 (CH), 54.9 (OMe).

4.4.2 Synthesis of pyridoanilines

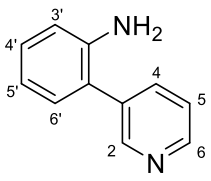

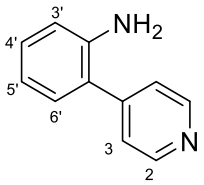

3-(2'-Aminophenyl)pyridine (4.38). 3-Pyridineboronic acid (324 mg. 2.6 mmol, 1.3 equiv), Na_2CO_3 (540 mg, 4 mmol, 4 equiv), $PdCl_2$(dppf) (5% mmol, 74 mg) and 2-bromoaniline (0.25 mL, 2 mmol, 1.0 equiv) were dissolved in a dioxane:H_2O (1:1). The reaction mixture was heated at 125 °C for 30 min in a Microwave reactor. Then, the reaction mixture was diluted with a 2 M aqueous solution of NaOH and 30 mL of CH_2Cl_2. The phases were separated and the resulting aqueous phase was extracted with of CH_2Cl_2 (3 x 30 mL). The combined organic phases were dried over Na_2SO_4, filtered and concentrated under pressure. The residue was purified by flash column chromatography (EtOAc) to furnish the *title compound* (327 mg, 96% yield) as a beige solid.

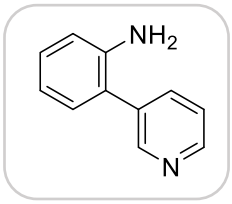

^{1}H NMR (600 MHz, Chloroform-*d*) δ 8.74 (1H, s, H-2), 8.62 (1H d, *J* 5.0, H-6), 7.81 (1H, d, *J* 8.0, 2.0, H-4), 7.38 (1H, dd, *J* 8.0, 5.0, H-5), 7.20 (1H, ddd, *J* = 8.0, 8.0, 1.5, H-4'), 7.10 (1H, dd, *J* 7.5, 1.5, H-6'), 6.85 (1H, ddd, *J* 8.0, 7.5, 1.0, H-5'), 6.79 (1H, dd, *J* 8.0, 1.0, H-3'), 3.54 (2H, s, NH_2).

4-(2'-Aminophenyl)pyridine (4.39). 4-Pyridineboronic acid (324 mg. 2.6 mmol, 1.3 equiv), Na_2CO_3 (540 mg, 4 mmol, 4 equiv), $PdCl_2$(dppf) (5% mmol, 74 mg) and 2-bromoaniline (0.25 mL, 2 mmol, 1.0 equiv) were dissolved in a dioxane:H_2O (1:1). The reaction mixture was heated at 125 °C for 30 min in a Microwave reactor. Then, the reaction mixture was diluted with a 2 M aqueous solution of NaOH and 30 mL of CH_2Cl_2. The phases were separated and the resulting aqueous phase was extracted with of CH_2Cl_2 (3 × 30 mL). The combined organic phases were dried over Na_2SO_4, filtered and concentrated under pressure. The residue was purified by flash column chromatography (EtOAc) to furnish the *title compound* (247 mg, 73% yield) as a beige solid.

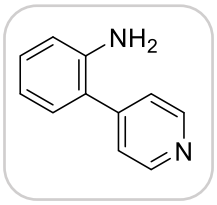

^{1}H NMR (600 MHz, Chloroform-*d*) δ 8.75 – 8.53 (2H, m, H-2), 7.43 (2H, m, H-3), 7.20 (1H, ddd, *J* 8.0, 7.5, 1.5, H-4'), 7.12 (1H, dd, *J* 7.5, 1.5, H-6'), 6.85 (1 H, ddd, *J* 7.5, 7.5, 1.0, H-5'), 6.77 (1 H, dd, *J* 8.0, 1.0, H-3').

2-(Pyridin-4'-yl)-5-methoxyphenylamine (4.40). Prepared according to General Procedure A using a solution of 2-bromo-5-methoxyaniline (404 mg, 2.0 mmol, 1.0 equiv.), 4-pyridylboronic acid (320 mg, 2.6 mmol, 1.3 0equiv.), Na_2CO_3 (848 mg, 8.0 mmol, 4.0 equiv.) and Pd(dppf)Cl_2 (73 mg, 5 mol%) in dioxane-water (1:1) (14 mL) in a pressure-rated sealed tube (35 mL). Purification by flash column chromatography on SiO_2 (12 g), eluting with CH_2Cl_2:MeOH (9:1) gave the *title compound* (0.25 g, 62%) as a colourless solid.

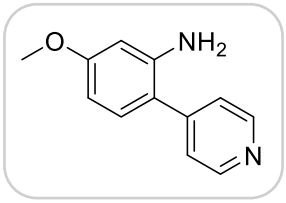

Mp: 147-148 °C (lit:[283] 143-145°C). **Purity (by LCMS):** 97%. **Found [ESI]:** MH^+, 201.1016. $C_{12}H_{13}N_2O$ [MH] requires 201.1022. **IR** (neat) *v*/cm^{-1} 3412, 3326 (NH_2), 2974 (C-H), 1609 (C-C), 1206 (C-O). **^{1}H NMR** (600 MHz, $CDCl_3$) 8.63 (2H, AA'XX', *J* 6.0, 1.5, H-3'), 7.42 (2H, AA'XX', *J* 6.0, 1.5, H-2'), 7.07 (1H, d, *J* 8.5, H-3), 6.44 (1H, dd, *J* 8.5, 2.5, H-4), 6.32 (1H, d, *J* 2.5, H-6), 3.81 (3H, s, OMe). **^{13}C NMR** (151 MHz, $CDCl_3$) δ 161.1 (C), 149.9 (CH), 147.8 (C), 144.7 (C), 131.3 (CH), 123.9 (CH), 117.4 (C), 105.0 (CH), 101.3 (CH), 55.2 (OMe).

2-(3'-Methylpyridin-4'-yl)-5-methoxyphenylamine (4.41). Prepared according to General Procedure A using a solution of 2-bromo-5-methoxyaniline (203 mg, 1.0 mmol, 1.0 equiv.), 2-methylpyridine-4-boronic acid (178 mg, 1.3 mmol, 1.3 equiv.), Na_2CO_3 (424 mg, 4.0 mmol, 4.0 equiv.) and Pd(dppf)Cl_2 (36 mg, 5 mol%) in dioxane-water (1:1) (14 mL) in a pressure-rated sealed tube (35 mL). Purification by flash column chromatography on SiO_2 (12 g), eluting with CH_2Cl_2:MeOH (9:1) gave the *title compound* (0.14 g, 66%) as a brown solid.

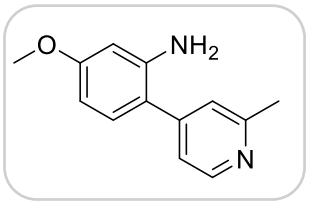

Mp: 137-139 °C. **Purity (by LCMS):** 98% **Found [ESI]:** MH^+, 215.1180. $C_{13}H_{15}N_2O$ [MH] requires 215.1179. **IR** (neat) *v*/cm^{-1} 3322, 3223 (NH_2), 3024 (C-H), 1644 (C-C), 1212 (C-O). **^{1}H NMR** (600 MHz, $CDCl_3$) δ 8.51 (1H, dd, *J* 5.0, 1.0, H-5'), 7.25 (1H, s, H-2'), 7.20 (1H, dd, *J* 5.0 H-6'), 7.05 (1H, d, *J* 8.5, H-3), 6.42 (1H, dd, *J* 8.5, 2.5, H-4), 6.31 (1H, d, *J* 2.5, H-6), 3.83 (2H, s, NH_2), 3.80 (3H, s, OMe), 2.59 (3H, s, Me),. **^{13}C NMR** (151 MHz, $CDCl_3$) δ 161.0 (C), 158.6 (CH), 149.0 (C), 148.2 (C), 144.7 (C), 131.2 (CH), 123.4 (CH), 121.0 (CH), 117.6 (C), 104.9 (CH), 101.3 (CH), 55.2 (OMe), 24.3 (Me).

2-(3'-Methoxypyridin-4'-yl)-5-methoxyphenylamine (4.42). Prepared according to General Procedure A using a solution of 2-bromo-5-methoxyaniline (404 mg, 2.0 mmol, 1.0 equiv.), 2-methoxypyridine-4-boronic acid (398 mg, 2.6 mmol, 1.3 equiv.), Na_2CO_3 (848 mg, 8.0 mmol, 4.0 equiv.) and $Pd(dppf)Cl_2$ (73 mg, 5 mol%) in dioxane-water (1:1) (14 mL) in a pressure-rated sealed tube (35 mL). Purification by flash column chromatography on SiO_2 (12 g), eluting with CH_2Cl_2:MeOH (9:1) gave the *title compound* (0.40 g, 87%) as a brown solid.

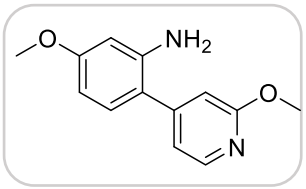

Mp: 124-125 °C. **Purity (LCMS):** 95%. **Found [ESI]:** MH^+, 231.1135. $C_{13}H_{15}N_2O_2$ [MH] requires 231.1134. **IR** (neat) *v*/cm^{-1} 3410, 3314 (NH_2), 2946 (C-H), 1610 (C-C), 1208 (C-O). **^{1}H NMR** (600 MHz, $CDCl_3$) δ 8.19 (1H, d, *J* 5.5, H-5'), 7.06 (1H, d, *J* 8.5, H-3), 6.98 (1H, ddd, *J* 5.5, 1.4, H-6'), 6.86 – 6.80 (1H, m, H-2'), 6.41 (1H, dd, *J* 8.5, 2.5, H-4), 6.30 (1H, d, *J* 2.5, H-6), 3.97 (3H, s, OMe), 3.86 (2H, s, NH_2), 3.80 (3H, s, OMe). **^{13}C NMR** (151 MHz, $CDCl_3$) δ 164.8 (C), 160.9 (C), 150.2 (C), 147.2 (CH), 144.6 (C), 131.1 (CH), 117.6 (C), 117.4 (CH), 110.43 (CH), 104.7 (CH), 101.1 (CH), 55.2 (OMe), 53.5 (OMe).

4.4.3 Synthesis of pyrido phenilazides

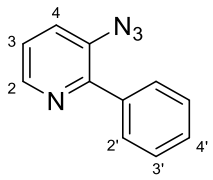

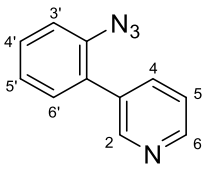

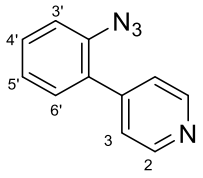

2-(Pyridin-4'-yl)-5-methoxyphenylazide (4.46). A solution of $NaNO_2$ (83 mg, 1.2 mmol, 1.2 equiv.) in H_2O (1.5 mL) was added to solution of 2-(pyridin-4'-yl)-5-methoxyphenylamine. (200 mg, 1 mmol, 1 equiv.) in 15% H_2SO_4 (5 mL) at 0 °C. After 20 min, urea (12 mg, 0.2 mmol, 0.2 equiv.) was added to eliminate the excess of sodium nitrite and 30 min later a solution of NaN_3 (111 mg, 1.7 mmol, 1.7 equiv.) in H_2O (1.5 mL) was added and the reaction mixture was stirred overnight at room temperature. The reaction was then neutralized with $NaHCO_3$ to pH~7 and exctracted with Et_2O (3 x 15

mL). The organic extracts were dried over anhydrous $MgSO_4$, filtered and concentrated under a reduced pressure to afford crude product as a brown solid (0.17 g. 77% yield) which was used on the next step without further purification.

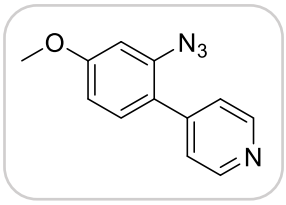

^{1}H NMR (600 MHz, $CDCl_3$) 8.62 – 8.60 (2H, d, *J* 5.5, H-3'), 7.37 (2H, d, *J* 5.5, H-2'), 7.28 (1H, d, *J* = 9.5 Hz, H-3), 6.80 – 6.76 (2H, m, H-1, H-4).

2-(3'-Methylpyridin-4'-yl)-5-methoxyphenylazide (4.47). A solution of $NaNO_2$ (54 mg, 0.8 mmol, 1.2 equiv.) in H_2O (1 mL) was added to solution of 2-(3'-methylpyridin-4'-yl)-5-methoxyphenylamine (140 mg, 0.7 mmol, 1.7 equiv.) in 15% H_2SO_4 (5 mL) at 0 °C. After 20 min, urea (8 mg, 0.1 mmol, 0.2 equiv.) was added to eliminate the excess of sodium nitrite and 30 min later a solution of NaN_3 (72 mg, 1.1 mmol, 1.7 equiv.) in H_2O (1 mL) was added and the reaction mixture was stirred overnight at room temperature. The reaction was then neutralized with $NaHCO_3$ to pH~7 and exctracted with Et_2O (3 x 15 mL). The organic extracts were dried over anhydrous $MgSO_4$, filtered and concentrated under a reduced pressure to afford crude product as a brown solid (138 mg, 88% yield) which was used on the next step without further purification.

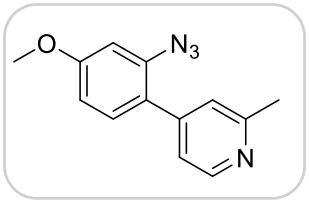

^{1}H NMR (600 MHz, $CDCl_3$) δ 8.49 (1H, d, *J* 5.0 Hz, H-5'), 7.28 – 7.24 (2H, m, H-2', H-3), 7.21 (1H, s, H-6), 7.16 (1H, dd, *J* 5.0, 2.0 Hz, H-6'), 6.77 (2H, m, H-4). 3.80 (3H, s, OMe). 2.59 (s, 3H, Me)

2-(3'-Methoxypyridin-4'-yl)-5-methoxyphenylazide (4.48). A solution of $NaNO_2$ (180 mg, 2.6 mmol, 1.2 equiv.) in H_2O (3 mL) was added to solution of 2-(3'-methoxypyridin-4'-yl)-5-methoxyphenylamine (500 mg, 2.2 mmol, 1.7 equiv.) in 15% H_2SO_4 (5 mL) at 0 °C. After 20 min, urea (26 mg, 0.4 mmol, 0.2 equiv.) was added to eliminate the excess of sodium nitrite and 30 min later a solution of NaN_3 (241 mg, 3.7 mmol, 1.7 equiv.) in H_2O (3 mL) was added and the reaction mixture was stirred overnight at room temperature. The reaction was then neutralized with $NaHCO_3$ to pH~7 and exctracted with Et_2O (3 x 15 mL). The organic extracts were dried over anhydrous $MgSO_4$, filtered and concentrated under a reduced pressure to afford crude product as a brown solid (438 mg, 79% yield) which was used on the next step without further purification.

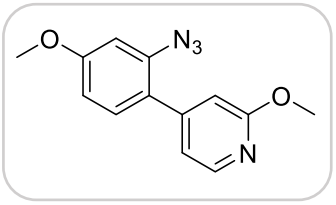

^{1}H NMR (600 MHz, $CDCl_3$) δ 8.17 (1H, d, *J* 5.5, H-5'), 7.26 (1H, dd, *J* = 8.5, Hz, H-3), 6.96 (1H, dd, *J* = 5.5, 1.5 Hz, H-6'), 6.81 (1H, s, H-2'), 6.78 – 6.73 (2H, m, H-4, H-6), 3.96 (3H, s, OMe), 3.87 (3H, s, OMe).

4.4.4 Synthesis of carbolines

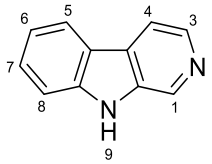

7-Methoxy-9*H*-β-carboline (4.52). A solution of 2-(pyridin-4'-yl)-5-methoxyphenylazide (113 mg, 0.5 mmol, 1 equiv.;) in dioxane (5 mL) was irradiated with 300 to 400 mn at 60 °C for 1 h using a UV-150 Photochemical Flow Reactor connected in-series. The solvent was evaporated *in vacuo* and the crude product was purified by flash column chromatography on SiO_2, eluting with CH_2Cl_2-MeOH (4:1) through a 12 g column using a Teledyne ISCO Combiflash Rf instrument, and recrystallization with methanol gave the *title compound* (58 mg, 59%) as a brown solid.

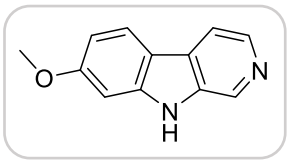

Mp: 215-217 °C (lit:[284] 215-216 °C). **Purity (LCMS):** 96%. **Found [ESI]:** MH^+, 199.0887. $C_{12}H_{11}N_2O$ [MH] requires 199.0871. **IR** (neat) *v*/cm^{-1} 3145 (NH), 2655 (C-H), 1627 (C-C), 1303 (C-O-C), 787, 774 (C-H). **^{1}H NMR** (600 MHz, d_6-DMSO) δ 11.44 (1H, s, NH), 8.76 (1H, s, H-1), 8.24 (1H, d, *J* 5.5, H-3), 8.06 (1 H, d, *J* 8.5, H-5), 7.95 (1H, d, *J* 5.5, H-4), 7.01 (1H, d, *J* 2.5, H-8), 6.82 (1H, dd, *J* 8.5, 2.5, H-6), 3.84 (3H, s, OMe). **^{13}C NMR** (151 MHz, d_6-DMSO) 160.8 (CH), 142.6 (C), 138.8 (CH), 136.6 (C), 133.7 (CH), 128.2 (C), 123.1 (CH), 114.7 (C), 114.3 (CH), 109.7 (CH), 95.0 (CH), 55.8 (Me).

1,7-Methoxy-9*H*-β-carboline (4.53). A solution of 2-(2-methoxy-pyridin-4'-yl)-5-methoxyphenylazide (128 mg, 0.5 mmol, 1 equiv.;) in dioxane (15 mL) was irradiated with 300 to 400 mn at 60 °C for 1 h using a UV-150 Photochemical Flow Reactor connected in-series. The solvent was evaporated *in vacuo* and the crude product was purified by flash column chromatography on SiO_2, eluting with CH_2Cl_2-MeOH (4:1) through a 12 g column using a Teledyne ISCO Combiflash Rf instrument, and recrystallization with methanol gave the *title compound* (51 mg, 45 %) as a brown solid

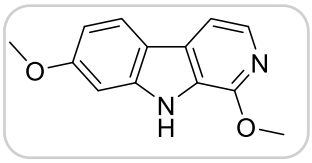

Mp: 202-204 °C. **Purity (LCMS):** 96%. **Found [ESI]:** MH^+, 229.0982. $C_{13}H_{13}N_2O_2$ [MH] requires 229.0977. **IR** (neat) *v*/cm^{-1} 3396 (NH), 2953 (C-H), 1629 (C-C), 1162 (C-O-C), 801 (C-H). **^{1}H NMR** (600 MHz, d_6-DMSO) δ 11.57 (1H, s, NH), 7.97 (1H, d, *J* 8.5, H-5), 7.79 (1H, d, *J* 5.5,

H-3), 7.57 (1H, d, *J* 5.6, H-4), 6.96 (1H, d, *J* 2.0, H-8), 6.80 (1H, dd, *J* 8.5, 2.0, H-6), 4.04 (3H, s, OMe), 3.82 (3H, s, OMe). **^{13}C NMR** (151 MHz, d_6-DMSO) 160.2 (C), 150.8 (C), 141.9 (C), 135.1 (CH), 129.4 (C), 123.6 (C), 122.7 (CH), 115.5 (C), 109.9 (CH), 109.4 (CH), 95.0 (CH), 55.7 (OCH_3), 53.2 (OCH_3).

CHAPTER 5: Conclusions

The importance of green chemistry and the arising interest in emerging technologies have seen an increasing use in chemistry laboratories in recent years especially in the pharmaceutical industry. Some of these emerging technologies such as microwave-assisted chemistry, mechanochemistry and sonochemistry are described in Chapter 1, highlighting flow chemistry, which is one of the key factors in this thesis. Also, an overview of carbazoles, their medicinal properties and methods of synthesis is reported and discussed, as they are the main target compounds of this work. Therefore, this thesis aimed to investigate a new route to access to carbazoles and some derivates by photocyclization of biaryl precursors efficiently accessed using emerging technologies. The incorporation of a photocyclization step into a continuous flow process has been studied, and this improved method could be utilized for the synthesis of carbazoles of biological interest and adapted for the synthesis of other heterocyclic scaffolds with similar structures.

Chapter 2 describes the development and optimization of a novel synthetic pathway for the synthesis of 17 *N*-ethylated carbazoles adapted to reagentless technologies. The synthetic method started with a Suzuki-Miyaura cross-coupling reaction conducted using microwave chemistry. This reaction allowed the preparation of biphenylamines that were transferred to a flow reactor, where they underwent a two-step reaction, including azide formation and subsequent photocyclization, passing through a PFA and a photochemical coil reactor consecutively. The conversion into the corresponding carbazole was efficient enough to proceed to the final step of *N*-ethylation, which was promoted using sonochemistry, to provide full conversion under mild conditions to the final product. **Scheme 113** shows a general scheme for the whole synthetic process. The method enabled the continuous production of carbazole scaffolds on gram scale.

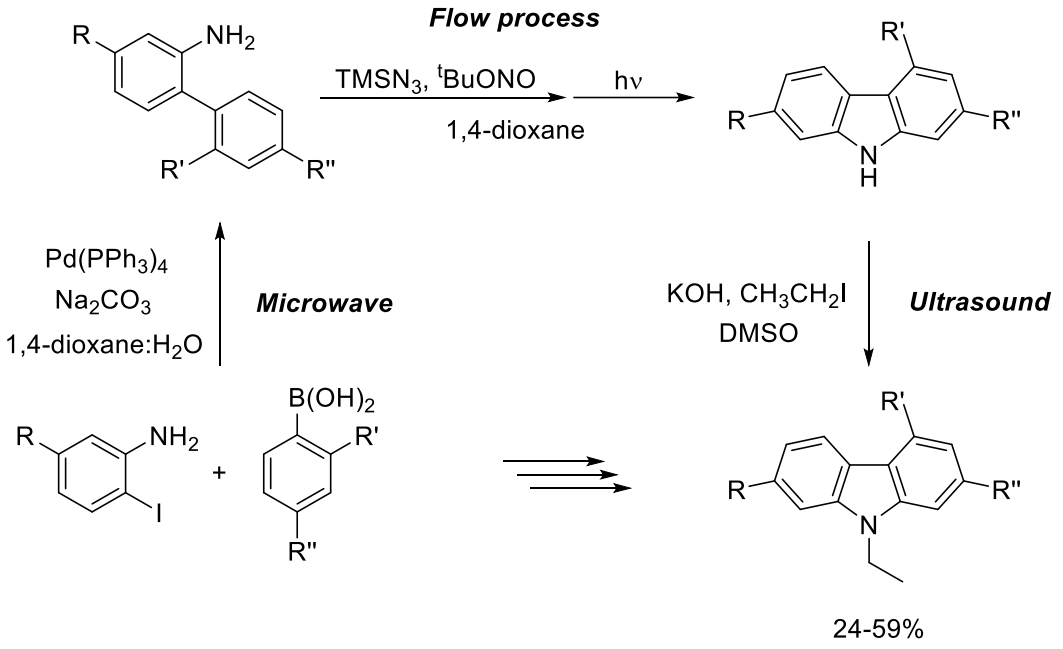

Scheme 113. *Novel synthetic pathway for the synthesis of N-ethylated carbazoles adapted to reagentless technologies.*

Chapter 3 discussed the characteristics of the p53 Y220C mutation, as well as strategies to reactivate the gene in cancer cells. For this purpose, the synthesis of 5 analogues of PK083 (**3.1**), the lead molecule, have been studied, providing an efficient alternative to existing synthetic routes, which proved to be less effective for electron poor carbazoles. Hence, a route to two carbazole 6-carboxylic acids (compounds **3.20** and **3.21**, **Scheme 114**) and three PK083 analogues (compounds **3.22**, **3.23** and **3.24**, **Scheme 115**) has been developed to facilitate their biological testing.

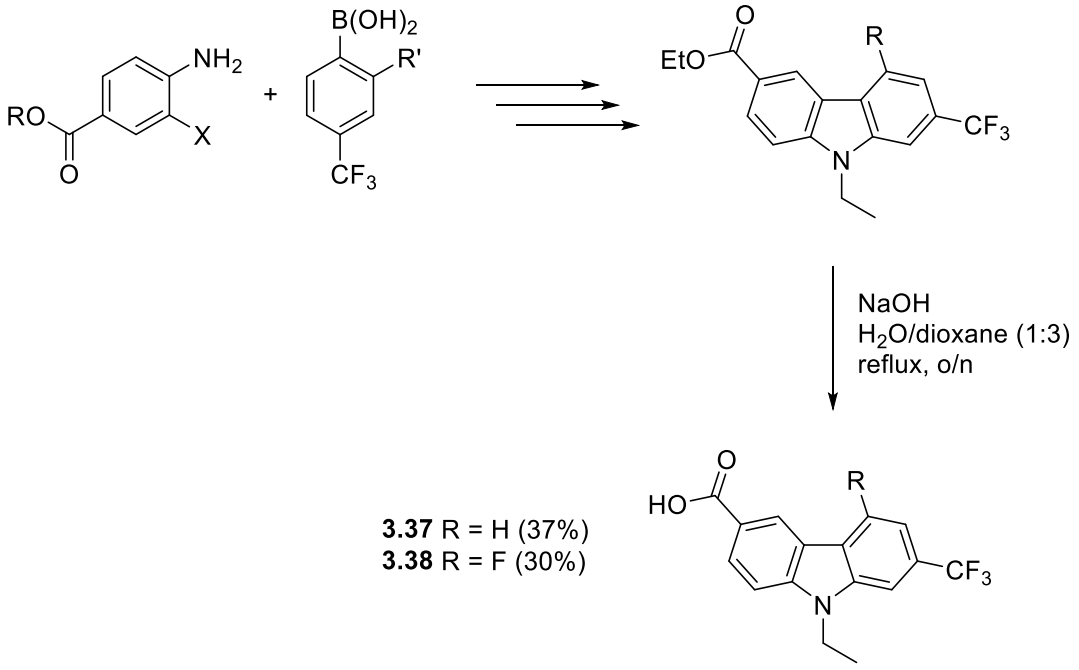

Scheme 114. *Total synthesis of compounds **3.20** and **3.21**. Total yields for the whole synthesis reported.*

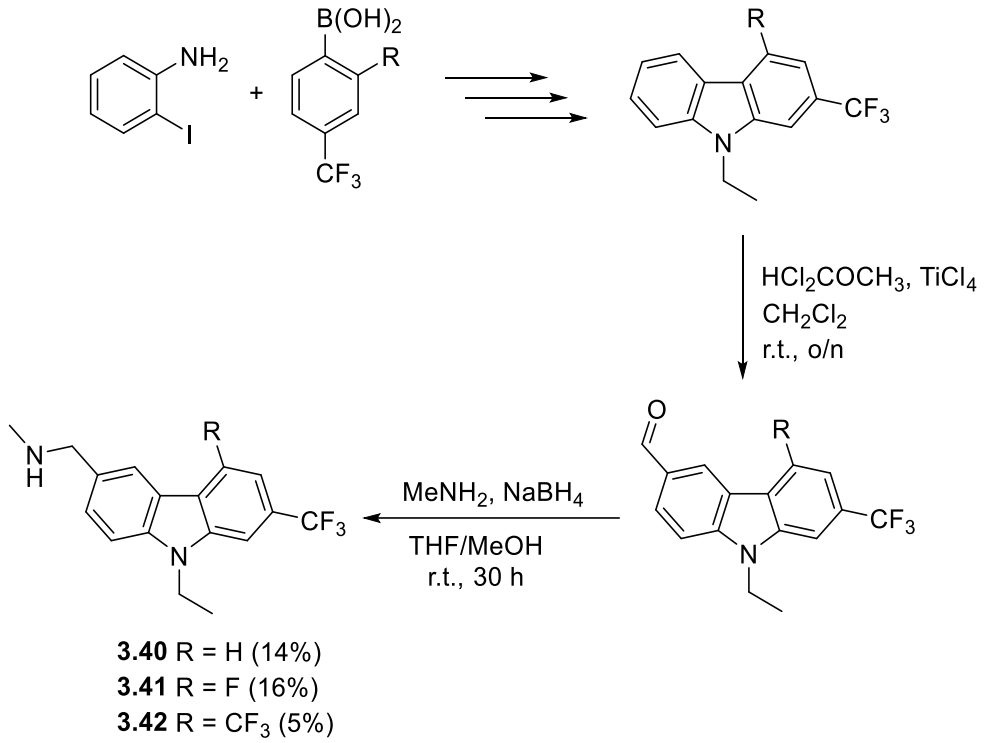

Scheme 115. *Total synthesis of compounds **3.22**, **3.23** and **3.24**. Total yields for the whole synthesis reported.*

Subsequently, five compounds were tested as reactivators of the p53 Y220C mutated gene. The potency of the p53 reactivators was initially determined by differential scanning fluorimetry to compare the changes in the thermal denaturation temperature by Dr Andreas Joerger's group (SGC, Institute of Pharmaceutical Chemistry, Goethe University, Frankfurt). Compound **3.40** was the only compound of the series that showed an increase in melting temperature (+ 1.04 °C), which was even superior than the lead molecule PK083 (**3.1**) (+ 0.55 °C), and its crystal structure in the protein was determined (**Figure 55**). The dissociation constant (K_D) obtained for **3.22** by isothermal calorimetry (ITC) was 4.7 ± 7.8 μM, showing improvement over the reported K_D for PK083 (**3.1**) (K_D = 125 ± 10.30).

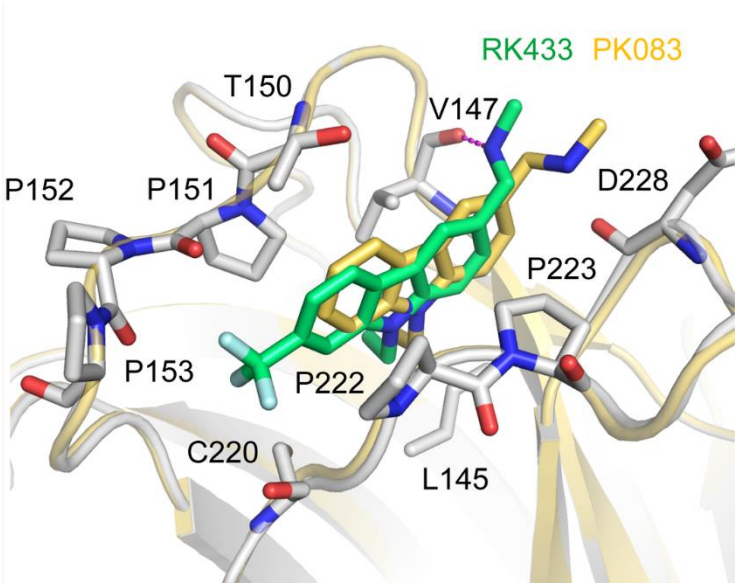

Figure 55. *Superposition of **3.40** (green) and PK083 (**3.1**) (yellow) in the Y220C cavity of p53.*

In Chapter 4, the focus was to adapt the synthetic method described in Chapter 2 to provide a highly efficient novel route to carbazole-containing natural products utilizing reagentless techniques. Thus, clausine C (**4.1**) and clausine N (**4.2**) were synthesised utilizing the methodology developed in Chapter 2 but without the *N*-ethylation step (**Scheme 116**) and were isolated and fully characterized. Clausine V (**4.8**) was synthesised (supported by the ^{1}H-NMR spectrum of the crude reaction mixture) but could not be purified and characterized.

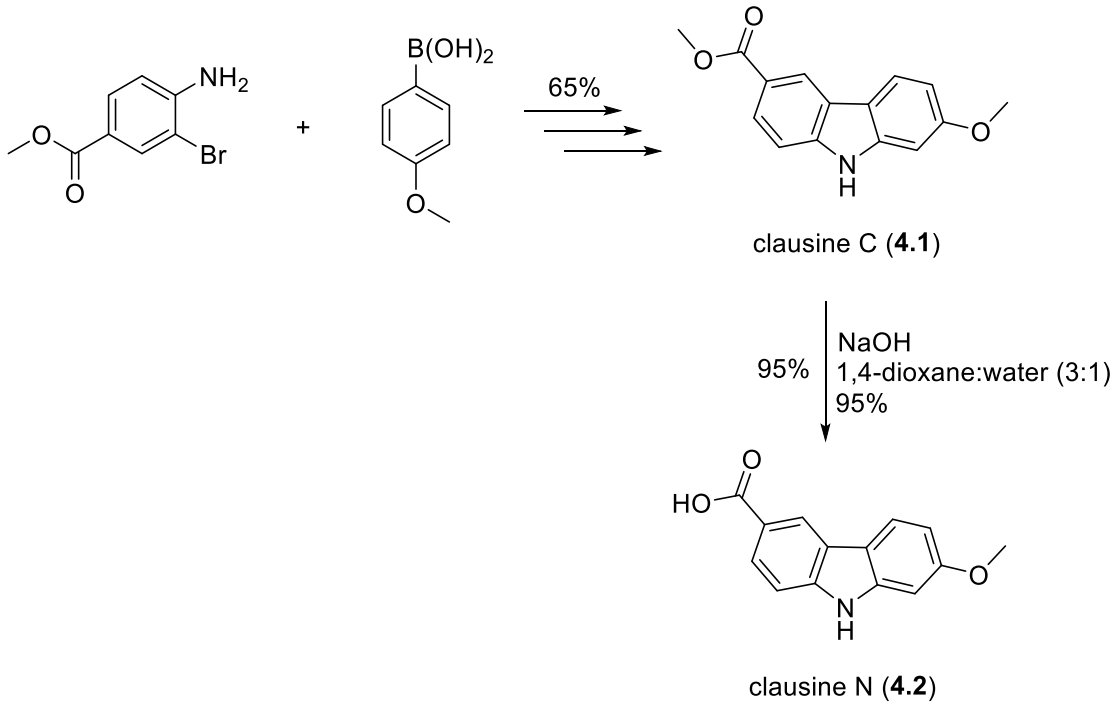

Scheme 116. *Synthetic route for the synthesis of clausine C (**4.1**) and clausine N (**4.2**).*

Besides, chapter 4 explored the adaptation of the developed methods to the synthesis of carboline scaffolds based on harmine's (**4.15**) structure. Although the method could not be exactly applied, as the azide formation reaction from the pyridoaniline precursors could not be transferred to a flow process, *β*-carbolines **4.52** and **4.53** were synthesised in moderate overall yield from the pyridineboronic acids (**Scheme 117**). However, harmine (**4.15**) could not be isolated due to regioselectivity problems in photocyclization.

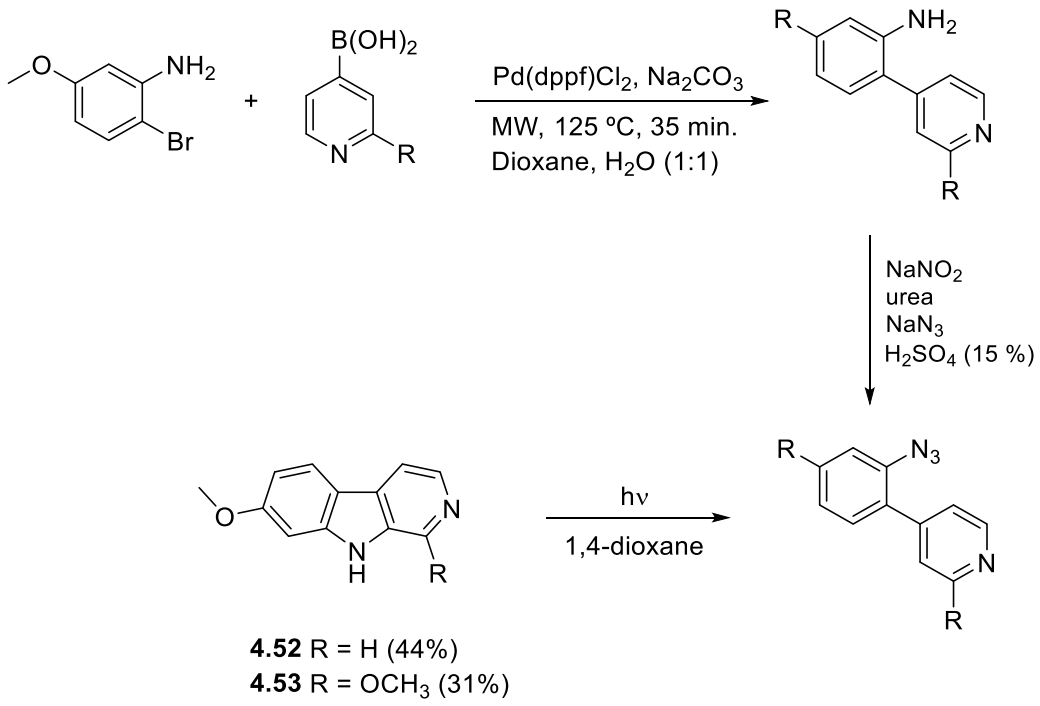

Scheme 117. *Adapted synthetic pathway for the synthesis of β-carbolines using reagentless technologies.*

5.1 Thesis outcomes

Poster presentations:

• A. Jose, S. Ortoll, J. Spencer and M. Bagley "Scaffold synthesis using flow and microwave chemistry" Labfact management and collaboration meeting on 16th and 17th January, 2019, Caen, France.

Oral presentations:

• S. Ortoll, M. Bagley and J. Spencer "Synthesis of heterocyclic scaffolds using reagentless tecniques" PhD symposium 2021, University of Sussex.

5.2 Future work

After investigating PhiKan083 (**3.1**) analogues with a mono-, di-, or trifluoroethyl anchor, John Spencer *et al.* found that the *N*-2,2,2-trifluoroethyl substituted carbazole **5.1** increased stability of the p53-Y220C DBD by 1.2 K at a compound concentration of 125 μM, showing a clear improvement over their *N*-ethyl substituted counterparts PhiKan083. The trifluoro-substituted carbazole was a potent compound and showed K_D values of 28 μM, which corresponds to a 5-fold increase in affinity compared to the nonfluorinated parent. [229] In the crystal structure of **5.1**, the CF_3 group interacts with the backbone carbonyl groups of Leu145 and Trp146 as well as with the thiol group of Cys220 (**Figure 56**).

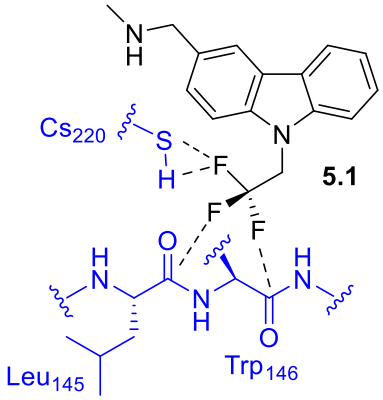

Figure 56. *p53-Y220C with bound trifluoro-derivative **5.1** of PhiKan083 (**3.1**).*

These aspects may be considered when designing the next generation of carbazole-based Y220C mutant stabilizers to incorporate the CF_3 moiety in the *N*-ethyl anchor, in order to improve the potency of the compounds already tested. Hence, a potential future line of investigation would be the synthesis of *N*-2,2,2-trifluoroethyl substituted carbazole analogues of **5.1**, which could potentially be conducted by substitution of the alkylating agent in the *N*-ethylation step described for the method.

Given the success in synthesising simple carbazole natural products, the synthesis of other simply functionalized carbazoles could be attempted. One example could be the investigation of the nature of the group attached to nitrogen, which could lead to compounds like rimcazole (**5.2**) (**Figure 57**), an antipsychotic drug,and even expanded to the synthesis of more complex carbazoles, such as compound **5.3** (**Figure 57**), a hole-transporting material in OLEDs which comprises two fused carbazoles, testing the applicability of the method to azide formation and cyclization of multiple groups in the same precursor.[285]

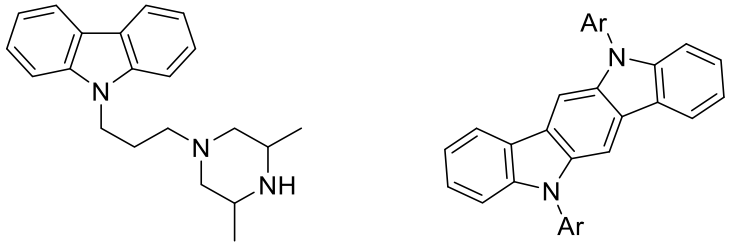

rimcazole (**5.2**) **5.3**

Figure 57. *Structures of rimcazole (**5.2**) and the bicarbazole **5.3**.*

For carboline future work, an alternative synthetic pathway could be studied changing from pyrido anilines to phenyl amino pyridines. Although the starting materials would be much more expensive and less accessible, the retrosynthetic proposal showed in **Scheme 118** could provide the triflate substrates **5.4** needed for the cross-coupling step from the oxidation of aminopyridines.

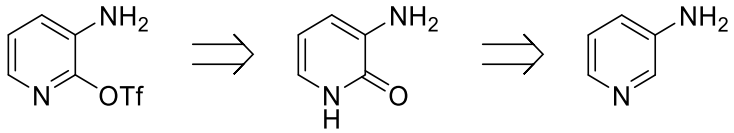

5.4

Scheme 118. *Retrosynthetic proposal for triflates **5.4.***

This approach should be suitable for the coupling and the azide formation and would avoid the regioselectivity problems that appear on the photocyclization step and could improve significantly the scope of the reaction, especially for the synthesis of libraries of *β*-carbolines.

ANNEX 1: Acridines

Acridines (**A1**) are nitrogen heterocycles from the family of alkaloids. These planar molecules are structurally related to anthracene with one of the central CH groups replaced by nitrogen (**Figure A1**), and the parent molecule was first isolated in 1870 from coal tar by Carl Gräbe and Heinrich Caro.[286] Like the related molecules pyridine and quinoline, acridine is mildly basic.

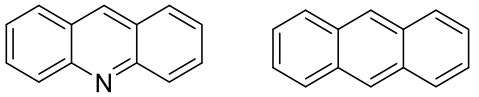

A1 anthracene (**A2**)

Figure A1. *The acridine nucleus (**A1**) and related anthracene (**A2**) structure.*

Acridine/acridone alkaloids are naturally occurring chemical compounds with a wide range of pharmacological activities such as anti-inflammatory, anticancer, antimicrobial, antitubercular, antiparasitic, antimalarial, antiviral and fungicidal activities.[287] To date, the literature describes a number of these scaffolds which have been tested as anticancer, antibacterial and antimalarial agents and against Alzheimer's disease. Examples of these compounds include cystodytin A (**A3**), isolated from various marine organisms, and acronycine (**A4**), isolated from the bark of the Australian scrub ash tree,

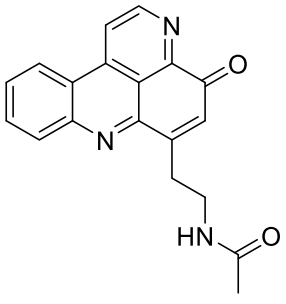

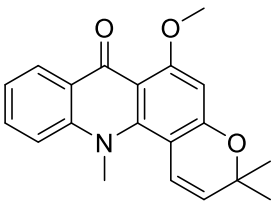

cystodytin A (**A3**) acronycine (**A3**)

shown in **Figure A2**.[288,289]

Figure A2. *Structure of cystodytin A (**A3**) and acronycine (**A4**).*

Acridine derivatives have been studied in some detail as potential anticancer drugs. They are well-known for their high cytotoxic activity and exhibit valuable biological properties such as fluorescent probes, anti-bacterial drugs, anti-protozoal drugs and anti-HIV drugs.[288] Acridine scaffolds are also of interest due to their affinity for DNA and intercalative properties, emerging as an important pharmacophore for the design of antitumour drugs targeting nucleic acids. The acridine skeleton consists of a series of three fused aromatic rings with planar π-conjugated structure as shown in **Figure A1**.[31] The mechanism of their intercalation with DNA is based on π-stacking interactions with base pairs of double-stranded nucleic acids. The heterocyclic, polyaromatic flat structure of acridine fits effectively into the cleft between two chains of polynucleotides. This intercalation of the acridine disturbs the crucial role of nucleic acids in cell division and is necessary for their antitumour activity. Substitution at positions on the heterocycle is crucial for specific biological activity and selectivity towards tumour cells.[288]

Acridines are fluorescent compounds of high quantum yield. Hence, these fluorescent heterocyclic compounds are of interest in many disciplines, including applications as fluorescence probes in chemosensors and molecular probes for biochemical research.[290] Fluorescence sensing is the method of choice for the detection of analytes with very high sensitivity, and often has outstanding selectivity thanks to specially designed fluorescent molecular sensors. Fluorescence is also a powerful tool for investigating the structure and dynamics of matter or living systems at a molecular or supramolecular level.[291] Among them, acridine-containing cyano dyes have been given considerable attention because of their relative chemical stability, high molar absorptivity and fluorescence quantum yield.

Novel acridine ligands were previously synthesized in the Viseux group, with the potential for further transformation to cationic gold(I) complexes to provide new fluorescent tools for the study of their mechanism of action using confocal microscopy. The results of cell viability assays showed good cytotoxic properties against the human HepG2 cancer cell line.[292] The conditions for the formation of acridines have been reported by Dr. Fatai Afolabi.[293] His previous work in the Viseux group optimised studies previously reported by Więcław in 2015.[294] The synthetic process has two main reaction steps. The first step is the deprotonation of the benzyl cyanide benzylic proton using *tert*-BuOK and subsequent attack of the conjugate base at the ortho position of a nitrobenzene, forming the σ^H-adduct intermediate (**A5**) as shown in **Scheme A1**. The R^1 group appeared to have an important effect on the stability of this adduct. This was observed experimentally, since this intermediate had a characteristic dark blue colour which disappeared when *tert*-$BuMe_2SiCl$ was added, turning the mixture orange. The *tert*-$BuMe_2SiCl$ was rationalized to facilitate the silylation of the σ^H-adduct, followed by the elimination of silanol to form the *ortho*-substituted nitrosoarene (**A6**). This nitrosoarene (**A6**) was further transformed to the silylated oxime (**A7**) by the addition of an excess of TBDMSCl, which facilitated electrocyclization followed by aromatization to give the corresponding acridine (**A8**).[293]

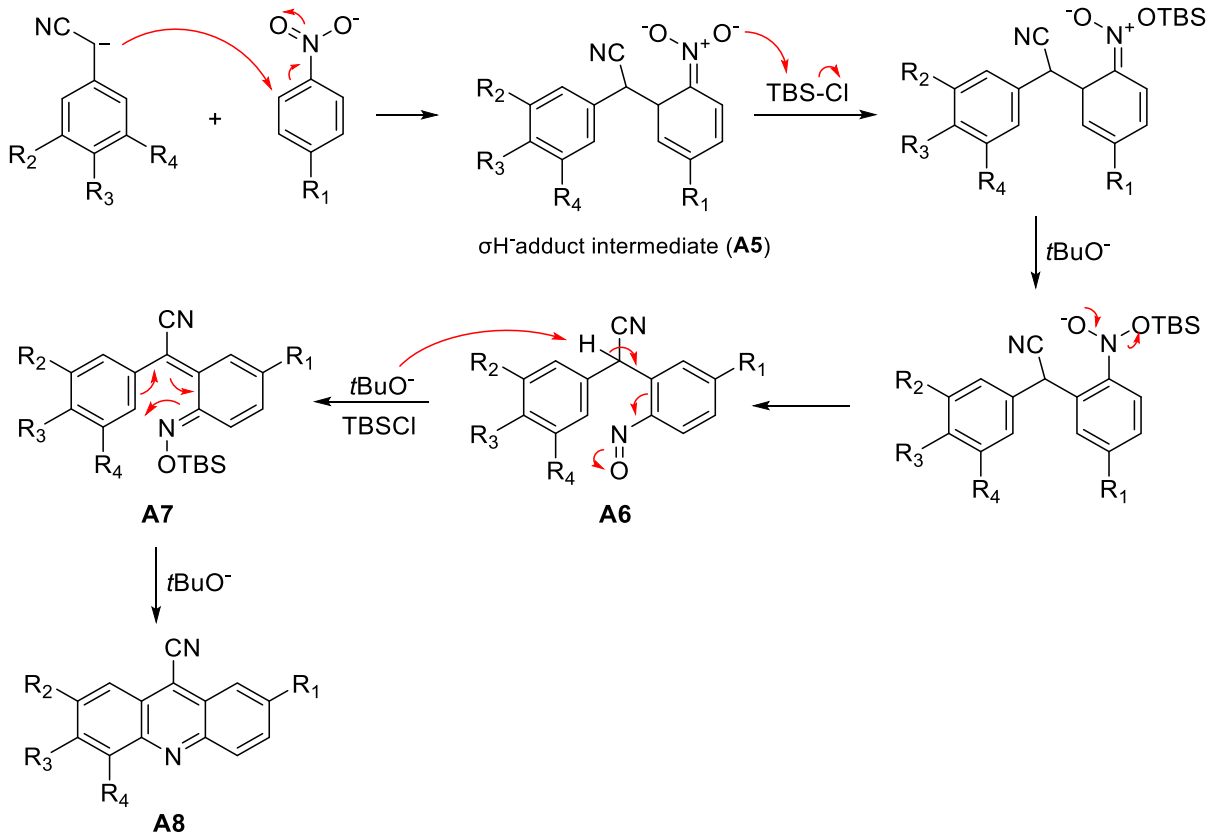

Scheme A1. *Proposed mechanism proposed and investigated by Dr. Fatai Afolabi.*

The promising results obtained by Dr. Fatai Afolabi encouraged the pursuit of further acridine analogues which could be synthesized in useful quantities for biological evaluation, focusing on the presence of the pentafluorosulfanyl (*SF_5*) moiety. The distinctive properties of the SF_5 group make it an attractive substituent in medicinal chemistry. Recent years have seen applications of pentafluorosulfanylated compounds in known drugs with the aim of studying its effect on drug activity. Such studies commonly substitute antecedent functional groups NO_2 or halogen atoms with SF_5 as a bioisostere.[292,295]

A1. Syntheis of acridine scaffolds

Following Dr. Afolabi's conditions, we aimed to synthesise different acridine analogues. Firstly, 2-chloroacridine was resynthesised in order to consolidate the chemistry and reactions conditions. The experimental process consists of adding a solution of *tert*-BuOK in anhydrous THF to a solution of the corresponding nitrobenzene and benzyl cyanide to form the σ^H-adduct intermediate (**A5**). Then, *tert*-$BuMe_2SiCl$ in THF is added followed by a second addition of *tert*-BuOK. The general reaction scheme and the results for the synthesis of different acridines are shown in **Table A1**.

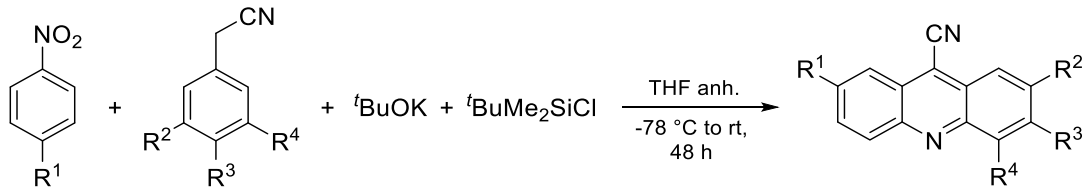

Table A1. *Acridines mediated by TBDMSCl.*

Entry	R_1	R_2	R_3	R_4	R_5	Compound	Yield (%)[a]
1	Cl	H	H	H	H	**A9**	51
2	Cl	H	H	NH_2	H	**A10**	-
3	SF_5	H	H	H	H	**A11**	-
4	H	SF_5	H	H	H	**A12**	35
5	H	SF_5	H	SF_5	H	**A13**	-
6	H	SF_5	SF_5	H	H	**A14**	-

a) Isolated yield after purification by flash chromatography.

2-Chloroacridine (**A9**) was resynthesised by this method in 51% yield (entry 1), confirming the success of the methodology, and prompting the investigation of new substitution patterns. The synthesis of 2-chloro-7-aminoacridine (**A10**) (entry 2) was investigated subsequently, but the reaction appeared incompartible with amino substituents. Avoiding the use of amino groups and given several halogenated acridines had already been synthesised and tested in the past, it was time to focus on analogues containing the pentafluorosulfanyl group. Although a first attempt with 4-pentafluorosulfanylnitrobenzene yielded the corresponding acridine **A12** (entry 4) in low yield, other regioisomers (entries 4-6) did not proceed as expected, and the 2-pentafluorosulfanylacridine (**A12**) was the only new scaffold produced by this methodology.

A9 and **A12** were synthesised in low and moderate yields (51 and 35%, respectively). The pentafluorosulfanyl group decreased substrate reactivity and only provided the corresponding product **A12** in position R_2. The stability of the corresponding σ^H-adduct intermediate was studied due to its potential dependence on the R^1 group, but no conclusions were reached. The reaction did not work for aminated substrates, and the pentafluorosulfanyl group reduced reactivity allowing only one analogue to be synthesised.

Given the poor success, alternative routes towards the synthesis of acridines were studied. The reaction described by Pordel in 2012[22] consisted of dissolving both reagents in a solution of KOH in MeOH and stirring for 24-48 h at 50 °C. This method provided the possibility of adapting the synthesis of this scaffold into a flow chemistry process.

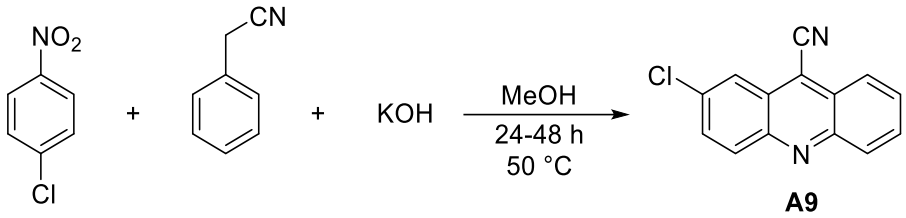

Scheme A2. *Acridine formation described by Pordel.*[22]

Given the poor success synthesising acridine scaffolds containing a pentafluorosulfanyl (SF_5) group and the promise of new conditions suitable for flow chemistry, it was decided to try to adapt this reaction into a flow process. For this purpose, as shown in **Table A2**, benzyl cyanide and the corresponding nitrobenzene were mixed under different conditions in order to find the best method for the synthesis of target compound, using a Vapourtec R2C+/R4 system, using a standard PFA coil reactor and/or a stainless-steel high temperature tube reactor, showed in **Figure A3**.

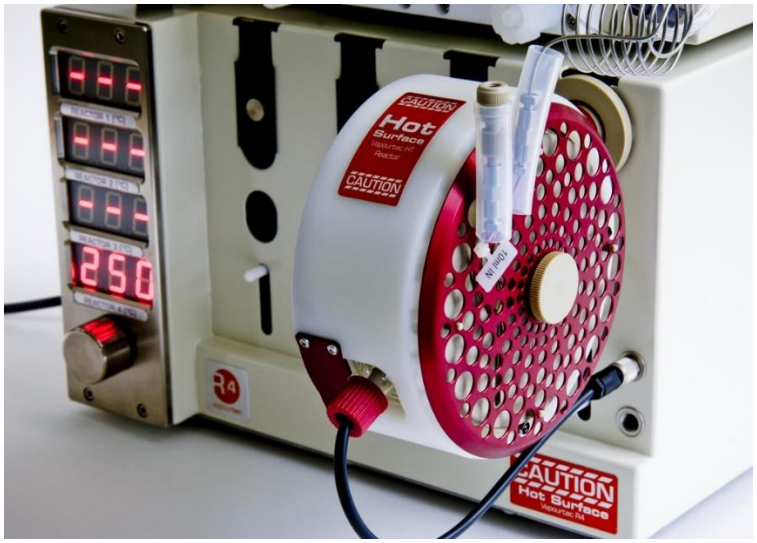

Figure A3. *High temperature tube reactor by Vapourtec.*

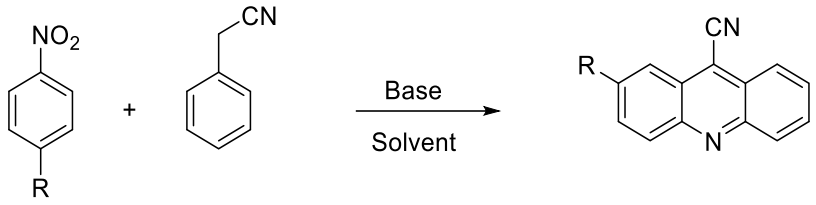

A15

Table A2. *Reaction conditions and materials employed in the synthesis of acridines using flow processing.*

Entry	Solvent	R_t (min)	T /°C	R	Eq. CN	Base	Eq. base	[A15]	Outcome[b]	Conv%[c]
1	MeOH	90	50	Cl	1	KOH	2	0.1	SM	-
2	MeOH	90	100	Cl	1	KOH	2	0.1	**A18**/ **A17** (2:1)	87
3	MeOH	90	120	Cl	1	KOH	2	0.1	**A18**/ **A17** (11:1)	77
4	MeOH	90	120	Cl	1	KOH	2	0.5	**A18**/ **A17** (6:1)	56
5	MeOH	60	80	OCH_3	2	KOH	2	0.2	SM	-
6	MeOH	60	110	OCH_3	2	KOH	2	0.2	SM	-
7	MeOH	60	150	OCH_3	2	KOH	2	0.2	SM	-
8	MeOH	120	25	OCH_3	2	KOH	2	0.2	SM	-
9	THF	60	100	Cl	2	*t*BuOK	3	0.33	mixture	-
10	THF	90[a]	25	OCH_3	2	*t*BuOK	3	0.08	SM	-
11	DMF	60[a]	80	Cl	2	*t*BuOK	3	0.015	**A20**	85
12	DMF	90[a]	25	Cl	2	*t*BuOK	3	0.015	**A20**/ **A21** / **A20** (40/1.5/1)	97

a) *Back pressure regulator present (8 + 250 psi), reactions at 30-35 bar.*

b) *SM = Starting Material; numbers in parentheses refer to the ratio of products, as determined by ^{1}H-NMR spectroscopic analysis after concentration under pressure*

c) *Conv% is ratio of starting material and products, as determined by ^{1}H-NMR spectroscopic analysis.*

The first attempts were conducted in methanol (**Table A2**, entries 1-4), with 1-chloro-4-nitrobenzene (**A16**) and KOH as base, following Pordel's original conditions,[31,32] as this conditions appeared as the most convenient approach to adapt to flow reactor characteristics and limitations. After a failed attempt at 50 °C (entry 1), the temperature was increased and the formation of two new compounds was observed (entries 2-4). One of the compounds was identified as anthranil (**A17**), and other compound, the major compound in all cases, was 4-nitroanisole (**A18**) resulting from the substitution of chloride by a methoxy group. Therefore, it was decided to change the aryl substituent R from chloride to methoxy to eliminate this side reaction. However, when 4-nitroanisole (**A18**) was submitted to the reaction conditions (entries 5-8) no reaction was observed for a range of temperatures and reaction times. Due to the poor results in adapting Pordel's conditions to the synthesis of acridines, it was decided to adapt the conditions employed by Nicolas Fay in his Master's studies, changing the base to *t*BuOK and increasing the base equivalents from 2 to 3 with THF as a solvent to test if flow chemistry might be suitable for the synthesis of amides **A19**, of general structure as shown in **Figure A4**.

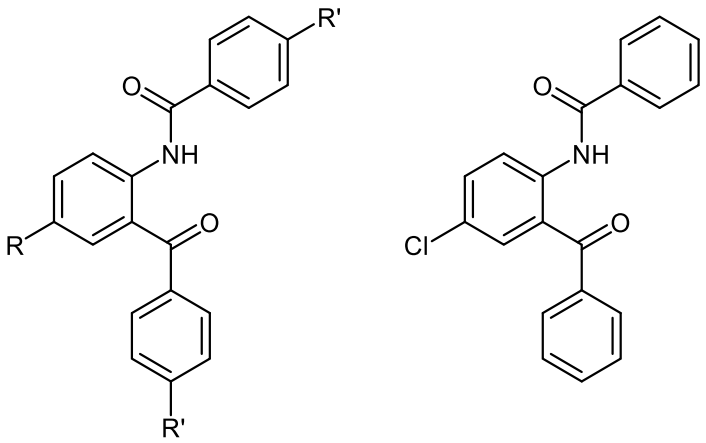

A19 **A21**

Figure A4. *Structure of amides **A19** previously synthesised in the group and its chlorinated analogue **A21**.*

The reaction with 4-nitroanisole (**A18**) in THF, again, did not provide any result (entry 10). The solvent was changed to DMF and the substrate to 1-chloro-4-nitrobenzene (**A16**), in order to remove any solubility problems, and this led to the appearance of compound **A20**, an unidentified compound already reported in previous work (potentially a combination of chloronitrosobenzene and benzoic acid). Increasing the reaction time at room temperature led an unidentified compound **A19**, with traces of the amide **A21** and **A20** (entry 12), although the low solubility of *t*BuOK in the solvent compromised significantly the reproducibility of the method.

Further attempts using two reactors in series provided encouraging preliminary results, with increased conversions to the amide product. Nonetheless, the poor homogeneity of the *t*BuOK solution, both in DMF and THF, caused issues with pump malfunction and compromised the reproducibility of the method. For this reason, the adoption of a flow processed route to these compounds was abandoned.

Before the route was abandoned, an investigation of two new potential scaffolds was made to expand the substrate scope of this process (**Scheme A3**). These studies utilized the same conditions previously studied for the synthesis of acridines or amides, but using 1,2-bis(cyanomethyl)benzene (**A22**) instead of benzylcyanide to facilitate intramolecular cyclization into scaffolds **A23** and **A24**.

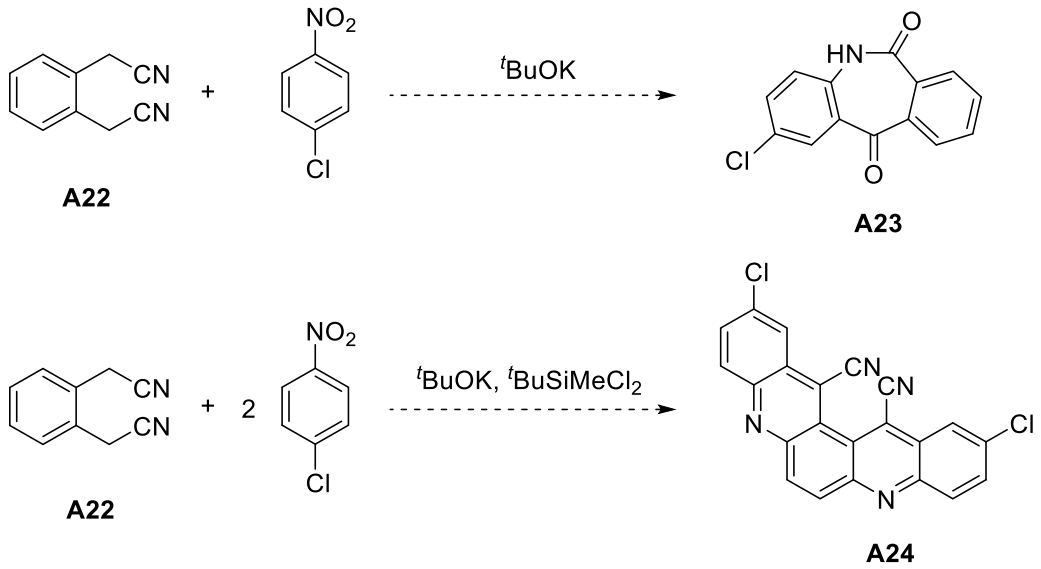

Scheme A3. *Investigation of a route to novel scaffolds **A20** and **A21**.*

Submitting both reactions to the established flow conditions provided poor results. The formation of amide **A20** provided poor conversion and gave a mixture of compounds, which couldn't be isolated and identified due to the low quantities of material. For the preparation of diacridine **A21**, only starting materials were observed by 1H-NMR spectroscopic analysis of the crude reaction mixture. The results suggested that new conditions were required for these more complex systems, which due to time limitations were not investigated.

A2. Conclusions

Two acridines, one of them novel, were synthesised in low to moderate yield. Pentafluorosulfanyl substitution was only successful for the synthesis of scaffold **A12** with this group in position R_2 (**Figure A5**). The reaction did not work for amine-containing substrates.

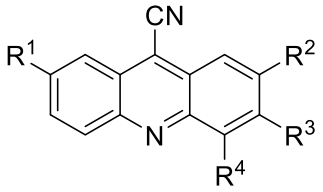

Figure A5. *Acridine substitution pattern.*

Different substrates and conditions were tested to adapt this type of reaction to flow processing, but without success. The poor results suggested that the low temperature and inert atmosphere were crucial for this reaction, and the poor solubility of *t*BuOK caused blockages and pump malfunction in this flow system. All these facts led to this approach being abandoned in favour of more promising flow processed reactions.

A brief study was carried out with bis(cyanomethyl)benzene to explore access of a new, more complex scaffold, but the poor initial results suggested that this chemistry needed thorough investigation and optimization to discover successful conditions. Hence, further studies into the synthesis of acridines was abandoned with no profitable results.

A3. Experimental

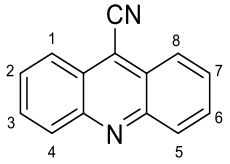

2-Chloroacridine-9-carbonitrile (A9). 1-Chloro-4-nitrobenzene (788 mg, 5.0 mmol, 1.0 equiv) and benzylcyanide (0.6 mL, 5.0 mmol, 1.0 equiv.) were dissolved in anhydrous THF and cooled to −78 °C under an argon atmosphere. A solution of *tert*-BuOK (0.79 g, 7.0 mmol, 1.4 equiv.) in anhydrous THF was added dropwise. After stirring for 20 min, a solution of *tert*-$BuMe_2SiCl$ (3.77 g, 25 mmol, 5.0 equiv.) in anhydrous THF was added to the mixture. The reaction mixture was stirred for a further 20 minutes before a solution of *tert*-BuOK (0.790 g, 7.0 mmol, 1.4 equiv) in anhydrous THF was added. The solution was warmed to room temperature, stirred for 42 h and evaporated *in vacuo*. Purification by flash column

chromatography on SiO_2, eluting with hexane-EtOAc (4:1), and an EtOAc solid-liquid extraction in a sonic bath gave the title compound (0.61 g, 51%) as a yellow solid.

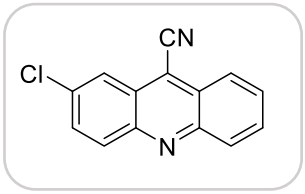

Mp: 206-207 °C (lit,[296] mp 204-205 °C). **Purity (LCMS):** 96%. **Found [ESI]:** MH^+, 239.0377. $C_{14}H_8ClN_2$ [MH] requires 239.0371. **IR** (neat) *v*/cm^{-1} 3051 (C-H), 2618 (CN) 1562 (C-C), 1072 (C-Cl). **^{1}H NMR** (600 MHz, $CDCl_3$) δ 8.39 – 8.34 (2H, m, H-1, H-7), 8.31 (1H, ddd, *J* 9.0, 9.0, 1.0, H-5), 8.26 (1H, d, *J* 9.0, H-3), 7.91 (1H, ddd, *J* 9.0, 6.5, 1.5, H-6), 7.84 – 7.79 (2H, m, H-4, H-8). **^{13}C NMR** (151 MHz, $CDCl_3$) δ 148.3 (C), 146.6 (C), 135.7 (C), 132.5 (CH), 132.0 (CH), 131.3 (CH), 130.5 (CH), 129.8 (CH), 126.4 (C), 126.4 (C), 125.2 (CH), 123.6 (CH), 114.7 (C), 114.4 (C).

3-Pentafluorosulfanyl-9-carbonitrile (A12). 3-Nitrophenylsulphur pentafluoride (0.45 mL, 3.0 mmol, 1.0 equiv.) and benzylcyanide (0.35 mL, 3.0 mmol, 1.0 equiv.) were dissolved in anhydrous THF (15 mL) and cooled to −78 °C under an argon atmosphere. A solution of *tert*-BuOK (1.03 g, 8.4 mmol, 2.8 equiv.) in anhydrous THF (7.5 mL) was added dropwise. After stirring for 20 min, a solution of *tert*-$BuMe_2SiCl$ (2.26 g, 15 mmol, 5 equiv.) in anhydrous THF (7.5 mL) was added to the mixture. The reaction mixture was stirred for a further 20 minutes before a solution of *tert*-BuOK (0.790 g, 7.0 mmol, 1.4 equiv) in anhydrous THF (7.5 mL) was added. The solution was warmed to room temperature, stirred for 42 h and evaporated *in vacuo*. Purification by flash column chromatography on SiO_2, eluting with hexane-EtOAc (4:1), and an EtOAc solid-liquid extraction in a sonic bath gave the title compound (0.35 g, 35%) as a golden solid.

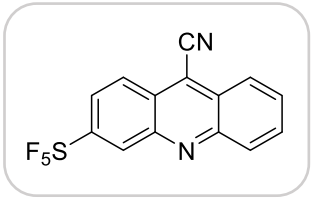

Mp: 206-207 °C. **Purity (LCMS):** 96%. **Found [ESI]:** MH^+, 331.0327. $C_{14}H_8F_5N_2S$ [MH] requires 331.0328. **IR** (neat) *v*/cm^{-1} 2229 (CN), 1625 (C-C), 754 (S-F). **^{1}H NMR** (600 MHz, $CDCl_3$) δ 8.79 (1H, d, *J* 2.0, H-4), 8.44 (1 H, d, *J* 9.5, H-1), 8.40 (1H, ddd, *J* 9.0, 0.5, 0.5, H-8), 8.35 (1H, d, *J* 9.0, H-5), 8.07 (1H, dd, *J* 9.5, 2.0, H-2), 7.98 (1H, ddd, *J* 9.0, 7.0, 1.5, H-6), 7.87 (1H, ddd, *J* 9.0, 7.0, 1.0, H-7). **^{13}C NMR** (151 MHz, $CDCl_3$) δ 154.8 (t, $^2J_{CF}$ 19, C), 149.5 (CH), 146.7 (C), 132.1 (CH), 130.7 (CH), 130.7 (CH), 129.4 (t, $^3J_{CF}$ 5, CH), 127.1 (C), 126.2 (CH), 126.0 (C), 125.3 (CH), 125.2 – 125.1 (m, C), 115.7 (CN), 114.3 (C).

Bibliography

1 K. C. Nicolaou, *Isr. J. Chem.*, 2018, **58**, 104–113.

2 M. F. Wohler, *Philos. Mag.*, 1828, **4**, 309–310.

3 A. Kekulé, *Ann. der Chem. und Pharm.*, 1866, **137**, 129–196.

4 M. Tswett, *Ber. Dtsch. Bot. Ges.*, 1906, **24**, 316–323.

5 M. Tswett, *Ber. Dtsch. Bot. Ges.*, 1906, 384–393.

6 I. I. Rabi, J. R. Zacharias, S. Millman and P. Kusch, *Phys. Res. Columbia Univ.*, 1938, **7**, 318.

7 Willard Libby and Radiocarbon Dating (Accessed on January 12, 2020)., https://www.acs.org/content/acs/en/education/whatischemistry/landmarks/radiocarbon-dating.html#:~:text=Carbon-14 was first discovered,California Radiation Laboratory in Berkeley.

8 R. B. Woodward, F. Sondhbimbr Cambridge and M. David Taub, *The total synthesis of colesterol*, Miescher and Fischer, 1937, vol. 20.

9 R. B. Woodward, F. Sondheimer and D. Taub, *J. Am. Chem. Soc.*, 1951, **73**, 4057.

10 R. B. Woooward, 1960, **3800**, 383–404.

11 R. B. Woodward, *Pure Appl. Chem.*, 1973, **33**, 145–178.

12 P. S. Baran, *J. Am. Chem. Soc.*, 2018, **140**, 4751–4755.

13 R. A. Holton, C. Somoza, H. B. Kim, F. Liang, R. J. Biediger, P. D. Boatman, M. Shindo, C. C. Smith, S. Kim, H. Nadizadeh, Y. Suzuki, C. Tao, P. Vu, S. Tang, P. Zhang, K. K. Murthi, L. N. Gentile and J. H. Liu, *J. Am. Chem. Soc.*, 1994, **116**, 1597–1598.

14 R. A. Holton, H. B. Kim, C. Somoza, F. Liang, R. J. Biediger, P. D. Boatman, M. Shindo, C. C. Smith, S. Kim, H. Nadizadeh, Y. Suzuki, C. Tao, P. Vu, S. Tang, P. Zhang, K. K. Murthi, L. N. Gentile and J. H. Liu, *J. Am. Chem. Soc.*, 1994, **116**, 1599–1600.

15 F. Tavares, J. P. Lawson and A. I. Meyers, *J. Am. Chem. Soc.*, 1996, **118**, 3303–3304.

16 L. M. Chapman, J. C. Beck, L. Wu and S. E. Reisman, *J. Am. Chem. Soc.*, 2016, **138**, 9803–9806.

17 Y. A. Ivanenkov, B. A. Zagribelnyy and V. A. Aladinskiy, *J. Med. Chem.*, 2019, **62**, 10026–10043.

18 H. C. Kolb, M. G. Finn and K. B. Sharpless, *Angew. Chemie Int. Ed.*, 2001, **40**, 2004–2021.

19 H. C. Kolb and K. B. Sharpless, *Drug Discov. Today*, 2003, **8**, 1128–1137.

20 S. S. van Berkel, A. J. Dirks, S. A. Meeuwissen, D. L. L. Pingen, O. C. Boerman, P. Laverman, F. L. van Delft, J. J. L. M. Cornelissen and F. P. J. T. Rutjes, *ChemBioChem*, 2008, **9**, 1805–1815.

21 V. Aucagne and D. A. Leigh, *Org. Lett.*, 2006, **8**, 4505–4507.

22 S. V Ley and I. R. Baxendale, *Chimia (Aarau).*, 2008, **62**, 162–168.

23 The Top Ten Emerging Technologies in Chemistry (Accessed on January 14, 2020), https://iupac.org/top-ten-emerging-technologies-call-2020/.

24 F. Gomollón-bel, *Chem. Int.*, 2019, **41**, 12–17.

25 J. H. Clark, *Green Chem.*, 1999, **1**, 1.

26 J. L. Tucker, *Org. Process Res. Dev.*, 2006, **10**, 315–319.

27 P. Anastas and J. Warner, *Green Chemistry: Theory and Practice*, Oxford University press, 1998.

28 S. L. Y. Tang, R. L. Smith and M. Poliakoff, *Green Chem.*, 2005, **7**, 761–762.

29 R. Gedye, F. Smith, K. Westaway, H. Ali, L. Baldisera, L. Laberge and J. Rousell, *Tetrahedron Lett.*, 1986, **27**, 279–282.

30 R. J. Giguere, T. L. Bray, S. M. Duncan and G. Majetich, *Tetrahedron Lett.*, 1986, **27**, 4945–4948.

31 D. M. P. Mingos and D. R. Baghurst, *Chem. Soc. Rev.*, 1991, **20**, 1–47.

32 CEM Discover (Accessed on July 22, 2022), https://cem.com/en/discover.

33 C. Gabriel, S. Gabriel, E. H. Grant, B. S. J. Halstead and D. Michael P Mingos, *Chem. Soc. Rev.*, 1998, **27**, 213–223.

34 R. Van Eldik, F.-G. Klårner and F. Zaragoza Dærwald, *High Pressure Chemistry Organic Synthesis on Solid Phase Solvent-free Organic Synthesis*, WILEY-VCH, 2nd edn., 2002.

35 C. O. Kappe, *Compr. Med. Chem. II*, 2006, **3**, 837–860.

36 J. L. Howard, Q. Cao and D. L. Browne, *Chem. Sci.*, 2018, **9**, 3080–3094.

37 K. Wright, *Paléorient*, 1991, **17**, 19–45.

38 L. Takacs, *J. Met.*, 2000, 12–13.

39 A. A. L. Michalchuk, I. A. Tumanov, V. A. Drebushchak and E. V. Boldyreva, *Faraday Discuss.*, 2014, **170**, 311.

40 S. L. James, C. J. Adams, C. Bolm, D. Braga, P. Collier, T. Frišcic, F. Grepioni, K. D. M. Harris, G. Hyett, W. Jones, A. Krebs, J. Mack, L. Maini, A. G. Orpen, I. P. Parkin, W. C. Shearouse, J. W. Steed and D. C. Waddell, *Chem. Soc. Rev.*, 2012, **41**, 413–447.

41 Retsch Mixer mill MM 400 (Accessed on July 22, 2022), https://www.retsch.com/products/milling/ball-mills/mixer-mill-mm-400/function-features/.

42 Lord Rayleigh O.M. F.R.S. (1917):, *Philos. Mag. Ser. 6*, 1917, **34**, 94–98.

43 W. T. Richards and A. L. Loomis, *J. Am. Chem. Soc.*, 1927, **49**, 3086–3100.

44 A. L. Loomis and R. w. Wood, *Philos. Mag. J. Sci.*, 1927, 417–436.

45 T. Ando, S. Sumi, T. Kawate, J. I. Née Yamawaki and T. Hanafusa, *J. Chem. Soc. - Ser. Chem. Commun.*, 1984, 439–440.

46 V. A. Akulichev, *Ultrasonics*, 1986, **24**, 8–18.

47 R. Cella and H. A. Stefani, *Tetrahedron*, 2009, **65**, 2619–2641.

48 L. H. Thompson and L. K. Doraiswamy, *Ind. Eng. Chem. Res.*, 1999, 1215–1249.

49 T. J. Mason, *Chem. Soc. Rev.*, 1997, **26**, 443–451.

50 B. Savun-Hekimoğlu, *Acoustics*, 2020, **2**, 766–775.

51 D. T. McQuade and P. H. Seeberger, *J. Org. Chem.*, 2013, **78**, 6384–6389.

52 C. E. Brocklehurst, H. Lehmann and L. La Vecchia, *Org. Process Res. Dev.*, 2011, **15**, 1447–1453.

53 M. Baumann, A. M. Rodriguez Garcia and I. R. Baxendale, *Org. Biomol. Chem.*, 2015, **13**, 4231–4239.

54 J. Pelleter and F. Renaud, *Org. Process Res. Dev.*, 2009, **13**, 698–705.

55 J. Britton and C. L. Raston, *Chem. Soc. Rev.*, 2017, 46, 1250–1271.

56 A. Polyzos, M. O'Brien, T. P. Petersen, I. R. Baxendale and S. V Ley, *Angew. Chemie - Int. Ed.*,

2011, **50**, 1190–1193.

57 C. A. Shukla and A. A. Kulkarni, *Beilstein J. Org. Chem.*, 2017, **13**, 960–987.

58 P. R. D. Murray, D. L. Browne, J. C. Pastre, C. Butters, D. Guthrie and S. V. Ley, *Org. Process Res. Dev.*, 2013, **17**, 1192–1208.

59 J. Hartwig, S. Ceylan, L. Kupracz, L. Coutable and A. Kirschning, *Angew. Chemie - Int. Ed.*, 2013, **52**, 9813–9817.

60 L. Kupracz and A. Kirschning, *Adv. Synth. Catal.*, 2013, **355**, 3375–3380.

61 The R-Series modular flow chemistry system (Accessed on July 22, 2022), https://www.vapourtec.com/products/r-series-flow-chemistry-system-overview/.

62 L. Ürge, J. Alcazar, L. Huck and G. Dormán, in *Annual Reports in Medicinal Chemistry*, 2017, vol. 50, pp. 87–147.

63 J. C. Pastre, D. L. Browne and S. V Ley, *Chem. Soc. Rev.*, 2013, **42**, 8849–8869.

64 K. Loubière, M. Oelgemöller, T. Aillet, O. Dechy-Cabaret and L. Prat, *Chem. Eng. Process. - Process Intensif.*, 2016, **104**, 120–132.

65 J. Mattay and A. G. Griesbeck, *Photochemical Key Steps in Organic Synthesis*, Weinheim, VCH, 2012.

66 A. Albini, L. Germani, A. Albini and M. Fagnoni, *Handbook of Synthetic Photochemistry*, 2010.

67 J. D. Coyle, *Introduction to Organic Photochemistry*, Great britain, Wiley, 1986.

68 M. Fischer, *Angew. Chemie Int. Ed. English*, 1978, **17**, 16–26.

69 E. B. Corcoran, J. P. McMullen, F. Lévesque, M. K. Wismer and J. R. Naber, *Angew. Chemie*, 2020, 2–7.

70 Vapourtec, The Future of Photochemistry with Vapourtec's UV-150, https://www.vapourtec.com/news/the-future-of-photochemistry-with-vapourtecs-uv-150/, (accessed 28 April 2020).

71 J. D. Williams, Y. Otake, G. Coussanes, I. Saridakis, N. Maulide and C. O. Kappe, *ChemPhotoChem*, 2019, **3**, 229–232.

72 M. Di Filippo, C. Bracken and M. Baumann, *Molecules*, *2020, **25**, 356*.

73 D. Cambié and T. Noël, *Top. Curr. Chem.*, 2018, 376.

74 G. L. Patrick, *Introduction to medicinal chemistry*, Fifth edition, Oxford, Oxford University press, 2013.

75 T. L. Lemke and D. A. Williams, *Foye's principles of medicinal chemistry*, Sixth edition, Baltimore, Lippincott Williams & Wilkins, 2006.

76 T. Nogrady and D. F. Weaver, *Medicinal Chemistry: A Molecular and Biochemical Approach.* Third Edition, 2005.

77 P. Shah and A. D. Westwell, *J. Enzyme Inhib. Med. Chem.*, 2007, **22**, 527–540.

78 C. Heidelberger, N. K. Chaudhuri, P. Danneberg, R. Duschinsky, R. J. Schnitzer, E. Pleven and J. Scheiner, *Nature*, 1957, **179**, 663–666.

79 S. Purser, P. R. Moore, S. Swallow and V. Gouverneur, *Chem. Soc. Rev.*, 2008, **37**, 320–330.

80 J. E. True, T. D. Thomas, R. W. Winter and G. L. Gard, *Inorg. Chem.*, 2003, **42**, 4437–4441.

81 Y. Zafrani, D. Yeffet, G. Sod-Moriah, A. Berliner, D. Amir, D. Marciano, E. Gershonov and S. Saphier, *J. Med. Chem.*, 2017, **60**, 797–804.

82 W. Zhu, J. Wang, S. Wang, Z. Gu, J. L. Aceña, K. Izawa, H. Liu and V. A. Soloshonok, *J. Fluor. Chem.*, 2014, **167**, 37–54.

83 G. Lewandowski, E. Meissner and E. Milchert, *J. Hazard. Mater.*, 2006, **136**, 385–391.

84 A. Coqueiro and R. Verpoorte, in *Encyclopedia of Analytical Science*, Leiden, Elsevier, 2019.

85 C. Graebe and C. Glaser, *Justus Liebigs Ann. Chem.*, 1872, **163**, 343–360.

86 G. R. Clemo and W. H. Perkin, *J. Chem. Soc. - Perkin Trans. 1*, 1924, 1804–1814.

87 D. P. Chakraborty, B. K. Barman and P. K. Bose, *Tetrahedron*, 1965, **21**, 681–685.

88 K. C. Das, D. P. Chakraborty and P. K. Bose, *Experientia*, 1964, **573**, 340.

89 H. Jiang, J. Sun and J. Zhang, *Curr. Org. Chem.*, 2012, **16**, 2014–2025.

90 Y. Tao, C. Yang and J. Qin, *Chem. Soc. Rev.*, 2011, **40**, 2943–2970.

91 M. Manickam, P. Iqbal, M. Belloni, S. Kumar and J. A. Preece, *Isr. J. Chem.*, 2012, **52**, 917–934.

92 Y. W. Park, *Chem. Soc. Rev.*, 2010, **39**, 2352–2353.

93 A. Gluszynska, *Eur. J. Med. Chem.*, 2015, **94**, 405–426.

94 O. Thau-Zuchman, E. Shohami, A. G. Alexandrovich, V. Trembovler and R. R. Leker, *J. Neurotrauma*, 2012, **29**, 375–384.

95 W. M. O'Brien and G. F. Bagby, *Pharmacother. J. Hum. Pharmacol. Drug Ther.*, 1987, **7**, 16–24.

96 B. P. Bandgar, L. K. Adsul, H. V. Chavan, S. S. Jalde, S. N. Shringare, R. Shaikh, R. J. Meshram, R. N. Gacche and V. Masand, *Bioorganic Med. Chem. Lett.*, 2012, **22**, 5839–5844.

97 A. Chakraborty, B. K. Chowdhury and P. Bhattacharyya, *Phytochemistry*, 1995, **40**, 295–298.

98 F. F. Zhang, L. L. Gan and C. H. Zhou, *Bioorganic Med. Chem. Lett.*, 2010, **20**, 1881–1884.

99 O. P. S. Patel, A. Mishra, R. Maurya, D. Saini, J. Pandey, I. Taneja, K. S. R. Raju, S. Kanojiya, S. K. Shukla, M. N. Srivastava, M. Wahajuddin, A. K. Tamrakar, A. K. Srivastava and P. P. Yadav, *J. Nat. Prod.*, 2016, **79**, 1276–1284.

100 A. A. Pieper, S. Xie, E. Capota, S. J. Estill, J. Zhong, J. M. Long, G. L. Becker, P. Huntington, S. E. Goldman, C. H. Shen, M. Capota, J. K. Britt, T. Kotti, K. Ure, D. J. Brat, N. S. Williams, K. S. MacMillan, J. Naidoo, L. Melito, J. Hsieh, J. De Brabander, J. M. Ready and S. L. McKnight, *Cell*, 2010, **142**, 39–51.

101 K. S. MacMillan, J. Naidoo, J. Liang, L. Melito, N. S. Williams, L. Morlock, P. J. Huntington, S. J. Estill, J. Longgood, G. L. Becker, S. L. McKnight, A. A. Pieper, J. K. De Brabander and J. M. Ready, *J. Am. Chem. Soc.*, 2011, **133**, 1428–1437.

102 D. Zhu, M. Chen, M. Li, B. Luo, Y. Zhao, P. Huang, F. Xue, S. Rapposelli, R. Pi and S. Wen, *Eur. J. Med. Chem.*, 2013, **68**, 81–88.

103 I. Tasset, C. Espínola, F. J. Medina, M. Feijóo, C. Ruiz, E. Moreno, M. M. Gómez, J. A. Collado, C. Muñoz, J. Muntané, P. Montilla, I. Túnez, E. More-No and P. Mon-, *J Physiol Biochem*, 2009, **65**, 291–296.

104 J. Wang, K. Ono, D. L. Dickstein, I. Arrieta-Cruz, W. Zhao, X. Qian, A. Lamparello, R. Subnani, M. Ferruzzi, C. Pavlides, L. Ho, P. R. Hof, D. B. Teplow and G. M. Pasinetti, *Neurobiol. Aging*, 2011, **32**, 2321.e1–2321.e12 a.

105 Y. Ouyang, Z. Chen, M. Tan, A. Liu, M. Chen, J. Liu, R. Pi and J. Fang, *Biochem. Biophys. Res. Commun.*, 2013, **441**, 917–922.

106 R. L. Siegel, K. D. Miller and A. Jemal, *CA. Cancer J. Clin.*, 2016, **66**, 7–30.

107 F. Aldabbagh, *Compr. Org. Funct. Gr. Transform. II*, 2004, **3**, 99–133.

108 M. Gehringer and S. A. Laufer, *J. Med. Chem.*, 2019, **62**, 5673–5724.

109 M. F. Brana, M. Cacho, A. Gradillas, B. de Pascual-Teresa and A. Ramos, *Curr. Pharm. Des.*, 2005, **7**, 1745–1780.

110 S. Issa, A. Prandina, N. Bedel, P. Rongved, S. Yous, M. Le Borgne and Z. Bouaziz, *J. Enzyme Inhib. Med. Chem.*, 2019, **34**, 1321–1346.

111 C. Graebe and F. Ullmann, *F. Liebigs Ann. Chem*, 1896, **291**, 16–17.

112 F. Ullmann, *Ann. der chemie*, 1904, **332**, 82.

113 W. G. Preston and S. Horwood, 1942, 500–504.

114 E. Drechsel, *J. für Prakt. Chemie*, 1888, **38**, 65–74.

115 W. Borsche, *Liebigs Ann. Chem.*, 1907, **356**, 49–80.

116 E. Fischer and F. Jourdan, *Berichte der Dtsch. Chem. Gesellschaft*, 1883, **16**, 2241–2245.

117 J. I. G. Cadogan, R. K. Mackie, R. J. G. Searle and M. Cameron-Wood, 1964, **2078**, 4831–4837.

118 A. W. Freeman, M. Urvoy and M. E. Criswell, *J. Org. Chem.*, 2005, **70**, 5014–5019.

119 R. Sanz, J. Escribano, M. R. Pedrosa, R. Aguado and F. J. Arnáiz, *Adv. Synth. Catal.*, 2007, **349**, 713–718.

120 A. W. Schmidt, K. R. Reddy and H. J. Knölker, *Chem. Rev.*, 2012, **112**, 3193–3328.

121 M. Kobayashi and T. Kuzuyama, *Biomolecules*, 2020, **10**, 1–15.

122 S. Huang, S. S. Elsayed, M. Lv, J. Tabudravu, M. E. Rateb, R. Gyampoh, K. Kyeremeh, R. Ebel, M. Jaspars, Z. Deng, Y. Yu and H. Deng, *Chem. Biol.*, 2015, **22**, 1633–1642.

123 Y. Liu, L. Su, Q. Fang, J. Tabudravu, X. Yang, K. Rickaby, L. Trembleau, K. Kyeremeh, Z. Deng, H. Deng and Y. Yu, *J. Org. Chem.*, 2019, **84**, 16323–16328.

124 H. J. Knölker, *Top. Curr. Chem.*, 2005, **244**, 115–148.

125 T. Aggarwal, Sushmita and A. K. Verma, *Org. Biomol. Chem.*, 2019, **17**, 8330–8342.

126 J. Jia, J. Shi, J. Zhou, X. Liu, Y. Song, H. E. Xu and W. Yi, *Chem. Commun.*, 2015, **51**, 2925–2928.

127 Y. Qiu, W. Kong, C. Fu and S. Ma, *Org. Lett.*, 2012, **14**, 6198–6201.

128 R. K. Saunthwal, K. M. Saini, M. Patel and A. K. Verma, *Tetrahedron*, 2017, **73**, 2415–2431.

129 S. Kotha, V. R. Aswar and A. K. Chinnam, *Tetrahedron Lett.*, 2017, **58**, 4360–4362.

130 J. Wang, H. T. Zhu, Y. F. Qiu, Y. Niu, S. Chen, Y. X. Li, X. Y. Liu and Y. M. Liang, *Org. Lett.*, 2015, **17**, 3186–3189.

131 K. Huang, G. Sheng, P. Lu and Y. Wang, *Org. Lett.*, 2017, **19**, 4114–4117.

132 S. Chen, Y. Li, P. Ni, H. Huang and G. J. Deng, *Org. Lett.*, 2016, **18**, 5384–5387.

133 Z. G. Yuan, Q. Wang, A. Zheng, K. Zhang, L. Q. Lu, Z. Tang and W. J. Xiao, *Chem. Commun.*, 2016, **52**, 5128–5131.

134 X. Yang and D. Wang, *ACS Appl. Energy Mater.*, 2018, **1**, 6657–6693.

135 J. A. Jordan-Hore, C. C. C. Johansson, M. Gulias, E. M. Beck and M. J. Gaunt, *J. Am. Chem. Soc.*, 2008, **130**, 16184–16186.

136 C. Suzuki, K. Hirano, T. Satoh and M. Miura, *Org. Lett.*, 2015, **17**, 1597–1600.

137 B. Liégault, D. Lee, M. P. Huestis, D. R. Stuart and K. Fagnou, *J. Org. Chem.*, 2008, **73**, 5022–5028.

138 Z. Liu and R. C. Larock, *Org. Lett.*, 2004, **6**, 3739–3741.

139 L. Ackermann, A. Althammer and P. Mayer, *Synthesis (Stuttg).*, 2009, 3493–3503.

140 H. Dong, M. Shen, J. E. Redford, B. J. Stokes, A. L. Pumphrey and T. G. Driver, *Org. Lett.*, 2007, **9**, 5191–5194.

141 M. Shen, B. E. Leslie and T. G. Driver, *Angew. Chemie - Int. Ed.*, 2008, **47**, 5056–5059.

142 B. J. Stokes, H. Dong, B. E. Leslie, A. L. Pumphrey and T. G. Driver, *J. Am. Chem. Soc.*, 2007, **129**, 7500–7501.

143 B. J. Stokes, B. Jovanovic, H. Dong, K. J. Richert, R. D. Riell, T. G. Driver and W. T. Street, *J. Org. Chem.*, 2009, **2**, 3225–3228.

144 L. Yang, Y. Zhang, X. Zou, H. Lu and G. Li, *Green Chem.*, 2018, **20**, 1362–1366.

145 X. Tian, L. Song and A. S. K. Hashmi, *Angew. Chemie - Int. Ed.*, 2020, **59**, 12342–12346.

146 H. Dong, R. T. Latka and T. G. Driver, *Org. Lett.*, 2011, **13**, 2726–2729.

147 D. Milstein and J. K. Stiile, *J. Am. Chem. Soc.*, 1978, **100**, 3636–3638.

148 S. Baba and E. ichi Negishi, *J. Am. Chem. Soc.*, 1976, **98**, 6729–6731.

149 N. Miyaura and A. Suzuki, *Chem. Rev.*, 1995, **95**, 2457–2483.

150 M. T. Reetz, R. Breinbauer and K. Wanninger, *Tetrahedron Lett.*, 1996, **37**, 4499–4502.

151 S. Pathak, M. T. Greci, R. C. Kwong, K. Mercado, G. K. S. Prakash, G. A. Olah and M. E. Thompson, *Chem. Mater. 2000, 12, 1985-1989 Synth.*, 2000, **146**, 1985–1989.

152 Y. Li, E. Boone and M. A. El-Sayed, *Langmuir*, 2002, **18**, 4921–4925.

153 M. Larhed, G. Lindeberg and A. Hallberg, *Tetrahedron Lett.*, 1996, **37**, 8219–8222.

154 L. Bai, J. X. Wang and Y. Zhang, *Green Chem.*, 2003, **5**, 615–617.

155 D. Villemin and F. Caillot, *Tetrahedron Lett.*, 2001, **42**, 639–642.

156 S. F. Nielsen, D. Peters and O. Axelsson, *Synth. Commun.*, 2000, **30**, 3501–3509.

157 F. Schneider, A. Stolle, B. Ondruschka and H. Hopf, *Org. Process Res. Dev.*, 2009, **13**, 44–48.

158 T. Seo, T. Ishiyama, K. Kubota and H. Ito, *Chem. Sci.*, 2019, **10**, 8202–8210.

159 J. Freitag, M. Hermann, M. Nüchter, B. Ondruschka, F. Schneider and A. Stolle, *Opt. Appl.*, 2005, **35**, 745–752.

160 C. Schmöger, T. Szuppa, A. Tied, F. Schneider, A. Stolle and B. Ondruschka, *ChemSusChem*, 2008, **1**, 339–347.

161 A. Migliorini, C. Oliviero, T. Gasperi and M. A. Loreto, *Molecules*, 2012, **17**, 4508–4521.

162 T. Seo, T. Ishiyama, K. Kubota and H. Ito, *Chem. Sci.*, 2019, **10**, 8202–8210.

163 F. Schneider and B. Ondruschka, *ChemSusChem*, 2008, **1**, 622–625.

164 J. Zhu, J. A. Beamish, C. Tang, K. Kottke-Marchant and R. E. Marchant, *Macromolecules*, 2006, **39**, 1305.

165 R. Kaushik, M. Chand and S. C. Jain, *Synth. Commun.*, 2018, **48**, 1308–1315.

166 U. Galli, O. Mesenzani, C. Coppo, G. Sorba, P. L. Canonico, G. C. Tron and A. A. Genazzani, *Eur. J. Med. Chem.*, 2012, **55**, 58–66.

167 P. Griess, *Philos. Trans. R. Soc. London*, 1864, 36–102.

168 F. Tiemann, *Ber. Dtseh. Chem. Ges*, 1891, **24**, 4162–4167.

169 Z. P. Demko and K. B. Sharpless, *J. Org. Chem.*, 2001, **66**, 7945–7950.

170 C. J. Smith, C. D. Smith, N. Nikbin, S. V Ley and I. R. Baxendale, *Org. Biomol. Chem.*, 2011, **9**, 1927–1937.

171 C. J. Smith, N. Nikbin, S. V Ley, H. Lange and I. R. Baxendale, *Org. Biomol. Chem.*, 2011, **9**, 1938–1947.

172 W. F. Sager and A. J. Fatiadi, *Hexhydroxybenzene*, UTC, 1973, vol. 5.

173 G. Burdzinski, J. C. Hackett, J. Wang, T. L. Gustafson, C. M. Hadad and M. S. Platz, *J. Am. Chem. Soc.*, 2006, **128**, 13402–13411.

174 W. Trotter and A. C. Testa, *J. Am. Chem. Soc.*, 1968, **90**, 7044–7046.

175 A. Cu and A. C. Testa, *J. Phys. Chem.*, 1975, **79**, 644–646.

176 W. Y. Lai, Q. Y. He, D. Y. Chen and W. Huang, *Chem. Lett.*, 2008, **37**, 986–987.

177 M. K. Kim, J. Kwon, T. H. Kwon and J. I. Hong, *New J. Chem.*, 2010, **34**, 1317–1322.

178 K. Guzow, M. Czerwińska, A. Ceszlak, M. Kozarzewska, M. Szabelski, C. Czaplewski, A. Łukaszewicz, A. A. Kubicki and W. Wiczk, *Photochem. Photobiol. Sci.*, 2013, **12**, 284–297.

179 N. Choubdar, M. Golshani, L. Jalili-Baleh, H. Nadri, T. T. Küçükkilinç, B. Ayazgök, A. Moradi, F. H. Moghadam, Z. Abdolahi, A. Ameri, F. Salehian, A. Foroumadi and M. Khoobi, *Bioorg. Chem.*, 2019, **91**, 103164.

180 M. Ben Braiek, F. Aloui and B. Ben Hassine, *Tetrahedron Lett.*, 2016, **57**, 2763–2766.

181 S. S. Soni, K. B. Fadadu, J. V. Vaghasiya, B. G. Solanki, K. K. Sonigara, A. Singh, D. Das and P. K. Iyer, *J. Mater. Chem. A*, 2015, **3**, 21664–21671.

182 T. Bzeih, T. Naret, A. Hachem, N. Jaber, A. Khalaf, J. Bignon, J. D. Brion, M. Alami and A. Hamze, *Chem. Commun.*, 2016, **52**, 13027–13030.

183 S. Zaho, J. Kang, Y. Du, J. Kang, X. Zhao, Y. Xu, R. Chen, Q. Wang and X. Shi, *J. Heterocycl. Chem.*, 2014, **51**, 424–428.

184 F. Ullmann, *Berichte der Dtsch. Chem. Gesellschaft*, 1903, **36**, 2382–2384.

185 H. Ma and X. Jiang, *J. Org. Chem.*, 2007, **72**, 8943–8946.

186 M. Hosseini-Sarvari and Z. Razmi, *RSC Adv.*, 2014, **4**, 44105–44116.

187 T. X. Métro, X. J. Salom-Roig, M. Reverte, J. Martinez and F. Lamaty, *Green Chem.*, 2015, **17**, 204–208.

188 G. P. Fan, Z. Liu and G. W. Wang, *Green Chem.*, 2013, **15**, 1659–1664.

189 G. Kaupp, J. Schmeyers and J. Boy, *Adv. Synth. Catal.*, 2000, **342**, 269–280.

190 A. Beillard, E. Golliard, V. Gillet, X. Bantreil, T. X. Métro, J. Martinez and F. Lamaty, *Chem. - A Eur. J.*, 2015, **21**, 17614–17617.

191 A. Briš, M. Dud and D. Margetić, *Beilstein J. Org. Chem.*, 2017, **13**, 1745–1752.

192 D. J. Byron, G. W. Gray, A. Ibbotson and B. M. Worrall, *Mesomorphism aqad Chem. Cortstitution*, 1959, **11**, 2246–2256.

193 Y. T. M. Takechi, C. Uno, *Chem. Pharm. Bull.*, 1994, **17**, 1460–1462.

194 H. Lund, P. Lunde and F. Kaufmann, *Acta Chemica Scandinavica,* 1966, **20**, 1631–1644.

195 H. Erdtman, F. Haglid and N. E. Stjernström, *Acta Chem. Scand.*, 1961, **15**, 1761–1764.

196 T. Akiyama, Y. Wada, M. Yamada, Y. Shio, T. Honma and S. Shimoda, *Org. Lett.*, 2020, 0–119.

197 H. R. Bjørsvik and V. Elumalai, *J. Org. Chem.*, 2016, **2016**, 5474–5479.

198 X. Kong, H. Zhang, C. Cao, S. Zhou, G. Pang and Y. Shi, *Bioorganic Med. Chem.*, 2016, **24**, 1376–1383.

199 M. A. Ziemer, A. Mason and D. M. Carlson, *J. Biol. Chem.*, 1982, **257**, 11176–11180.

200 S. Surget, M. P. Khoury and J. C. Bourdon, *Onco. Targets. Ther.*, 2013, **7**, 57–67.

201 A. C. Joerger and A. R. Fersht, *Cold Spring Harb. Perspect. Biol.*, 2010, **2**, 1–20.

202 X. Sun, H. Shimizu and K. Yamamoto, *Mol. Cell. Biol.*, 1995, **15**, 4489–4496.

203 M. T. N. Le, C. Teh, N. Shyh-Chang, H. Xie, B. Zhou, V. Korzh, H. F. Lodish and B. Lim, *Genes Dev.*, 2009, 1–9.

204 M. M. Candeias, L. Malbert-Colas, D. J. Powell, C. Daskalogianni, M. M. Maslon, N. Naski, K. Bourougaa, F. Calvo and R. Fåhraeus, *Nat. Cell Biol.*, 2008, **10**, 1098–1105.

205 A. M. Bode and Z. Dong, *Nat. Rev. Cancer*, 2004, **4**, 793–805.

206 E. S. Helton and X. Chen, *J. Cell. Biochem.*, 2007, **100**, 883–896.

207 K. H. Vousden, *J. Cell Sci.*, 2006, **119**, 5015–5020.

208 M. B. Kastan, Q. Zhan, W. S. El-Deiry, F. Carrier, T. Jacks, W. V. Walsh, B. S. Plunkett, B. Vogelstein and A. J. Fornace, *Cell*, 1992, **71**, 587–597.

209 J. C. Garbe, C. R. Holst, E. Bassett, T. Tlsty and M. R. Stampfer, *Cell Cycle*, 2007, **6**, 1927–1936.

210 D. R. Green and J. E. Chipuk, *Cell*, 2006, **126**, 30–32.

211 J. G. Teodoro, A. E. Parker, X. Zhu and M. R. Green, *Science*, 2006, **313**, 968–971.

212 M. Taura, A. Eguma, M. A. Suico, T. Shuto, T. Koga, K. Komatsu, T. Komune, T. Sato, H. Saya, J.-D. Li and H. Kai, *Mol. Cell. Biol.*, 2008, **28**, 6557–6567.

213 L. Roger, G. Gadea and P. Roux, *Biol. Cell*, 2006, **98**, 141–152.

214 X. Yu, S. L. Harris and A. J. Levine, *Cancer Res.*, 2006, **66**, 4795–4801.

215 I. Goldstein, V. Marcel, M. Olivier, M. Oren, V. Rotter and P. Hainaut, *Cancer Gene Ther.*, 2011, **18**, 2–11.

216 A. Feki and I. Irminger-Finger, *Crit. Rev. Oncol. Hematol.*, 2004, **52**, 103–116.

217 D. Dittmer, S. Pati, G. Zambetti, S. Chu, A. K. Teresky, M. Moore, C. Finlay and A. J. Levine, *Nat. Genet.*, 1993, **4**, 42–46.

218 G. A. Lang, T. Iwakuma, Y. A. Suh, G. Liu, V. A. Rao, J. M. Parant, Y. A. Valentin-Vega, T. Terzian, L. C. Caldwell, L. C. Strong, A. K. El-Naggar and G. Lozano, *Cell*, 2004, **119**, 861–872.

219 K. P. Olive, D. A. Tuveson, Z. C. Ruhe, B. Yin, N. A. Willis, R. T. Bronson, D. Crowley and T. Jacks, *Cell*, 2004, **119**, 847–860.

220 S. Shangary and S. Wang, *Clin Cancer Res*, 2008, **14**, 1–7.

221 P. Hainaut and M. Hollstein, *Adv. Cancer Res.*, 1999, **77**, 81–86.

222 A. Binayke, S. Mishra, P. Suman, S. Das and H. Chander, *Cancer Chemother. Pharmacol.*, 2019, **83**, 0.

223 A. C. Joerger and A. R. Fersht, *Oncogene*, 2007, **26**, 2226–2242.

224 M. R. Bauer, A. Kra, G. Settanni, R. N. Jones, X. Ni, R. Khan Tareque, A. R. Fersht, J. Spencer

and A. C. Joerger, *Cite This ACS Chem. Biol*, 2020, **15**, 668.

225 R. N. Jones, *Towards the design and synthesis of a p53 mutant Y220C rescue drug,* 2017, University of Sussex.

226 A. C. Joerger, M. R. Bauer, R. Wilcken, M. G. J. Baud, H. Harbrecht, T. E. Exner, F. M. Boeckler, J. Spencer and A. R. Fersht, *Structure*, 2015, **23**, 2246–2255.

227 M. R. Bauer, A. Krämer, G. Settanni, R. N. Jones, X. Ni, R. Khan Tareque, A. R. Fersht, J. Spencer and A. C. Joerger, *ACS Chem. Biol.*, 2020, **15**, 657–668.

228 M. R. Bauer, R. N. Jones, R. K. Tareque, B. Springett, F. A. Dingler, L. Verduci, K. J. Patel, A. R. Fersht, A. C. Joerger and A. C. Joerger, *Future Med. Chem.*, 2019, **11**, 2491–2504.

229 M. R. Bauer, R. N. Jones, M. G. J. Baud, R. Wilcken, F. M. Boeckler, A. R. Fersht, A. C. Joerger and J. Spencer, *ACS Chem. Biol.*, 2016, **11**, 2265–2274.

230 S. Prajapati, A. Prasoon Mishra and A. Srivastava, *Ijpcbs*, 2012, **2012**, 52–62.

231 Ë. Pretsch, P. Bühlmann, M. Badertscher, *Structure Determination of Organic Compounds*, Fourth edition, Berlin, Springer, 2009.

232 L. Lu, Y. Li and X. Jiang, *Green Chem.*, 2020, **22**, 5989–5994.

233 A. A. Passchier, *J. Phys. Chem.*, 1967, **71**, 937–942.

234 Z. Ludwig, L. Gernot, P. Olaf, K. Joachim, N. Jens, B. Nico, B. Thorsten, T. L. Antonius and K. Stefan, *Novel benzimidazole derivatives as Ep4 antagonists*, 2016.

235 R. Bautista, P. A. Montoya, A. Rebollar, E. Burgueño and J. Tamariz, *Molecules*, 2013, **18**, 10334–10351.

236 K. G. Andrews, D. M. Summers, L. J. Donnelly and R. M. Denton, *Chem. Commun.*, 2016, **52**, 1855–1858.

237 E. L. Stoll, T. Tongue, K. G. Andrews, D. Valette, D. J. Hirst and R. M. Denton, *Chem. Sci.*, 2020, **11**, 9494–9500.

238 R. Köppe and P. H. Kasai, *Chem. Phys.*, 1994, **189**, 401–413.

239 D. L. F. DeTar and T. Kosuge, *J. Am. Chem. Soc.*, 1958, **80**, 6072–6077.

240 W. Reusch, Reactions of Aryl Diazonium Salts Arenediazonium Salts (Accesseed on November 30, 2022),

https://chem.libretexts.org/Bookshelves/Organic_Chemistry/Supplemental_Modules_(Organic_Chemistry)/Amines/Reactivity_of_Amines/Reactions_of_Aryl_Diazonium_Salts.

241 Z. Tavakkoli, H. Goljani, H. Sepehrmansourie, D. Nematollahi and M. A. Zolfigol, *RSC Adv.*, 2021, **11**, 25811–25815.

242 R. R. Petrov, L. Knight, S. R. Chen, J. Wager-Miller, S. W. McDaniel, F. Diaz, F. Barth, H. L. Pan, K. Mackie, C. N. Cavasotto and P. Diaz, *Eur. J. Med. Chem.*, 2013, **69**, 881–907.

243 N. V. Alekseeva, A. I. Bokanov, L. M. Alekseeva and V. G. Granik, *Pharm. Chem. J.*, 2002, **36**, 318–323.

244 Y. J. Pu, R. K. Vaid, S. K. Boini, R. W. Towsley, C. W. Doecke and D. Mitchell, *Org. Process Res. Dev.*, 2009, **13**, 310–314.

245 A. Rieche, H. Gross and E. Höft, *Org. Synth.*, 1967, **47**, 1.

246 T. M. Cresp, M. V Sargent, J. A. Elix and D. P. H. Murphy, *J. Chem. Soc. Perkin Trans. 1*, 1973, **32**, 340–345.

247 O. García, E. Nicolás and F. Albericio, *Tetrahedron Lett.*, 2003, **44**, 4961–4963.

248 I. Ramos-Tomillero, M. Paradís-Bas, I. De Pinho Ribeiro Moreira, J. M. Bofill, E. Nicolás and F. Albericio, *Molecules*, 2015, **20**, 5409–5422.

249 D. Rennison, S. M. Gueret, O. Laita, R. J. Bland, I. A. Sutherland, I. K. Boddy and M. A. Brimble, *Aust. J. Chem.*, 2016, **69**, 1268–1276.

250 F. Han, L. Chi, X. Liang, S. Ji, S. Liu, F. Zhou, Y. Wu, K. Han, J. Zhao and T. D. James, *J. Org. Chem.*, 2009, **74**, 1333–1336.

251 C. Luparello, I. Cruciata, A. C. Joerger, C. A. Ocasio, R. Jones, R. K. Tareque, M. C. Bagley, J. Spencer, M. Walker, C. Austin, T. Ferrara, P. D'Oca, R. Bellina, R. Branni and F. Caradonna, *Int. J. Mol. Sci.*, 2021, **22**, 1–14.

252 F. Boeckler, A. Joerger, G. Jaggi, T. Rutherford, D. Veprintsev and A. Fersht, *Chemtracts*, 2008, **21**, 236–237.

253 V. K. Srivastava and R. Yadav, *Data Processing Handbook for Complex Biological Data Sources*, Elsevier Inc., 2019.

254 Schrodinger (Accessed on October 19, 2022), https://www.schrodinger.com/.

255 Maestro CEM Discover (Accessed on October 19, 2022),

https://schrodinger.digitalchalk.com/delivery/dashboard.

256 A. G. Atanasov, B. Waltenberger, E.-M. Pferschy-Wenzig, T. Linderd, C. Wawroscha, P. Uhrine, V. Temmlf, L. Wanga, S. Schwaigerb, E. H. Heissa, J. M. Rollingera, D. Schusterf, J. M. Breusse, V. Bochkovg, M. D. Mihovilovicd, B. Koppa, R. Bauerc, V. M. Dirscha and H. Stuppnerb, *Biotechnol Adv*, 2015, 1582–1614.

257 A. L. Harvey, R. Edrada-Ebel and R. J. Quinn, *Nat. Rev. Drug Discov.*, 2015, **14**, 111–129.

258 G. R. Geen, J. M. Evans and A. K. Vong, *Compr. Heterocycl. Chem. II A Rev. Lit. 1982-1995*, 1996, **5**, 469–500.

259 M. Sorokina and C. Steinbeck, *J. Cheminform.*, 2020, **12**, 1–51.

260 G. L. Points and C. M. Beaudry, *Org. Lett.*, 2021, **23**, 6882–6885.

261 M. P. Krahl, A. Jäger, T. Krause and H. J. Knölker, *Org. Biomol. Chem.*, 2006, **4**, 3215–3219.

262 T. V. Nykaza, A. Ramirez, T. S. Harrison, M. R. Luzung and A. T. Radosevich, *J. Am. Chem. Soc.*, 2018, **140**, 3103–3113.

263 X. Tian, L. Song and A. S. K. Hashmi, *Angew. Chemie - Int. Ed.*, 2020, **59**, 12342–12346.

264 T. Chatterjee, G. B. Roh, M. A. Shoaib, C. H. Suhl, J. S. Kim, C. G. Cho and E. J. Cho, *Org. Lett.*, 2017, **19**, 1906–1909.

265 Y. Qiu, D. Ma, C. Fu and S. Ma, *Org. Biomol. Chem.*, 2013, **11**, 1666–1671.

266 R. Forke, A. Jäger and H. J. Knölker, *Org. Biomol. Chem.*, 2008, **6**, 2481–2483.

267 F. Goebel, *Ann. der Chemie und Pharm.*, 1841, **38**, 363.

268 T. Herraiz, D. González, C. Ancín-Azpilicueta, V. J. Arán and H. Guillén, *Food Chem. Toxicol.*, 2010, **48**, 839–845.

269 A. S. N. Formagio, L. T. D. Tonin, M. A. Foglio, C. Madjarof, J. E. de Carvalho, W. F. da Costa, F. P. Cardoso and M. H. Sarragiotto, *Bioorg. Med. Chem.*, 2008, **16**, 9660–9667.

270 S. Y. Son, J. Ma, Y. Kondou, M. Yoshimura, E. Yamashita and T. Tsukihara, *Proc. Natl. Acad. Sci. U. S. A.*, 2008, **105**, 5739–5744.

271 R. B. Herbert and J. Mann, *J. Chem. Soc. Perkin Trans. 1*, 1982, 1523–1525.

272 J. Berlin, C. Rügenhagen, N. Greidziak, I. N. Kuzovkina, L. Witte and V. Wray, *Phytochemistry*, 1993, **33**, 593–597.

273 J. Berlin, C. Rügenhagen, I. N. Kuzovkina, L. F. Fecker and F. Sasse, *Plant Cell. Tissue Organ Cult.*, 1994, **38**, 289–297.

274 R. M. Kostrzewa and T. Archer, *Isoquinolines and Beta-Carbolines as Neurotoxins and Neuroprotectants*, 2012.

275 T. R. Govindachari and W. M. Whaley, *Org. React.*, 1951, **6**, 151.

276 S. U. Dighe, S. K. Samanta, S. Kolle and S. Batra, *Tetrahedron*, 2017, **73**, 2455–2467.

277 B. N. A. Buschler, *Berichte der Deutschen Chemischen Gesellschaft,* 1893, **22**, 1903–1908.

278 T. P. Singh and O. M. Singh, *J. Chem. Sci.*, 2016, **128**, 565–572.

279 T. Kametani, T. Yamanaka and K. Ogasawara, *Chem. Commun.*, 1968, 996–997.

280 A. L. Pumphrey, H. Dong and T. G. Driver, *Angew. Chemie - Int. Ed.*, 2012, **51**, 5920–5923.

281 W. Yang, J. Zhou, B. Wang and H. Ren, *Chem. Eur. J.*, 2011, **17**, 13665–13669.

282 T. S. Wu, S. C. Huang, P. L. Wu and C. S. Kuoh, *Phytochemistry*, 1999, **52**, 523–527.

283 H. Shigyo, S. Sato, K. Shibuya and Y. Takashi, *Chem. Pharm. Bull.*, 1994, **17**, 1460–1462.

284 R. C. Elderfield and O. L. Mccurdy, *J. Org. Chem.*, 1956, **21**, 295–296.

285 T. N. Poudel and Y. R. Lee, *Chem. Sci.*, 2015, **6**, 7028–7033.

286 C. Graebe and H. Caro, *Berichte der Dtsch. Chem. Gesellschaft*, 1883, **16**, 2828–2832.

287 M. Gensicka-Kowalewska, G. Cholewiński and K. Dzierzbicka, *RSC Adv.*, 2017, **7**, 15776–15804.

288 G. Cholewiński, K. Dzierzbicka and A. M. Kołodziejczyk, *Pharmacol. Reports*, 2011, 63, 845.

289 H. K. H. Fong and B. R. Copp, *Mar. Drugs*, 2013, **11**, 274–299.

290 M. Rahimizadeh, M. Pordel, M. Bakavoli and H. Eshghi, *Dye. Pigment.*, 2010, **86**, 266–270.

291 V. Pakjoo, M. Roshani, M. Pordel and T. Hoseini, *Arkivoc*, 2012, **2012**, 195–203.

292 J. M. Coteron, M. Marco, J. Esquivias, X. Deng, K. L. White, J. White, M. Koltun, F. El Mazouni, S. Kokkonda, K. Katneni, R. Bhamidipati, D. M. Shackleford, I. Angulo-Barturen, S. B. Ferrer, M. B. Jiménez-Díaz, F. J. Gamo, E. J. Goldsmith, W. N. Charman, I. Bathurst, D. Floyd, D. Matthews, J. N. Burrows, P. K. Rathod, S. A. Charman and M. A. Phillips, *J. Med. Chem.*, 2011, **54**, 5540–5561.

293 F. Afolabi, *Synthesis of novel fluorescence cationic gold(i) complexes as potent anti cancer agent,* 2018, University of Sussex.

294 M. Więcław, M. Bobin, A. Kwast, R. Bujok, Z. Wróbel and K. Wojciechowski, *Mol. Divers.*, 2015, **19**, 807–816.

295 C. Alverez, M. R. Arkin, S. L. Bulfer, R. Colombo, M. Kovaliov, M. G. Laporte, C. Lim, M. Liang, W. J. Moore, R. J. Neitz, Y. Yan, Z. Yue, D. M. Huryn and P. Wipf, *ACS Med. Chem. Lett.*, 2015, **6**, 1225–1230.

296 Z. Vejdelek, M. Rajsner, A. Dlabac and M. Ryska, *Japanese J. Gastroenterol. Surg.*, 1980, **13**, 3593–3615.